

Off-the-rack instead of Tailor-made Module-based Plant Design at Equipment Level

Zur Erlangung des akademischen Grades eines
Dr.-Ing.
von der Fakultät Bio- und Chemieingenieurwesen
der Technischen Universität Dortmund
genehmigte Dissertation

vorgelegt von
M.Sc. Heiko Radatz
aus
Forst (L.)

Tag der mündlichen Prüfung: 25.10.2021
1. Gutachter: Prof. Dr.-Ing. Gerhard Schembecker
2. Gutachter: Prof. Dr.-Ing. Marcus Grünewald

Dortmund - 2021

An apple a day keeps the Dr. away.

Acknowledgements

The work leading to this doctoral thesis has been conducted during my employment at the Laboratory of Plant and Process Design (APT) from the department of Biochemical and Chemical Engineering (BCI) at TU Dortmund University.

First and foremost, I would like to thank Prof. Dr.-Ing Gerhard Schembecker for giving me the opportunity of working and writing my thesis under his supervision. His critical thinking, his resilience and his ability to directly see the heart of the matter have impressed and shaped me over the years. Furthermore, I am thankful for the support and the critical and fruitful discussions with Dr.-Ing. Christian Bramsiepe, who lead the group of Module-based Plant Design in the first years. The freedom to pursue and explore own ideas without knowing where they will lead is something I really appreciate.

I am very grateful to all the colleagues as well as the numerous bachelor and master students whose work I supervised. Especially, I would like to thank Matthias, Martin, Christian and Ramy from the module-based plant design group and my office mate Marie for all the motivating discussions and critical perspectives. As I was also part of the EU-funded research project TOP-REF, I would like to thank my TOP-REF colleagues from all over Europe - I enjoyed collaborating with all of you.

I would also like to mention my friends who have accompanied me along the way. Special thanks to Lukas for reading my work and your support along the entire path.

Finally, I would like to thank my family for their encouragement, support and patience on this long journey.

Abstract

Module-based plant design facilitates a paradigm shift in chemical and biochemical industry to decrease the time needed for plant design. Instead of a tailored design of apparatuses for a target production rate, modules are selected off-the-rack to set up a production plant.

Within the scope of this thesis, four important areas of module-based plant design at equipment level are investigated. First, the determination of a plants' overall operating window, a prerequisite for equipment module selection and evaluation is improved by considering the so far neglected non-linear dependency between the operating constraints and the production rate of a plant.

Second, the currently accepted view that investment costs are determining the decision on the use of equipment modules for different process units is disproved and novel preselection approaches are proposed, applied and evaluated. A preselection approach based on investment and operating costs is rated most suitable to decide on the use of equipment modules for a case study. The third area explored is equipment module selection for a constant market demand, aiming at flexibility in production rate at low investment costs, as well as for a market demand development. It is shown by case studies that modular production plants offer a promising alternative to conventionally designed plants. Finally, an approach to design equipment modules for flexibility in production rate is introduced and applied. For the case study of a heat exchanger it is shown that a four times larger operating window can be obtained at only 14 % higher total annual costs compared to a conventionally designed heat exchanger.

Hence, this work investigates four key areas in module-based plant design at equipment level beyond current state of the art contributing to a paradigm shift in plant design.

Zusammenfassung

Modulbasierte Anlagenplanung ermöglicht einen Paradigmenwechsel in der chemischen und biochemischen Industrie, um die Zeit der Anlagenplanung zu verkürzen. Anstelle einer maßgeschneiderten Auslegung von Apparaten für einen Auslegungspunkt werden Module von der Stange ausgewählt, um eine Produktionsanlage zu errichten.

Im Rahmen dieser Arbeit werden vier wichtige Bereiche der modulbasierten Anlagenplanung auf Equipmentebene untersucht. Erstens wird die Bestimmung des Gesamtbetriebsfensters einer Anlage, eine Voraussetzung für die Auswahl von Equipmentmodulen und Bewertung von modularen Anlagen, durch die Berücksichtigung der bisher vernachlässigten und nichtlinearen Abhängigkeit zwischen den Betriebsgrenzen und der Produktionsrate einer Anlage verbessert. Zweitens werden aktuelle Entscheidungskriterien für den Einsatz von Equipmentmodulen für verschiedene Prozesseinheiten in Frage gestellt und neue Vorauswahlmethoden vorgeschlagen, angewendet und bewertet. Dabei wird die derzeit akzeptierte Ansicht, dass Investitionskosten bestimmend sind, widerlegt. Eine Vorauswahlmethode, um über die Verwendung von Equipmentmodulen zu entscheiden, die auf Investitions- und Betriebskosten basiert, wird für eine Fallstudie als am geeignetsten bewertet. Der dritte untersuchte Bereich behandelt die Auswahl von Equipmentmodulen für eine konstante Marktnachfrage, mit dem Ziel einer hohen Flexibilität in der Produktionsrate bei niedrigen Investitionskosten, sowie für eine Marktnachfrageentwicklung. Anhand von Fallstudien wird gezeigt, dass modulare Produktionsanlagen eine vielversprechende Alternative zu konventionell ausgelegten Anlagen darstellen. Abschließend wird ein Ansatz zur Auslegung von Equipmentmodulen für eine hohe Flexibilität in der Produktionsrate vorgestellt und angewendet. Am Beispiel eines Wärmeübertragers wird gezeigt, dass ein viermal größeres Betriebsfenster für nur 14 % höhere jährliche Gesamtkosten im Vergleich zu einem konventionell ausgelegten Wärmeübertrager erreicht werden kann.

Somit untersucht diese Arbeit vier wichtige Bereiche der modulbasierten Anlagenplanung auf Equipmentebene über den aktuellen Stand der Technik hinaus und liefert ihren Beitrag für einen Paradigmenwechsel in der Anlagenplanung.

List of Publications

Journal Papers

- Radatz, H., Kragl, A., Kampwerth, J., Stark, C., Herden, N., Schembecker, G.
Application and evaluation of preselection approaches to decide on the use of equipment modules
Chemical Engineering Research and Design, 2021, 173, pp. 89–107
- Radatz, H., Kühne, K., Bramsiepe, C., Schembecker, G.
Comparison of capacity expansion strategies for chemical production plants
Chemical Engineering Research and Design, 2019, 143, pp. 56–78
- Radatz, H., Schröder, M., Becker, C., Bramsiepe, C., Schembecker, G.
Selection of equipment modules for a flexible modular production plant by a multi-objective evolutionary algorithm
Computers and Chemical Engineering, 2019, 123, pp. 196–221
- Eilermann, M., Post, C., Radatz, H., Bramsiepe, C., Schembecker, G.
A general approach to module-based plant design
Chemical Engineering Research and Design, 2018, 137, pp. 125–140
- Radatz, H., Elischewski, J.M., Heitmann, M., Schembecker, G., Bramsiepe, C.
Design of equipment modules for flexibility
Chemical Engineering Science, 2017, 168, pp. 271–288
- Radatz, H., Schembecker, G., Raffray, G., Sellis, D., Boto, F., Echeverria, Z., Carrion, A., Herce, C., Oto, F., Gil, A., Arias, A., Borrego, R., Romero, J., Jacinto, J. T.,
Improving resource efficiency of industrial processes with TOP-REF methodology - Part 1
Hydrocarbon Processing / January 2019
- Radatz, H., Schembecker, G., Raffray, G., Sellis, D., Boto, F., Echeverria, Z., Carrion, A., Herce, C., Oto, F., Gil, A., Arias, A., Borrego, R., Romero, J., Jacinto, J. T.
Improving resource efficiency of industrial processes with the TOP-REF methodology – Part 2
Hydrocarbon Processing / February 2019

Oral presentations

- H. Radatz, A. Kragl, G. Schembecker
Müssen die Kosten bei der Verwendung von Equipment-Modulen immer steigen?
Jahrestreffen der Fachgemeinschaft “Prozess-, Apparate- und Anlagentechnik“ (PAAT), Würzburg, DE (2017)
- H. Radatz
TOP-REF Workshop – Methodologies & Tools for decision-making (Modeling and global sensitivity analysis)
World Congress of Chemical Engineering, Barcelona, ES (2017)
- H. Radatz
The TOP-REF Approach to Improve the Resource Efficiency of Energy Intensive Industrial Processes - Coupling of Models
4. Treffen Arbeitskreis Prozesssimulation, Berlin, DE (2017)
- H. Radatz, T. Hellenkamp, G. Schembecker, C. Bramsiepe
The Top-Ref Approach to Improve the Resource Efficiency of Energy Intensive Industrial Processes
2016 AIChE Annual Meeting, San Francisco, CA, USA (2016)

- H. Radatz, K. Kühne, G. Schembecker, C. Bramsiepe
Comparison of capacity expansion strategies for chemical production plants
ProcessNet-Jahrestagung und 32. DECHEMA-Jahrestagung der Biotechnologen,
Aachen, DE (2016)
- T. Hellenkamp, H. Radatz, C. Bramsiepe, G. Schembecker
The TOP-REF approach for identification of critical process parameters for process monitoring and optimization
ProcessNet-Jahrestagung und 32. DECHEMA-Jahrestagung der Biotechnologen,
Aachen, DE (2016)
- H. Radatz, J.M. Elischewski, G. Schembecker, C. Bramsiepe
Design of Flexible Equipment Modules
Jahrestreffen der ProcessNet-Fachgemeinschaft "Prozess-, Apparate- und Anlagentechnik" (PAAT), Bruchsal, DE (2015)
- H. Radatz, T. Seifert, M. Heitmann, G. Schembecker, C. Bramsiepe
Application of a multi-objective Evolutionary Algorithm for the Selection of Modular Plant Setups
Jahrestreffen der ProcessNet-Fachgemeinschaft "Prozess-, Apparate- und Anlagentechnik" (PAAT), Lüneburg, DE (2014)
- H. Radatz, T. Seifert, G. Schembecker, C. Bramsiepe
Einbindung von Flexibilitätsanalysen und Anlagenerweiterungsstrategien in die Anlagenplanung
Jahrestreffen der ProcessNet-Fachgemeinschaft "Prozess-, Apparate- und Anlagentechnik" (PAAT), Bruchsal, DE (2013)

Poster presentations

- H. Radatz, N. Herden, C. Stark, G. Schembecker, C. Bramsiepe
Module-based plant design meets biochemical production
Himmelfahrtstagung: Models for Developing and Optimising Biotech Production, Neu-Ulm, DE (2017)
- H. Radatz, K. Kühne, G. Schembecker, C. Bramsiepe
Comparison of Capacity Expansion Strategies for Chemical Production Plants and Consideration of Alternative Modular Reactors with a Larger Operating Window
(incl. CAST Division Rapid Fire Presentation)
2016 AIChE Annual Meeting,
San Francisco, CA, USA (2016)
- N. Wolters, H. Radatz, L. Bolenz, G. Schembecker, C. Bramsiepe, J. Merz
Optimization of feeding strategies for the fermentative production of Erinacine C and evaluation of industrial-scale production
Himmelfahrtstagung: New Frontiers for Biotech-Processes, Koblenz, DE (2016)
- H. Radatz, C. Stark, J. Kampwerth, C. Bramsiepe, G. Schembecker
A Novel Approach to decide on Modularization: Application to a biochemical Production Process
5th European Process Intensification Conference EPIC, Nice, FR (2015)
- H. Radatz, G. Schembecker, C. Bramsiepe
Module-based Plant Design for Chemical and Biochemical Production Plants
1st Industrial Bioprocess-Development Academy, Ludwigshafen, Germany (2015)

H. Radatz, M. Heitmann, G. Schembecker, C. Bramsiepe
Design of Equipment Modules regarding Flexibility
ProcessNet-Jahrestagung und 31. DECHEMA-Jahrestagung der Biotechnologen,
Aachen, DE (2014)

Other

CEN Workshop Agreement CWA 17185:2017
Methodology to measure and improve the resource efficiency of resource intensive processes
Danish Standards Foundation / European Committee for Standardization
Date of approval: 2017-09-11

Declaration

Parts of this work have already been published by the author in scientific journals and were reused in this thesis with permission. In addition, some chapters contain methods and simulations resulting from student theses supervised by the author at the Laboratory of Plant and Process Design (Department of Biochemical and Chemical Engineering, TU Dortmund University). The corresponding chapters, scientific papers and student theses of which parts were used in this work are listed below.

Chapter 1		Partly modified from	[D]
Chapter 3	3.1	Partly modified from	[B,C]
	3.2	Partly modified from	[A,b,e,i]
	3.3.1	Partly modified from	[C,a,k]
	3.3.2	Partly modified from	[B,d]
	3.4	Partly modified from	[E,f,j,k]
Chapter 4	4.2.1	Partly modified from	[A,b,e,i]
	4.2.2	Partly modified from	[A,e]
	4.2.3	Partly modified from	[A,b,e,i]
	4.2.4	Partly modified from	[A,e]
	4.3	Partly modified from	[B,C,a,d]
		Algorithm development and implementation partly from	[a,c,d,e,g]
	4.4	Partly modified from	[E,F,G,f,j]
		Method development and implementation partly from	[f,h,j,b,l,o]
Chapter 5	5.1	Partly modified from	[C,a]
		Process simulation partly developed in	[a]
	5.2	Partly modified from	[B,d,g,h]
		Process simulation partly developed in	[d,g,h,e]
	5.3	Partly modified from	[A,b,c,e,n]
		Process simulation partly developed in	[b,c,e]
Chapter 6	6.1	Partly modified from	[C]
	6.2	Partly modified from	[A,e]
	6.3.1	Partly modified from	[C,a]
	6.3.2	Partly modified from	[C]
	6.3.3	Partly modified from	[B,d]
	6.4	Partly modified from	[E,f]
Chapter 7		Partly modified from	[A,B,C,D,E]
Chapter 8		Partly modified from	[A,B,C,D,E]

Publications

- [A] Radatz, H., Kragl, A., Kampwerth, J., Stark, C., Herden, N., Schembecker, G.
Application and evaluation of preselection approaches to decide on the use of equipment modules
Chemical Engineering Research and Design, 2021, 173, pp. 89–107
- [B] Radatz, H., Kühne, K., Bramsiepe, C., Schembecker, G.
Comparison of capacity expansion strategies for chemical production plants
Chemical Engineering Research and Design, 2019, 143, pp. 56–78
- [C] Radatz, H., Schröder, M., Becker, C., Bramsiepe, C., Schembecker, G.
Selection of equipment modules for a flexible modular production plant by a multi-objective evolutionary algorithm
Computers and Chemical Engineering, 2019, 123, pp. 196–221
- [D] Eilermann, M., Post, C., Radatz, H., Bramsiepe, C., Schembecker, G.
A general approach to module-based plant design
Chemical Engineering Research and Design, 2018, 137, pp. 125–140
- [E] Radatz, H., Elischewski, J.M., Heitmann, M., Schembecker, G., Bramsiepe, C.
Design of equipment modules for flexibility
Chemical Engineering Science, 2017, 168, pp. 271–288
- [F] Radatz, H., Schembecker, G., Raffray, G., Sellis, D., Boto, F., Echeverria, Z., Carrion, A., Herce, C., Oto, F., Gil, A., Arias, A., Borrego, R., Romero, J., Jacinto, J. T.,
Improving resource efficiency of industrial processes with TOP-REF methodology – Part 1
Hydrocarbon Processing / January 2019
- [G] Radatz, H., Schembecker, G., Raffray, G., Sellis, D., Boto, F., Echeverria, Z., Carrion, A., Herce, C., Oto, F., Gil, A., Arias, A., Borrego, R., Romero, J., Jacinto, J. T.,
Improving resource efficiency of industrial processes with the TOP-REF methodology – Part 2
Hydrocarbon Processing / February 2019
-

Supervised student theses

- [a] C. Becker
Improvement of a multi-objective evolutionary algorithm for the selection of modular plant setups
Bachelor thesis, Laboratory of Plant and Process Design, TU Dortmund University, 2014
- [b] C. Stark
Application of exergoeconomic criteria for the decision on modularization of unit operations to a fermentative production process
Bachelor thesis, Laboratory of Plant and Process Design, TU Dortmund University, 2014
- [c] N. Herden
Selection of equipment modules for modular plant setups – application to a biochemical production process
Master thesis, Laboratory of Plant and Process Design, TU Dortmund University, 2016
- [d] K. Kühne
Comparison of capacity expansion strategies for chemical production plants
Master thesis, Laboratory of Plant and Process Design, TU Dortmund University, 2015
- [e] A. Kragl
Application and evaluation of preselection criteria to decide on the use of equipment modules
Master thesis, Laboratory of Plant and Process Design, TU Dortmund University, 2017

-
- [f] J. Elischewski
Design of equipment modules regarding flexibility
Master thesis, Laboratory of Plant and Process Design, TU Dortmund University, 2015
- [g] M. Schröder
Investigation of reactor modeling depths for equipment module selection
Master thesis, Laboratory of Plant and Process Design, TU Dortmund University, 2017
- [h] M. Eilermann
An approach for the generation and application of equipment module databases for modular plant setups
Master thesis, Laboratory of Plant and Process Design, TU Dortmund University, 2014
- [i] J. Kampwerth
Entwicklung von Entscheidungskriterien für/gegen Modularisierung basierend auf thermoökonomischen Analysen am Beispiel eines Steam Crackers
Bachelor thesis, Laboratory of Plant and Process Design, TU Dortmund University, 2014
- [j] V. Booshanan
An approach to investigate the influence of equipment design parameters on volume flexibility
Master thesis, Laboratory of Plant and Process Design, TU Dortmund University, 2014
- [k] B. Mistry
Modeling, simulation and flexibility analysis of a crude distillation and fractionation unit
Master thesis, Laboratory of Plant and Process Design, TU Dortmund University, 2015
- [l] E. Carsanba
An approach to develop a generally applicable equipment module databased
Bachelor thesis, Laboratory of Plant and Process Design, TU Dortmund University, 2016
- [m] M. Franz
Metamodellierung von Prozesssimulationen für Sensitivitätsanalysen
Bachelor thesis, Laboratory of Plant and Process Design, TU Dortmund University, 2015
- [n] L. Bolenz
Optimization of feeding strategies for the fermentative production of erinacine C and evaluation of industrial-scale production
Master thesis, Laboratory of Plant and Process Design, TU Dortmund University, 2016
(supervised together with N. Wolters)
- [o] I. Kalisch
Investigating the operating limits of evaporators concerning mechanical design constraints
Master thesis, Laboratory of Plant and Process Design, TU Dortmund University, 2015
(supervised together with M. Eilermann)
-

Nomenclature

Abbreviations

CIP	cleaning-in-place
DCW	dry cell weight
EA	evolutionary algorithm
ES	equipment set
FBD	fluidized bed dryer
FERM	fermenter
IPA	isopropanol

Latin Symbols

a_p	[m ² /m ³]	volume specific surface of particle
A	[m ²]	area
A_{ab}	[-]	absorption factor
A_{est}	[m ²]	estimated heat transfer area
Ar	[-]	<i>Archimedes</i> number
A_{req}	[m ²]	required heat transfer area
A_s	[m ²]	shell cross flow area
b_c	[%]	baffle cut
BEC	[\$]	bare equipment costs
c	[-]	dispersion factor in decanter
c	[\$/J]	specific exergy costs
C	[\$] or [-]	investment costs or empirical constant
\dot{C}	[\$/s]	cost stream
Cap	[%]	capacity
Cap_{fac}	[-]	ratio of simulated production rate to a reference production rate
Cap_{mean}	[kg/h] or [t/h]	mean capacity of overall operating window
Cap_{min}	[kg/h] or [t/h]	minimum capacity
Cap_{max}	[kg/h] or [t/h]	maximum capacity
ΔCap	[kg/h] or [t/h]	size of an operating window
ΔCap_{rel}	[-]	relative size of an operating window
C_{el}	[\$/year]	annual electricity costs
$CEPCI$	[-]	Chemical Engineering Plant Cost Index
CEX	[-]	cost-capacity-exponent
$c_{DCW,initial}$	[g/m ³]	initial dry cell weight concentration
C_i	[\$]	total investment costs
CL	[-]	tube layout constant
C_{op}	[\$/year]	annual operating costs
c_p	[J/kg/K]	specific heat
C_{tot}	[\$/year]	total annual costs
CTP	[-]	tube count calculation constant
d or D	[m]	diameter
\bar{d}	[\$/a]	mean distance
d_p	[m]	diameter of catalyst pellet or particle
d_e	[m]	equivalent (or hydraulic mean) diameter
$D:F$	[-]	distillate to feed ratio
d_h	[m]	sieve hole diameter
d_i	[m]	inner tube diameter
$d_{i,nozz}$	[m]	inner nozzle diameter

d_o	[m]	outer tube diameter
$d_{o,nozz}$	[m]	outer nozzle diameter
d_T	[m]	tube diameter
DPC	[\$]	direct plant costs
d_s	[m]	shell inside diameter
d_{tr}	[m]	diameter of tie rods
\tilde{e}_{ch}	[J/mol]	specific chemical exergy
\dot{E}	[J/s]	exergy stream
E_A	[kJ/kmol]	activation energy
EAA	[\$]	equivalent annual annuity
E_i	[-]	interaction effects
f	[-]	<i>Fanning</i> friction factor
f_0	[-]	mean
f_{vapor}	[-]	vapor fraction
F	[Pa ^{0.5}]	flooding factor
f_b	[-]	baffle spacing factor
FCF	[\$]	free cash flow
FCI	[\$]	fixed capital investment
FOB	[\$]	free on board costs
F_t	[-]	temperature correction factor
g	[m ² /s]	standard gravitational acceleration
$\gamma_{i,L}^\infty$	[-]	activity coefficient of component i
G_s	[kg/s/m ²]	shell-side mass velocity
h	[m] or [W/m ² /K]	height / heat transfer coefficient
h_l	[m]	distance below the stirrer
h_u	[m]	distance above the stirrer
$\Delta h_{stirrer}$	[m]	distance between the stirrer blades
Δh_c	[kJ/g]	heat of combustion
ΔH_{rxn}	[kJ/mol]	heat of reaction
\dot{H}	[J/s]	enthalpy stream
$HETP$	[m]	height equivalent of a theoretical plate
h_{tot}	[h]	total number of working hours
HTU_G	[m]	height of gas-film transfer unit
HTU_L	[m]	height of liquid-film transfer unit
HTU_{OG}	[m]	height of overall gas transfer unit
i	[-]	number of components
ICF	[\$] or [-]	interim cash flow or Investment Cost Factor
ID	[mm]	inner diameter
$instr.$	[\$]	costs for instrumentation excluding valves
j	[-]	index of process units
j_f	[-]	friction factor
j_h	[-]	heat transfer factor
	[-]	design vapor velocity factor
k	[-]	number of input parameters for sampling
	[1/s] or [m ³ /kmol/s]	rate constant
K	[-]	equilibrium constant
k_f	[W/m/K]	thermal conductivity of the liquid
$k_{vert.}$	[-]	design vapor velocity factor of vertical vapor-liquid separator
k_w	[W/m/K]	thermal conductivity of the tube wall material
K_1	[-]	empirical factor

L	[m]	length
l_b	[m]	baffle spacing
L_{eff}	[m]	effective length
L_f	[m]	necessary flow distance of decanter
l_{nozz}	[m]	length of nozzles
L_T	[m]	tube length filled with catalyst
$L_{T,total}$	[m]	total tube length
\dot{m}	[kg/s]	mass flow rate
m	[kg]	mass
\dot{m}	[kg/s]	mass flow rate
MIRR	[%]	modified internal rate of return
n	[-]	number / exponent / number of moles
\dot{n}	[mol/s] or [kmol/s]	molar flow rate
N	[-]	population size
N'	[-]	archive size (Number of Pareto-optimal modular equipment sets)
N_{base}	[-]	number of base samples
N'	[-]	archive size
N_b	[-]	number of baffles
n_{op}	[h/year]	annual operating hours
NPV	[\$]	net present value
$N_{S,pass}$	[-]	number of shell passes
N_T	[-]	number of tubes
NTP	[-]	number of theoretical plates
$N_{T,pass}$	[-]	number of tube passes
n_{tr}	[-]	number of tie rods
n_{nozz}	[-]	number of nozzles
Nu	[-]	<i>Nusselt</i> number
Nu_m	[-]	mean <i>Nusselt</i> number
OD	[mm]	outer diameter
$OPEX$	[\$]	operating expenses
p	[bar] or [Pa]	pressure
p_i^{LV}	[Pa]	vapor pressure of component i
p_{rec}	[-]	recombination probability
p_{mut}	[-]	mutation probability
P	[kW]	power
P_p	[-]	position factor for a process unit at position p
Pr	[-]	<i>Prandtl</i> number
PR	[-]	tube pitch ratio
p_t	[m]	tube pitch
Δp	[bar]	pressure drop
$price_{el}$	[\$/kWh]	price of electric power
$price_h$	[\$/h]	price per working hour
$price_M$	[\$/kg]	price per kg of used material
$price_u$	[\$/t]	price of utility
\dot{Q}	[W] or [kW]	heat duty / heat stream
q_{fill}	[-]	liquid content
q_p	[-]	heat generation potential
r	[%]	interest rate
r	[kmol/s/m ³]	reaction rate
r_{mut}	[-]	mutation rate
R	[-]	temperature ratio

Re	[-]	<i>Reynolds</i> number
Re_p	[-]	particle related <i>Reynolds</i> number
R_f	[m ² °C/W]	fouling resistance
$R_{f,i}$	[m ² °C/W]	inside fouling resistance
$R_{f,o}$	[m ² °C/W]	outside fouling resistance
RR	[-]	actual reflux ratio
S	[-]	temperature ratio
$S.Fac$	[-]	vapor-liquid separation factor
S_i	[-]	first-order sensitivity index
<i>size</i>	e.g. [m ³]	characteristic size
S_{Ti}	[-]	total order sensitivity index
\dot{S}	[J/s/K]	entropy stream
t	[s] or [h] or [year]	time
T	[°C] or [K]	temperature
TCI	[\$]	total cost of investment
$TCI_{initial}$	[\$]	initial total cost of investment
ΔT_m	[°C]	true mean temperature difference
ΔT_{ln}	[°C] or [K]	mean logarithmic temperature difference
U	[W/m ² /K]	overall heat transfer coefficient
$U_{O,ass}$	[W/m ² /K]	assumed heat transfer coefficient
$U_{O,calc}$	[W/m ² /K]	overall heat transfer coefficient
v	[m/s]	velocity
v_f	[m/s]	forward velocity of continuous phase
V	[m ³]	volume
\dot{V}	[m ³ /s]	volume flow rate
Var	[-]	total variance
Var_{X_i}	[-]	variance of parameter X_i
$Var_{X \sim i}$	[-]	variance of all parameters but X_i
W	[J]	work
x_i	[mole-%] or [mole/mole]	molar concentration / fraction of component i
X	[mole/mole]	loading of liquid
X_c	[kg/kg]	critical solids moisture content
X_e	[kg/kg]	equilibrium solid moisture content
Y	[mole/mole]	loading of vapor stream
y_i	[mole/mole]	molar fraction of vapor
\dot{Z}	[\$/s]	system costs stream
Z_{FBD}	[m]	actual bed height in fluidized bed dryer
$Z_{FBD,min}$	[m]	bed height at minimum fluidization $Z_{FBD,min}$
Z_{Dryer}	[m]	height of the dryer

Greek Symbols

α	[°]	tube layout angle
α	[W/m ² /K]	heat transmission coefficient
	[-]	Correlation exponents for the operating constraints
δ_b	[m]	baffle thickness
δ_s	[m]	shell thickness
δ_t	[m]	tube thickness
δ_{ts}	[m]	tubesheet thickness
ε	[-]	void fraction / bed voidage
ε_{min}	[-]	minimum fluidization void fraction

η	[Pa s]	dynamic viscosity
η	[-]	pumping efficiency
θ	[°]	angle
λ	[W/m/K] or [-]	thermal conductivity or number of offspring individuals
μ	[Pa s]	dynamic viscosity
ν	[m ² /s]	kinematic viscosity
ξ_t	[-]	tube side friction coefficient
ρ	[kg/m ³]	mass density
σ	[N/m]	liquid surface tension
τ	[s] or [h]	residence time
τ_{shear}	[Pa]	shear forces
Φ	[-]	ratio of sieve hole area to tray active area

Subscripts

0	reference state
<i>av</i>	avoidable
<i>b</i>	baffles
<i>BM</i>	biomass
<i>cat</i>	catalyst
<i>ch</i>	chemical
<i>cold</i>	cold side fluid
<i>cryst</i>	crystallizer
<i>drain</i>	draining
<i>ex. loss</i>	external exergy losses
<i>fill</i>	filling
<i>fluid</i>	fluid
<i>g</i>	gas
<i>h</i>	heavy phase
<i>heads</i>	heat exchanger heads
<i>horiz.</i>	horizontal
<i>hot</i>	hot side fluid
<i>hyd</i>	hydraulic
<i>in</i>	incoming
<i>irrev</i>	irreversibility
<i>kin</i>	kinetic
<i>l</i>	light phase
<i>L</i>	liquid
<i>lb</i>	longitudinal baffles
<i>loss</i>	losses
<i>mat</i>	material
<i>max</i>	maximum
<i>min</i>	minimum
<i>mix</i>	mixing
<i>MS</i>	molten salt
<i>nozz</i>	nozzles
<i>N – source</i>	nitrogen source
<i>out</i>	outgoing
<i>overall</i>	overall
<i>p</i>	index for position of process unit in process
<i>P</i>	products
<i>ph</i>	physical

<i>plant</i>	entire production plant / modular equipment set
<i>pot</i>	potential
<i>PU</i>	process unit
<i>req</i>	required
<i>ref</i>	reference
<i>RM</i>	raw material
<i>s</i>	solid
<i>S</i>	substrate
<i>shell</i>	shell side
<i>T</i>	tubes
<i>t</i> or <i>tube</i>	tube side
<i>tb</i>	tube bundle
<i>tot</i>	total
<i>trod</i>	tie rods
<i>ts</i>	tubesheet
<i>unav</i>	unavoidable
<i>Uti</i>	utilities
<i>V</i>	vapor
<i>W</i>	work

Table of content

Acknowledgements	III
Abstract.....	IV
Zusammenfassung.....	V
List of Publications.....	VII
Declaration.....	XI
Nomenclature	XV
Table of content.....	XXI
List of figures	XXIII
List of tables	XXVII
1 Introduction and motivation	1
2 Scope of this thesis	7
3 State of the art	9
3.1 Determination of a plants' overall operating window	9
3.2 Preselection approaches to decide on the use of equipment modules for process units.....	10
3.3 Equipment module selection.....	11
3.3.1 Selection of equipment modules for a flexible modular production plant.....	12
3.3.2 Selection of equipment modules for capacity expansions.....	14
3.4 Equipment design for flexibility.....	16
4 Methods.....	19
4.1 Determination of a plants' operating window.....	19
4.2 Preselection approaches to decide on the use of equipment modules for process units.....	24
4.2.1 Preselection based on investment costs <i>Inv</i>	24
4.2.2 Preselection based on investment and operating costs <i>Inv&Op</i>	25
4.2.3 Preselection based on exergoeconomics <i>ExEco</i>	28
4.2.4 Evaluation of preselection approaches	33
4.3 Equipment module selection.....	34
4.4 Method to design equipment for flexibility	41
4.4.1 Mathematical model.....	42
4.4.2 Sampling generation.....	42
4.4.3 Determination of Cap_{min} , Cap_{max} and ΔCap	43
4.4.4 Global sensitivity analysis.....	43
4.4.5 Development of a two-step design approach	45
4.4.6 Deduction of design rules of thumb	46
4.5 Economic evaluation methods	46
4.5.1 Total capital investment (TCI)	46
4.5.2 Operating expenditures (OPEX)	47
4.5.3 Net present value (NPV).....	47
4.5.4 Equivalent annual annuity (EAA)	47
4.5.5 Modified internal rate of return (MIRR).....	48
5 Example processes	49
5.1 Styrene production process.....	49
5.2 Acetone production process.....	54
5.3 Fermentative succinic acid production	59

6 Applications.....	63
6.1 Determination of a plants' overall operating window	63
6.2 Preselection approaches to decide on the use of equipment modules for process units	65
6.2.1 Preselection based on investment costs <i>Inv</i>	65
6.2.2 Preselection based on investment and operating costs <i>Inv&Op</i>	66
6.2.3 Preselection based in exergoeconomics <i>ExEco</i>	67
6.2.4 Rating impact of using equipment modules on investment and operating costs.....	70
6.2.5 Evaluation of preselection approaches	71
6.3 Equipment module selection by evolutionary algorithm	74
6.3.1 Settings of evolutionary algorithm	74
6.3.2 Constant market demand	74
6.3.3 Market demand development.....	83
6.4 Design for flexibility	97
6.4.1 Development of the design approach and deduction of design rules of thumb	97
6.4.2 Evaluation of the design approach and the design rules of thumb for flexible shell and tube heat exchanger designs	108
7 Major achievements.....	115
8 Outlook & general conclusion	121
9 References.....	123
10 Appendix.....	133
Curriculum vitae	185

List of figures

Figure 1-1: Typical phases of a process and plant design project (durations adapted from [5–7])	1
Figure 1-2: General approach to module-based plant design [13]	3
Figure 1-3: Depiction of module-based plant design at equipment level - migration from sequence of process units to a modular equipment set.....	4
Figure 4-1: Depiction of individual operating constraints of HX6, R1 and C1 of the styrene production process example.....	20
Figure 4-2: Comparison of relationships between the plant's production rate and the values of operating constraints of different process units (@sp = at simulation point, equal to <i>Capfac</i> =1)	20
Figure 4-3: Exemplary operating constraint (shell side velocity of heat exchanger HX6) over different simulated production rates of the styrene production plant shown as capacity factor <i>Capfac</i>	22
Figure 4-4: <i>Inv</i> -approach - decision tree based on investment costs to decide on the use of equipment modules for process units (* critical CEX-value from [28])	25
Figure 4-5: Example consisting of three process units for the calculation of affected costs of <i>CRM</i> , <i>av</i> , <i>CUti</i> and <i>CTCI</i> according to the preselection approach <i>Inv&Op</i>	27
Figure 4-6: Decision tree for <i>Inv&Op</i> approach to decide on the use of equipment modules for process units (* critical CEX-value from [28])	28
Figure 4-7: Exemplary exergoeconomic cost balance for a system consisting of two process units (<i>C</i> – exergetic cost stream, <i>Z</i> – system costs stream)	30
Figure 4-8: Decision tree for <i>ExEco</i> approach to decide on the use of equipment modules for process units (* critical CEX-value from [28])	32
Figure 4-9: Scheme describing the evaluation of the preselection approaches by the distance of the Pareto fronts for the preselection approaches to case <i>Conv</i>	34
Figure 4-10: General framework to select equipment modules for modular equipment sets	35
Figure 4-11: Translation of the characteristics of the optimization problem to select equipment modules for modular equipment sets to the characteristics of a living organism in nature.....	36
Figure 4-12: Example for recombination and mutation operators.....	38
Figure 4-13: Working principle of the implemented SPEA to select equipment modules for modular equipment sets	38
Figure 4-14: Schematically illustration of the approach to determine the required expansion steps to follow a given market demand development.....	39
Figure 4-15: Exemplary stepwise capacity expansion strategy for a given market demand development.....	40
Figure 4-16: Graphical representation of the method to develop a design approach and deduce design rules of thumb for flexible equipment modules.....	41
Figure 5-1: Flowsheet of styrene production process (partly based on based on [84,85])	50
Figure 5-2: Flowsheet of acetone production process (based on [99]).....	56
Figure 5-3: Concentration profile for a serial reaction (modified from [107])	58
Figure 5-4: Reactor selectivity plotted over IPA-conversion	58

Figure 5-5: Comparison of reactor selectivity at different production rates for the conventionally designed reactor modules and the reactor modules with a larger operating window (dashed grey lines indicate lower selectivity operating constraint, <i>Capfac</i> = ratio of simulated production rate to a reference production rate)	59
Figure 5-6: Flowsheet of the fermentative succinic acid production process (partly based on process description of [115]).....	61
Figure 6-1: Comparison of operating windows of the process units based on the different determination approaches for the conventional design of the styrene case study (green bars: proposed correlation approach of this work, red bars: approach assuming an equal and linear relationship [23]) ...	64
Figure 6-2: TCI of process units of succinic acid production plant based on shortcut design	66
Figure 6-3: Exergetic losses of process units of the succinic acid production plant based on shortcut design.....	68
Figure 6-4: Exergoeconomic costs for process units of succinic acid production plant based on shortcut design.....	68
Figure 6-5: Pareto front of case <i>All</i> after 200 generations (blue rhombs) and conventional case <i>Conv</i> (black dot) (details of all Pareto-optimal modular equipment sets can be found in Table A.4-11)	70
Figure 6-6: Overall operating windows of case <i>Conv</i> (black) and Pareto-optimal modular equipment sets of case <i>All</i> (blue, numbered consecutively as shown in Table a.4-11 from left to right)	71
Figure 6-7: Final Pareto fronts of succinic acid case study after 200 generations (* annual TCI calculated with depreciation period of 10 years, details of all Pareto-optimal modular equipment sets can be found in Table A.4-11, the resulting overall operating windows are shown in appendix A.4.7)	72
Figure 6-8: TCI-distribution of grouped process units for the conventional design	75
Figure 6-9: TCI-distribution of all process units for the conventional design sorted by contribution	75
Figure 6-10: Evolution of Pareto front over the generations of Run3 (interpolated surfaces and projections to bottom area are used for a better visibility)	76
Figure 6-11: Pareto fronts after 250 generations for three independent optimization runs (interpolated surfaces and projections to bottom area are used for a better visibility).....	77
Figure 6-12: Two-dimensional view (TCI vs. Cap_{max}) of the three Pareto sets depicted as dots and the overall explored search space shown as interpolated area of the simulated operable modular equipment sets	77
Figure 6-13: Two-dimensional view (Cap_{min} vs. Cap_{max}) of the three Pareto sets depicted as dots and the overall explored search space shown as interpolated area of the simulated operable modular equipment sets	77
Figure 6-14: Two-dimensional view (TCI vs. Cap_{min}) of the three Pareto sets depicted as dots and the overall explored search space shown as interpolated area of the simulated operable modular equipment sets	77
Figure 6-15: All Pareto-optimal sets found within the three optimization runs till the 250 th generation (interpolated surfaces and projections to bottom area are used for a better visibility)	78
Figure 6-16: Operating windows of exemplary modular equipment sets of the different regions from the overall Pareto fronts.....	79
Figure 6-17: Approximation of the combined Pareto fronts of all three runs by 3 rd order polynomial according to Eq. 6-1 ($TCI_{conv, design} = \$ 15.8271536$ million, $A1 = 0.4045$, $A2 = -0.01902$, $A3 = 0.0003427$, $B1 = -0.4568$, $B2 = -0.0175$, $B3 = -0.0002307$)	80

Figure 6-18: Frequency of occurrence of the limiting process units to $Cap_{max,plant}$ and $Cap_{min,plant}$ for all Pareto sets and all simulated and operable sets without Pareto sets.....	82
Figure 6-19: Illustration of the general evaluation framework to compare the different capacity expansion strategies.....	84
Figure 6-20: Operating windows of all process units from the reference plant representing the conventional case.....	85
Figure 6-21: Distribution of total FOB costs for all process units of the reference plant	85
Figure 6-22: Comparison of conventional case to the 20 %- and 40 %-production lines regarding production rate (lines) and the overall TCI (dots)	87
Figure 6-23: Production rate and overall TCI of production lines (blue) and its corresponding equipment-wise capacity expansion strategy (green)	88
Figure 6-24: Pareto front of the equipment-wise capacity expansion strategies after the 200 th generation, highlighting ES1 with the lowest $TCl_{initial}$ and ES2 with the highest NPV	89
Figure 6-25: Production rate (lines) and overall TCI (dots) of modular equipment set ES1 (smallest $TCl_{initial}$) and modular equipment set ES2 (largest NPV)	89
Figure 6-26: Results of all expansion strategies in terms of the objectives $TCl_{initial}$ and NPV.....	91
Figure 6-27: Pareto fronts of equipment-wise capacity expansion strategies with conventional reactor modules and reactor modules with a larger operating window.....	92
Figure 6-28: Production rate (lines) and overall TCI (dots) of modular equipment set $ES_{LargeOpWin}$ (reactor modules with larger operating window) and modular equipment set ES2 (reactor modules designed for 90 % conversion).....	93
Figure 6-29: ES2 process units' operating windows after determining the required number of equipment modules to serve the market demand development at 70 kt/a.....	95
Figure 6-30: $ES_{LargeOpWin}$ process units' operating windows after determining the required number of equipment modules to serve the market demand development at 70 kt/a	95
Figure 6-31: Sketch of the methanol cooler example	97
Figure 6-32: Sensitivity indices and interaction effects regarding ΔCap , bars represent the mean of three runs, $N_{base} = 1023$ per run.....	100
Figure 6-33: Sensitivity indices and interaction effects regarding Cap_{min} , bars represent the mean of three runs, $N_{base} = 1023$ per run	100
Figure 6-34: Sensitivity indices and interaction effects regarding Cap_{max} , bars represent the mean of three runs, $N_{base} = 1023$ per run	101
Figure 6-35: Two-step approach to design flexible liquid/liquid shell and tube heat exchangers without phase change.....	102
Figure 6-36: Distributions of the values for the exchanger configuration NS, passNT, pass in the considered intervals of Cap_{min}	103
Figure 6-37: Distributions of the values for the shell diameter ds in the considered intervals of Cap_{min}	103
Figure 6-38: Distributions of the values for the tube OD do in the considered intervals of Cap_{min}	104
Figure 6-39: Distributions for the values of the tube length L in the considered intervals of Cap_{min}	105
Figure 6-40: Distributions of the values for the number of baffles Nb in the considered intervals of Cap_{min}	106
Figure 6-41: Distributions of the values for the tube pitch ratio PR in the considered intervals of Cap_{min}	106

Figure 6-42: Operating window of the shell and tube heat exchanger designed for flexibility with design parameters listed in Table 6-14	109
Figure 6-43: Comparative illustration of the operating windows of the designed shell and tube heat exchangers with $Cap_{min} = 100 - 200$ t/h	112
Figure 6-44: Comparative illustration of the operating windows of numbered-up conventional design and the shell and tube heat exchanger design for flexibility within $Cap_{min} = 100 - 200$ t/h	113

List of tables

Table 3-1:	Overview of works aiming at the selection of equipment modules.....	13
Table 3-2:	Works aiming at evaluating capacity expansion strategies	15
Table 3-3:	Works aiming to design equipment for flexibility	17
Table 4-1:	Used upper and lower operating constraints for different process units.....	23
Table 4-2:	Overview of investigated cases.....	24
Table 4-3:	Calculated affected costs for the exemplary process of Figure 4-5 according to the preselection approach <i>Inv&Op</i>	27
Table 5-1:	Kinetics of IPA dehydrogenation [99] and dehydration.....	55
Table 6-1:	Correlation exponents for the operating constraints of each process unit (conventional design case of styrene production plant)	63
Table 6-2:	Costs affected by using equipment modules per process unit of the succinic acid production plant based on the shortcut design	66
Table 6-3:	Mean absolute distances between TCI and OPEX of the modular equipment sets in the Pareto fronts with applied preselection approaches and the conventional production plant for the succinic acid case study.....	72
Table 6-4:	Parameters of evolutionary algorithm	74
Table 6-5:	Number and size of equipment modules of two equipment-wise capacity expansion strategies	90
Table 6-6:	Comparison of all expansion strategies by investment costs, NPV, EAA, MIRR and market satisfaction (PL = production line, EW = Equipment-wise)	91
Table 6-7:	Number and size of equipment modules of ES2 and ES _{LargeOpWin}	93
Table 6-8:	Adapted shell and tube heat exchanger design parameters and their possible values [122,126]	98
Table 6-9:	Considered operating constraints for liquid/liquid shell and tube heat exchangers without phase change [122,126]	99
Table 6-10:	Summary of influential design parameters on Cap_{min} , ΔCap and Cap_{max}	101
Table 6-11:	Recommended values for the selection of the exchanger configuration.....	104
Table 6-12:	Ratio of shell diameter to number of tube passes depending on Cap_{min} interval	105
Table 6-13:	Recommended values for the ratio B to select the number of baffles	107
Table 6-14:	Design parameters of the exemplarily designed shell and tube heat exchanger with a large operating window for a desired Cap_{min} -interval of 100 to 200 t/h.	109
Table 6-15:	Data of compared shell and tube heat exchangers for $Cap_{min} = 100 - 200$ t/h	111
Table 6-16:	Data of compared shell and tube heat exchangers for $Cap_{min} = 100 - 200$ t/h	113

1 Introduction and motivation

Applying a structured approach to design a chemical or biochemical production plant started around 100 to 130 years ago [1,2]. In 1901 the Englishman George E. Davis introduced the concept of ‘unit operations’ and later ‘unit processes’ which was coined by Arthur D. Little in 1915 [1,3].

Plant design today, as illustrated in Figure 1-1, is still based on the concept of unit operations and has not changed fundamentally. After product development, process design determines the best sequence of unit operations and characteristic equipment dimensions, resulting in a block diagram. Plant design is regarded as the realization phase which typically starts with a feasibility study where the technical, economic and financial feasibility of the most promising process must be demonstrated [4]. In this phase, the target production rate of the industrial plant is fixed. A typical document generated is the process flow diagram (PFD). If it is economical to realize the process as an industrial plant, the basic engineering phase follows, fully defining the plant and its functions in all components. This includes the detailed equipment dimensioning and the generation of the piping and instrumentation diagram (P&ID). Prior to commissioning, the technical data sheets are prepared during the detail engineering phase. Additionally, the P&ID is finalized, and the plant layout is accomplished, including a CAD model and the complete pipeline planning. Procurement, construction, start-up and operation complete the project execution phase. [5]

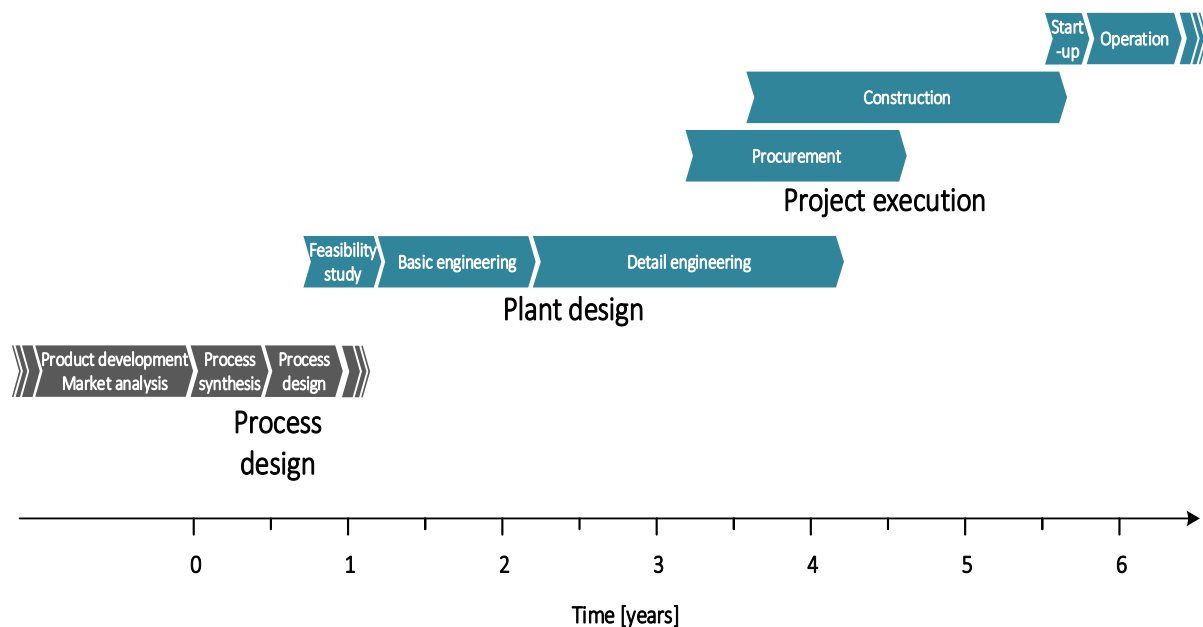


Figure 1-1: Typical phases of a process and plant design project (durations adapted from [5–7])

Within plant design, the design work is usually carried out by several specialized teams focusing on different unit operations, guided and controlled by project management [8].

Depending on size and complexity of the project, plant design can take typically two to four years [5].

The continuously increasing international competition and decreasing product life cycles in chemical and biochemical industry require a significant reduction in the time needed from a product idea to its introduction to the market [7]. Since plant design occupies much time and workforce, it is a potential lever to achieve a shorter time-to-market. To decrease the time for plant design, it is tried to speed up each individual step and to conduct as many parallel activities as possible [4,8]. Replacing the use of a pilot plant prior to production scale by miniplant technology to investigate for example a possible accumulation of components or the corrosion behavior of equipment, can lead to a reduction in costs and time within process and plant design [7,9]. However, although the economic environment changed from formerly steady and predictable markets [10] to volatile and unpredictable markets, a fundamental change in the plant design approach to decrease time and effort did not take place so far. Still, the requirements of each equipment are defined on an overall level and the equipment is specifically designed by corresponding unit operation experts. A verification, whether all the conventionally designed apparatuses work together as required, is most often performed on a simplified level of detail. Hence, the detailed design of an equipment is done decoupled from the detailed design of the other equipment.

To cope with the increasing uncertainty in market demand and its development, modern plant design

- needs to be accelerated and
- needs to aim at flexibility in production rate or adaptability to a market demand development.

A faster plant design can be achieved by using apparatuses off-the-rack, called equipment modules, to set up a production plant [11,12]. The detailed and time-consuming design of equipment tailored for a specific application is replaced by a selection and configuration of predefined modules. This approach is called module-based plant design. Simultaneously, equipment module selection can be performed with the objective of a large operating window or incorporating a market demand development over time to cope with the increasing uncertainty of market demand developments. Besides saving the time required for a tailored design of equipment, the reuse of equipment module designs or physical equipment modules offers additional cost saving potential.

Within module-based plant design, modules are defined as unmodifiable, project-independent and reusable elements [13]. By applying module-based plant design, the same essential planning documents as in conventional plant design are created like PFD, P&ID, technical data sheets, and a 3D-layout. 'Modular' is thereby regarded as an assembly of two

or more modules [14]. The general approach to module-based plant design developed together with colleagues as part of this work is shown in Figure 1-2. The starting point is set by the block diagram (BD) with additional information according to ISO 10628-1 [15] representing the best sequence of unit operations as well as results from lab experiments.

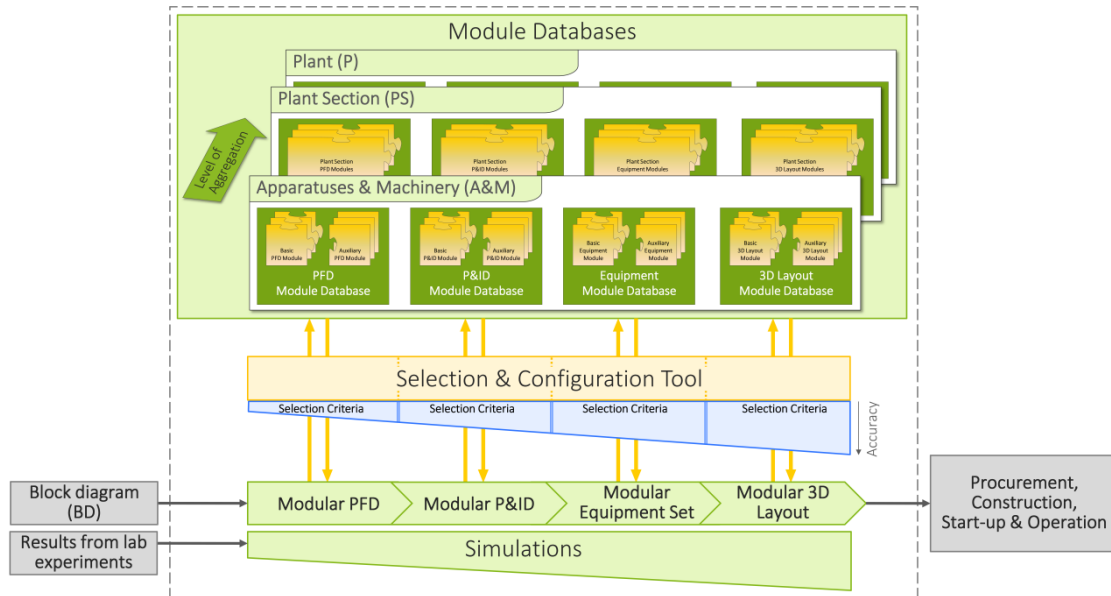


Figure 1-2: General approach to module-based plant design [13]

To accomplish each of the four sequential major design tasks from a *Modular PFD* via the *Modular P&ID* and the *Modular equipment set* to a *Modular 3D layout*, modules are selected from the corresponding module databases. Process simulation supports module selection, whereby the level of detail and accuracy is increasing over the different design tasks. When no suitable modules are available, it is possible to complete the design steps for specific blocks in particular design tasks conventionally. A key advantage of module-based plant design rarely recognized so far is the availability of detailed information about the modules from the module databases right from the beginning of plant design. Hence, an operability check or a detailed cost estimation can be performed earlier and with an increased precision. In conventional plant design, this information is gained by time-consuming engineering effort.

One of the most challenging and complex tasks in module-based plant design is the equipment module selection to get a modular equipment set. This task is referred to module-based plant design at equipment level and aims at setting the detailed equipment specifications of a modular production plant. Hence, it is a way to migrate from a process design as a sequence of process units applying physical and chemical changes to a modular production plant, called modular equipment set, consisting of single or multiple equipment modules for each process unit as depicted in Figure 1-3. The type of equipment is specified

(i.e. a tubular fixed-bed reactor or a shell and tube heat exchanger with fixed tubesheets) and the suitable design of the equipment (i.e. length, diameter, number of tubes), the specific equipment module(s), must be selected. As exemplarily depicted in Figure 1-3, two shell and tube heat exchanger modules HX-4 with a specified tube length, tube diameter, number of tubes, etc. have been selected for Process Unit I and one tubular fixed-bed reactor module R-2 has been selected for Process Unit II. The utilization of multiple equipment modules for a process unit is also often called numbering-up.

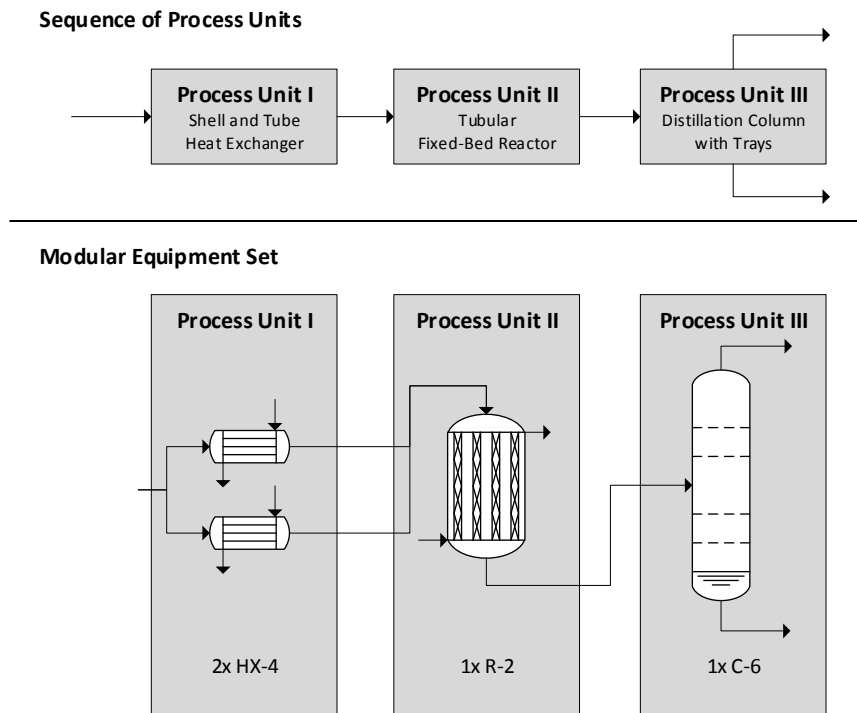


Figure 1-3: Depiction of module-based plant design at equipment level - migration from sequence of process units to a modular equipment set

The detailed design parameters stored for each equipment module in the equipment module database enable an equipment module selection based on rigorous and detailed simulation models. This allows to verify in detail whether one or multiple equipment modules for a process unit are operable within the overall plant considering for example the process task and hydrodynamics. The operating windows of the individual process units are determined by specific operating constraints of each process unit, for example by fluid velocity limitations in heat exchangers or by flooding and weeping conditions described by an F-factor in distillation columns. The detailed and rigorous simulation models allow to determine the values of the operating constraints of a process unit based on the design parameters of the selected equipment module(s). The resulting operating window of a process unit can be described by the capacity range in which the process unit is operable,

whereas the lower limit is called $Cap_{min,PU}$ and the upper limit $Cap_{max,PU}$. This operating window can be expressed as a percentage related to the target production rate of the plant. When a plant shall produce for instance 100 kg/h and an operating window of a process unit of that plant is determined to -2 % to +7 %, this process unit can operate between 98 kg/h and 107 kg/h. Utilizing numbering-up can change the operating window in two ways. If two equipment modules of the same size are used instead of one, the corresponding operating window of that process unit can be increased. Using two smaller equipment modules instead of a single equipment module also allows to realize smaller production rates. The operating window of the entire plant results from the range of production rates at which all operating windows of a modular equipment set overlap and is described by $Cap_{min,plant}$ and $Cap_{max,plant}$. However, the detailed design parameters that come along with each equipment module pose also a major challenge for module-based plant design at equipment level, since equipment modules need to be selected for all process units simultaneously to account for interactions resulting in a high complexity.

Due to its key role and importance within module-based plant design, this thesis focuses on module-based plant design at equipment level. By utilizing detailed design parameters of the equipment modules for an entire plant, the investigations are beyond solely economic considerations to investigate and judge on module-based plant design.

Hence, the aim of this thesis is to provide methods for and insights to important areas of module-based plant design at equipment level contributing to a paradigm shift in plant design.

2 Scope of this thesis

Usually, the operating window is not a key part in conventional plant design, whereas it plays an essential role in module-based plant design at equipment level. The operating window of a process unit cannot be determined a priori solely based on the design parameter values of an equipment module, because information on the process stream(s) that are processed in the corresponding equipment module, e.g. its composition and properties, are required to determine it. Additionally, the often non-linear relation of the process units' operating constraints to the production rate of the plant, as for example for the velocity in a heat exchanger, needs to be considered. Since determining the operating window of the individual process units and an entire modular equipment set is a basic requirement of module-based plant design at equipment level, it is the first objective of this work.

Furthermore, equipment modules off-the-rack are not designed specifically to the application of a process task and the requirements of a corresponding process unit in a process. Depending on the process unit and the overall plant, the use of equipment modules might have a high impact on the costs for certain process units. Hence, using equipment modules off-the-rack should be avoided for process units if the use of non-tailored apparatuses results in a strong cost increase. A suitable preselection approach to identify process units that show a high impact on costs when using equipment modules sets the second objective of this work.

The third objective is the development of a general methodology to enable a multi-objective selection of equipment modules for modular production plants. This multi-objective equipment module selection approach will be utilized to evaluate the potential of module-based plant design at equipment level. On the one hand, the trade-off between investment costs and flexibility in production rate to cope with market induced fluctuations will be investigated. On the other hand, equipment module selection for a changing market demand development will be explored to find the best trade-off solutions between initial investment risk and adaptability by stepwise capacity expansions.

The investigation of capacity expansion strategies reveals that equipment modules designed for flexibility offer significant advantages. The larger operating window leads to less expansion steps required and avoids a gap in the operating window by numbering-up. This results in the fourth objective of this work, the development of a generally applicable and simple method to design equipment modules for flexibility.

In essence, this work tackles four major areas in the field of module-based plant design at equipment level:

- (1) The determination of a plants' overall operating window
- (2) Preselection approaches to decide on the use of equipment modules for process units
- (3) The selection of equipment modules and investigation of trade-offs
- (4) The design of equipment modules for flexibility

The following chapters 3.1 to 3.4 give an overview of the state of the art for each of the four areas that are investigated. Afterwards, the methods developed for each of the four areas are introduced in the chapters 4.1 to 4.4 and chapter 4.5 introduces the economic indicators used for evaluation. Details of the three example processes, their implementation in Aspen Plus®V8.4 and the generation of the equipment module database will be described in chapter 5. The application results of the methods developed are shown and discussed for the four investigation areas in the chapters 6.1 to 6.4. Finally, the major achievements are summarized in chapter 7, before an outlook is given and a general conclusion is drawn in chapter 8.

3 State of the art

This chapter gives an overview of the current state of the art for each of the four major areas that are investigated in this work. Each area is first characterized, the challenges are summarized and the requirements to address these challenges are stated. Key works that tried to address the challenges are cited and it is described where they have fallen short. Finally, the gap bridged by this thesis is identified.

3.1 Determination of a plants' overall operating window

The determination of a plants' operating window is a basic requirement for equipment module selection in module-based plant design at equipment level, since it is necessary to check the plants' operability. Moreover, the overall operating window can be used as equipment module selection objective for example to realize a modular plant with a large operating window.

Two main challenges, already mentioned decades ago in 1964 by Coleman and York [16], arise when determining the plants' overall operating window:

- (i) A design dependency between the process units exists.
- (ii) The capacity of a process unit may not be a linear function of the plants' production rate.

By design dependency it is meant that the design of a single process unit directly affects the design of other process units of the process due to an interconnection of all process units via continuous material and energy streams. Although it needs to be looked at the other way round in module-based plant design, since the design is given by the equipment modules and the operating window is to be determined, the design dependency is valid. Recently Bruns et al. [17] investigated and proved this design dependency. To take the design dependency into account, it is necessary to determine the operating window of a single process unit in context of all other process units. Hence, the entire modular equipment set needs to be considered. To account for the often non-linear relationship between capacity of a process unit and production rate of a plant, a detailed process simulation that allows to determine the specific process-technological and mechanical operating constraints is required.

A widespread approach to evaluate flexibility, and thus the operating window of a process or an equipment design is based on the flexibility index introduced by Grossmann et al. [18–22]. The focus of these works lies in the quantification and evaluation of the operating window in different dimensions. Since the approach is based on solving non-linear programming (NLP) or mixed integer non-linear programming (MINLP) formulations, it becomes impractical and

difficult to solve considering detailed equipment designs including the large number of discrete design parameters for an entire plant. Seifert [23] proposed an approach to determine the operating windows of the individual process units based on process-technological and hydraulic operating constraints considering the entire modular equipment set. However, he assumed an equal and linear relationship between the plants' production rate and the different operating constraints of each process unit. Hence, Seifert mastered the design dependency, but neglected the often non-linear dependency of the process units' operating constraints on the production rate of the plant.

Many other authors who investigate module-based plant design at equipment level either neglect the operating windows and focus on economic considerations only or they assume fixed operating windows [16,24–35].

It can be summarized that an approach to determine the plants' operating window considering the design dependency and the often non-linear relationship between the capacity of a process unit and the production rate of a plant is currently not available. Thus, this work will close this gap and set the basis for module-based plant design at equipment level by an approach that determines the plants' overall operating window taking the design dependency and the non-linear relation into account.

3.2 Preselection approaches to decide on the use of equipment modules for process units

Since equipment modules are not tailor-made, costs might increase by module-based plant design. If the use of non-tailored apparatuses results in a strong cost increase for a process unit, using equipment modules off-the-rack should be avoided. So far, there has been extensive work on the impact of using equipment modules on investment costs, for instance by [12,23,28,36,37], because fixed budgets are authorized for planning and designing a production plant. The impact of using multiple equipment modules for a process unit on investment costs is thereby determined based on Eq. 3-1 [38]:

$$C = C_{ref} \cdot \left(\frac{size}{size_{ref}} \right)^{CEX} \quad \text{Eq. 3-1}$$

The cost-capacity-exponent *CEX* reflects the relationship between investment costs *C* and the characteristic size *size* of different process unit. The smaller the *CEX*, the more expensive it is to use multiple or smaller equipment modules for a process unit compared to using a single large equipment module. In particular, Oldenburg et al. [28] used this in combination with a product sales forecast to decide between gradually increasing the installed capacity or building a large capacity at once. Based on the same idea, Seifert et al. [36] and Seifert

[23] analyzed modular equipment sets by the share of overall investment costs of process units and its *CEX*-values. They evaluated whether equipment modules can be used without the risk of a large cost increase. Another preselection approach that is limited to investment costs based on Eq. 3-1 was proposed by Seifert [23]. Assuming the number of equipment modules used for a process unit to be lower than five, Seifert introduced the so-called Investment Cost Factor *ICF*. The *ICF* combines the proportion of a process unit's share on the overall investment costs and the economy of scale by the *CEX*-value of a process unit, describing the increase in total cost of investment *TCI* when multiple equipment modules are used for a process unit. Process units with a large *ICF* have a high impact on the investment costs.

One key drawback of the aforementioned approaches is that, when an equipment module for a process unit is not tailor-made to meet its specific requirements, operating costs will be affected as well, since the equipment module operates away from its design point. Thus, investment as well as operating costs must be considered when deciding on the use of equipment modules for process units.

This work will introduce, apply and evaluate two preselection approaches that consider both, investment and operating costs, whereby one is based on investment and operating costs directly and the other is based on exergoeconomics. These preselection approaches are compared to a preselection approach that is solely based on investment costs.

3.3 Equipment module selection

A basic requirement for equipment module selection is a proper determination of the operating window of each process unit and the entire modular equipment set. The design dependency and the often non-linear relationship between the plant's production rate and the operating constraints that limit the operating window of each process unit need to be considered. Furthermore, the size and number of the equipment modules that need to be selected for each process unit lead to many discrete variables. Hence, the exchange of equipment modules for process units results in a discrete and non-monotonic search space. This leads to an optimization problem that is hard to solve for entire production plants.

In the following, a literature review on equipment module selection in light of two different goals will be given:

- (i) Equipment module selection for a constant market demand and the goal of flexibility in production rate
- (ii) Equipment module selection for a changing market demand development with the goal of adaptability by sequential capacity expansion steps

3.3.1 Selection of equipment modules for a flexible modular production plant

An overview of works aiming at selecting equipment modules for a flexible modular production plant is summarized in Table 3-1. Goyal and Ierapetritou [25] select standardized designs based on a demand plot and a clustering approach by solving a MINLP optimization problem. Detailed equipment design parameters are not included, and the flexibility of the designs is not determined consequently by process-technological or mechanical operating constraints of the process units. Additionally, no selection of equipment module sizes and numbers is included. Later Goyal and Ierapetritou extended their approach to a multi-objective selection including costs, model robustness and solution robustness [26]. Sirdeshpande et al. [27] applied a similar approach based on a MINLP optimization to select standardized designs, but suffer from the same shortcomings as Goyal and Ierapetritou. In summary, all three works are more focused on process synthesis rather than on equipment module selection taking into consideration equipment module sizes and numbers. Harwardt et al. [32] use a superstructure-based MINLP approach to select equipment sizes for a distillation column and the required condenser and the reboiler area from discrete values. The total annualized costs are used as objective for the selection of the equipment sizes. Their approach is very promising, although it does not consider detailed design parameters for the heat exchangers and flexibility is not considered as objective. Additionally, the resulting MINLP becomes difficult to solve when selecting equipment modules for an entire production plant. A workflow for equipment module selection for an entire plant is proposed by Seifert et al. [39] using a 'module design space' which is a fixed operating window of the equipment modules and a 'process design space' defined by the user. Based on reference sizes for the processing units determined by a shortcut design, Seifert et al. select different equipment module sizes for each process unit by hand. 'Crucial' process units that influence the operation of other process units like a membrane separator upstream of a mixer-settler extraction, are excluded from module selection and flexibility is not considered. Seifert [23] used a multi-objective evolutionary algorithm to select equipment modules for a large volume flexibility (VF) at low investment costs. However, the VF used as objective is unspecific and does not describe the flexibility in production rate of a plant. Using VF as objective favors enlarging the lower capacity limit. Thus, Seifert did not investigate the trade-off between flexibility in production rate at low investment costs.

Table 3-1: Overview of works aiming at the selection of equipment modules for a flexible modular production plant

Ref.	Approach	Shortcomings
[25–27]	Selection of standardized designs by solving a mixed-integer nonlinear programming (MINLP) model	<ul style="list-style-type: none"> - no detailed equipment design parameters are considered - flexibility not determined consequently by process-technological or mechanical operating constraints of the single process units - no selection of equipment module sizes and numbers
[32]	Superstructure-based MINLP approach to select discrete equipment sizes for a distillation column and corresponding condenser and reboiler areas	<ul style="list-style-type: none"> - does not consider detailed design parameters for the heat exchangers - resulting MINLP becomes difficult to solve when selecting equipment modules for an entire plant
[39]	Workflow-based equipment module selection by hand for an entire plant using a ‘module design space’ and a ‘process design space’	<ul style="list-style-type: none"> - selection by hand - reference sizes needed for selection - process units that influence other process units are excluded from module selection - flexibility not considered
[23]	Automated selection by a multi-objective evolutionary algorithm using volume flexibility (VF) as objective	<ul style="list-style-type: none"> - volume flexibility (VF) as flexibility objective is unspecific and does not describe flexibility in production rate of a plant - operating constraints are related linearly to production rate of the plant - implemented multi-objective evolutionary algorithm is a kind of a blind search considering also non-operable modular equipment sets

The key drawback is the assumption of an equal and linear relationship between the plants’ production rate and the operating constraints of each process unit. This has a large influence on the resulting operating window of the overall plant as will be shown in chapter 6.1. Lastly, the implemented multi-objective evolutionary algorithm was a kind of a blind search considering also non-operable modular equipment sets. This was compensated by a very large population size and by merging the results of several optimization runs into a single Pareto front.

It can be summarized that a working approach to select equipment modules for an entire modular production plant that identifies trade-off solutions between flexibility in production rate and additional investment costs is not available. A promising approach for equipment module selection is given by the work of Seifert [23].

In contrast to the approaches mentioned, this work introduces an approach to select equipment modules of different sizes and numbers for an entire modular production plant to identify trade-off solutions between flexibility in production rate and additional investment costs. A detailed process simulation enables the determination of the process-technological and mechanical operating constraints of each process unit considering

detailed equipment design parameters. A key improvement is the consideration of the often non-linear relationship between the operating constraints of the process units to the production rate of the entire plant. This allows the identification and investigation of trade-off solutions between flexibility in production rate and additional investment costs.

3.3.2 Selection of equipment modules for capacity expansions

Basically, there are two options for sequential capacity expansion strategies in light of a changing market demand development:

- (i) Line-wise capacity expansions
- (ii) Equipment-wise capacity expansions

In case of line-wise capacity expansions, an entire copy of the plant is added when a single process unit reaches its maximum capacity. This already gives a certain adaptability to a growing market demand and reduces the investment risk but results in idle capacities of the process units that do not limit the operating window of the entire plant. In contrast, these idle capacity potentials are utilized in case of equipment-wise capacity expansions, where only limiting process units are expanded. Different works aiming at evaluating capacity expansion strategies for chemical production plants, for both, line- and equipment-wise capacity expansions, are summarized in Table 3-2. Works investigating line-wise capacity expansion strategies are for example [30,31,33,35]. The focus lies on an economic investigation while neglecting the individual operating constraints of the process units that determine their operating window.

The early work by Coleman and York [16] investigates equipment-wise capacity expansion strategies. Based on the cost capacity exponent they proposed a solely economic consideration of sequential capacity expansions for a growing market. Ishii et. al [24] proposed an iterative heuristic procedure to adapt the plant's capacity to the market development based on the profile of opportunity costs to decide whether an equipment-wise capacity expansion is suitable or not. It was shown that the overall profitability increases when a stepwise capacity expansion is taken into account. However, it is an economic consideration only, assuming that $Cap_{max,PU}$ is known a priori and constant and $Cap_{min,PU}$ is not taken into account. Other works proposing an investment planning model for the development of equipment-wise capacity expansion strategies [28,29] assumed a linear relationship between the minimum and maximum capacities of the process units and the production rate of the entire plant. Instead of considering the individual operating constraints of the process units, specific operating ranges for some of the process units are assumed.

Table 3-2: Works aiming at evaluating capacity expansion strategies for chemical production plants

	Ref.	Contribution	Shortcomings
Line-wise capacity expansion	[30,31]	Showed that line-wise capacity expansion can improve profitability	<ul style="list-style-type: none"> - economic consideration only - no consideration of process units' operating constraints
	[33]	Comparison of line-wise expansion strategies using different cost capacity exponents and learning rates	<ul style="list-style-type: none"> - economic consideration only - expansion steps are fixed by decision rules - no consideration of process units' operating constraints
	[35]	Investigated expansion strategies of small scale continuously operated modular multi-product plants based on a decision tree analysis	<ul style="list-style-type: none"> - no operating windows considered
Equipment-wise capacity expansion	[16]	Investigated the minimum present value of total costs for a single equipment at different demand growth rates	<ul style="list-style-type: none"> - economic consideration only
	[24]	Iterative heuristic procedure to adapt plant capacity to the market demand development based on the profile of opportunity costs by equipment-wise capacity expansion steps	<ul style="list-style-type: none"> - economic consideration only - assume that $Cap_{max,PU}$ is known and fix - do not consider $Cap_{min,PU}$
	[28,29]	Investment planning model for the development of stepwise capacity expansion strategies	<ul style="list-style-type: none"> - no consideration of process units' operating constraints - $Cap_{min,PU}$ & $Cap_{max,PU}$ are assumed and related linearly to production rate of the entire plant
	[34]	Iterative framework based on a mixed-integer linear programming (MILP) model to find optimum capacity plan for a production plant	<ul style="list-style-type: none"> - no consideration of the process units' operating constraints
	[36,40,41]	Showed that equipment-wise capacity expansion can improve profitability	<ul style="list-style-type: none"> - used shortcut calculations - conversion and selectivity in reactor are fixed - operating constraints are related linearly to the production rate of the plant
	[23]	Used an evolutionary algorithm to find modular equipment sets for different market demand developments minimizing the total cost of investment (TCI) and maximizing the net present value (NPV)	<ul style="list-style-type: none"> - operating constraints are related linearly to the production rate of the plant - implemented multi-objective evolutionary algorithm is a kind of a blind search considering also non-operable modular equipment sets

An iterative framework based on a mixed-integer linear programming (MILP) model to find the optimum capacity plan for a production plant, neglecting the operating constraints of each process unit is proposed by Geraili et al. [34]. The works of Seifert et al. showed that equipment-wise capacity expansion can improve profitability of the plant [36,40,41]. However, they have used shortcut calculations and the operating constraints were related linearly to the production rate of the plant. Additionally, in [36] the conversion and selectivity

in the reactor are assumed to be constant over different production rates. In his doctoral thesis Seifert used an evolutionary algorithm to select equipment modules for modular equipment sets considering a market demand development with the objectives of minimizing the TCI and maximizing the NPV [23]. The key drawback in the work of Seifert is the determination of the operating window of the entire modular equipment sets and the implemented multi-objective evolutionary algorithm as described in the previous chapter already.

It can be summarized that a proper determination and comparison of different capacity expansion strategies for chemical production plants to quantify the compromise between additional initial investment and a good adaption to a demand development is not available so far. To the authors knowledge, no work compared the conventional design approach, building a large capacity at once to profit from economy of scale effects, to a line-wise capacity expansion strategy as well as an equipment-wise capacity expansion strategy. Additionally, most of the works mentioned performed a purely economic evaluation without a detailed process simulation and thus neglecting the operating constraints of the individual process units. A promising idea to determine the best equipment sizes and the best time of an equipment-wise expansion was given by the work of Seifert [23], but a proper determination of the plant's operating window, which influences the required expansion steps, is missing, as well as a comparison to a line-wise capacity expansion strategy.

In contrast to the approaches mentioned, this work shows a comparison of different capacity expansion strategies for chemical production plants to quantify the compromise between additional initial investment and a better adaptability to a demand development considering the process units' operating constraints. On top of that, reactors designed for a larger operating window are investigated in light of equipment-wise capacity expansion, offering important advantages that will be demonstrated and discussed.

3.4 Equipment design for flexibility

Design parameters of equipment such as for example diameters and lengths are predominantly discrete due to the nature of the manufacturing process for tubes or metal sheets. Hence, a lot of discrete design parameters that influence the operating window need be selected when designing equipment for flexibility in production rate. A method to design equipment for flexibility should consider all design parameters that need to be selected. Additionally, it should be structured, generic and easy to apply. This turns optimization-based approaches to be impractical for a detailed design considering all, mostly discrete, design parameters. Different works aiming to design equipment for flexibility are summarized in Table 3-3.

Table 3-3: Works aiming to design equipment for flexibility

Ref.	Contribution	Shortcomings
[18–22]	Optimization-based evaluation of flexibility for a given design by flexibility index (can be used to take redesign actions)	<ul style="list-style-type: none"> - more an evaluation than a design method - can become impractical and difficult to solve for a detailed design including many discrete design parameters
[42]	Optimization-based design strategy using a flexibility factor	<ul style="list-style-type: none"> - prior flexibility analysis is required
[43]	Evaluation and consideration of flexibility within design approach by flexibility map	<ul style="list-style-type: none"> - one-at-a-time analysis - transfer of concept to equipment with larger number of design parameters is impractical

A widespread approach to evaluate the flexibility of a process or an equipment design is based on the flexibility index [18–22]. These works focus on the quantification and evaluation of flexibility in different dimensions, rather than on the design of equipment. Hence, they cannot be considered as design approach, although the resulting evaluation of flexibility of a design can be used to take redesign actions. Furthermore, the approach to evaluate the flexibility is based on solving NLP or MINLP formulations which can become impractical and difficult to solve when considering a detailed design of equipment including many discrete design parameters. Hoch and Eliceche [42] go a step further by introducing a design strategy based on a prior flexibility analysis. Sudhoff et al. [43] suggest a graphical tool called ‘flexibility map’ which they use in a design approach for rotating packed beds for distillation. This approach is easy to understand and apply due to its graphical depiction. However, it is based on a one-at-a-time analysis of the design parameters which makes the approach impractical when applying it to other types of equipment with a larger number of design parameters. A way to simplify optimization-based equipment design approaches is a preceding global sensitivity analysis to reduce the number of parameters. An example is the work of Fesanghary et al. [44], who apply a global sensitivity analysis prior to an economic design optimization for a heat exchanger.

It can be summarized that a method to design equipment for flexibility that considers all design parameters in a structured, generic and easy to apply way is not available so far.

In contrast to the approaches mentioned, this work introduces a method for detailed equipment design including all design parameters with the aim of increased flexibility in terms of production rate. This method is based on a global sensitivity analysis to develop a two-step design approach. Additionally, design rules of thumb are deduced by an analysis of the sampling results to enable a quick design of flexible equipment.

4 Methods

The following chapter describes the methods developed in the scope of this work for each of the four major areas investigated. Additionally, section 4.5 introduces five economic indicators required to apply, evaluate and compare the methods developed.

4.1 Determination of a plants' operating window

An appropriate determination of the plants operating window is of utmost importance in module-based plant design at equipment level, because it is used to ensure operability and hence sets the basis for equipment module selection. As described in chapter 3.1, the challenge is to consider the design dependency and the often non-linear relationship between the operating constraints of a process unit and the overall production rate of the plant.

To illustrate this challenge, details of the styrene production process example are anticipated (see chapters 5.1 and 6.1 for details) and heat exchanger HX6, reactor R1 and distillation column C1 of the styrene production process example are considered. Each process unit has its specific operating constraints. In case of the heat exchanger this is for example the velocity on the shell side. The pressure drop might be an operating constraint of the reactor and the operation of the column might be limited by the F-factor with its boundaries of flooding and weeping. To determine the operating windows of the three process units within the entire process, a simulation is performed at a certain production rate. Based on the resulting shell side velocity of HX6, the pressure drop in R1 and the F-factor of C1 at the simulated production rate, the distance to the minimum and maximum values of the corresponding operating constraint limits to the simulation point can be determined. The resulting individual operating windows of the process units are shown in Figure 4-1 for a simulated production rate of 2500 kg/h. The column can for example operate between -22 % and +54 % of its F-factor at the simulated point. A lower operating boundary is determined for the heat exchanger in terms of the minimum shell side velocity and for the reactor in terms of the pressure drop to -16 %, respectively. Such a representation could lead to the conclusion that the overall operating window of these three process units ranges from -16 % to +54 %. However, this is a false perception because it relates the different operating constraints such as the velocity, the pressure drop and the F-factor in a linear and equal way to the production rate of the plant. Previous works like [23] implicitly assumed such a linear and equal relationship between the plant's production rate and all operating constraints of each process unit. To explain and demonstrate why this assumption is

incorrect, the relationship between the different operating constraints to the production rate of the plant is investigated in more detail.

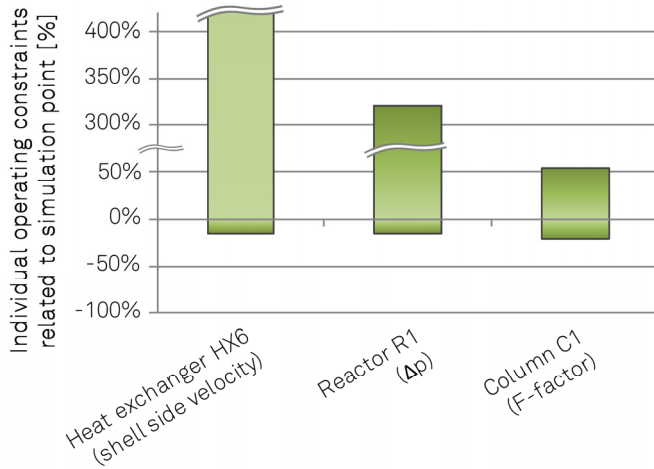


Figure 4-1: Depiction of individual operating constraints of HX6, R1 and C1 of the styrene production process example

Therefore, different production rates are simulated, and the resulting values of the specific operating constraints are observed. The production rate of the styrene production process example is varied in 5 %-steps from 60 % to 120 % of the target production rate of 2500 kg/h. The values of the operating constraints as the shell side velocity of the heat exchanger HX6, the pressure drop of reactor R1 and the F-factor of column C1 are plotted in Figure 4-2 in relative scale to the simulation point. All three operating constraints can serve as minimum and maximum operating constraint (cf. Table 4-1). The relative scale of the plants' production rate on the x-axis is described by the capacity factor of the plant Cap_{fac} , which is the ratio of a production rate to the production rate at the simulation point (sp), where $Cap_{fac} = 1$. The operating constraints on the y-axis are displayed as ratio of the operating constraint values at different Cap_{fac} -values to the operating constraint value at the simulation point (@sp).

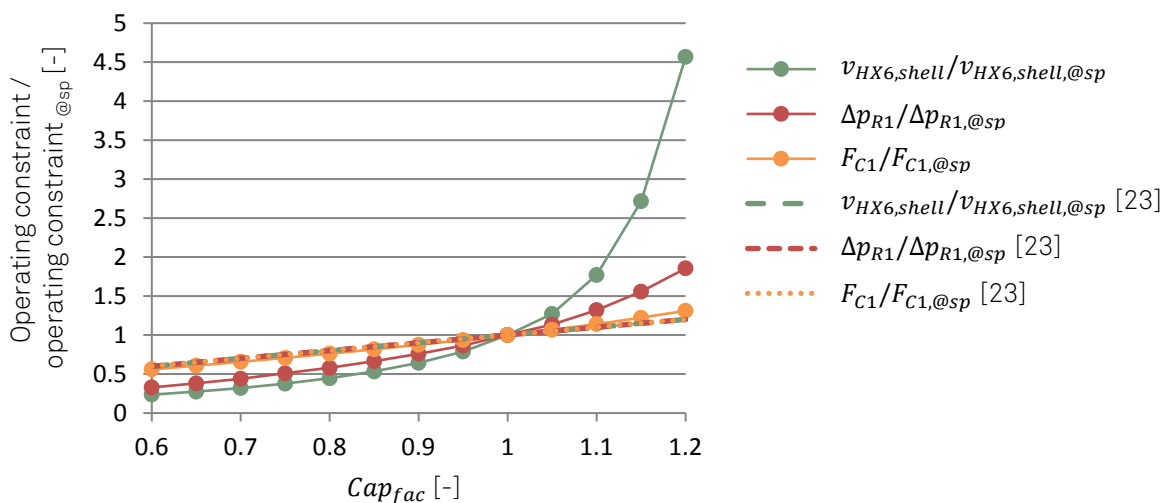


Figure 4-2: Comparison of relationships between the plant's production rate and the values of operating constraints of different process units (@sp = at simulation point, equal to $Cap_{fac} = 1$)

The dots interpolated by a solid line in Figure 4-2 show the resulting relationships between the plants' production rate and the different operating constraints of the process units based on the process simulations. It is evident that the relationships are not linear. Furthermore, they are not changing equally with the production rate of the plant. Assuming a linear and equal relationship results in the dashed lines. They are identical for all three operating constraints considered, meaning that the same relationship between the plants' production rate and the values of the operating constraints of each process unit is assumed. In case of the F-factor the difference, and hence the non-linearity, might be negligible, but for the pressure drop in the reactor and the velocity in the heat exchanger, they are not.

This investigation shows that a new approach to determine the operating window of a plant is required. A possible approach to tackle this challenge is an iterative bisection-approach to determine $Cap_{min/max,PU}$ in terms of the plant's production rate. However, this is too costly in simulation time. Therefore, a correlation approach using a power function for each operating constraint of each process unit to the production rate of the plant is proposed in this work to approximate the non-linear relationships between the process units' operating constraints and the production rate of the plant. A constraint for the approximation function is that the correlation matches the operating constraint values at the simulation point in order to accurately depict the region around the target production rate of the plant. To illustrate how the process units' operating constraints can be related to the production rate of the plant, the shell side velocity of heat exchanger HX6 is used as an example. The entire production plant is simulated over a range of production rates. Next, the values of the operating constraint 'shell side velocity' for each of the simulated production rates are plotted, as shown by the black dots in Figure 4-3. The lower limit of $v_{HX,shell,min} = 0.6$ m/s, which is the minimum velocity to avoid fouling, is depicted as red dashed line. The implicitly assumed linear dependency as in [23] is shown by the grey line and the correlation approach introduced in this work by the green line. The difference in the determined $Cap_{min,HX6}$ between the assumed linear dependency and the correlation approach of this work is visible by the different Cap_{fac} -values where the respective curve is crossing the minimum shell side velocity of 0.6 m/s with 0.85 and 0.98, respectively. This difference results in a $Cap_{min,HX6}$ of 85 % for the assumed linear dependency and of 98 % for the correlation approach of this work. Hence, the determined lower boundary of the operating window differs by 13 %. How the correlation approach of this work is derived is explained in the following.

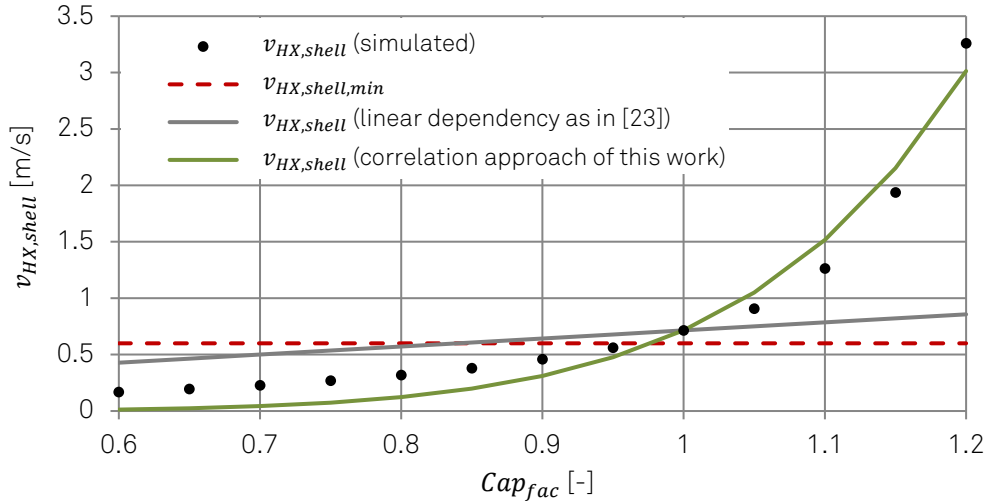


Figure 4-3: Exemplary operating constraint (shell side velocity of heat exchanger HX6) over different simulated production rates of the styrene production plant shown as capacity factor Cap_{fac}

To account for the non-linear behavior of the shell side velocity over the different simulated production rates, the shell side velocity is approximated by a power function with Cap_{fac} as shown in Eq. 4-1 by adjusting the correlation exponent α .

$$v_{HX,shell @Cap_{fac}} = v_{HX,shell @Cap_{fac}=1} \cdot (Cap_{fac})^{\alpha} \quad \text{Eq. 4-1}$$

$v_{HX,shell @Cap_{fac}}$ represents the shell side velocity of the heat exchanger at different capacity factors Cap_{fac} and $v_{HX,shell @Cap_{fac}=1}$ at the simulation point.

The minimum capacity of the plant $Cap_{min,plant}$ in terms of the production rate of the plant \dot{m}_{plant} is in general determined by Eq. 4-2:

$$Cap_{min,plant} = \frac{\dot{m}_{plant,min}}{\dot{m}_{plant,@sp}} \quad \text{Eq. 4-2}$$

To determine $Cap_{min,plant}$ in terms of \dot{m}_{plant} , the definition of Cap_{fac} and a rearrangement of Eq. 4-1 can be used as shown below:

$$Cap_{fac} = \frac{\dot{m}_{plant @Cap_{fac}}}{\dot{m}_{plant,@sp}} = \left(\frac{v_{HX,shell @Cap_{fac}}}{v_{HX,shell,@sp}} \right)^{\frac{1}{\alpha}}$$

This rearrangement allows to describe any shell side velocity of the heat exchanger HX6 as a function of Cap_{fac} . Hence, if $v_{HX,shell @Cap_{fac}}$ is equal to $v_{HX,shell,min}$ the related mass flow rate of the plant is $\dot{m}_{plant,min}$. Accordingly, the minimum capacity of the plant $Cap_{min,plant}$ in terms of \dot{m}_{plant} can be determined by Eq. 4-3:

$$Cap_{min,plant} = \left(\frac{v_{HX,shell,min}}{v_{HX,shell,@sp}} \right)^{\frac{1}{\alpha}} \quad \text{Eq. 4-3}$$

Thus, using the suggested correlation approach with the correlation exponent α relates the operating constraints of a process unit to the production rate of the plant considering the nonlinearities.

To apply the proposed correlation approach and determine the operating window of different process units as well as an entire modular equipment set, operating constraints for different process units are required. In general, operating constraints that limit the operating windows of a process unit can be for example of process-technological or mechanical nature. Flooding and weeping in a distillation column are examples of process-technological operating constraints. Examples of mechanical operating constraints are velocity limitations in heat exchangers to avoid erosion or critical vibrations. Table 4-1 summarizes possible upper and lower operating constraints of different process units that are used in this work.

Table 4-1: Used upper and lower operating constraints for different process units

Process unit	Minimum operating constraint	Maximum operating constraint
Reactor	<ul style="list-style-type: none"> min. pressure drop selectivity^a 	<ul style="list-style-type: none"> max. pressure drop min. conversion^a
Heat Exchanger	<ul style="list-style-type: none"> min. tube velocity min. shell velocity (fouling) 	<ul style="list-style-type: none"> max. tube velocity max. shell velocity (vibrations) max. tube/shell pressure drop
Tray column	<ul style="list-style-type: none"> non-uniform distribution weeping 	<ul style="list-style-type: none"> flooding
Packed column	<ul style="list-style-type: none"> 40 % of fractional capacity 	<ul style="list-style-type: none"> 95 % of fractional capacity
Vapor-liquid separator	<ul style="list-style-type: none"> / 	<ul style="list-style-type: none"> max. gas velocity min. liquid residence time
Decanter	<ul style="list-style-type: none"> / 	<ul style="list-style-type: none"> max. <i>Reynolds</i> number
Fermenter	<ul style="list-style-type: none"> min. liquid level (sufficient liquid level above stirrer) 	<ul style="list-style-type: none"> max. liquid level (min. head space for liquid drop settling and foam deposition)
Rotary drum vacuum filter	<ul style="list-style-type: none"> min. pressure drop (0.2 bar) 	<ul style="list-style-type: none"> max. pressure drop (0.8 bar)
Crystallizer	<ul style="list-style-type: none"> min. liquid level 	<ul style="list-style-type: none"> max. liquid level required heat exchange area
Dryer	<ul style="list-style-type: none"> min. void fraction for fluidization min. fluidization velocity 	<ul style="list-style-type: none"> max. void fraction to avoid elutriation/pneumatic transport max. solids hold-up

^a only used for acetone production case study in chapter 6.3.3

To finally determine the individual operating constraint values based on design parameters of equipment modules, and hence enable the determination of operating windows, a detailed simulation is required. A detailed description of how the operating constraints shown in Table 4-1 are calculated can be found in appendix A5. The list of operating constraints in Table 4-1 can also be extended to consider further process-technological or mechanical operating constraints.

4.2 Preselection approaches to decide on the use of equipment modules for process units

A preselection approach to decide on the use of equipment modules must not only consider investment, but also operating costs since both are affected by using equipment modules. Hence, the aim of a preselection approach is the identification of process units with a high impact on investment and operating costs. For these process units, the use of equipment modules is not recommended to avoid a high cost increase.

Three preselection approaches are compared in this work. The preselection approach called *Inv* that is based on investment costs and has been proposed in literature is used as benchmark. Additionally, new preselection approaches that consider investment and operating costs, which consist of utility and raw material costs, are introduced. The investment and operating costs are either allocated to the process units where they are incurred by the preselection approach called investment and operating costs *Inv&Op*, or they are allocated using exergy streams by the preselection approach called exergoeconomics *ExEco*. As references, cases without any preselection using equipment modules for all process units *All* and a conventionally designed plant *Conv* are employed. If the applied preselection approach results in no use of equipment modules for a process unit, the conventionally designed equipment of case *Conv* is used. An overview of the different cases is summarized in Table 4-2.

Table 4-2: Overview of investigated cases

Case	Description
<i>Inv</i>	Preselection approach based on investment costs
<i>Inv&Op</i>	Preselection approach based on investment and operating costs
<i>ExEco</i>	Preselection approach based on exergoeconomics
<i>All</i>	Case using equipment modules for all process units
<i>Conv</i>	Conventionally designed production plant

The cases *Conv* and *All* are utilized to evaluate the impact of using equipment modules on the operating and investment costs, whereby case *All* is resulting in the modular equipment sets with the smallest investment and operating costs. Furthermore, case *Conv* sets the basis to compare the suitability of the three different preselection approaches.

4.2.1 Preselection based on investment costs *Inv*

The decision tree approach introduced by Oldenburg et al. [28] forms the basis for the preselection approach based on investment costs used. The modified decision tree is shown in Figure 4-4. Based on a shortcut design, a first step confirms whether a process unit contributes a large part to the overall TCI. If not, using equipment modules has little impact

on the TCI and equipment modules can be used for the corresponding process unit. If a process unit does have a major impact on the overall TCI, the CEX-value is taken as a criterion to confirm whether the increase in investment costs is significant when using multiple equipment modules for this process unit. If the CEX-value is above the critical value of 0.6, equipment modules can be used, otherwise the corresponding process unit is ruled out for using equipment modules. The critical CEX-value of 0.6 is adopted from Oldenburg et al. [28].

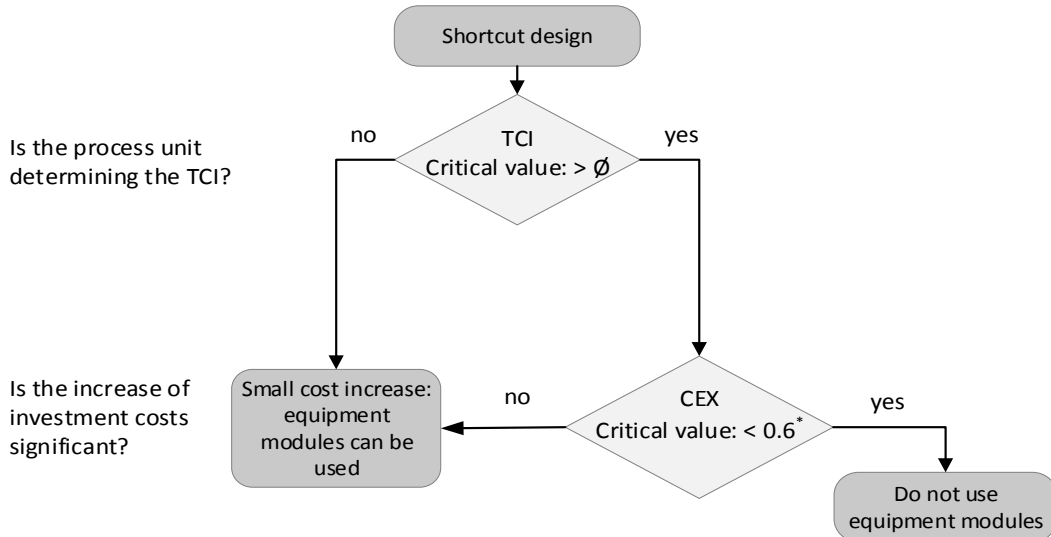


Figure 4-4: *Inv*-approach - decision tree based on investment costs to decide on the use of equipment modules for process units (* critical CEX-value from [28])

4.2.2 Preselection based on investment and operating costs *Inv&Op*

In contrast to the preselection approach that solely considers investment costs, the preselection approach *Inv&Op* takes both, investment and operating costs into account.

To combine investment and operating costs, both are considered as cost streams \dot{C} in [\$/h]. Hence, the TCI is converted to \dot{C}_{TCI} by a depreciation period of ten years and 8,000 operating hours per year. Operating costs include multiple types of utility costs \dot{C}_{Uti} , e.g. for cooling water, steam or electricity, and raw material costs \dot{C}_{RM} . \dot{C}_{TCI} and \dot{C}_{Uti} can easily be allocated to the process unit that affects the TCI or that requires the utility for its processing task. Such allocation is not that simple for raw material costs. While associated raw material costs are unavoidable, the amount of required raw material depends on the apparatus chosen for the corresponding process unit and may additionally increase when operated away from the design point. Therefore, costs for additional raw material that would not be used in case of a perfectly fulfilled processing task are defined as avoidable raw material costs $\dot{C}_{RM,av}$. To distinguish between avoidable and unavoidable raw material costs $\dot{C}_{RM,av}$ and $\dot{C}_{RM,unav}$, the following definition is used:

Definition:

Avoidable raw material costs represent the part of raw material costs that emerge due to a process unit not fulfilling its processing task perfectly. Two types of avoidable raw material are considered:

- Raw material that is not converted to the desired product or raw material that exits the process unaltered
- Product that is not exiting the process via the product stream

The costs are only considered to be avoidable, if they are influenced by using equipment modules.

Hence, examples of avoidable raw material are side products generated in a reactor or liquid droplets entrained by the gas stream of a vapor-liquid separator. In contrast, co-products or side products for which the amount does not change by using equipment modules are not viewed as loss and are thus not considered avoidable raw material costs.

Being sequentially processed in a production plant, the monetary value of the processed material stream increases with each processing step. If the material in a process unit has a higher monetary value compared to previous process units, the decision on using equipment modules is essential. Hence, it is crucial to consider the position of a process unit when deciding on the use of equipment modules. This can be realized by a position factor P for a process unit at position p using Eq. 4-4:

$$P_p = \frac{\dot{C}_{RM,unav} + \sum_{i=1}^p \dot{C}_{RM,av,i} + \sum_{i=1}^p \dot{C}_{Uti,i} + \sum_{i=1}^p \dot{C}_{TCI,i}}{\dot{C}_{RM,unav}} \quad \text{Eq. 4-4}$$

The value of P_p depends on the position of a process unit within the process and on the increase of costs that incurs up to the corresponding position p . This cost increase in relation to $\dot{C}_{RM,unav}$ is expressed as the sum of $\dot{C}_{RM,av}$, \dot{C}_{Uti} and \dot{C}_{TCI} up to position p of the corresponding process unit. Here, $\dot{C}_{RM,av}$ and \dot{C}_{Uti} reflect the costs that might increase by using equipment modules that are not tailor-made for the required process task. Furthermore, \dot{C}_{TCI} increases by the economy of scale effect when using multiple equipment modules for a process unit.

The calculation of the position factor P_p and the affected costs according to the preselection approach *Inv&Op* will be shown for an exemplary production process depicted in Figure 4-5. For each of the three process units, the TCI, the costs related to the required utility and the process data to calculate the amount of unavoidable raw material costs are given. Process unit 1 and 3 are heat exchangers that change the temperature of the process stream according to their processing task.

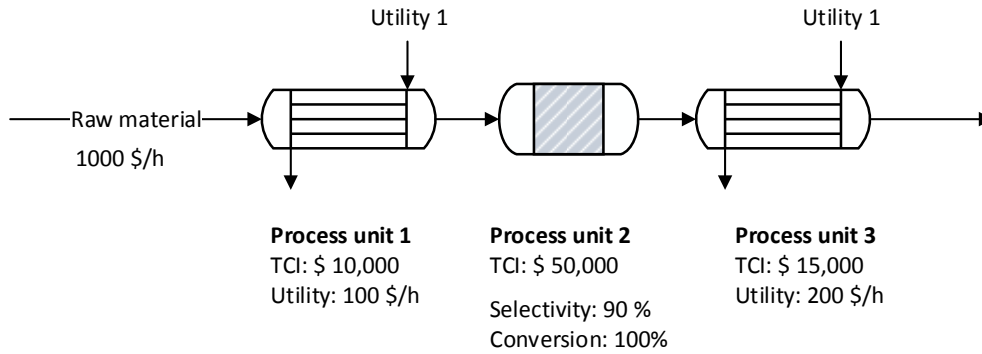


Figure 4-5: Example consisting of three process units for the calculation of affected costs of $\dot{C}_{RM,av}$, \dot{C}_{Uti} and \dot{C}_{TCI} according to the preselection approach *Inv&Op*

As the heat exchangers are process units that heat up or cool down without destroying or losing raw material or product, no avoidable raw material is lost according to the aforementioned definition. In contrast, a selectivity of 90 % is given for process unit 2, a reactor, for which raw material reacting in a side reaction is a raw material loss. Thus, the corresponding raw material costs are considered as avoidable raw material costs. The costs considered to be affected in the example process of Figure 4-5 are summarized in Table 4-3.

Table 4-3: Calculated affected costs for the exemplary process of Figure 4-5 according to the preselection approach *Inv&Op*

	\dot{C}_{TCI} [\$ /h]	\dot{C}_{Uti} [\$ /h]	$\dot{C}_{RM,av}$ [\$ /h]
Process unit 1	0.125	100	0
Process unit 2	0.625	0	100
Process unit 3	0.1875	200	0

The determination of the position factor for process unit 3 is shown by Eq. 4-5:

$$P_3 = \frac{900 \frac{\$}{h} + 100 \frac{\$}{h} + (100 + 200) \frac{\$}{h} + (0.125 + 0.625 + 0.1875) \frac{\$}{h}}{900 \frac{\$}{h}} \quad \text{Eq. 4-5}$$

resulting in $P_3 = 1.4455$.

$\dot{C}_{RM,av}$, \dot{C}_{Uti} and \dot{C}_{TCI} form the basis for a decision tree to determine the use of equipment modules for process units of a process considering the investment and operating costs. The developed decision tree is shown in Figure 4-6. First, the contribution of costs affected by using equipment modules for a process unit i in relation to the entire production plant consisting of j process units is determined. If this ratio is below the mean value, the impact on the affected costs is low and equipment modules can be used without expecting a significant cost increase. If the ratio is high, a second step determines whether \dot{C}_{TCI} affects the cost increase by using equipment modules. If this is the case, the CEX is used in a third

decision step. In case $\dot{C}_{RM,av}$ and \dot{C}_{Uti} result in a high ratio, it is desirable to quantify the effect of using equipment modules based on these costs.

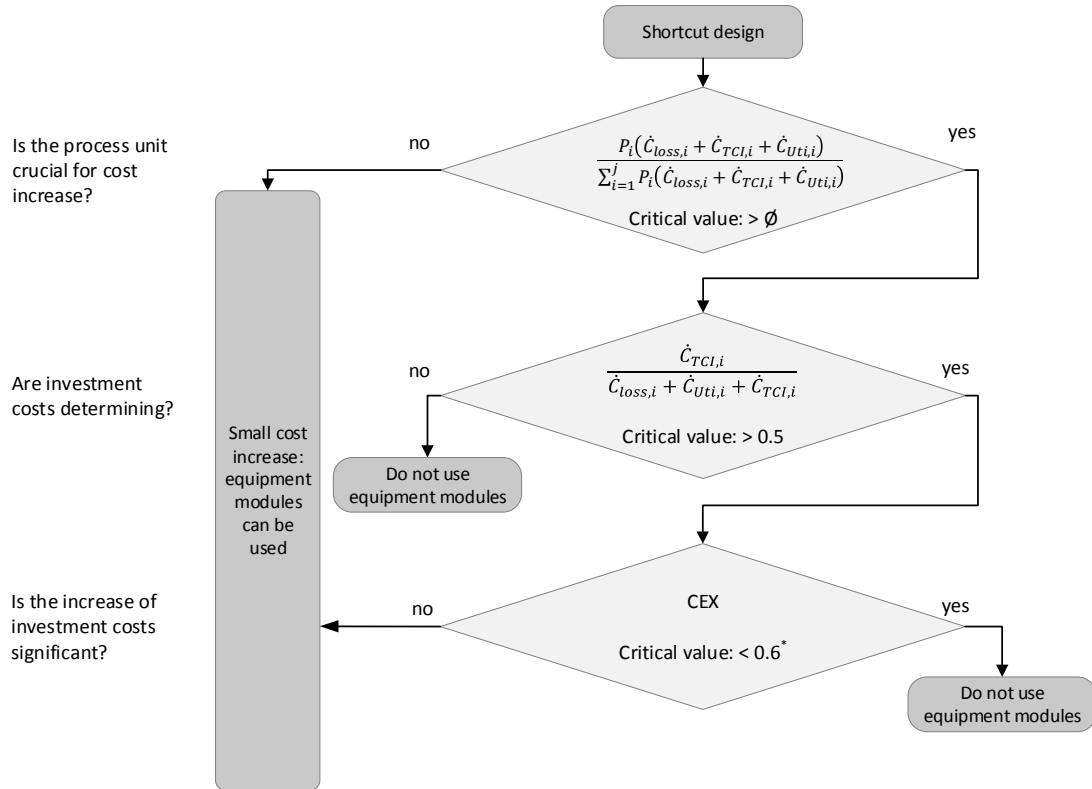


Figure 4-6: Decision tree for *Inv&Op* approach to decide on the use of equipment modules for process units (* critical CEX-value from [28])

However, no appropriate information about the effect of using equipment modules on $\dot{C}_{RM,av}$ and \dot{C}_{Uti} is known so far. Thus, using equipment modules is not recommended and the use of conventionally designed apparatuses is preferred. Once the effect of using equipment modules on $\dot{C}_{RM,av}$ and \dot{C}_{Uti} is known, the proposed decision tree should be extended.

4.2.3 Preselection based on exergoeconomics *ExEco*

The preselection approach *ExEco* considers both, investment and operating costs, while the operating costs are allocated by an exergoeconomic approach. To apply exergoeconomic decision criteria for the decision on using equipment modules for a process unit, an exergoeconomic analysis of a shortcut design needs to be performed. This can be split into three steps: A mass and energy balance, an exergy balance and the exergoeconomic balance. In general, the exergy of a material stream can originate from physical exergy \dot{E}_{ph} , mixing exergy \dot{E}_{mix} , chemical exergy \dot{E}_{ch} , kinetic exergy \dot{E}_{kin} and potential exergy \dot{E}_{pot} [45,46]. Already including mixing exergy, the physical exergy of a material stream can be calculated by Eq. 4-6 [46]:

$$\dot{E}_{ph} + \dot{E}_{mix} = \dot{H} - \dot{H}_0 - T_0 \cdot (\dot{S} - \dot{S}_0) \quad \text{Eq. 4-6}$$

wherein \dot{H} and \dot{S} refer to the enthalpy and entropy of the mixed stream and \dot{H}_0 and \dot{S}_0 refer to the enthalpy and entropy of the considered stream at reference conditions of $T_0 = 25^\circ\text{C}$ and $p_0 = 1 \text{ atm}$ [45–47]. Compared to physical exergy, kinetic and potential exergy of a material stream are small for industrial production processes and hence neglected for an exergoeconomic analysis in the scope of this work [46,48]. Chemical exergy refers to the part of the total exergy resulting from the difference in the chemical potential between the pure components of the considered material stream and the components of the reference environment in their respective concentrations. Exergy that enters a system and exits it as it cannot be transformed into another type of exergy is called transit exergy. Wall and Riedl propose to exclude transit exergy from exergoeconomic analysis, because transit exergy can have a high share on the overall exergy of a stream and is constant [48,49]. Hence, transit exergy can distort the operating cost allocation to process units and is therefore excluded from the exergoeconomic decision criteria to decide on using equipment modules. The specific chemical exergy $\tilde{e}_{ch,i}$ of a component depends on the amount of exergy that is released when it is decomposed to the individual components of the reference environment at equilibrium conditions [46]. Decomposition reactions to the individual components of the reference environment like nitrogen, oxygen and carbon dioxide cannot occur in any of the considered process units. Thus, the largest part of the chemical exergy is not available for transition. In process units that alter the composition of streams, the chemical exergy is changing. Such process units might be separation units, for example, in which chemical exergy is simply distributed to one of the outgoing streams, but not converted into another type of exergy. Other process units that change the composition of streams are process units in which reactions occur. Here, the enthalpy or entropy of a reaction causes a temperature or pressure change that necessitates the supply of heating or cooling exergy. However, this aspect is already considered by the physical exergy and the exergy of heat. For this reason, chemical exergy corresponds to transit exergy and is excluded from the exergy analysis that is applied to decide on the use of equipment modules in the scope of this work.

Besides exergy of a material stream \dot{E}_{mat} , which represents exergy associated with mass transfer, work and heat transfer must be considered in an exergy balance. Electrical energy can be fully transformed into work, hence Eq. 4-7 is used if electrical energy is supplied to a process unit to determine the corresponding exergy stream.

$$\dot{E}_W = W \quad \text{Eq. 4-7}$$

In case of heat transfer where a heat stream \dot{Q} is supplied, the maximum rate of conversion from thermal energy to work is described by Eq. 4-8 [45].

$$\dot{E}_Q = \dot{Q} \cdot \left(1 - \frac{T_0}{T}\right) \quad \text{Eq. 4-8}$$

To perform an exergy balance for a system with a defined system boundary, all incoming exergy streams $\dot{E}_{in,i}$ and outgoing exergy streams $\dot{E}_{out,i}$ associated with mass, heat transfer and work are taken into account as shown in Eq. 4-9.

$$\sum \dot{E}_{in,i} = \sum \dot{E}_{out,i} + \dot{E}_{irrev} + \dot{E}_{ex.loss} \quad \text{Eq. 4-9}$$

The exergy losses that occur in a system can either be caused by process irreversibility, called \dot{E}_{irrev} , or by exergy that is released to the environment, called external exergy losses $\dot{E}_{ex.loss}$. Since no data can be generated for the amount of exergy that is released to the environment by using a process simulator like Aspen Plus[®], external exergy losses cannot be determined and are neglected in the scope of this work. According to Nimkar et al. [50], the source of irreversibility depends on the type of process unit. In general, exergetic losses are low in case of a uniform process with a low driving force. For example, a source of irreversibility in a heat exchanger is the temperature difference between the hot and the cold medium. To reduce the irreversibility, the utility temperature should be adjusted to decrease the temperature difference. From an economic point of view, a lower temperature difference will increase the investment costs for a heat exchanger.

To extend an exergy analysis to an exergoeconomic analysis, a cost balance is required. Exemplary, this is shown in Figure 4-7 for a system consisting of two process units.

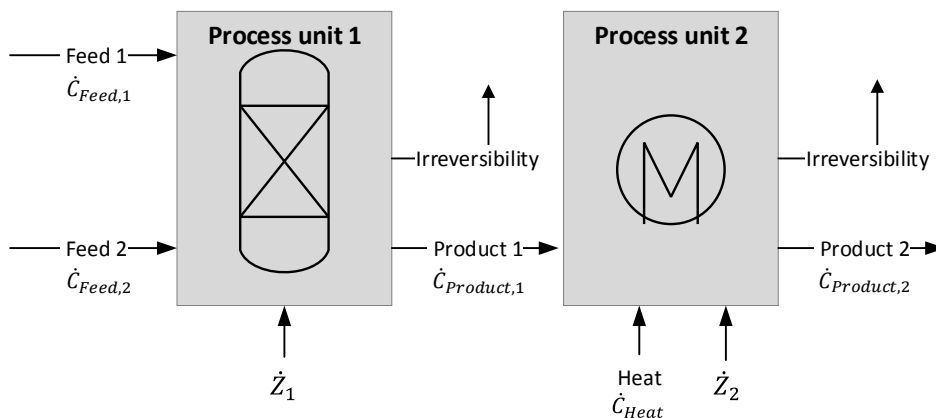


Figure 4-7: Exemplary exergoeconomic cost balance for a system consisting of two process units (\dot{C} – exergetic cost stream, \dot{Z} – system costs stream)

Balancing the costs for the first process unit yields Eq. 4-10, with $\dot{C}_{Feed,1}$ and $\dot{C}_{Feed,2}$ as material costs of Feed 1 and Feed 2.

$$\dot{C}_{Feed,1} + \dot{C}_{Feed,2} + \dot{Z}_1 = \dot{C}_{Product,1} \quad \text{Eq. 4-10}$$

\dot{Z}_1 refers to the system costs of process unit 1 representing the fixed costs that do not depend on the actual production rate.

System costs are composed of investment, labor and maintenance costs. As shown in Eq. 4-10, the outgoing product stream must defray all incoming cost streams. Furthermore, $\dot{C}_{Product,1}$ represents the ingoing cost stream to process unit 2. Consequently, a cost balance for process unit 2 includes heating costs \dot{C}_{Heat} and is shown in Eq. 4-11.

$$\dot{C}_{Product,1} + \dot{C}_{Heat} + \dot{Z}_2 = \dot{C}_{Product,2} \quad \text{Eq. 4-11}$$

To analyze a system exergoeconomically, the specific exergetic costs are defined. For the feed of process unit 1 they are shown in Eq. 4-12.

$$c_{Feed,1} = \frac{\dot{C}_{Feed,1} + \dot{C}_{Feed,2} + \dot{Z}_1}{\dot{E}_{Feed,1} + \dot{E}_{Feed,2}} \quad \text{Eq. 4-12}$$

For the feed of process unit 2, the specific exergetic costs are calculated by Eq. 4-13.

$$c_{Feed,2} = \frac{\dot{C}_{Product,1} + \dot{C}_{Heat} + \dot{Z}_2}{\dot{E}_{Product,1} + \dot{E}_{Heat}} \quad \text{Eq. 4-13}$$

According to Querol et al. [51], the specific exergetic costs enable the cost determination of the costs through exergetic losses \dot{C}_{loss} and basic costs \dot{C}_{basic} . Costs through exergetic losses represent the economic value that is allocated to the irreversibility of a process. Even in case of an economically ideal process that is fully reversible and has no system costs, basic costs are still in place as long as incoming exergy streams enter the system. Thus, the basic costs are thermodynamically needed to perform the process units' task. By using equipment modules, the basic costs ideally remain constant, whereas system costs might increase according to economy of scale effects. Exergetic losses may also increase due to an operation away from the optimal design point [48,51].

Using the specific exergy costs c_{Feed} and the outgoing exergy streams \dot{E}_{out} , the basic costs \dot{C}_{basic} are calculated by Eq. 4-14 [51]:

$$\dot{C}_{basic} = c_{Feed} \cdot \sum \dot{E}_{out} \quad \text{Eq. 4-14}$$

The costs through exergetic losses \dot{C}_{loss} are calculated using the exergetic losses \dot{E}_{irrev} as shown by Eq. 4-15:

$$\dot{C}_{loss} = c_{Feed} \cdot \dot{E}_{irrev} \quad \text{Eq. 4-15}$$

System costs, basic costs and costs through exergetic losses can now be calculated for process unit 1 and process unit 2 as final step of the exergoeconomic analysis, setting the basis for the decision on using equipment modules for process units. As only system costs \dot{Z} and costs through exergetic costs are influenced by using equipment modules, a decision on the use of equipment modules for a process unit can be made by comparing the exergetic

losses of the process units to each other. As described above, the incoming costs of a process unit also depend on the previous process units upstream. This is challenging for process units with incoming recycle streams. To still enable the calculation of exergoeconomic costs for these process units, the costs for entering and outgoing recycle streams are assumed to be zero. Accordingly, all costs of the process unit are allocated to the outgoing stream that is fed to the next process unit.

The decision tree to decide on the use of equipment modules for process units based on the *ExEco* approach is shown in Figure 4-8.

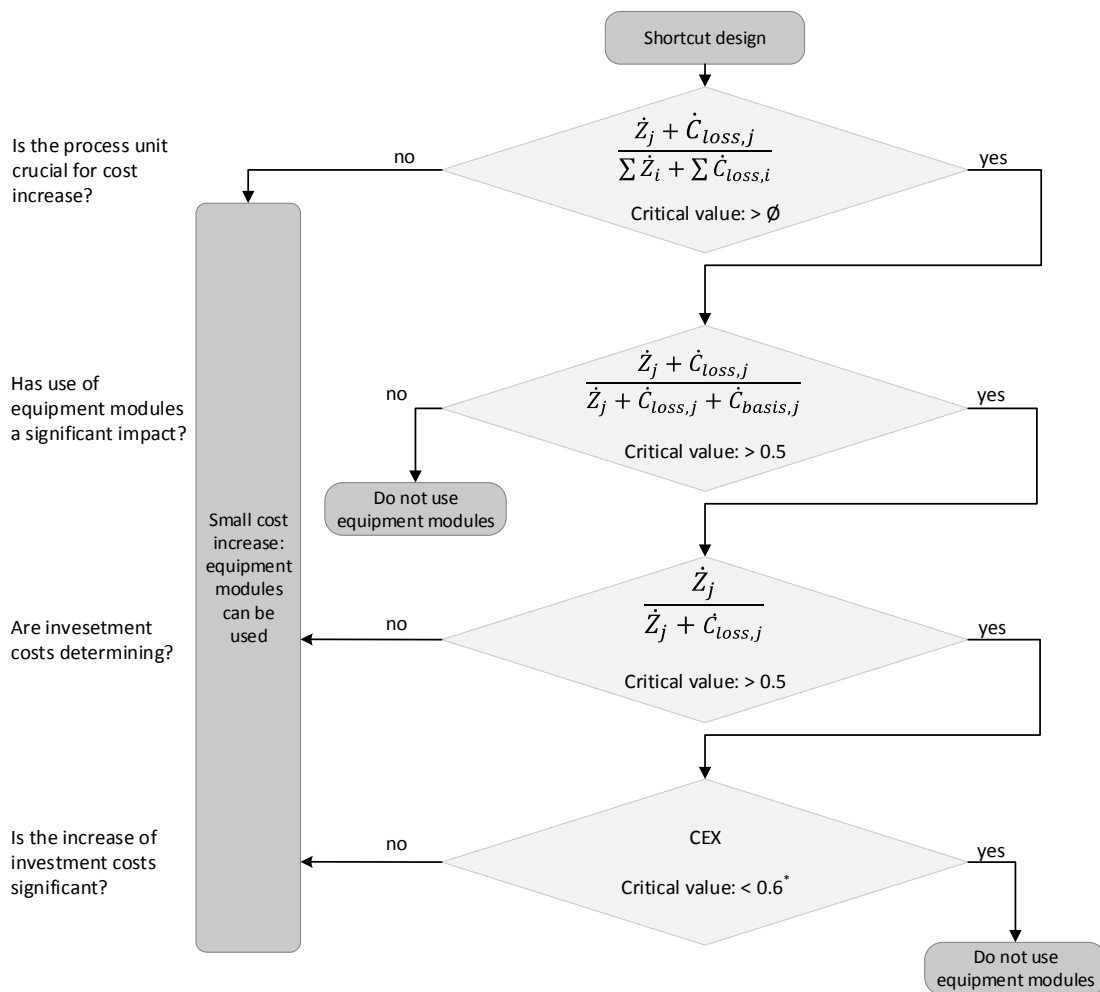


Figure 4-8: Decision tree for *ExEco* approach to decide on the use of equipment modules for process units (* critical CEX-value from [28])

In a first step, the share of system costs \dot{Z} and costs through exergetic losses \dot{C}_{loss} that are affected by using equipment modules on the total amount of system costs and costs through exergetic losses are evaluated for each process unit. The average of all process units of the considered production plant is selected as the critical value. If the value is lower than the critical value, a small exergetic cost increase in case of using equipment modules compared to the other process units is expected. Therefore, equipment modules can be used for the considered process unit. In a second step, the ratio of the affected costs and the overall

exergetic costs is investigated. If the ratio in the second step is below the critical value of 0.5, the cost increase by using equipment modules is small and equipment modules can be used as the largest part of costs cannot be avoided. If the cost increase is high, the third decision criterion applies. Both, the third and the fourth criterion, are similar to the economic decision tree. If the system costs result in high affected costs, the CEX-criterion will be applied. In contrast, the effect of using equipment modules on costs through exergetic losses cannot be properly estimated so far. Thus, the use of equipment modules in case of dominating costs through exergetic losses is not considered and the corresponding process unit is ruled out for the use of equipment modules.

4.2.4 Evaluation of preselection approaches

A shortcut design of the process equipment is used to apply the developed preselection approaches *Inv*, *Inv&Op* and *ExEco*. The application of the preselection approaches determines for which process units equipment modules can be used. Following each preselection, a multi-objective evolutionary algorithm is applied to select equipment modules for the respective process units minimizing TCI and OPEX as selection objectives (see chapter 4.3). This results in a Pareto front for each preselection case. To subsequently evaluate the different preselection approaches, the absolute location of each Pareto front is not important, but its distance to the conventional case *Conv* as illustrated in Figure 4-9. A preselection approach is called suitable, if the process units that influence TCI and OPEX the most are identified by the respective preselection and set to the conventionally designed apparatuses. Hence, the smaller the distance of the Pareto front based on the corresponding preselection approach to the conventional design *Conv*, the better is the preselection approach in identifying the process units with the largest impact on TCI and OPEX. If the impact of using equipment modules for a process unit on TCI and OPEX is low, the use of equipment modules is not leading to worse TCI and OPEX, while benefits of using equipment modules can be assumed.

With regard to the scheme shown in Figure 4-9 this means that preselection approach 1 is better compared to preselection approach 2 since the distance to case *Conv* is smaller. The absolute TCI and OPEX of the preselection approaches are in general smaller, because the selection of equipment modules from the equipment module databases offers a degree of freedom to minimize TCI and OPEX compared to case *Conv*.

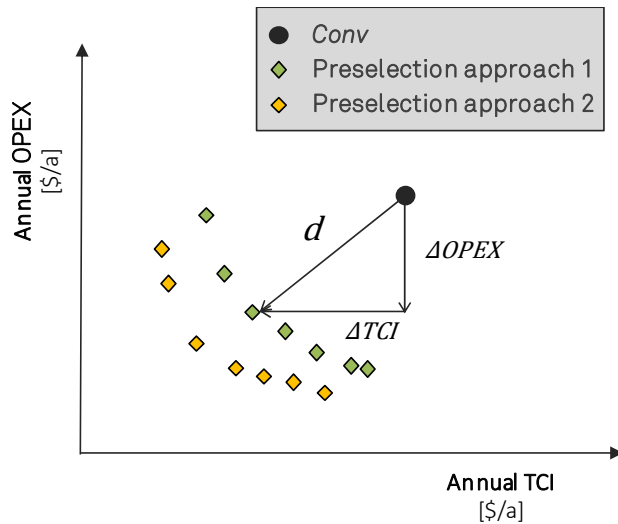


Figure 4-9: Scheme describing the evaluation of the preselection approaches by the distance of the Pareto fronts for the preselection approaches to case *Conv*

Quantitatively, the distance of a Pareto front consisting of the modular equipment sets i to the conventional design *Conv* is determined by the mean distance according to Eq. 4-16.

$$\bar{d} = \frac{1}{N} \cdot \sum_i^N \sqrt{\Delta TCI_i^2 + \Delta OPEX_i^2} \quad \text{Eq. 4-16}$$

4.3 Equipment module selection

Different methods are combined to a framework to select equipment modules for a modular production plant, as shown in Figure 4-10. The framework for equipment module selection is applied to select equipment modules for all process units of a process within the scope of this work. However, it is also applicable to select equipment modules for only some of the process units of a process.

The basis of the framework is an equipment module database consisting of different equipment modules for each process unit. Initially, a random modular equipment set is selected. To check if this modular equipment set is operable, it is simulated in Apen Plus® and Aspen EDR®. The results of the process simulation are transferred via an Aspen ActiveX interface to MS Excel VBA, which is also used to determine the objectives of the equipment module selection. Next, the values of the objective functions are utilized by the multi-objective evolutionary algorithm. Applying evolutionary operators as mutation, recombination and selection, the evolutionary algorithm is improving the modular equipment sets over the generations.

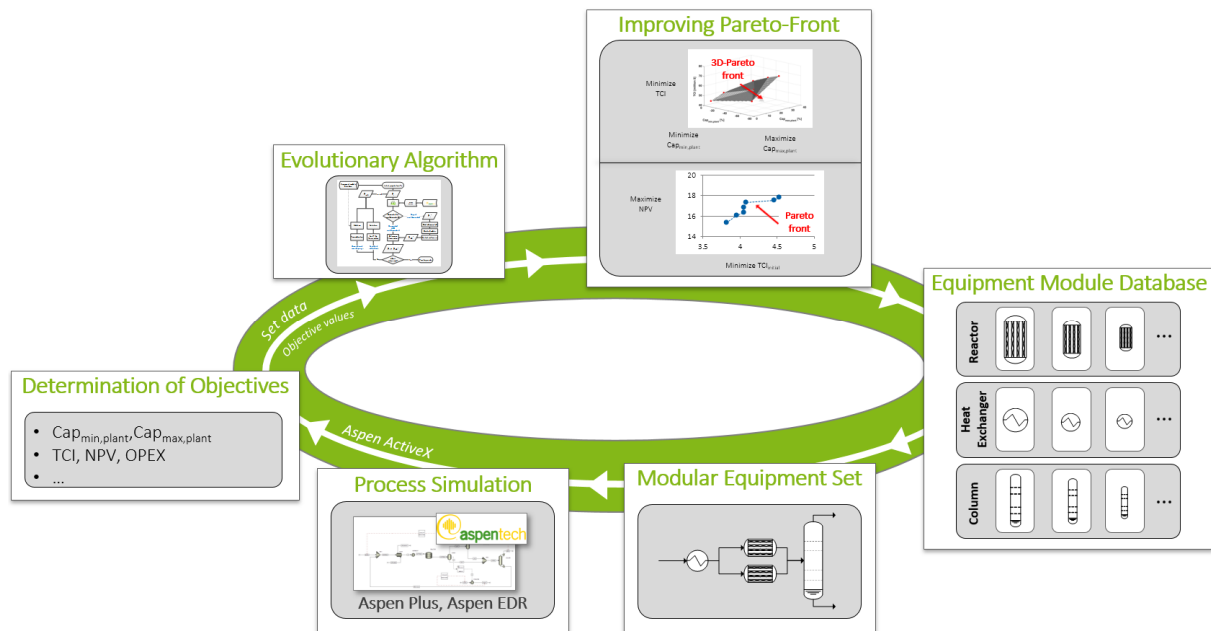


Figure 4-10: General framework to select equipment modules for modular equipment sets

The selection of different combinations of equipment module sizes and numbers contains a large number of discrete decision variables. This results in a discontinuous and non-monotonic search space. Additionally, multiple objectives need to be considered such as for example an increased operating window by minimizing $Cap_{min,plant}$, maximizing $Cap_{max,plant}$ and minimizing additional investment costs.

Due to the large number of discrete decision variables, as well as the discontinuous and non-monotonic search space, the problem cannot be solved by gradient based optimization algorithms [52]. Evolutionary algorithms (EAs) are suitable to handle multiple objectives and a large number of discrete decision variables [53]. They are population-based algorithms and use the concepts of evolution as recombination, mutation and selection to find better solutions inspired by living organisms in nature [54]. The applied evolutionary algorithm for equipment module selection is based on the Strength Pareto Evolutionary Algorithm (SPEA) developed by [55] and was implemented in MS Excel VBA. SPEA is an elitist evolutionary algorithm that maintains an external archive P' to store a fixed number of Pareto-optimal solutions.

For the selection of equipment modules to form modular equipment sets an equipment module with its corresponding size and number can be considered as a gene of a living organism in nature's evolution. A possible solution of an optimization problem, in this case a possible modular equipment set, is referred to as an individual. Similarly to a living organism in nature, this individual is part of a population, which describes the group of all current modular equipment sets within a generation. The number of individuals in a population is called population size N . This translation is illustrated in Figure 4-11.

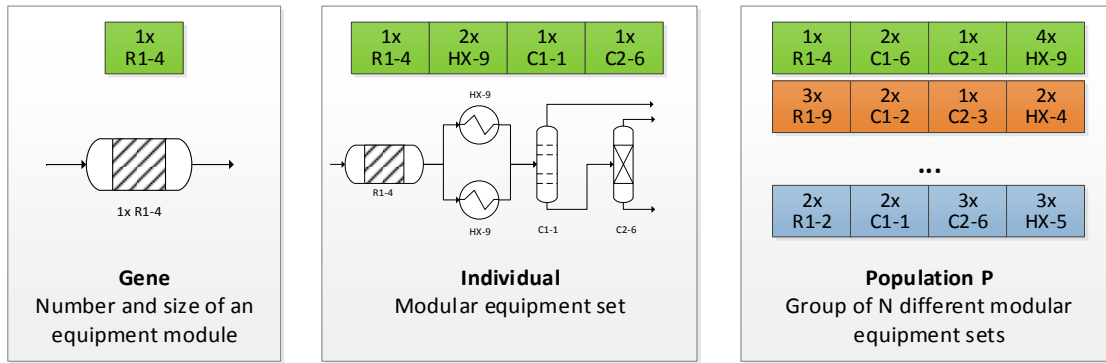


Figure 4-11: Translation of the characteristics of the optimization problem to select equipment modules for modular equipment sets to the characteristics of a living organism in nature

The overall working principle of the implemented SPEA can be separated into four main steps that are illustrated in Figure 4-13. It starts with a randomly created initial population P_0 of size N and an empty external archive P'_0 of size N' . Each initial individual is transferred to Aspen Plus® separately and evaluated by a simulation run. Only converging and operable modular equipment sets are used. If a modular equipment set does not converge or is not operable, the set is kicked out of the population and another modular equipment set is randomly chosen. Each modular equipment set that has been kicked out is saved in an extra array. To prevent simulating the same or not working individuals twice, every time before a new set is simulated, it is checked whether this set is already stored in the extra arrays called 'solutions' and 'errors sets'. Based on the values of the objectives, the EA selects the best individuals of the initial population to store them in the archive P' , which is the repository of the non-dominated and Pareto-optimal individuals. A modular equipment set A is non-dominated by a modular equipment set B, if it outperforms B in one objective and is at least equal in the other objectives. All non-dominated solutions form the Pareto front of a population P_i . The size of the archive P' or rather the number of solutions of the Pareto front, is limited to a maximum number of individuals called the archive size N' . Whenever new individuals are added to the archive throughout the generations, the dominance inside the archive is checked. Dominated individuals inside the archive are removed together with duplicates. If the archive still exceeds the maximum archive size N' , modular equipment sets with the smallest Euclidian distance between their objectives are selected and one of them is randomly deleted until the maximum archive size N' is reached. This maintains diversity inside the archive and thus a broad Pareto front [54].

When the new Pareto-optimal individuals, also called elites, are preserved for the next generation in the external archive P' , genetic operators are used to find a new population. Therefore, SPEA assigns a fitness value, called strength S_i , to each member i of the archive P' according to Eq. 4-17 [55]:

$$S_i = \frac{n_i}{N + 1} \quad \text{Eq. 4-17}$$

The strength S_i is proportional to the number of current population members n_i that a non-dominated solution i of the archive P' dominates. The smaller the fitness value, the better the individual is. A division of n_i by $(N + 1)$ assigns more strength (a lower fitness value) to the non-dominated solutions stored in the archive P' . Afterwards, each current population member j gets a fitness value F_j according to Eq. 4-18 [55]:

$$F_j = 1 + \sum_{i \in P_i, i \leq j} S_i \quad \text{Eq. 4-18}$$

Thus, the fitness of an individual $j \in P_i$ is calculated by summing up the strengths of all non-dominated solutions i of the archive P' that cover j . One is added in order to ensure that the members of the archive P' have a better fitness than members of the current population P_i [55].

After the external storage of the Pareto-optimal solutions in the archive and the assignment of the fitness values, the next step is the generation of new individuals, the so-called offspring individuals. To generate a certain number of offspring individuals λ for the next population P_{i+1} recombination, mutation and selection are applied subsequently. New individuals are generated based on the non-dominated as well as all dominated modular equipment sets, thus by combining P'_{i+1} and P_i .

To generate a new offspring, the genetic code of two individuals can be recombined. This means the offspring receives a part of its genetic code from individual A and the other part of individual B. As suggested by [55], a one-point crossover recombination is used in this work. Such a one-point crossover describes a recombination where the set of equipment modules is cut at one point resulting in two parts. The offspring receives one part of each individual, respectively [56]. In addition to recombination, the genetic code can also mutate subsequently to preserve diversity in the population. A mutation causes several genes to randomly change to another value. That means exchanging one of the equipment modules for a process unit with another one for this process unit from the equipment module database. Figure 4-12 illustrates the generation of new offspring individuals. The number of equipment modules changed by mutation is referred to as the mutation rate r_{mut} , the probability of recombination and mutation to happen is called recombination probability p_{rec} and mutation probability p_{mut} .

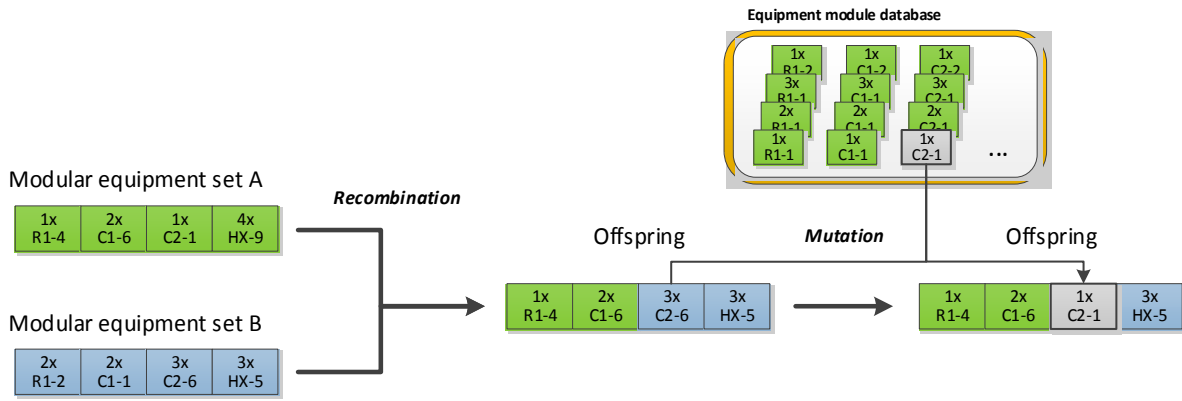


Figure 4-12: Example for recombination and mutation operators

Like the creation of the initial population, only one offspring at a time is passing through recombination and mutation. Afterwards, this offspring needs to be simulated in Aspen Plus® to receive its objective values. If this individual turns out not to converge or to be not operable, it is not saved as offspring, but as ‘error set’. In that case, a new offspring is generated. Each offspring generated is compared with those modular equipment sets that have been kicked out before. Offspring individuals are created until the desired number of offspring individuals λ is reached. This offspring array of size λ forms one part of the new population P_{i+1} for the following generation. The remaining places for the new population P_{i+1} are filled by ranking selection, which means that the individuals of P'_{i+1} and P_i are sorted according to their fitness values and P_{i+1} is filled up with the best ranked individuals until the population size N is reached.

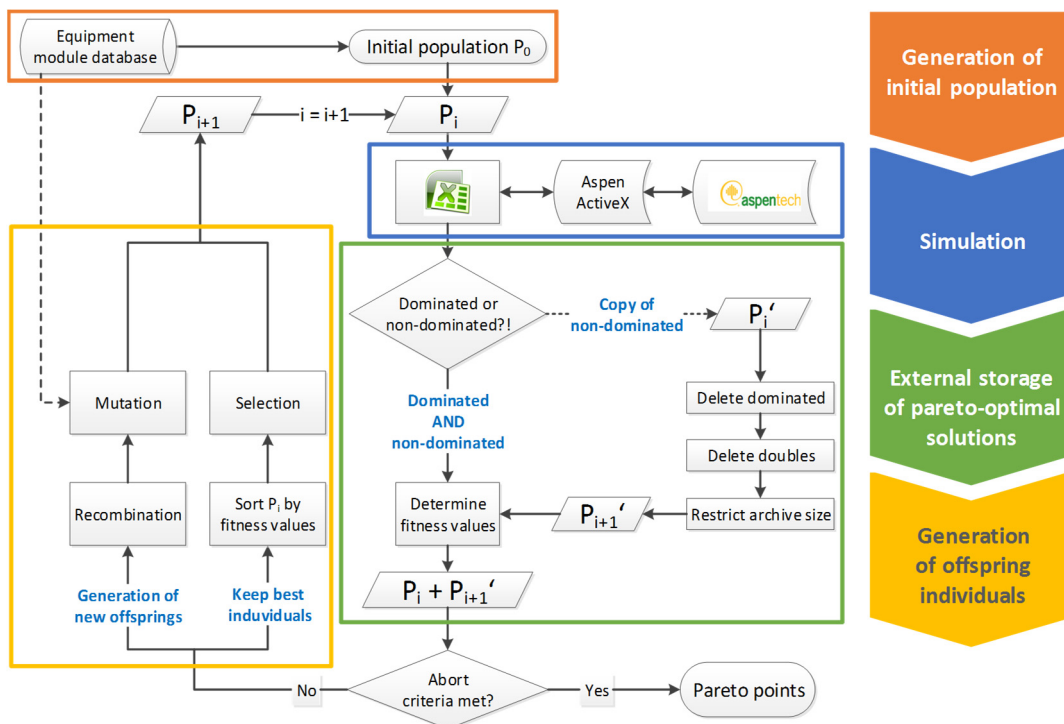


Figure 4-13: Working principle of the implemented SPEA to select equipment modules for modular equipment sets

As soon as the new population is generated, the evolutionary algorithm starts with the next generation. Throughout the generations the algorithm will find improved individuals and the Pareto front is moving towards the optimal solutions. This process is repeated until an abort criterion is fulfilled, in the framework of this work until no additional Pareto-optimal equipment sets are found over a specified number of generations.

To select equipment modules for a market demand development the general approach to select equipment modules needs to be extended by an approach to determine the best stepwise capacity expansion strategy. The market demand development over a certain period of time and the equipment module database are the starting point. In a first step, the required expansion steps to follow the market demand development need to be determined. The approach to determine the required expansion steps to follow the given market demand development is schematically illustrated in Figure 4-14. The market demand development is divided into discrete points. A modular equipment set is compiled out of the equipment module database, either randomly in the first generation of the evolutionary algorithm or by applying recombination, mutation and selection for the following generations. This modular equipment set is transferred to the *Process Simulation*, where a rigorous determination of the operating window is performed for the first demand point. If this modular equipment set is operable, meaning that the operating windows of all process units are covering the simulated production rate, it is taken as initial modular equipment set.

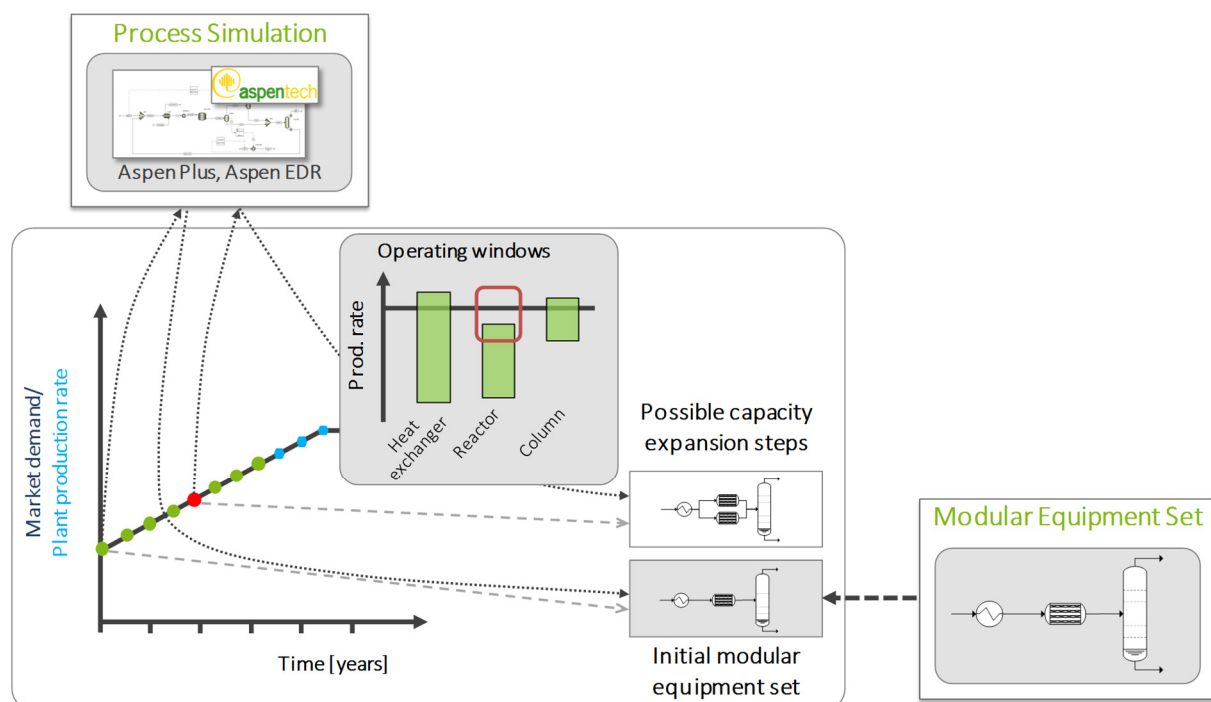


Figure 4-14: Schematically illustration of the approach to determine the required expansion steps to follow a given market demand development

Next, the following discrete market demand points are consecutively simulated, whereas the operability is checked, and the plants' operating window is determined for each point. This is done until an upper operating boundary of a process unit is below the simulated production rate. In Figure 4-14 this is exemplarily shown by the red dot, where the operating window of the reactor of the initial modular equipment set is too small. In such a case, an additional reactor equipment module is added and operated in parallel. When all discrete demand points are simulated, the possible equipment-wise capacity expansion steps required to meet the marked demand are determined for the initial modular equipment set.

Afterwards, the best expansion strategy needs to be selected. An exemplary stepwise capacity expansion is shown in Figure 4-15. The production starts utilizing a smaller production plant with little idle capacities at the beginning that is expanded later. The result is a production along the market demand with gaps in between. These gaps are capacities that neither the initial plant nor the expanded one can fulfill.

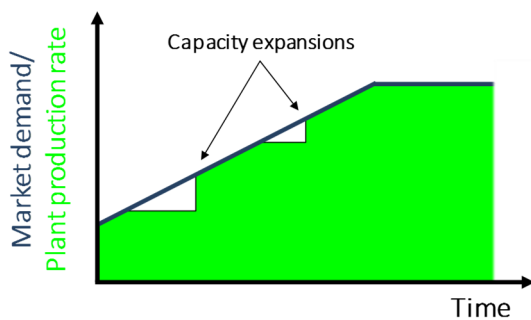


Figure 4-15: Exemplary stepwise capacity expansion strategy for a given market demand development

Hence, the plant operates below the market demand and as well leaves some production potential. However, these gaps can be decreased either by using smaller equipment modules or by earlier capacity expansions. The economic success is a trade-off between further earnings by filling these production gaps and the required additional investment for utilizing multiple smaller equipment modules or earlier expansion steps. To evaluate the best trade-off solutions between the initial investment risk and a better adaptability, the initial investment $TCl_{initial}$ should be minimized and the profit in terms of NPV should be maximized. The results of simulating a modular equipment set along the given market demand development are used to determine the expansion scenario with the maximum NPV between the extreme cases 'no expansion at all' and 'using all required expansion steps right from the beginning'. This best expansion scenario is forwarded together with the initial investment $TCl_{initial}$ to the evolutionary algorithm, which converges to the best modular equipment sets in terms of a low $TCl_{initial}$ and a maximum profit indicated by the NPV.

4.4 Method to design equipment for flexibility

The proposed method to design equipment modules for flexibility is shown in Figure 4-16. Its foundation is a mathematical model of the apparatus under consideration incorporating the key design parameters (1). Additionally, typical values or ranges of values for the design parameters are required and the operating constraints of the considered apparatus need to be identified. The design space of the design parameters is spanned by the number of design parameters and their possible values or value ranges. This design parameter space is explored by a sampling of apparatus designs (2), aiming for a high coverage rate.

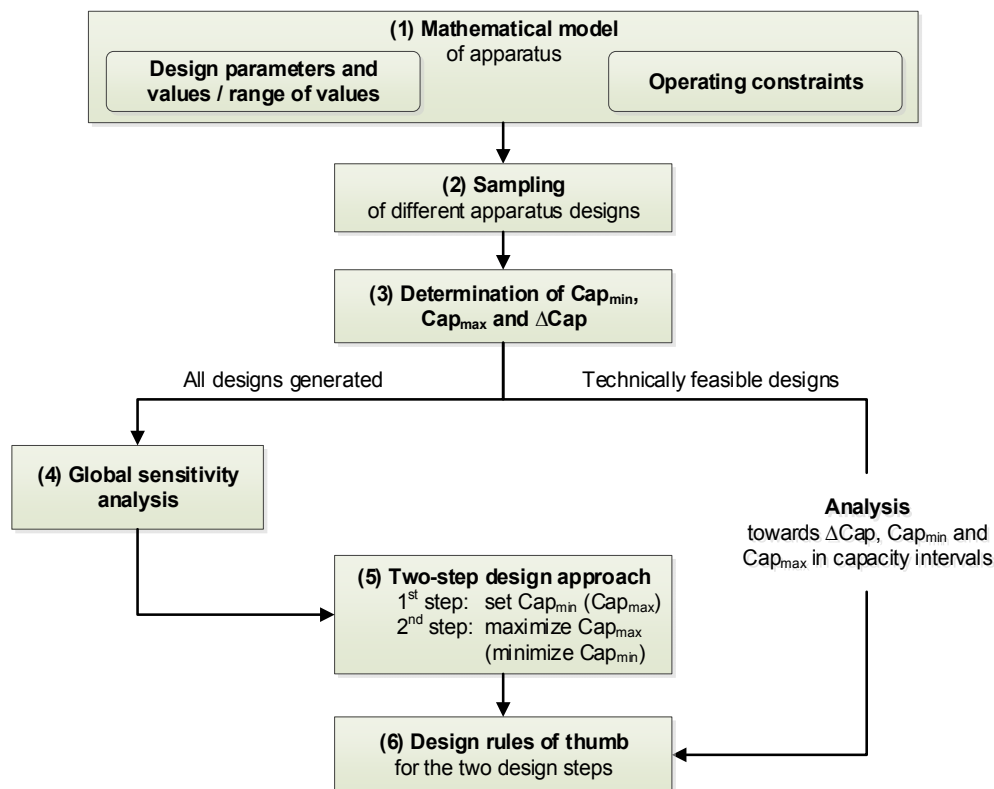


Figure 4-16: Graphical representation of the method to develop a design approach and deduce design rules of thumb for flexible equipment modules

Next, the lower capacity limit Cap_{min} , the upper capacity limit Cap_{max} and the size of the operating window $\Delta Cap = Cap_{max} - Cap_{min}$ need to be determined (3). Based on all sampled apparatus designs and their corresponding Cap_{min} -, Cap_{max} - and ΔCap -values, a global sensitivity analysis (4) is performed to identify the design parameters with the strongest impact on Cap_{min} , Cap_{max} and ΔCap . Ranking the design parameters according to their impact on Cap_{min} , Cap_{max} and ΔCap prepares the basis for the development of a two-step design approach (5) that leads to a large operating window. The technically feasible designs generated by the sampling are analyzed to deduce design rules of thumb (6) required to determine values for the design parameters to achieve an equipment design with a large operating window. A design is technically feasible, if Cap_{max} is larger than Cap_{min} . Applying a

global sensitivity analysis to develop the two-step design approach (left branch of Figure 4-16) requires the consideration of all sampled designs. It can happen that technically infeasible designs are generated. However, since the impact of a design parameter on for example Cap_{max} is of interest, the technically infeasible designs are no problem. In contrast, to deduce the design rules of thumb (right branch of Figure 4-16) only the technically feasible designs are used in order to generate feasible equipment designs with a large operating window. The software MS Excel and MS Excel VBA are used to implement the method. Each part of the method shown in Figure 4-16 is described in more detail in the following.

4.4.1 Mathematical model

The mathematical model of an apparatus needs to relate the design parameters to the description of the process step occurring in this apparatus. To explore the design parameter space, realistic or usual values or ranges of values of the design parameters need to be defined, based on for example norms and standards, information of manufacturers or the manufacturing process. An important requirement of the overall approach is the possibility to sample all design parameters independently from any design capacity or each other. Hence, adjustments of available models might be necessary to enable an independent sampling of the design parameters. Furthermore, the operating constraints of the considered apparatus need to be identified.

4.4.2 Sampling generation

An efficient sampling technique is required to distribute different apparatus designs in the space of the design parameters with a high coverage at a low number of samples. Classical pseudo-random number generators produce non-uniformly distributed numbers over the input space which results in gaps or clustered areas [57]. To improve the distribution uniformity of sampled points and thus the efficiency of the sampling method, the group of low-discrepancy numbers was developed [57]. By using low-discrepancy numbers, already sampled points are taken into consideration when defining the next sampling point, leading to a so-called quasi-random sampling. Well-established low-discrepancy sequences are for example the Halton [58–60], Faure [61,62], Sobol' [63,64] or Niederreiter [65] sequences. Sobol's sequence is the most popular low-discrepancy sequence due to its simplicity and efficiency of implementation and the good low-discrepancy properties compared to other sequences [66,67]. In this work, the Sobol' sampling based on Joe and Kuo's [68] and Antonov and Saleev's work [64] is used. The Sobol' sequence poses two drawbacks. First, it always provides the same set of sampling points for a given number of samples and dimensions. Thus, a sampling-based statistical error estimation is not possible [69]. The second

disadvantage is the decreasing uniformity of the Sobol sequence with an increasing number of dimensions [67]. To overcome these limitations techniques have been developed to randomize the sampling while maintaining the low-discrepancy properties [70]. These so-called scrambling methods combine low-discrepancy properties of quasi-random samplings and the possibility of a simple statistical error estimation [71]. The scrambling technique called Owen-like scrambling described in [72] is used in this work. In order to implement the Owen-like scrambling in MS Excel VBA, modifications as described in [66] are applied. To transform the quasi-random numbers of the Sobol' and the scrambled Sobol' sequence which lie between zero and one to the discrete design parameters values, the approach presented by Statnikov et al. [73] is used.

4.4.3 Determination of Cap_{min} , Cap_{max} and ΔCap

Depending on the apparatus under consideration, different operating constraints can limit the operating window. Cap_{min} and Cap_{max} for each operating constraint can be determined by calculating the mass flow rate of the process stream at the limiting values of the corresponding operating constraints. To describe the behavior of the apparatus, the related equations are implemented in MS Excel VBA. The mass flow rates of the process stream at the corresponding operating constraints are determined using the Goal Seek function in MS Excel VBA. This process mass flow rate represents the maximum or minimum capacity limitation regarding the related constraint. The same procedure is applied to all operating constraints. Finally, Cap_{max} is described by the minimum mass flow rate of the upper operating constraints and Cap_{min} is described by the maximum value of the lower operating constraints [74]. As a large operating window is the key investigation goal any economically driven design limitations are neglected.

4.4.4 Global sensitivity analysis

To identify design parameters with a big impact on Cap_{min} , Cap_{max} and ΔCap , a global sensitivity analysis is applied. Global sensitivity analysis methods consider the whole parameter range and enable a consideration of parameter interactions, since all input parameters are varied simultaneously [75]. The most frequently used global sensitivity analysis methods are variance-based methods [76] such as the Fourier Amplitude Sensitivity Test (FAST) and the Sobol' method. The main advantage of these methods is the model independence allowing the application to non-linear and complex models. The Sobol' method is used in this work and was implemented in MS Excel VBA. A short description of the method is given in the following:

- Generate two independent ($N_{base} \times k$) input matrices A and B by the sampling method. N_{base} is the number of base samples and can vary from a few hundreds to a few thousands [77]. In case of a Sobol' sampling, a value of 2^n is recommended by Sobol, whereas n is a natural number. The first row of the sequence is discarded to avoid anomalies [78,79]. This results in $N_{base} = 2^n - 1$ base samples. The value of k represents the number of input parameters, in this case the design parameters. Matrix A is generated by the Sobol' sampling and matrix B by applying the Owen-like scrambling to matrix A , as described in chapter 4.4.2.

$$A = \begin{bmatrix} X_{11} & \cdots & X_{1k} \\ \vdots & \ddots & \vdots \\ X_{N1} & \cdots & X_{Nk} \end{bmatrix}; B = \begin{bmatrix} X'_{11} & \cdots & X'_{1k} \\ \vdots & \ddots & \vdots \\ X'_{N1} & \cdots & X'_{Nk} \end{bmatrix} \quad \text{Eq. 4-19}$$

- Generate the matrices A_{B_i} , built up by all columns of A except for the i th column which is taken from matrix B .

$$A_{B_i} = \begin{bmatrix} X'_{1i} & \cdots & X_{1k} \\ \vdots & \ddots & \vdots \\ X'_{Ni} & \cdots & X_{Nk} \end{bmatrix} \quad \text{Eq. 4-20}$$

- Calculate the related model outputs for the input parameters and summarize them into ($N_{base} \times k$) vectors Y , respectively. The total number of required model evaluations amounts to $N_{base} \cdot (2 + k)$.

$$Y_A = f(A); Y_B = f(B); Y_{A_{B_i}} = f(A_{B_i}) \quad \text{Eq. 4-21}$$

- Compute the first-order and total-order sensitivity indices S_i , S_{T_i} and interaction effects E_i based on the related variances Var according to [67,77]:

$$\text{Mean} \quad f_0^2 = \left(\frac{1}{N_{base}} \sum_{j=1}^{N_{base}} Y_A(j) \right)^2 \quad \text{Eq. 4-22}$$

$$\text{Total variance} \quad Var(Y) = \frac{1}{N_{base}} \sum_{j=1}^{N_{base}} Y_A(j)^2 - f_0^2 \quad \text{Eq. 4-23}$$

$$\text{Main effect} \quad Var_{X_i}(E_{X_{\sim i}}(Y|X_i)) = \frac{1}{N_{base}} \sum_{j=1}^{N_{base}} Y_B(j) \cdot (Y_{A_{B_i}}(j) - Y_A(j)) \quad \text{Eq. 4-24}$$

$$\text{Variance that would be left if all factors but } X_i \text{ could be fixed} \quad E_{X_{\sim i}}(Var_{X_i}(Y|X_{\sim i})) = \frac{1}{2N_{base}} \sum_{j=1}^{N_{base}} (Y_A(j) - Y_{A_{B_i}}(j))^2 \quad \text{Eq. 4-25}$$

$$\text{First-order sensitivity indices} \quad S_i = \frac{Var_{X_i}(E_{X_{\sim i}}(Y|X_i))}{Var(Y)} \quad \text{Eq. 4-26}$$

$$\text{Total-order sensitivity indices} \quad S_{Ti} = \frac{E_{X_{\sim i}}(\text{Var}_{X_i}(Y|X_{\sim i}))}{\text{Var}(Y)} = 1 - \frac{\text{Var}_{X_{\sim i}}(E_{X_i}(Y|X_{\sim i}))}{\text{Var}(Y)} \quad \text{Eq. 4-27}$$

$$\text{Interaction effects} \quad E_i = S_{Ti} - S_i \quad \text{Eq. 4-28}$$

The first-order sensitivity index S_i represents the individual effect of the considered design parameter by measuring the main effect on the model output [75]. Therefore, it is the most meaningful index for this work because it represents the importance of a single design parameter. The total-order index S_{Ti} is defined as the sum of first-order plus all higher-order effects and hence, it includes effects due to interactions with other design parameters [75]. Subsequently, the interactions E_i can be calculated by subtracting the individual index from the total sensitivity index. As a result, for example regarding ΔCap , design parameters with a large value of S_i can be used to directly enlarge the operating window. A design parameter with an interaction effect larger than the individual effect can only be used together with other design parameters to enlarge the operating window.

4.4.5 Development of a two-step design approach

From an application point of view, it is reasonable to set the Cap_{\min} - or the Cap_{\max} -value into a desired capacity interval first and subsequently increase the Cap_{\max} -value or decrease the Cap_{\min} -value, respectively, as much as possible. This initial range of Cap_{\min} or Cap_{\max} can be defined by the expected minimum or maximum load of the considered equipment depending on the expected market demand and the companies' strategy. When a company is for example entering a new market, it will probably know the production rate required (Cap_{\min}) and if the market demand increases the equipment should be able to increase the production rate as much as possible. The other case, where Cap_{\max} shall be set at first and Cap_{\min} decreased as much as possible, is for example applicable in times of an economic crisis. If Cap_{\min} is more important and shall be set to a specified range, the main influencing design parameters on Cap_{\min} need to be selected in a first design step to ensure that Cap_{\min} lies in the required range. In a second design step Cap_{\max} should be increased as much as possible. If the main influencing design parameters on Cap_{\min} also have an impact on Cap_{\max} or ΔCap , this needs to be considered in the first design step and Cap_{\min} can be set into a specific range with the possibility towards a large operating window. In the second design step, the main influencing design parameters on Cap_{\max} need to be selected. Afterwards, the non-influential design parameters on Cap_{\min} , Cap_{\max} and ΔCap can be selected. If Cap_{\max} is more important, the approach begins with the selection of the main influencing design parameters on Cap_{\max} , accordingly.

4.4.6 Deduction of design rules of thumb

The approach to deduce design rules of thumb is described for the case that Cap_{min} is set in a first design step and Cap_{max} should be increased in the second design step. To deduce design rules of thumb, all technically feasible designs of the sampling runs are identified, combined and duplicates are deleted, because duplicate designs would get a too great weight in the deduction of the design rules of thumb. In the first design step, the sampled designs are classified into different Cap_{min} -intervals and sorted regarding their relative size of the operating window ΔCap_{rel} which is determined by Eq. 4-29, where Cap_{mean} describes the mean of Cap_{min} and Cap_{max} :

$$\Delta Cap_{rel} = \frac{Cap_{max} - Cap_{min}}{Cap_{mean}} \quad \text{Eq. 4-29}$$

20 % of the designs with the largest ΔCap_{rel} in each Cap_{min} -range form the basis to deduct design rules of thumb. The design rules of thumb are deduced by analyzing changes in the frequency distributions of the design parameter values over the different capacity intervals. For example, if the tube diameter of a shell and tube heat exchanger changes over the capacity intervals from a smaller to a larger value with an increasing capacity interval, the different tube diameters for each capacity interval can be used as design rule of thumb. If no such characteristic changes in the frequency distributions of the individual design parameters over the different capacity intervals can be identified, characteristic ratios of design parameters as the length to diameter ratio can be considered, depending on the type and function of the apparatus under consideration. In the second design step the sampled heat exchanger designs in the Cap_{min} -intervals are sorted by Cap_{max} to maximize the values of Cap_{max} . The design rules of thumb for the second design step are again deduced as described for the first design step.

4.5 Economic evaluation methods

4.5.1 Total capital investment (TCI)

The calculation of the total capital investment is based on the equipment costs of a plant. Free on board costs (FOB) refer to the costs of the assembled equipment ready for shipment. They are calculated with the capacity method shown in Eq. 4-30 [38]:

$$FOB = FOB_{ref} \cdot \left(\frac{size}{size_{ref}} \right)^{CEX} \cdot \frac{CEPCI}{CEPCI_{ref}} \quad \text{Eq. 4-30}$$

The costs of an equipment are determined in regard to a reference equipment with the costs FOB_{ref} and a characteristic reference size $size_{ref}$. The cost capacity exponent CEX describes the dependency between costs and size of the equipment. The Chemical Plant Cost Index

(CEPCI) accounts for the price development of chemical processing equipment. The current CEPCI as well as the $CEPCI_{ref}$ are used to adapt the price of the equipment to the current price level.

To calculate the TCI, the FOB costs are multiplied with factors that consider further expenses like delivery, plant construction, assembly and overhead costs (see Table A.1-2). The costs for instrumentation and control systems are considered with a fixed value for each equipment, because the expenses for a control system are nearly independent of the equipment size. Exemplarily for two small equipment items, the instrumentation costs are doubled in comparison to one bigger equipment. The instrumentation costs do not include control valves which have to be considered separately. The costs for engineering and construction are set to 35 % of the direct plant costs (DPC) as shown in Table A.1-2.

4.5.2 Operating expenditures (OPEX)

To calculate the OPEX, manufacturing costs for raw material \dot{C}_{RM} and utilities \dot{C}_{Uti} are summed up according to Eq. 4-31:

$$OPEX = \sum \dot{C}_{RM} + \sum \dot{C}_{Uti} \quad \text{Eq. 4-31}$$

Hence, indirect variable costs like costs for license fees and research expenses are not considered in OPEX calculation.

4.5.3 Net present value (NPV)

The NPV is a measure for the profitability of an investment taking the time value of money into account. In order to calculate the NPV, the free cash flow (FCF) needs to be determined first, representing the difference in yearly cash inflows and cash outflows. For the FCF determination, the net sales, the variable and fixed costs as well as taxes and depreciation are considered as shown in Table A.1-3. Net sales as well as variable costs are calculated from the mass and energy balance in Aspen Plus®. The NPV calculation shown in Eq. 4-32 discounts all free cash flows in the project lifetime t to their present value [80].

$$NPV = \sum_i^t \frac{FCF_i}{(1+r)^i} \quad \text{Eq. 4-32}$$

These cash flows include investments, either the initial investment $TCI_{initial}$ or investments for capacity expansions, as well as yearly profits in terms of the FCF. The net sales as well as the variable costs are calculated for each month and discounted to the middle of a year.

4.5.4 Equivalent annual annuity (EAA)

The EAA normalizes the absolute profit in terms of the NPV to a single year. Hence, NPV and EAA determine the absolute profit of an investment, whereby the EAA enables the evaluation

and comparison of projects with unequal durations [81]. The EAA is calculated as shown in Eq. 4-33 [80].

$$EAA = \frac{r \cdot NPV}{1 - (1 + r)^{-n}} \quad \text{Eq. 4-33}$$

The EAA can be interpreted as a mean amount of cash that could be drawn yearly out of the investment over a period of n years. It also uses the calculatory interest rate r .

4.5.5 Modified internal rate of return (MIRR)

The MIRR measures the relative profit and is calculated as shown in Eq. 4-34 [81]. The FCF of every year t is set in relation to every investment over the regarded time span n . Hence, the MIRR is the rate, with which all money invested in a project earns interest in a single year.

$$MIRR = \sqrt[n]{\frac{\sum_{t=0}^n FCF_t (1 + r)^{n-t}}{\sum_{t=0}^n TCI_t (1 + r)^t}} - 1 \quad \text{Eq. 4-34}$$

The equation assumes that all cash flows are reinvested at the calculatory interest rate r . Therefore, it gives a more realistic approach in contrast to the unmodified internal rate of return, where reinvestments grow with the internal rate of return itself [81].

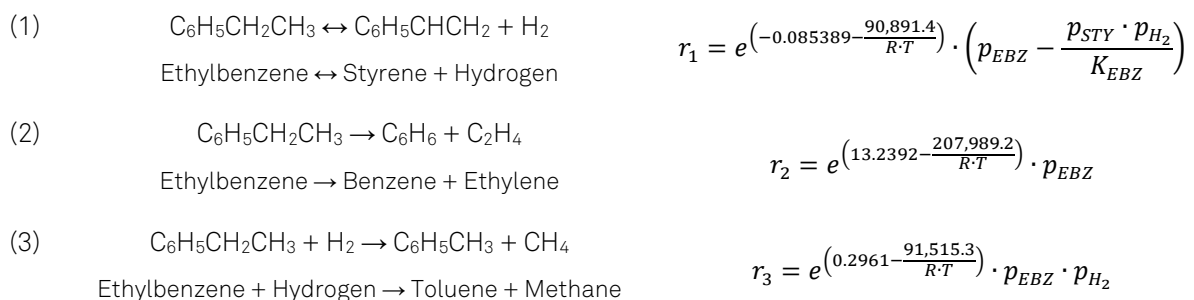
5 Example processes

Different example processes are used to illustrate, apply and evaluate the methods developed in the scope of this work. The detailed description of the example processes and their implementation shall give the ability to validate the results and enable researchers to utilize the example processes of this work for future investigations. In the following, the three example processes, their implementation in Aspen Plus® V8.4 and the generation of the equipment module database will be described. With the styrene and acetone production, two continuous chemical example processes of bulk products are used, whereas the succinic acid example process represents a small-scale biochemical process utilizing a fermentative batch reaction.

5.1 Styrene production process

The determination of a plants' overall operating window and the selection of equipment modules for a constant market demand development is demonstrated using the example of a styrene production plant. Styrene is an important industrial unsaturated monomer mainly used for polystyrene production. About 85 % of the commercially available styrene is produced via the direct dehydrogenation of ethylbenzene to styrene [82], which is also considered in this work.

The endothermic reaction is carried out in vapor phase, whereby the main reaction is the reversible endothermic conversion of ethylbenzene to styrene and hydrogen (1). As it is a reversible vapor-phase reaction producing 2 moles of product from 1 mole of ethylbenzene, low pressure favors the forward reaction. Considered thermal side reactions are the irreversible decomposition of ethylbenzene to benzene and ethylene (2) and the irreversible hydrodealkylation of ethylbenzene to toluene and methane (3). A steam injection is used to supply the necessary heat of reaction and to clean the catalyst by reacting with carbon to produce CO₂ and H₂ [82]. To describe the reaction kinetics the pseudo-homogeneous kinetic model from [83] is used, as summarized below:



The kinetic model neglects the side reactions (4) to (6) described by [83] involving steam. The equilibrium relation for reaction (1) is summarized by Eq. 5-1 to Eq. 5-3 based on [83].

$$K_{EBZ} = e^{\left(\frac{-\Delta F_0}{R \cdot T}\right)} \quad [bar] \quad \text{Eq. 5-1}$$

$$\Delta F_0 = a + bT + cT^2 \quad \left[\frac{kJ}{kmol} \right] \quad \text{Eq. 5-2}$$

$$K_{EBZ} = e^{\left(\frac{-122,725.157 + 126.267 \cdot T + 2.194 \cdot 10^{-3} \cdot T^2}{R \cdot T}\right)} \quad [bar] \quad \text{Eq. 5-3}$$

The flowsheet of the styrene production process is extended and refined based on [84] and [85] and shown in Figure 5-1. In a first step, the ethylbenzene feed EBZ is evaporated in heat exchanger HX1 using high-pressure steam (HPS). The subsequent superheater HX1B uses hot flue gas (FG). Afterwards, 42 bar superheated steam from the fired heater FH is injected to increase the inlet temperature of the first reactor to 640 °C [82]. Since the endothermic reaction in the adiabatic fixed-bed reactor R1 leads to a temperature decrease, the reactor outlet stream is heated up again to 640 °C by superheated steam before it enters the second adiabatic reactor R2. The outlet stream of reactor R2 is cooled and partially condensed by the heat exchangers HX3 and HX4 using boiler feed water (BFW), while high-pressure steam (HPS) and low-pressure steam (LPS) are generated, respectively. Heat exchanger HX5 cools the stream down to 60 °C with cooling water (CW) before mainly hydrogen is removed from the cooled product stream in a two-phase separator F1.

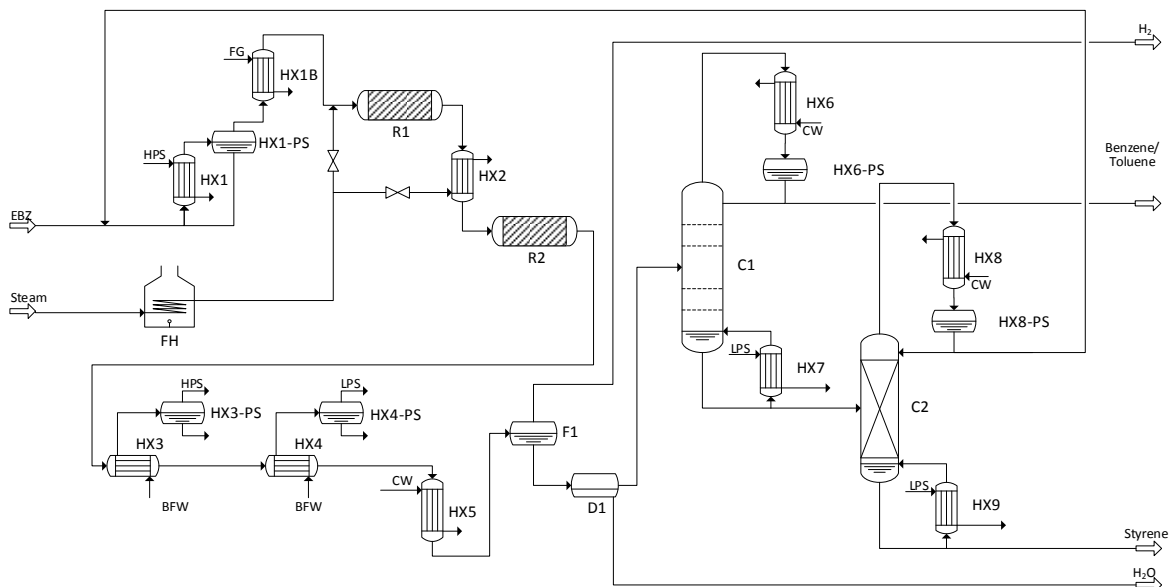


Figure 5-1: Flowsheet of styrene production process (partly based on based on [84,85])

The two-phase liquid stream consisting of a water- and a styrene-rich phase is fed to decanter D1 where the water phase is removed. Column C1 separates benzene and toluene from the styrene-rich stream coming from decanter D1. In column C2 the main product

styrene is purified to the final product purity of 99.9 wt.-%. The unconverted EBZ is recycled and mixed with the EBZ-feed stream. Within this work, all process units except for the fired heater FH are considered for the selection of equipment modules.

The target production rate of 20 kt/a is ensured by a design specification varying the EBZ feed stream. This target production rate is oriented at [86], whereas nowadays styrene production plants have a capacity of several hundred kt/a [87]. The Peng–Robinson equation of state is chosen as property method [85,88]. Further boundary conditions and the specifications of the available utilities are summarized in Table A.2-1.

To model the adiabatic fixed-bed reactors, the adiabatic *RPlug* model is used with a catalyst bed voidage ϵ of 0.4 and the corresponding catalyst mass. To consider the effect of a lower packing density at the tube walls, the pressure drop calculation according to [89] is implemented via calculator blocks as described in appendix A.6.1. To reduce simulation time, the detailed *RPlug*-calculations are isolated from the overall flowsheet simulation. Therefore, the reactors are simulated using shortcut *RStoic* models within the flowsheet. This assures a fast convergence of the flowsheet including all recycle streams. The resulting inlet conditions of the *RStoic* models are transferred to the *RPlug* models using *Transfer* blocks, where the reactors are rigorously simulated. The results of the detailed *RPlug* models as fractional conversion and pressure drop are transferred back to the *RStoic* models. To ensure that the shortcut models have the same results as the detailed *RPlug* models, a synchronization takes place via Excel VBA until the pressure drops of both models show a deviation below 1 %. The reactor equipment modules are designed for three cases in which one to three reactors are used in parallel. Both reactors R1 and R2 have equal length and diameter. The reactor length is determined by a design specification such that the pressure drop in R1 is 0.2 bar [90]. An overall conversion of 65 % [82] is ensured by changing the diameter of the reactor via a design specification. The resulting L/D-ratio of 0.8 is comparable to [86,91]. Based on this L/D-ratio of 0.8 the volume is varied by ± 15 % and the L/D-ratio by ± 0.2 to obtain different reactor module sizes for the equipment module database. The use of discrete diameter steps of 0.05 m leads to slight variations in the overall reactor volume. However, differences to the calculated volume are less than 5 %. This procedure ensures that the conversion, which among others strongly depends on the reactor volume, varies in a small range around 65 %. Additionally to the length and diameter, the catalyst mass is determined using a catalyst bulk density of 2 146.27 kg catalyst per m³ reactor [83,86,91]. The reactor equipment modules determined are summarized in appendix A.2.4.

The heat exchangers take a special position as they are simulated using Aspen Shell & Tube Exchanger Design & Rating (EDR) V8.4. This allows for a rigorous modeling of the heat exchangers that can be directly connected to a *HeatX*-model block. To reduce simulation time, the EDR-calculations are isolated from the overall flowsheet simulation. In a first step, all heat exchangers are simulated using shortcut models as *HeatX* blocks or a combination of two *Heater* blocks with an *HXFlux* block. This assures a fast convergence of the flowsheet including all recycle streams. The specifications of the implemented shortcut *HeatX* or *HXFlux* models are summarized in Table A.2-2. The resulting process requirements of the heat exchangers are subsequently transferred from the shortcut models to the detailed EDR simulations. Since the EDR models are not directly within the overall flowsheet, potential errors in the EDR simulations cannot affect the remaining flowsheet convergence iterations. This enables a separate check whether the heat exchangers are operable or not. In case all heat exchangers operate properly, a synchronization takes place. This approach allows to check, whether the heat exchangers can be operated together. Via Excel VBA the calculated pressure drops of the EDR models are written to the shortcut models. Next, the whole flowsheet is simulated again and the operability of each unit is checked. This is done iteratively until the pressure drops of both models deviate less than 1%. This synchronization concept offers the advantage that the shortcut models of the heat exchangers provide good initial values for the required utility flow rates helping to either avoid convergence problems or excessive computation times. These initial values of the utility flow rates are corrected in the rigorous EDR simulations to consider the excess heat exchange area of the heat exchangers. The heat exchanger equipment modules are designed for seven different cases in which the inlet streams to each heat exchanger are adjusted by multiplication blocks. The factors 0.4, 0.5, 2/3, 1, 1.5, 2, 2.5 are used, resulting in seven heat exchanger modules for each of the ten heat exchangers as summarized in Table A.2-6 to Table A.2-15 of appendix A.2.4.

Both distillation columns are simulated with the *RadFrac* model, whereas C1 is a tray column with a partial-vapor condenser and C2 is a packed column with a total condenser. The numbers of theoretical plates *NTP* and the feed stage are determined as described in appendix A.5.2. A summary of the design parameters is given in Table A.2-3. Sinnott recommends sieve holes with a diameter of $d_h = 5$ mm [92]. The ratio of hole area to active area is set to 12% and the tray spacing to 0.6 m as suggested by Coker [93]. To determine the maximum flooding factor of the sieve tray column C1 the constant K_1 is determined to 0.1 [92]. The structured packing MellapakPlus 252.Y from SULZER is used column C2. The HETP value (height equivalent of a theoretical plate) is taken from *SULZER* as 0.38 m. After

determining the basic design parameters of the distillation columns C1 and C2, the column equipment modules for both columns are designed for three cases in which one to three columns are used in parallel and the *NTP* is varied by ± 5 stages. This results in nine different column equipment modules for C1 and C2, respectively. The determined diameter is rounded up to the next norm diameter of DIN 28105:2002-0 [94]. The adjacent larger and smaller norm diameters are also included. This results in 27 column equipment modules for C1 and C2, respectively, summarized in Table A.2-5.

All vapor-liquid separators are implemented using a *Flash2* model block. The equipment modules for the vapor-liquid separators are designed based on the volume flow rates and densities of the gas and liquid stream. Due to a large liquid volume fraction compared to the gas volume fraction, horizontal vapor-liquid separators are used. The resulting diameters and lengths are rounded up to the first digit. Since the vapor-liquid separation factor *S.Fac* for C2-COND-PS calculated according to Eq. A5-13 is not in the range of validity [95,96], the maximum velocity is set to 0.15 m/s [97]. To generate an equipment module database for the vapor-liquid separators, the heat exchanger modules designed are utilized in combination with their corresponding multiplication factors. The same multiplication factors are applied to the vapor-liquid separators. Afterwards, the volume flow rates and densities of the vapor and liquid streams are used as basis for vapor-liquid separator design. In cases where no heat exchanger module could be designed, the multiplication factors for the vapor-liquid separators are applied and the nearest heat exchanger equipment modules are utilized. Additionally to the heat exchanger multiplication factors, 1/3 and 3 are used to design the vapor-liquid separator equipment modules. This results in 9 different vapor-liquid separator modules for each vapor-liquid separator (see Table A.2-17).

The decanter is modeled using a *Decanter* model block. The dispersion factor *c* determined by Eq. A5-17 with a value of 0.351 indicates that the light phase, mainly styrene, should be the dispersed phase. To design the decanter modules the norm diameters according to DIN 28105 [94] are used. A diameter of the vessel which results in $7\,000 < Re < 8\,000$ is selected. The calculated total length L_{tot} is rounded up to the next 0.05 m. In order to create an equipment module database the three smaller and larger normed diameters of the first selected one are picked. The corresponding total length L_{tot} is determined and rounded up accordingly. By this 7 equipment modules are designed. In addition, the process stream is divided by 2 and 3 and the described procedure is repeated. Using the exact flowrates from the simulation file would lead to a design at the upper operating limit of the decanter. To allow larger flowrates a design flowrate of 110 % is used for the described decanter design. This results in 21 decanter modules for the decanter D1 (see Table A.2-16).

To model different numbers of equipment modules used in parallel for a process unit, *Multiplicator* blocks are used before and after each process unit.

5.2 Acetone production process

The example process of producing acetone via the dehydrogenation of isopropanol (IPA) is used to select equipment modules for a market demand development and to compare different capacity expansion strategies.

The dehydrogenation of IPA has been an important route to produce acetone. In 1970 approximately 50-60 % of the total US acetone production was based on this route, whereas nowadays, the cumene oxidation process with acetone as co-product is the main source of worldwide acetone [98]. However, the dehydrogenation of IPA is still a viable alternative. Its main advantage is the absence of aromatic impurities, particularly benzene. For this reason, acetone produced by IPA may be preferred by the pharmaceutical industry due to the tight restrictions placed on solvents by the Food and Drug Administration (FDA) [84].

Table 5-1 summarizes the reaction equations and the kinetic data of the reversible dehydrogenation of IPA to acetone and hydrogen and the most important side reaction, the dehydration of IPA to propene and water [98]. The reaction rates and activation energies are taken from Luyben [99]. These activation energies were confirmed by [100,101]. The dehydration of IPA to propene and water as most important side reaction was unfortunately neglected by Luyben and other authors and thus no kinetic data are available. However, selectivity is a major concern for the design of a reactor and will be especially important for the calculation of its operating boundaries. Hence, a kinetic equation was generated in this work. The side reaction is assumed to be a first order reaction and irreversible as the equilibrium conversion is determined to 88 % using an *RGibbs* reactor model. Activation energies of the dehydration are available from [100]. The side reaction has a higher activation energy compared to the main reaction and thus, is promoted by higher reaction temperatures. The ratio of the activation energies of the main to the side reaction of Rioux were applied to the activation energy used by Luyben, resulting in 77 430 kJ/kmol. Finally, the rate constant k needs to be determined. Patents show a selectivity of acetone of around 99 % for the specified conversion of 90 % [102,103]. Hence, the side reaction is kinetically controlled. A rate constant k is determined to reach similar results. At its design production rate, the reactor operates at 90 % conversion. Since in this work not only the design production rate is considered, the reactor is also operated at flow rates below this design production rate. With a decreased throughput, the residence time in the reactor increases, leading to a decreased selectivity. For the reactor design it is assumed that the reactor has to operate above 99 % selectivity, when the reactor is operated at 70 % of its design

production rate. The rate constant k of the side reaction is determined to 154 s^{-1} such that both conditions are fulfilled.

Table 5-1: Kinetics of IPA dehydrogenation [99] and dehydration

	r [kmol/(s·m ³)]	k	E_A [kJ/kmol]
Dehydrogenation (main reaction)			
<i>IPA</i> ↔ <i>Acetone</i> + H_2	(forward) $r = c_{IPA} \cdot k \cdot e^{\frac{-E_A}{RT}}$	^a $22 \cdot 10^6$	72 380
$(\Delta H_R = +62.9 \text{ kJ/mol})$ [99]	(reverse) $r = c_{Ace} \cdot c_{H_2} \cdot k \cdot e^{\frac{-E_A}{RT}}$	^b 1000	9 480
Dehydration (side reaction)			
<i>IPA</i> → <i>Propene</i> + H_2O	$r = c_{IPA} \cdot k \cdot e^{\frac{-E_A}{RT}}$	^a 154	77 430
$(\Delta H_R = +50.6 \frac{\text{kJ}}{\text{mol}})$ [104]			
^a k in [s^{-1}] for dehydrogenation (forward) and dehydration			
^b k in [$\text{m}^3/(\text{kmol s})$] for dehydrogenation (reverse)			

Plant design and process parameters used in this work are based on a publication of Luyben [99]. The basic flowsheet is shown in Figure 5-2. An azeotropic mixture of IPA (67 mole-%) and water enters the process as feed at 1 atm. It is mixed with the recycle of unreacted IPA and water and its pressure is raised to 18 atm in pump P1. Afterwards, the process flow is vaporized in HX1 using high-pressure steam (HPS) at 45 bar. All evaporators in this process are designed as forced circulation evaporators, whereby 15 % of the process stream is evaporated. The remaining liquid is separated in the vapor-liquid separator HX1-PS and recycled back to the heat exchanger HX1. After its evaporation, the process stream is fed to the multi-tubular reactor R1, where the gas phase catalytic reaction occurs. The reaction is endothermic and heated counter currently by molten salt (MS). The mixture enters the reactor as saturated vapor at around 200 °C. The first section of the reactor does not contain catalyst in order to overheat the stream to 250 °C and thereby avoiding condensation at the catalyst pellets. The reaction mixture leaves the reactor at around 480 °C and is partially condensed and cooled down to 47 °C in the two subsequent heat exchangers HX2 and HX3. The first condenser HX2 operates with boiler feed water (BFW) at 5 bar, while low pressure steam (LPS) is generated. HX3 is operated with cooling water (CW) at 20 °C. The remaining vapor fraction of the reactor product stream is removed in vapor-liquid separator HX3-PS. This gas stream mainly consists of hydrogen as well as the main fraction of propene. However, it also contains acetone and IPA, which are washed out in the absorption column AB1 using water. Thereby, 99 mole-% of the gaseous acetone is recovered and mixed with the liquid flow of HX3-PS. This mixture enters the distillation column C1, where acetone is

separated from the process stream. The column uses a partial condenser C1-COND and the acetone product stream leaves as condensate. The purity of the acetone product stream is set to 99.8 mole-%. The vapor that leaves the partial condenser C1-COND consists of remaining hydrogen. The bottom stream of distillation column C1 consists of unreacted IPA and water. To recycle unreacted IPA, the bottom stream of column C1 is sent to a second distillation column C2. The distillate stream of column C2, a near azeotropic mixture¹ of IPA (65 mole-%) and water, is recycled back and mixed with the feed stream. Excess water is removed at the bottom of C2 with an impurity of 0.1 mole-%. Both distillation columns are tray columns and operate at atmospheric pressure. The condensers C1-COND and C2-COND use cooling water, the reboilers C1-REB and C2-REB use low-pressure steam (LPS) at 5 bar.

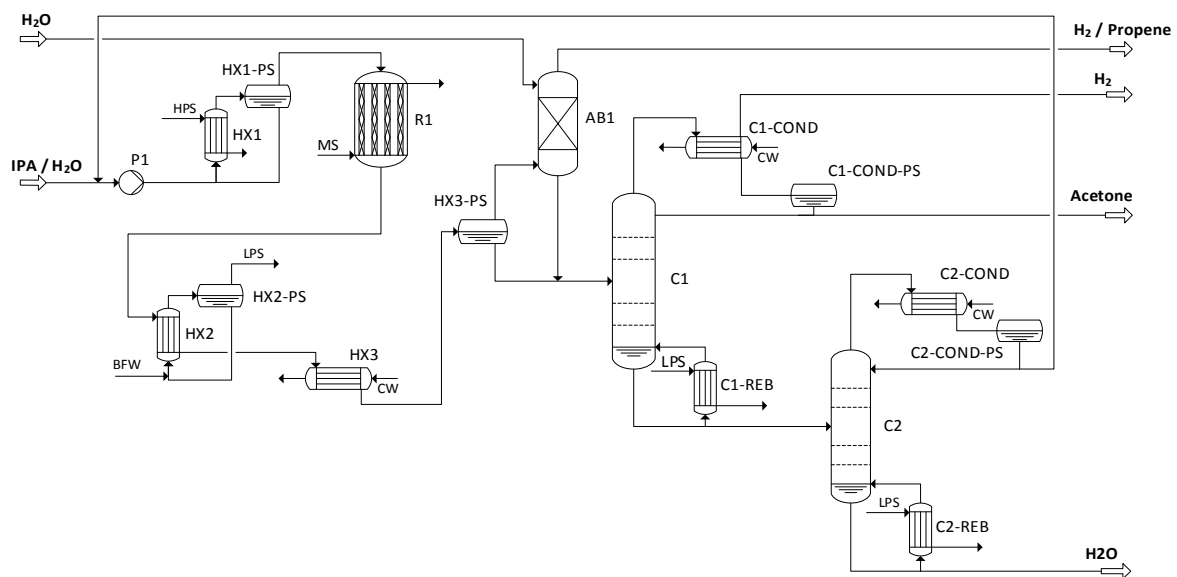


Figure 5-2: Flowsheet of acetone production process (based on [99])

All process units described except pump P1 are considered for the capacity expansion strategies. The target production rate is ensured by a design specification varying the flow rate of the feed stream. The UNIQUAC property method is used [84,99].

To design equipment modules the process is simulated at ten different production rates from 7 to 70 kt acetone and 8000 operating hours per year. For each of these production rates, all process units are designed conventionally which results in up to ten different equipment modules per process unit. The number of equipment modules per process unit may be less than ten, because two different production rates can lead to the same design based on the discrete design parameter values used.

¹ Azeotropic mixture at atmospheric pressure is 67 mole-% IPA and 33 mole-% water ([99])

Since the heat generation potential q_p of the main reaction is with 17.5 larger than ten, a multi-tubular reactor is used [105]. The heat for the reaction is supplied by molten salt at a temperature of 761 K, whereby the temperature change along the reactor is assumed to be constant [99]. The detailed design procedure of the multi-tubular reactor modules is described in appendix A.5.4. It results in tubes with a diameter of 25 mm and a tube length L_T of 4.35 m filled with catalyst. Adding the overheating section results in a total tube length of 4.7 m. The pressure drop in the reactor tubes is calculated as described in appendix A.6.1 and the calculation of the heat transfer is described in detail in appendix A.5.4. *Calculator* blocks are used to implement the calculations of pressure drop and heat transfer in the multi-tubular reactor model block *RPlug*. The detailed *RPlug*-calculations are isolated from the overall flowsheet simulation as described for the styrene production process in the previous chapter 5.1.

The heat exchangers are rigorously modeled using Aspen EDR with the synchronization concept described in the previous chapter 5.1. The specifications of the shortcut *HeatX* models are summarized in Table A.3-1. The heat exchanger modules are designed as described in appendix A.5.1 using Aspen EDR. Both distillation columns C1 and C2 are modeled using the *RadFrac* model with the parameters described in the previous chapter 5.1. The numbers of theoretical plates *NTP* and the feed stage are determined as described in appendix A.5.2 and a summary of the design parameters is given in Table A.3-2. Internal *Design Specs* of the *RadFrac* model block are used to assure the specified purities by varying the reflux ratio and the distillate to feed ratio. The randomly packed absorption column AB1 is modeled using a *RadFrac* model block. Applying the general conventional design calculations as described in appendix A.5.3 leads to an *NTP* of 9. However, based on economic considerations by Luyben [99], an *NTP* value of 10 is used. Raschig rings with a diameter of 25 mm are used as internals [84] resulting in a *HETP* value of 0.649. A *Desig Spec* is used to achieve an acetone yield of 99 % [99]. All vapor-liquid separators are implemented using a *Flash2* model in Aspen Plus®. Due to a large liquid volume fraction compared to the gas volume fraction, horizontal vapor-liquid separators are used. The equipment modules for the vapor-liquid separators are designed based on the volume flow rates and densities of the gas and liquid stream from the Aspen Plus® simulation as described in detail in appendix A.5.5. It is assumed that for horizontal separators the vapor flow \dot{V}_V makes up 15 % of the cross-sectional area and the liquid surge volume is 85 % [106]. The resulting diameters and lengths are rounded up to the first digit.

Since a reactor is often an expensive process unit, it plays a major role in capacity expansion strategies. Reactors with a larger operating window require less expansion steps within a

capacity expansion strategy and might consequently be economically advantageous. Therefore, an approach to design reactor modules with a larger operating window is proposed and investigated in light of equipment-wise capacity expansions. For many applications, the reactor selectivity is important and is therefore regarded as operating constraint that limits the operating window. A parameter that influences selectivity is the conversion, since for many reaction systems, the selectivity decreases with increasing conversion. Examples are reactions occurring in series or parallel [107]. Figure 5-3 shows a typical concentration progress of reactions occurring in series.

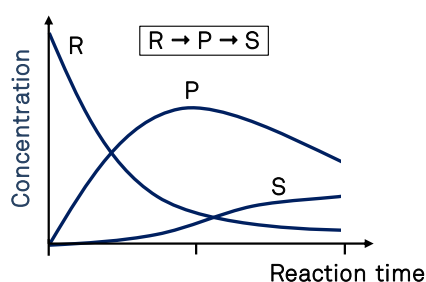


Figure 5-3: Concentration profile for a serial reaction (modified from [107])

With an increasing concentration of product P, the consecutive reaction towards the side product S will be enhanced and thereby the selectivity towards P decreases. In case of parallel reactions, high conversions can also result in a lower selectivity, for example due to different reaction orders [107], required temperature profiles that promote the side reactions [108] or equilibrium reactions which have slower reaction rates near the equilibrium conversion. A favorable operating point of a reactor is often a trade-off between conversion and selectivity [109]. On the one hand, costs related to the recycle of unreacted raw material favor high conversion. On the other hand, costs related to reactant loss or side product separation favor high selectivity [110,111]. A lower conversion also leads to smaller reactor sizes and consequently decreased investment costs. The trade-off between conversion and selectivity in case of the dehydrogenation of IPA to acetone is shown in Figure 5-4. It can be seen that with increasing conversion, the selectivity decreases.

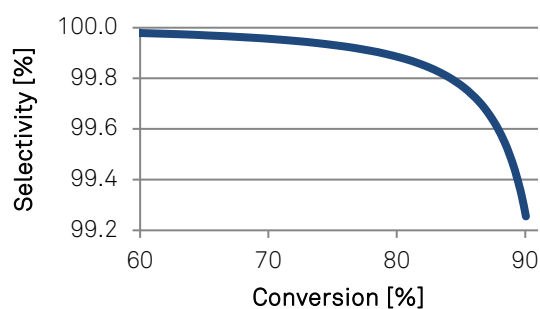


Figure 5-4: Reactor selectivity plotted over IPA-conversion

To enlarge the operating window of a reactor module, the reactor modules are designed for a lower conversion of 85 % instead of 90 % as in the conventional case. This leads to an increased selectivity enlarging the operating window in terms of the selectivity operating

constraint. The resulting total tube length for the reactor with a larger operating window is 3.5 m compared to the 4.7 m for a conversion of 90 %. The resulting increase in operating window is illustrated in Figure 5-5 where the reactor is simulated over a range of different production rates described as capacity factor Cap_{fac} . The operating window of the reactor modules could be increased by approximately 34 %.

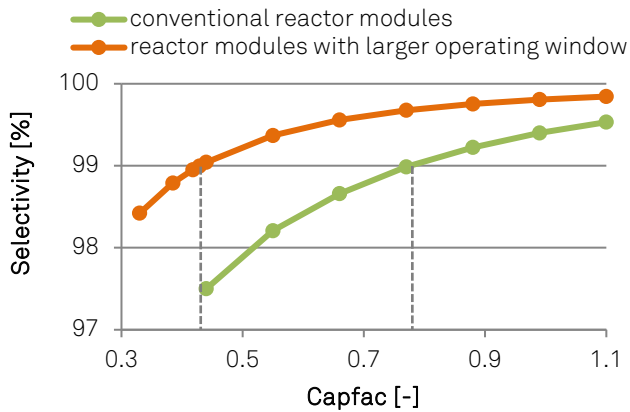


Figure 5-5: Comparison of reactor selectivity at different production rates for the conventionally designed reactor modules and the reactor modules with a larger operating window (dashed grey lines indicate lower selectivity operating constraint, Cap_{fac} = ratio of simulated production rate to a reference production rate)

All resulting equipment modules of the acetone process are summarized in appendix A.3.4. The correlation exponents of the operating constraints are determined by simulating different production rates in 5 %-steps from 50 % to 130 % of the target production rate of 28 kt/a. The resulting correlation exponents of each process unit and its operating constraints of the conventional plant are summarized in Table A.3-9.

5.3 Fermentative succinic acid production

The biochemical production of succinic acid via batch fermentation from crude glycerol is used as case study to apply and evaluate the proposed preselection approaches to decide on the use of equipment modules.

Succinic acid is a platform chemical with a high potential. An estimated global succinic acid market of around 50 kt/a in 2016 is expected to reach approximately 94 kt/a in 2025 [112]. Currently, it is mainly synthesized from petrochemicals via hydrogenation of maleic acid [113]. However, crude glycerol is a co-product in biodiesel production with a large-scale availability at low costs [114] and offers a promising alternative for succinic acid production. To model the succinic acid production by *Actinobacillus succinogenes*, the unstructured kinetic model that considers substrate and product inhibition of [114] is used. Due to the very low byproduct formation of acetic acid and formic acid with respect to succinic acid, it is assumed that the byproducts do not affect the specific growth rate or the substrate mass balance [114]. The initial glycerol and dry cell weight concentration is adjusted to 21.5 g/L and 0.2 g/L, respectively. If the residual concentration of glycerol in the fermenter is below zero or if the final concentration of succinic acid exceeds a concentration of 29.3 g/L, the

fermentation is stopped. The limit of the maximum succinic acid concentration is set to consider the maximum achieved concentration in experimental studies [114].

The process flow diagram used in this work as shown in Figure 5-6 is partly based on the process description by Vlysidis et al. [115]. Crude glycerol from biodiesel production consisting of 80 wt.-% glycerol, 19 wt.-% water and 1 wt.-% methanol is used as feedstock and diluted with process water to adjust the initial glycerol concentration to 21.5 g/L for the batch fermentation, including the inoculum. Next, the mixed stream is continuously sterilized using low-pressure steam (LPS) in heat exchanger HX1 by raising the temperature up to 140 °C [116] and the pressure to 4 bar. After sterilization, the stream is cooled down in HX2 to the fermentation temperature of 37 °C [114]. In the fermenter, 1 vol.-% inoculum is added containing the microorganism *Actinobacillus succinogenes*, yeast extract, anti-foam and glycerol that initializes the anaerobic, exothermic fermentation described by Eq. 5-4:



Besides CO_2 for succinic acid production, *Actinobacillus succinogenes* is capnophilic, grows better and forms less ethanol under a surplus of CO_2 [117]. To keep the pH value between 6 to 7.4 during acid formation [117], sodium hydroxide is added continuously [118]. Since the fermentation takes place in batch fermenters, buffer tanks before and after the fermentation are installed. The rotary drum vacuum filter RDVF1 is operated at 0.7 bar to separate the residual biomass from the product stream leaving the fermenter [115]. Afterwards, water and most impurities are separated in the three forced circulation evaporators HX3, HX4 and HX5 to a concentration of 485 g/L succinic acid. The succinic acid concentration of 485 g/L after water separation is chosen to the solubility of succinic acid at 70 °C [119]. In the subsequent crystallizer cascade CrystCas, succinic acid crystals are formed due to its lower solubility in water compared to the byproducts acetic and formic acid and their salt forms [119]. Total supersaturation reduction is assumed in each of the four mixed-suspension mixed-product-removal (MSMPR) crystallizers, which are arranged in a cascade. A temperature of 20 °C in the last crystallizer is chosen to enable the use of moderately low temperature refrigerated water as utility stream with an inlet temperature of 5 °C and an outlet temperature of around 15 °C [84]. The temperature steps in the four-staged MSMPR crystallizer cascade are set to 64.4 °C, 56.5 °C, 44.4 °C and 20.0 °C to achieve an equal yield in each crystallization vessel. After the last crystallization vessel, the remaining succinic acid in solution amounts to 62.0 g/L.

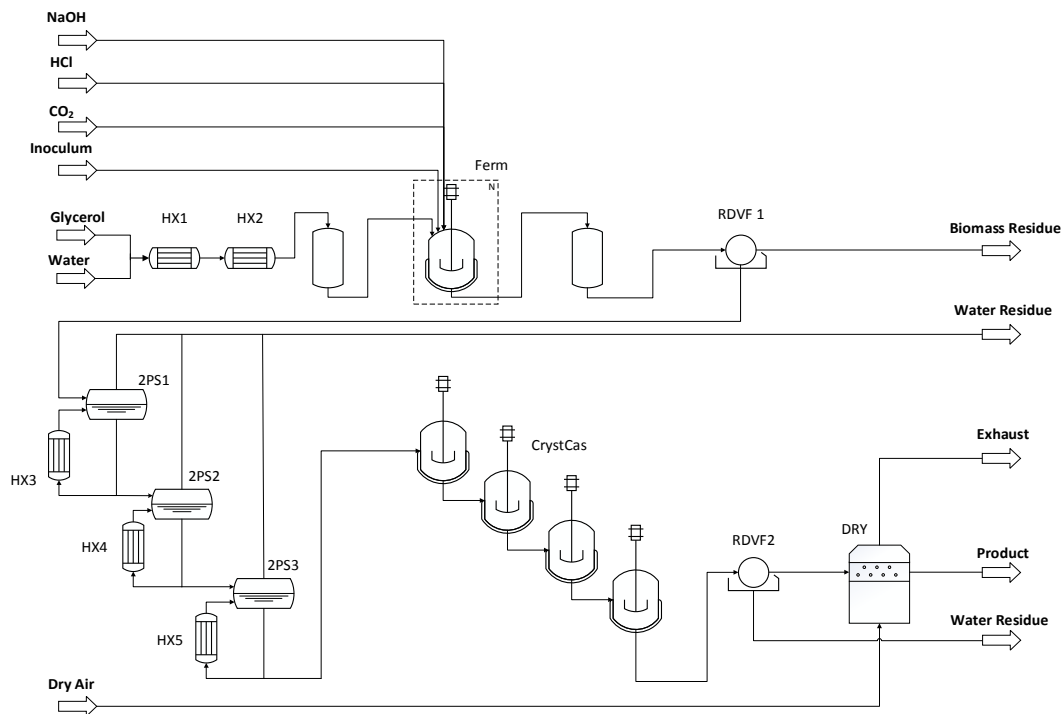


Figure 5-6: Flowsheet of the fermentative succinic acid production process (partly based on process description of [115])

To separate the crystals from the liquid phase, an additional rotary drum vacuum filter RDVF2 operating at 0.69 bar is used before the succinic acid crystals are dried with 125 °C hot air in the fluidized bed dryer DRY.

All process units described except the buffer tanks are considered for equipment module selection. The target production rate amounts to 4 kt succinic acid per year.

The described fermentative succinic acid production process from crude glycerol is implemented in Aspen Plus® V8.4, where the entire mass and energy balance is modelled, and MATLAB 2010, which is used to model the fermentation kinetics and the fermenter scheduling for each Aspen Plus® run. The target production rate is ensured by a design specification varying the flow rate of the feed stream. As global property method, SOLIDS is used to account for the microorganisms in the fermenter and the succinic acid crystals in the crystallizer cascade and the subsequent process units. Additionally, NRTL-HOC is used for the heat exchangers and the vapor-liquid separators to better estimate the non-ideal behavior caused by the carboxylic acids forming dimers in the vapor phase. To model the batch fermenters in Aspen Plus® a *User2* model is used transferring inlet stream data from Aspen Plus® via MS Excel to MATLAB where the reaction kinetics and a batch sequence determination are implemented (see appendix A.5.7 for details). The composition of the inoculum is adopted from experiments [114] in small anaerobic reactors using the most relevant ingredients, whereby magnesium carbonate is equimolarly replaced by hydrochloric

acid and sodium hydroxide. Yeast extract of the inoculum is considered as L-Glutamic acid in the process simulation. The heat exchangers are rigorously modeled using Aspen EDR with the synchronization concept described in chapter 5.1. The specifications of the shortcut *HeatX* models are summarized in Table A.4-3. The heat exchanger modules are designed as described in appendix A.5.1 using Aspen EDR. All vapor-liquid separators are implemented using a *Flash2* model. Both rotary drum vacuum filters RDVF1 and RDVF2 are modeled using a *Drum Filter* model. The Brownell filtration is used and washing and deliquoring are not taken into account. It is assumed that the filter cake is incompressible and that the separation efficiency of solids equals one. Thus, the filtrate does not contain any remaining solids. All required input parameters of RDVF1 and RDVF2 in design mode are listed in Table A.5-5. The *Crystallizer* model block is used together with the temperatures and the solubility curve to model the crystallizer cascade. To model the fluidized bed dryer a convective *Dryer* model with cross-flow gas direction and an ideally mixed solids flow is used. The parameters describing the drying curve, the solids residence time and the heat transfer coefficient are summarized in Table A.5-4.

To design equipment modules the process is simulated at ten different production rates from 0.5 to 5 kt succinic acid and 8000 operating hours per year. For each of these production rates, all process units are designed conventionally resulting in up to ten different equipment modules per process unit. The number of equipment modules per process unit can be less than ten, because two different production rates can lead to the same design based on the discrete design parameter values used. The conventionally designed plant with a single equipment module for each process unit is simulated in 5 %-increments from 70 % to 140 % of the target production rate of 4 kt/a to determine the correlation exponents α to relate the process units' specific operating constraints to the overall production rate of the plant. The resulting correlation exponents of each process unit and its operating constraints of the conventional plant are summarized in Table A.4-2.

6 Applications

6.1 Determination of a plants' overall operating window

The difference in determining the operating window by assuming a linear and equal relationship between the plant's production rate and the values of the operating constraints as in [23] to the suggested correlation approach developed in this work is shown for the conventional design of the styrene production plant. To relate the specific operating constraints to the overall production rate of the plant, a correlation exponent α for each operating constraint of each process unit is used as described in chapter 4.1. Therefore, the conventionally designed plant with a single equipment module for each process unit is simulated for different production rates from 60 % to 120 % of the target production rate of 20 kt/a in 5 %-steps. The resulting correlation exponents of each process unit and its operating constraints of the conventional plant are summarized in Table 6-1.

Table 6-1: Correlation exponents for the operating constraints of each process unit (conventional design case of styrene production plant)

Process units	Correlation exponents		Process units	Correlation exponents	
Heat exchangers	$\alpha_{v_{tube}}$	$\alpha_{v_{shell}}$	Reactors	$\alpha_{\Delta p}$	
HX1	1.44	1.37	R1	2.92	
HX1B	1.44	1.64	R2	3.04	
HX2	1.65	0.89	Vap-liq separators	α_{τ}	α_v
HX3	1.76	1.41	HX1-PS	1.29	1.43
HX4	1.82	1.75	HX3-PS	1.26	1.41
HX5	1.87	4.97	HX4-PS	1.34	1.80
HX6	1.13	7.90	HX6-PS	1.03	0.92
HX7	1.24	1.24	HX8-PS	1.42	0.36
HX8	1.57	2.74	F1	1.31	0.96
HX9	1.57	1.59	Decanter	α_{Re}	
Dist. columns	$\alpha_{F-factor}$		D1	1.42	
C1	1.25				
C2	1.57				

For the maximum pressure drop of the heat exchangers no specific correlation exponent could be found due to variations based on small convergence deviations. Instead, the correlation exponents of the velocities are used for the maximum pressure drop operating constraint, too.

Figure 6-1 visualizes the differences of the operating windows for each process unit and the resulting overall operating window. Depending on the process unit, a large difference in the resulting operating windows of the individual process units is apparent. The approach assuming an equal and linear relationship between the operating constraints and the production rate of the plant always overestimates the size of the operating window. In

particular, large differences can be observed for Cap_{max} of both reactors and the heat exchanger HX8.

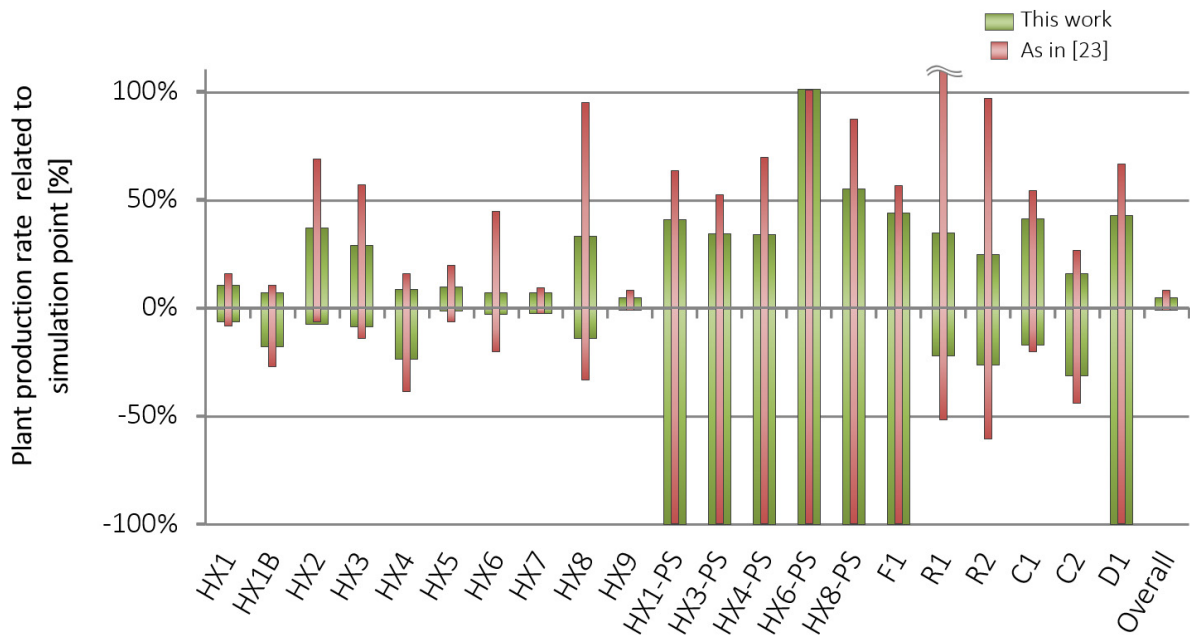


Figure 6-1: Comparison of operating windows of the process units based on the different determination approaches for the conventional design of the styrene case study (green bars: proposed correlation approach of this work, red bars: approach assuming an equal and linear relationship [23])

These differences also impact the overall operating window of the entire plant. Although the limiting process unit regarding $Cap_{min,plant}$ and $Cap_{max,plant}$ is with HX9 equal, the approach assuming an equal and linear relationship results in an operating window of -1.4 % and +8.1 %, whereas the correlation-based approach of this work which considers the often non-linear relationship results in an overall operating window of -0.9 % and +5.1 %. The absolute difference of 12.5 kg/h regarding $Cap_{min,plant}$ and 75 kg/h regarding $Cap_{max,plant}$ between both approaches sounds small, but it results in 100 t/a and 600 t/a, respectively, and is hence not negligible.

6.2 Preselection approaches to decide on the use of equipment modules for process units

The preselection approaches to decide on the use of equipment modules for process units introduced in chapter 4.2 are applied to the example process of fermentative succinic acid production (see chapter 5.3). First, the results of applying the preselection approaches based on a shortcut design of the process equipment are shown and discussed. Next, the impact of using equipment modules on investment and operating costs is rated. Finally, the preselection approaches are evaluated.

The basis for applying and evaluating the preselection approaches is a shortcut design based on design heuristics. Most of the equipment modules in the equipment module databases are generated via a shortcut design, too (see appendix A.4.7). An exception are the heat exchangers, for which a shortcut design is used to apply the preselection approaches, while the heat exchanger equipment modules are designed rigorously by Aspen EDR[®]. The estimated overall heat transfer coefficients are summarized in Table A.4-1. The equipment module databases can be found in appendix A.4.5. To rate the impact of using equipment modules on investment and operating costs and to evaluate the preselection approaches, the multi-objective evolutionary algorithm (see chapter 4.3) is applied to select equipment modules for the respective process units using a minimization of TCI and OPEX as selection objectives. The parameters for TCI and OPEX determination are summarized in appendix A1. Besides investment costs, the exergoeconomic analysis requires the consideration of system costs including labor, maintenance, and other fixed costs [120]. Therefore, maintenance costs and sundry expenses are considered for the system costs determination by 7.5 % and 6 % of the TCI, respectively [111]. A five-shift system is used for the case study, including a required number of workers and a supervisor per shift, one technician and an operation manager. The required number of workers depends on the type of process units in the plant as per Table A. 1-4. To transfer the system costs into a cost stream, 8,000 operating hours per year and a depreciation period of 10 years are assumed.

6.2.1 Preselection based on investment costs *Inv*

As can be seen in Figure 6-2, the main contribution to the TCI is caused by a single process unit, the fermenter. Since all other process units have a TCI below average, their influence on the overall TCI of the production plant is low and equipment modules can be used.

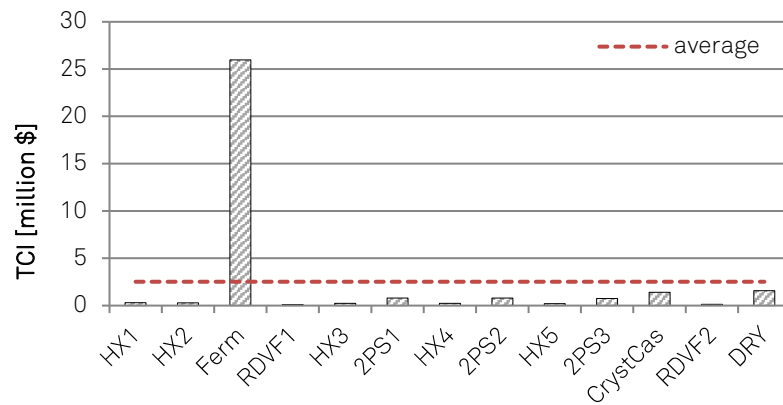


Figure 6-2: TCI of process units of succinic acid production plant based on shortcut design

The CEX-value of the fermenters is 0.51 and thus below the critical CEX-value of 0.6. According to the preselection approach based on investment costs, the fermenter is the only process unit for which no equipment modules should be used.

6.2.2 Preselection based on investment and operating costs *Inv&Op*

For the succinic acid production plant, the share of affected costs to the overall production costs is 20.0%. In case of the preselection approach *Inv&Op*, only this share of costs is considered to decide on using equipment modules for process units. The affected costs for the process units of the succinic acid production plant based on the shortcut design are summarized in Table 6-2. Heat exchangers and vapor-liquid separators are assumed to be processed one after another according to the main direction of the process stream. The position factor has a value of 1.249 for the dryer as the last process unit.

Table 6-2: Costs affected by using equipment modules per process unit of the succinic acid production plant based on the shortcut design

Position	Process unit	Costs [\$/h]			P_p [-]
		$\dot{C}_{Glycerol,av}$	\dot{C}_{TCI}	\dot{C}_{uti}	
0	Feedmix		0	0	1.000
1	HX1		3.7	131.8	1.023
2	HX2		3.6	46.2	1.031
3	Ferm	0.000	324.6	199.3	1.118
4	RDVF1		1.3	18.6	1.122
5	2PS1	0.002	10.0	0.0	1.123
6	HX3		3.0	294.9	1.173
7	2PS2	0.003	9.9	0.0	1.175
8	HX4		2.8	211.2	1.211
9	2PS3	0.020	9.3	0.0	1.212
10	HX5		2.5	165.8	1.240
11	CrystCas		17.6	0.5	1.243
12	RDVF2		1.7	0.9	1.244
13	DRY		19.6	14.6	1.249
Sum:		0.025	409.6	1083.7	

As can be seen in Table 6-2, the avoidable glycerol losses are very small. This is due to the fact that the fermenter models used do not show a correlation between the amount of

byproduct and the equipment used for fermentation. Therefore, no raw material losses are considered for the fermenters according to the definition (see chapter 4.2.2) and raw material losses occur in the vapor-liquid separators only, where small amounts of succinic acid leave the process via the vapor stream. The utility costs show the largest contribution to the avoidable costs. In case of the fermenters, cooling water, electricity for the stirrers and the excess of carbon dioxide that does not react but is supplied to support succinic acid production cause high utility costs. Considering the evaporators HX3, HX4 and HX5, the high utility costs emerge due to the price of steam and the large amount of the process stream that must be evaporated.

In the first step of the decision tree, HX1, Ferm, HX3, HX4 and HX5 lead to an above average ratio of costs affected by using equipment modules compared to the overall costs affected by using equipment modules. The second step of the decision tree reveals that for the process units HX1, HX3, HX4 and HX5, the investment costs are not mainly affected. Instead, utility and avoidable raw material costs are deciding factors. Since no information about the effect of using equipment modules on utility and avoidable raw material costs is available up to this point, using equipment modules is not recommended for HX1, HX3, HX4 and HX5. In case of the fermenter, the investment costs are the main affected costs and the third criterion in the decision tree is confirmed. The CEX-value of 0.51 indicates that the use of equipment modules could lead to a high cost increase. Thus, the use of equipment modules for the fermenter is not recommended. For all other process units, equipment modules can be used with little cost increase expected according to the *Inv&Op* preselection approach. The position of a process unit along the process stream has a small impact within the decision tree only.

6.2.3 Preselection based in exergoeconomics *ExEco*

To understand exergoeconomic costs of process units, the results of the foregoing exergy and exergoeconomic analysis will be discussed prior to presenting the results of the preselection approach *ExEco*.

The exergetic losses of the process units from the succinic acid production plant based on the shortcut design are summarized in Figure 6-3. Since the temperature difference in all heat exchangers of the succinic acid production plant are similar, the exergetic losses in the heat exchangers are comparable. Supplying cold and hot utilities to the cascade of crystallizers CrystCas and the dryer DRY, both process units have lower exergetic losses due to the small process stream in comparison to the heat exchangers.

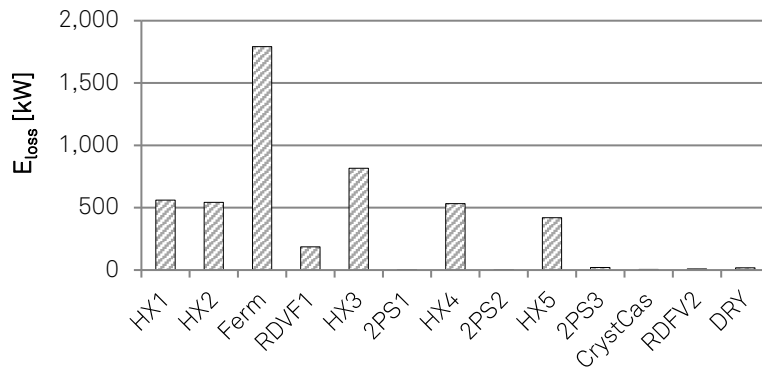


Figure 6-3: Exergetic losses of process units of the succinic acid production plant based on shortcut design

The vapor-liquid separators show very low exergetic losses of 2 to 20 kW because the streams separated are in thermodynamic equilibrium. Although the processing conditions in the fermenters are moderate, they cause the largest exergetic loss. This is a result of stirring since the electrical energy provided is almost completely dissipated into the fermentation broth. A similar effect can be observed for both rotary drum vacuum filters RDVF1 and RDVF2, although the power consumption is far lower compared to the stirring in the fermenters. In both cases, the electrical exergy supplied cannot be transferred to the outgoing streams and represents a source of irreversibility.

Figure 6-4 shows the exergetic costs consisting of basic costs, system costs and costs through exergetic losses for each process unit of the succinic acid production plant. Higher specific exergoeconomic costs of the feed stream to a process unit, resulting from a smaller incoming exergy of heat, can be observed for HX2 in comparison to HX1, HX3, HX4 and HX5. The electrical exergy supplied to RDVF1, RDVF2 and the fermenters is smaller compared to the amounts of heat exergy supplied to the evaporators HX3, HX4 and HX5. Hence, the specific exergoeconomic costs are higher for process units consuming electrical energy compared to evaporators, ultimately leading to high exergetic costs through losses.

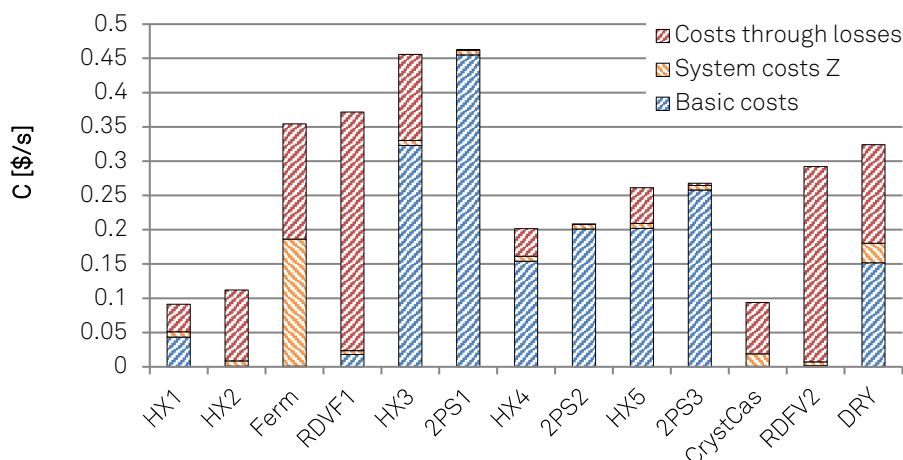


Figure 6-4: Exergoeconomic costs for process units of succinic acid production plant based on shortcut design

As the dryer DRY is the last process unit in the succinic acid production process, the process stream is small and mainly consists of solid material resulting in a low exergy of the incoming and outgoing streams. The low exergy of the incoming streams leads to high specific costs c_{Feed} , which results in high overall exergetic costs of around 0.32 \$/s. Two process units that have large basic costs are 2PS1 and HX3 with approximately 0.46 \$/s and 0.32 \$/s, respectively. Both process units combined represent the first forced circulation evaporator. In contrast to the subsequent forced circulation evaporators HX4 and HX5, the temperature of the process stream is with 37 °C low when entering HX3. This leads to comparably higher specific exergy costs that are forwarded to 2PS1. The basic costs of 2PS1 are even higher, as no additional exergy is supplied to the vapor-liquid separator resulting in a further increase of specific exergy costs. Process units with very low basic costs are CrystCas, HX2 and Ferm since the outgoing exergy streams are low according to their moderate temperature and pressure conditions.

Going through the decision tree based on exergoeconomics (c.f. Figure 4-8), Ferm, RDVF1, HX3, RDVF2 and DRY show an above average share of costs that are affected by using equipment modules \dot{C}_{loss} and \dot{Z} per process unit compared to the overall plant. Thus, these process units are crucial when considering the cost increase. In case of HX3, the ratio of costs through losses and system costs compared to the basic costs is lower than 0.5, leading to the decision against using equipment modules. For the remaining crucial process units Ferm, RDVF1, RDVF2 and DRY, this ratio is larger than 0.5 and the third decision tree criterion is confirmed. The system costs are thereby only crucial for the process unit Ferm. No information about the effect of using equipment modules on the costs in relation to exergetic losses is available. Therefore, the use of equipment modules for RDVF1, RDVF2 and DRY is not recommended. In case of the fermenter, the third decision tree criterion is examined and since the CEX-value of 0.51 is lower than the critical value of 0.6, no equipment modules should be used. For all other process units, equipment modules can be used according to the preselection approach *ExEco*.

In summary, RDVF1 and RDVF2 are ruled out for using equipment modules due to the exergetic inefficiency of stirring and rotating. In case of the fermenter, the high share of system costs in combination with the low CEX-value lead to the decision against using equipment modules. The dryer has high exergetic costs based on the low exergy of the incoming stream, due to which the use of equipment modules cannot be recommended. In case of the first evaporator HX3, the high share of the basic costs leads to the recommendation against using equipment modules.

6.2.4 Rating impact of using equipment modules on investment and operating costs

To rate the impact of using equipment modules on investment and operating costs, the conventional case *Conv*, where the equipment is designed for the target production rate, is compared to the Pareto front of case *All*, where equipment modules are selected for all process units (see Figure 6-5).

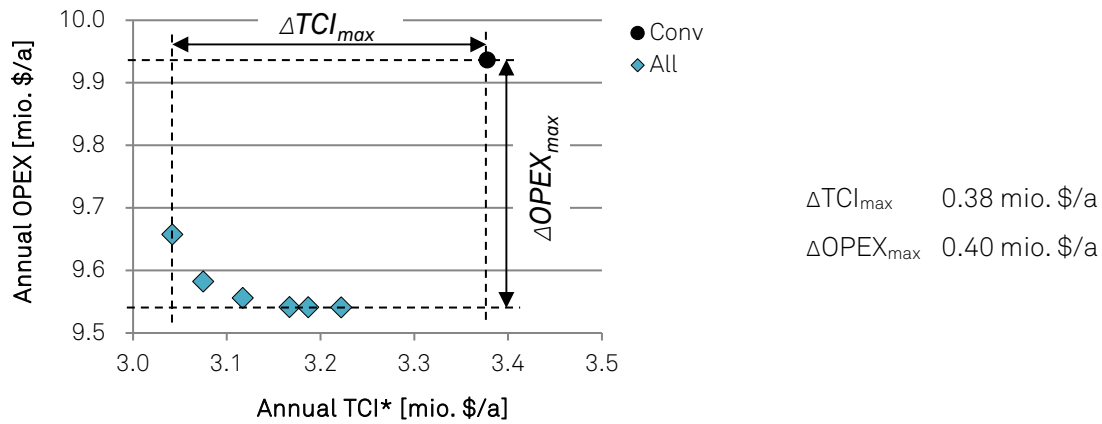


Figure 6-5: Pareto front of case *All* after 200 generations (blue rhombs) and conventional case *Conv* (black dot) (details of all Pareto-optimal modular equipment sets can be found in Table A.4-11)

The maximum difference in annual investment costs ΔTCI_{max} of 0.38 mio. \$/a is comparable to the maximum difference in operating costs $\Delta OPEX_{max}$ of 0.40 mio. \$/a. This leads to the conclusion that both TCI and OPEX are equally important for the case study when deciding on the use of equipment modules.

Furthermore, it is apparent that the modular equipment sets of case *All* show lower OPEX and TCI values compared to the conventionally designed production plant *Conv*. The conventional production plant is designed for the target production rate considering design heuristics that take operating and investment costs indirectly into account while enabling to operate each apparatus in a well-balanced operating window that is centered at the design production rate. As can be seen in Figure 6-6, applying the design heuristics results in a well-balanced operating window ranging from -13.5 % to 8.3 % around the desired production rate for case *Conv*. This ensures operability around the design production rate. In contrast, the equipment modules of case *All* are selected with the sole objective to minimize TCI and OPEX while ensuring that the modular equipment set is operable at the required production rate only. To minimize the TCI, the operating window of the modular equipment sets from case *All* is reduced. Especially an operating window above the desired production rate requires an increased TCI.

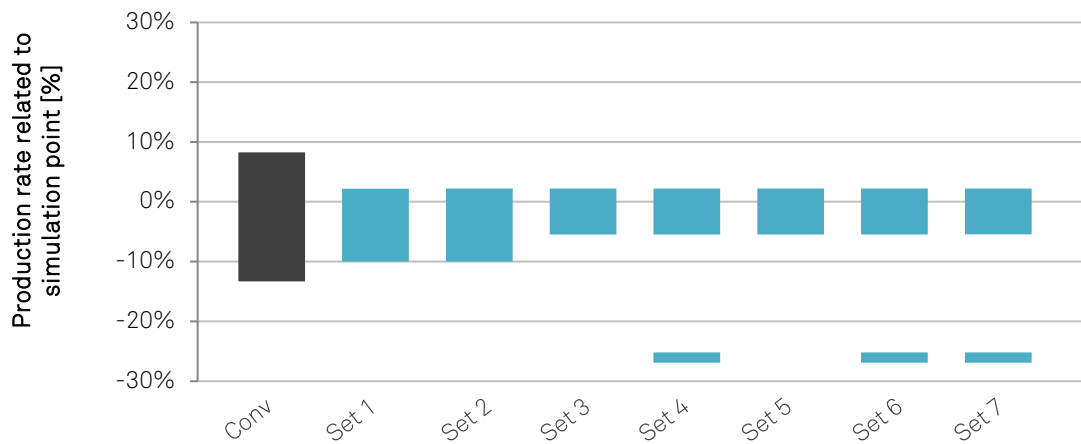


Figure 6-6: Overall operating windows of case *Conv* (black) and Pareto-optimal modular equipment sets of case *All* (blue, numbered consecutively as shown in Table a.4-11 from left to right)

This leads to a lower Cap_{max} for all modular equipment sets of case *All* compared to case *Conv* and thereby also to a lower TCI. In addition, Set 4, Set 6 and Set 7 show a small operable range at lower production rates due to the selection of multiple smaller equipment modules. However, a gap occurs since the use of multiple of these smaller equipment modules does not offer a continuous operation over the entire range of production rates.

6.2.5 Evaluation of preselection approaches

Figure 6-7 shows the different Pareto fronts of the equipment module selection runs based on the different preselection approaches *Inv*, *Inv&Op* and *ExEco*. Additionally, the reference cases *Conv* and *All* are depicted. The selection of equipment modules for all process units (case *All*) results in the Pareto front with the lowest annual TCI and OPEX. Thus, case *All* represents the largest number of degrees of freedom for TCI and OPEX minimization as expected. Most of the Pareto-optimal modular equipment sets with a previously applied preselection are located between the TCI and OPEX of case *Conv* and the Pareto front of case *All*. This is based on the applied preselection approaches that either result in using the conventionally designed equipment module for a process unit or allow a selection of equipment modules from the equipment module database by the evolutionary algorithm. Compared to case *All*, the Pareto front of case *Inv* moved closer to the TCI of the conventional design *Conv*, leading to the conclusion that the fermenter, which is fixed to the conventional design, is the process unit with the highest impact on the TCI. The OPEX of case *Inv* are comparably far away from case *Conv* as from case *All*, which reveals that no process unit with a high impact on OPEX could be identified by the preselection *Inv*.

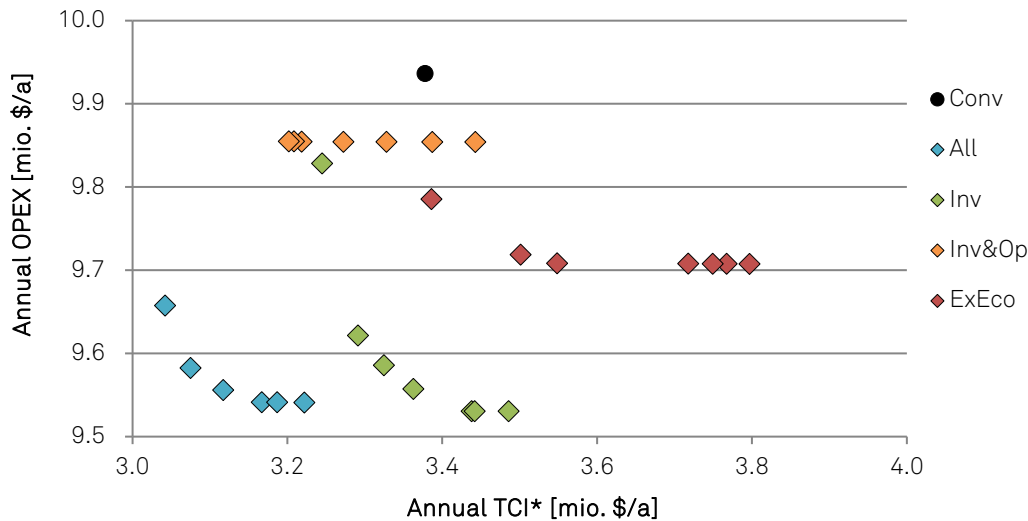


Figure 6-7: Final Pareto fronts of succinic acid case study after 200 generations (* annual TCI calculated with depreciation period of 10 years, details of all Pareto-optimal modular equipment sets can be found in Table A.4-11, the resulting overall operating windows are shown in appendix A.4.7)

The Pareto front of case *Inv&Op* shows nearly no range in OPEX and is closest to the conventional design *Conv*. Thus, by fixing the conventionally designed equipment for the process units HX1, Ferm, HX3, HX4 and HX5, the major process units with an effect on OPEX could be identified.

The preselection based on exergoeconomics *ExEco* shows a Pareto front that lies at equal or higher annual TCI compared to the conventional design case *Conv*, whereas the OPEX are closer to case *Conv* compared to case *Inv*.

A short distance between the conventional case *Conv* and a Pareto front of a respective preselection approach reflects that the process units with a high impact on OPEX and TCI have been determined correctly. The mean values of the absolute distance between case *Conv* and the Pareto fronts are summarized in Table 6-3.

Table 6-3: Mean absolute distances between TCI and OPEX of the modular equipment sets in the Pareto fronts with applied preselection approaches and the conventional production plant for the succinic acid case study

Preselection approach	\bar{d}_{TCI} [Mio. \$/a]	\bar{d}_{OPEX} [Mio. \$/a]	\bar{d} [Mio. \$/a]
<i>All</i>	0.26	0.35	0.45
<i>Inv</i>	0.14	0.34	0.39
<i>Inv&Op</i>	0.10	0.08	0.14
<i>ExEco</i>	0.26	0.22	0.35

A value of $\bar{d}_{TCI} = 0.10$ mio. \$/a for case *Inv&Op* compared to 0.14 mio. \$/a for case *Inv* indicates that preselection *Inv&Op* is a slightly more suitable preselection approach in terms of investment costs. Although the difference is small, it could be expected that a preselection

based solely on investment costs has lower and thus better \bar{d}_{TCI} values compared to case *Inv&Op*. A detailed look at the modular equipment set of case *Inv* with the highest TCI (see Table A.4-11) reveals that eight equipment modules have been selected for 2PS1, ten for 2PS2, eight for 2PS3 and five for RDVF1. Meanwhile, the number of equipment modules for the other Pareto-optimal modular equipment sets of case *Inv* amount to one, five, one and one, respectively. This lower number of equipment modules decreases the annual TCI by 0.47 mio. \$/a and thus decreases \bar{d}_{TCI} for case *Inv* to 0.07 mio \$/a. This reveals that, on the one hand, the single optimization run with 200 generations raises small uncertainties regarding the derived conclusions of this case study. On the other hand, it proves that a generalized conclusion can be made by considering the details of the Pareto-optimal modular equipment sets.

Comparing the preselection approaches *Inv&Op* and *ExEco*, it can be concluded that *Inv&Op* is the more suitable preselection approach for the case study investigated due to the smaller distance in investment costs \bar{d}_{TCI} , in operating costs \bar{d}_{OPEX} and hence a smaller overall distance \bar{d} .

In summary, the most suitable preselection approach to consider investment and operating costs for the succinic acid production case study is the preselection approach *Inv&Op*, due to the low value of \bar{d}_{TCI} and the lowest value of \bar{d}_{OPEX} .

6.3 Equipment module selection by evolutionary algorithm

6.3.1 Settings of evolutionary algorithm

In general, the parameters of an evolutionary algorithm need to be adapted to the specific optimization problem by parameter tuning [53]. However, this is not possible for the current work due to the high computational effort. The parameters used for the multi-objective evolutionary algorithm SPEA are listed in Table 6-4. The size of the population is chosen based on experience whereby a larger population would lead to long simulation times and a smaller population results in too few individuals in the Pareto front. The size of the archive is limited to one quarter of the population size [55].

Table 6-4: Parameters of evolutionary algorithm

Parameter	Value [-]
Population size N	28
Archive size N'	7
Number of offspring individuals λ	14
Recombination probability p_{rec}	1
Mutation probability p_{mut}	0.5
Mutation rate r_{mut}	5
Abort criterion	10

The number of offspring individuals λ is set to 14 to have a high selection pressure since a larger number of offspring individuals leads to the removal of more individuals from the current population. The parameters describing the evolutionary operations recombination and mutation to find new solutions are the recombination probability p_{rec} , the mutation probability p_{mut} and the mutation rate r_{mut} . With a recombination probability of one, each new offspring is generated by recombination. A subsequent mutation is performed with a probability of 50 %. A selected mutation rate of five means that equipment modules for five process unit are randomly exchanged with other equipment modules from the equipment module database. The mutation and recombination probability as well as the mutation rate are selected to provide a high diversity of the offspring individuals. If the number of individuals in a population and the offspring individuals are too similar, the algorithm takes longer to leave local optima. 10 generations without the addition of a new individual into the archive are used as abort criterion.

6.3.2 Constant market demand

The styrene production process example (see chapter 5.1) is used to select equipment modules for a constant market demand. The goal is a flexible modular production plant with a large operating window for a minimum of required investment. Hence, the selection

objectives are to minimize $Cap_{min,plant}$ and maximize $Cap_{max,plant}$ to get a large operating window while minimizing the total cost of investment TCI.

First, the results of the conventional design of the styrene production plant are evaluated. An evaluation of the equipment module selection approach follows. Finally, the modular equipment sets of the Pareto front that represent the best trade-off solutions of flexible modular equipment sets with a low TCI are evaluated in detail.

The conventional design offers an operation between -0.9% and $+5.1\%$ of the target production rate of 20 kt/a (cf. chapter 6.1) for a TCI of \$ 15.8 million. More than 50 % of the TCI are made up by the heat exchangers, as shown in Figure 6-8. Considering the TCI-distribution of all process units in Figure 6-9, it can be seen that three process units, the distillation column C2 and the heat exchangers HX2 and HX3, are dominating the costs.

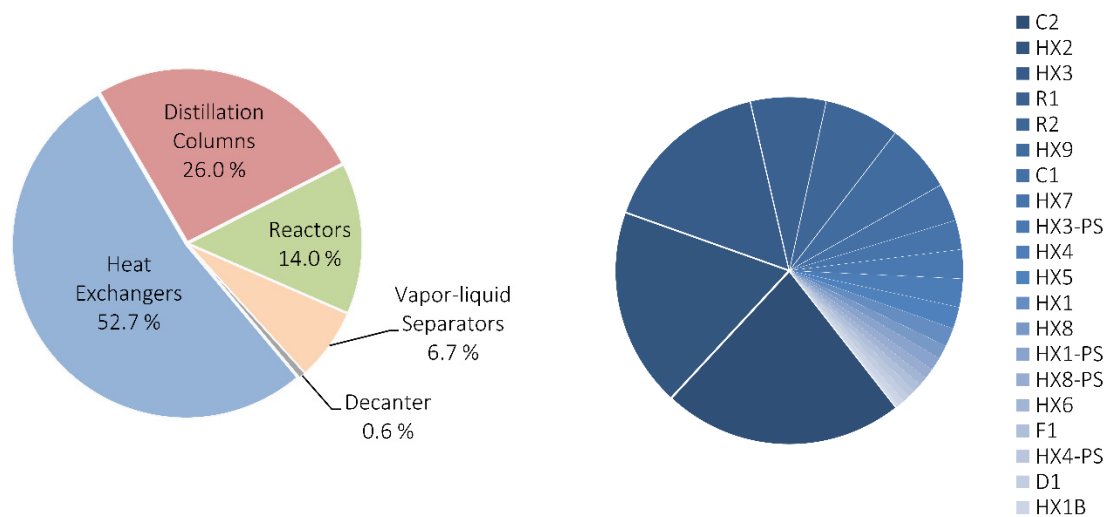


Figure 6-8: TCI-distribution of grouped process units for the conventional design

Figure 6-9: TCI-distribution of all process units for the conventional design sorted by contribution

Relating the operating windows of C2, HX2 and HX3 (cf. chapter 6.1) to the share on the TCI it becomes clear that the large $Cap_{max,PU}$ of these process units might be the reason for their large share in the TCI since all three main cost drivers offer a relatively large $Cap_{max,PU}$. Thus, they are not designed to fit tightly on the edge.

Three independent optimization runs are performed to select equipment modules (see chapter 4.3). The conventional design is added to the initial population P_0 in all three runs. As can be exemplarily seen in Figure 6-10 for Run3, the Pareto front is evolving from generation 1 over generation 10 to generation 250 towards better modular equipment sets with a large operating window at a low TCI. From the 150th generation on, only minor improvements are observed in the Pareto front. However, the algorithm runs are continued to the 250th generation for all three runs and stopped after an overall simulation time of three weeks. In case of all three runs the abort criterion is not reached until the 250th generation.

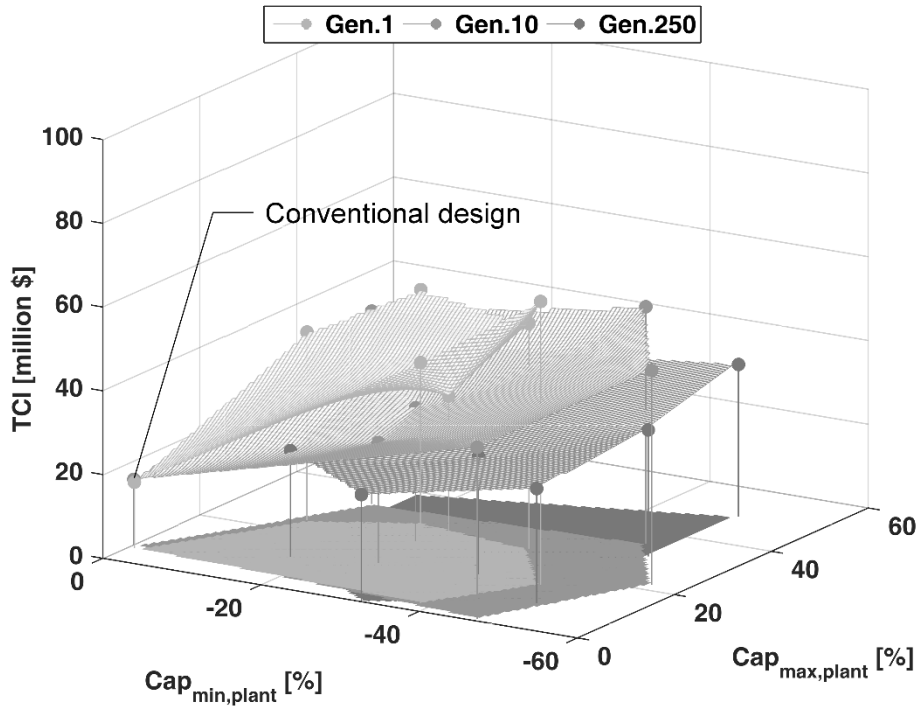


Figure 6-10: Evolution of Pareto front over the generations of Run3 (interpolated surfaces and projections to bottom area are used for a better visibility)

Additionally, it can be observed in Figure 6-10 that the conventional design with the lowest TCI of \$ 15.8 million is not part of the final Pareto front of the 250th generation. The reason is the restriction of the archive size N' , whereby one of the modular equipment sets with the smallest Euclidian distance between the Pareto sets in the search space is deleted from the archive P' .

A comparison of the Pareto sets of the three independent runs is shown in Figure 6-11, where red is used for Run1, blue for Run2 and green for Run3. Ideally, all three Pareto fronts should be identical, which is not the case for the three runs after the 250th generation. To examine the reasons, the three 2-dimensional views of the Pareto sets and the overall explored search space depicted as interpolated area of the simulated operable modular equipment sets are shown in Figure 6-12 to Figure 6-14. First, it can be seen that the explored search spaces of the three runs do not differ as much as the difference in their Pareto sets in Figure 6-11 implies. Second, it stands out that the Pareto sets of the three runs are not always located at the edges or corners of the explored search space as it might be assumed, especially for low TCI-, large Cap_{max} - or low Cap_{min} -values.

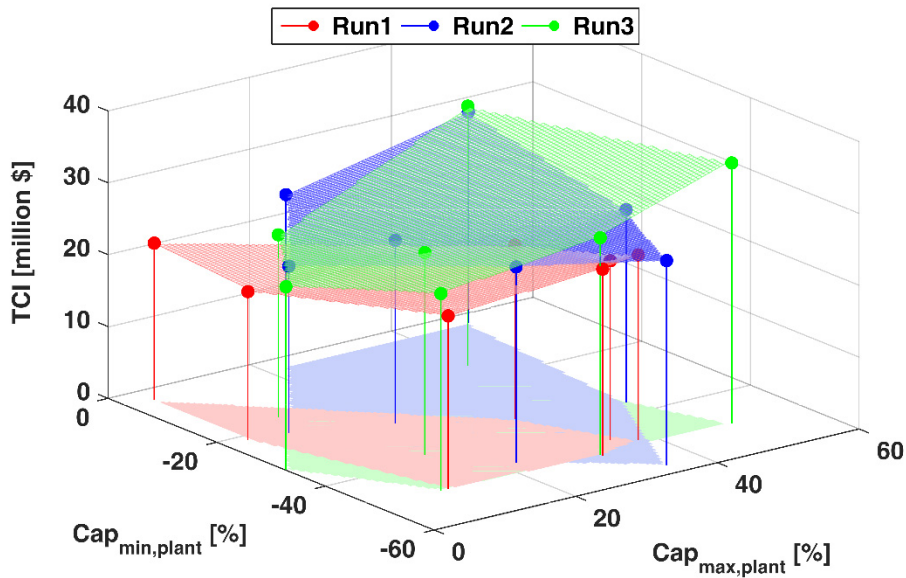


Figure 6-11: Pareto fronts after 250 generations for three independent optimization runs (interpolated surfaces and projections to bottom area are used for a better visibility)

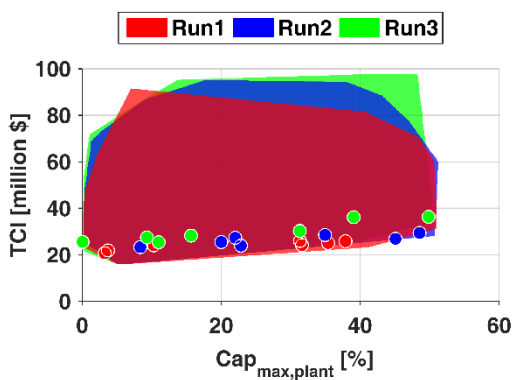


Figure 6-12: Two-dimensional view (TCI vs. Cap_{max}) of the three Pareto sets depicted as dots and the overall explored search space shown as interpolated area of the simulated operable modular equipment sets

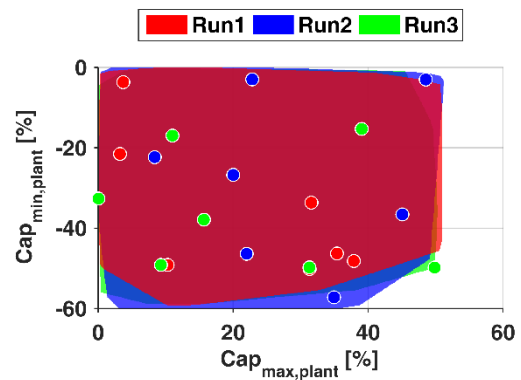


Figure 6-13: Two-dimensional view (Cap_{min} vs. Cap_{max}) of the three Pareto sets depicted as dots and the overall explored search space shown as interpolated area of the simulated operable modular equipment sets

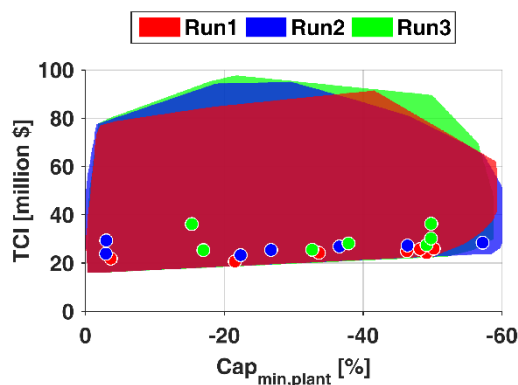


Figure 6-14: Two-dimensional view (TCI vs. Cap_{min}) of the three Pareto sets depicted as dots and the overall explored search space shown as interpolated area of the simulated operable modular equipment sets

Thus, there must be more Pareto sets than the seven sets that are stored in the archive P' . Investigating all modular equipment sets that were simulated during the optimization runs for Pareto-optimal sets reveals 138, 103 and 107 Pareto sets for each run, respectively. On the one hand, a restriction of the archive size N' is necessary to maintain a high selection pressure and thus preventing the optimization process from slowing down [55]. On the other hand, the archive size N' should not be too small to adequately represent the characteristics of the Pareto front. Hence, in future works the archive size N' should be increased for the investigated case to adequately represent the Pareto front consisting of the three objectives $Cap_{min,plant}$, $Cap_{max,plant}$ and TCI for the used equipment module database. Furthermore, using an alternative clustering approach for the restriction of N' would help to keep a uniform distribution of the Pareto sets stored in the archive.

Figure 6-15 shows all Pareto-optimal modular equipment sets found during the three optimization runs until the 250th generation. It can be seen that the overall Pareto fronts of the three independent runs are quite similar.

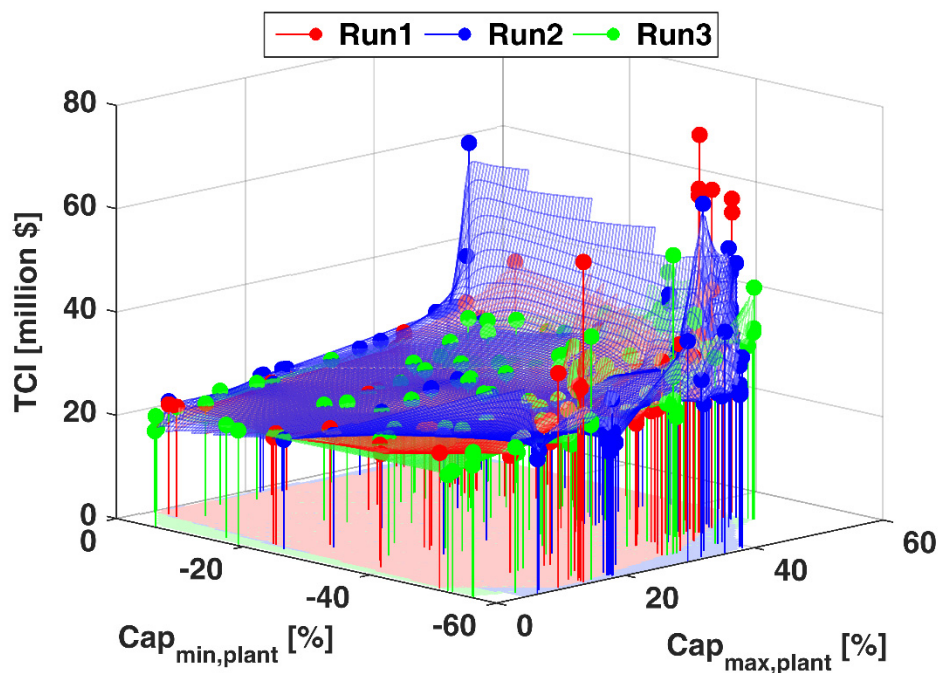


Figure 6-15: All Pareto-optimal sets found within the three optimization runs till the 250th generation (interpolated surfaces and projections to bottom area are used for a better visibility)

A large plateau can be observed for all Pareto-optimal modular equipment sets with a capacity range from -50% to 40% where the TCI lies in the range of \$20 million to \$25 million and does not increase sharply. This plateau is the most interesting region of Figure 6-15 because it shows that modular equipment sets with a higher flexibility in

production rate can be realized without having to spend much more in TCI. On the edges of the lowest $Cap_{min,plant}$ - and $Cap_{max,plant}$ -values a large increase in TCI can be observed. Thus, the costs for modular equipment sets with a $Cap_{min,plant}$ -value lower than -50 % or a $Cap_{max,plant}$ -value of more than 40 % increase exponentially. If a modular equipment set shall have both, a $Cap_{min,plant}$ lower than -50 % and a $Cap_{max,plant}$ larger than 40 % the cost increase is even higher. Furthermore, in the corner of low flexibility an additional decrease from the 'plateau' towards the conventional design with the lowest TCI is visible.

The operating windows of some exemplary modular equipment sets from the different regions of the overall Pareto fronts are shown in Figure 6-16. Three examples of Pareto sets from the plateau are set1, set2 and set3, whereby set1 offers a flexibility range from - 16.9 % to + 15.7 % for \$ 22.4 million and set2 a range from - 38.1 % to + 31.6 % for \$ 23.4 million. Thus, more than a 5- or 11-fold operating window can be obtained compared to the conventional design for a 1.4 or 1.5-times higher TCI. Set4 and set5 are examples of enlarging $Cap_{min,plant}$ and $Cap_{max,plant}$ even further leaving the plateau of the Pareto front where the TCI increases more steeply. An example of a comparably-balanced operating window to the conventional design is shown by set6 with a $Cap_{min,plant}$ of - 11.0 % and a $Cap_{max,plant}$ with + 51.0 %. Thus, set6 offers around 10 times the $Cap_{min,plant}$ - and $Cap_{max,plant}$ -value of the conventional design for 2.5 times more investment.

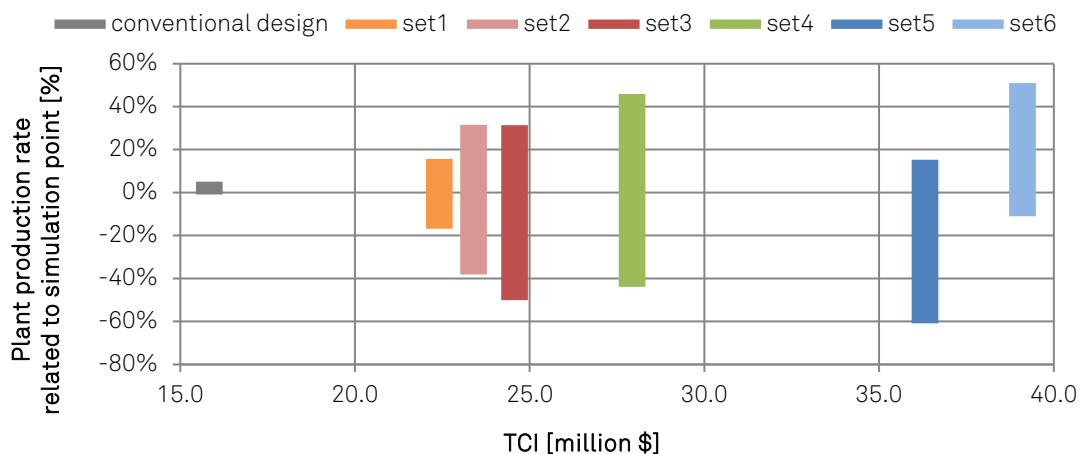


Figure 6-16: Operating windows of exemplary modular equipment sets of the different regions from the overall Pareto fronts

Details about the equipment modules selected for each process unit of the exemplary modular equipment sets and the conventional design can be found in Table A.2-18 of appendix A.2.5. To approximate the characteristic surface of the Pareto front a two-dimensional polynomial function of 3rd order as shown in Eq. 6-1 can for example be used.

$$TCI = TCI_{conv,design} + A_1 \cdot Cap_{max} + A_2 \cdot Cap_{max}^2 + A_3 \cdot Cap_{max}^3 + B_1 \cdot Cap_{min} + B_2 \cdot Cap_{min}^2 + B_3 \cdot Cap_{min}^3 \quad \text{Eq. 6-1}$$

Figure 6-17 shows an approximation of the combined Pareto fronts of all three runs. It can be seen that the characteristic form of the Pareto front can be represented by the approximation using Eq. 6-1. The accuracy of the surface approximation can be measured by the adjusted R-square value $adj - R^2$, which is the square of the correlation between the response values and the predicted response values adjusted based on the residual degrees of freedom. $adj - R^2$ can take any value less than or equal to 1, with a value closer to 1 indicating a better fit [121]. The accuracy of the combined Pareto front-approximation has an $adj - R^2$ -value of 0.946.

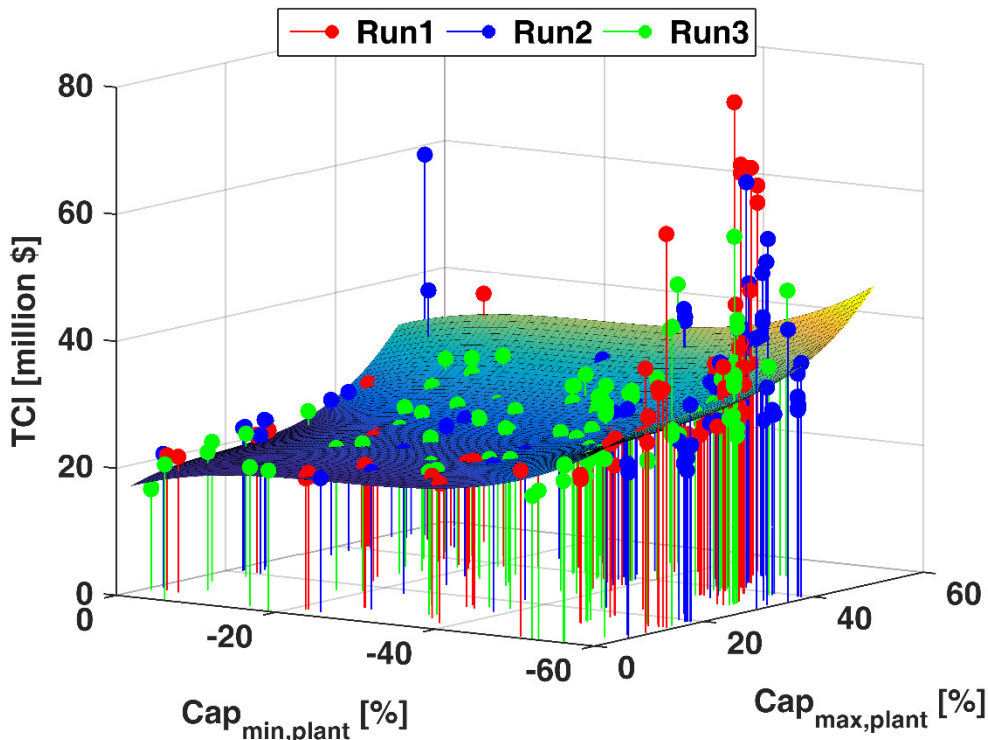


Figure 6-17: Approximation of the combined Pareto fronts of all three runs by 3rd order polynomial according to Eq. 6-1
 $(TCI_{conv,design} = \$ 15.8271536 \text{ million}, A_1 = 0.4045, A_2 = -0.01902, A_3 = 0.0003427,$
 $B_1 = -0.4568, B_2 = -0.0175, B_3 = -0.0002307)$

Such approximation of a Pareto front can for example be used to prepare fast proposals by engineering companies that offer modular production plants in collaboration with equipment suppliers. When a customer asks for a modular production plant with a certain target production rate and a certain flexibility range the engineering company can quickly give a first cost estimation and already has an initial Pareto-optimal design that can be finally adjusted to the specific requirements of the customer. Thus, if a customer wants a low cost modular styrene production plant with the target production rate of 20 kt/a and a capacity range from - 25 % to + 30 % based on the used equipment module database, they have to spend around \$ 24.18 million. The TCI of a modular equipment set from all Pareto

sets found with a comparable capacity range from - 24.8 % to + 30.1 % is \$ 25.25 million. However, for reliable shortcut cost estimations more Pareto-optimal modular equipment sets are necessary to enable a better approximation of the Pareto front.

To investigate the equipment modules present in the Pareto sets of the three runs, the frequency of occurrence within all Pareto sets is investigated. Furthermore, the Pareto sets are sorted regarding $Cap_{\min,plant}$ and $Cap_{\max,plant}$, respectively, and divided into capacity ranges of 10 %. This allows to investigate for example, whether particular equipment modules are selected for a $Cap_{\min,plant}$ - or $Cap_{\max,plant}$ -range. Furthermore, this allows to identify changes in the equipment modules selected over the $Cap_{\min,plant}$ - and $Cap_{\max,plant}$ -ranges. Considering all Pareto sets of the three runs, all equipment modules are present, except the largest modules for HX1, HX2 and HX8, although they can be found in the simulated and operable sets. To improve $Cap_{\min,plant}$ and $Cap_{\max,plant}$ numbering-up and the use of large modules are observable for all process units. Thus, also for the process units with the highest share in TCI of the conventional design as C2, HX2 and HX3, the use of multiple small or large equipment modules can be observed. In case of the heat exchangers, nearly no single equipment modules are present in the Pareto front for $Cap_{\min,plant}$ -values smaller - 10 % and $Cap_{\max,plant}$ -values larger + 10 %. The reason might be the relatively small operating window of the heat exchangers. Considering the equipment modules used for reactor R1 in larger $Cap_{\max,plant}$ -ranges, only larger equipment modules with an increased volume and a large L/D-ratio are used. For $Cap_{\max,plant}$ -values larger + 20 % no smaller norm diameter equipment modules of the columns C1 and C2 are selected.

Summarizing the analysis of the frequency of occurrence no peculiarity could be identified since no specific equipment module is preferably selected for the same process unit of the Pareto sets. Also no shift in the equipment modules used over the capacity ranges except for the described process units is visible. Thus, no statement can be made whether numbering-up or the use of oversized equipment modules for a process unit is preferred to increase the operating window of process units while keeping the TCI low. This observation might change for a different equipment module database. Within this work, the equipment modules are conventionally designed for different production rates of the process units. However, if also equipment modules designed for flexibility as shown in chapter 6.4 are present in the equipment module database, the need for a numbering-up of equipment modules for process units might be reduced. This could lead to a preferred use of such flexible equipment modules for the process units of the Pareto sets.

So far it was not investigated whether a particular process unit is always limiting the overall operating window of the Pareto-optimal modular equipment sets. To analyze the limiting

process units of the Pareto sets, Figure 6-18 shows the limiting process units that determine $Cap_{min,plant}$ and $Cap_{max,plant}$ for all identified Pareto sets as well as all simulated and operable sets without the Pareto sets. As can be seen in Figure 6-18, the limiting process units of the Pareto sets that determine $Cap_{min,plant}$ and $Cap_{max,plant}$ are different. This is visible for both, all Pareto sets as well as all simulated sets without the Pareto sets. $Cap_{min,plant}$ is most often limited by the process units R1 and R2, whereas $Cap_{max,plant}$ is most often limited by C2 and HX2. To realize lower $Cap_{min,plant}$ -values, it is necessary to use multiple smaller equipment modules for a process unit. The reactors have the lowest cost capacity exponent (cf. Table A.1-1 in appendix A1) and thus it is most expensive to use multiple equipment modules for them. To keep the TCI low for a low $Cap_{min,plant}$, the equipment modules of the reactors need to be selected in such a way that their operating windows fit tightly on the edge. That is why they are most often limiting $Cap_{min,plant}$, especially for the Pareto sets. For the process units that are most often limiting $Cap_{max,plant}$ as C2 and HX2, no such clear observation is possible. To increase $Cap_{max,plant}$ of a modular equipment set, the process units with the largest share on the TCI of the conventional design seem to be crucial, because C2 and HX2 are most often limiting $Cap_{max,plant}$ of the Pareto sets. However, the share on TCI of the different process units of a modular equipment set can change because multiple equipment modules can be chosen for a process unit to increase its operating window. This leads to a change in the TCI-distribution of all process units.

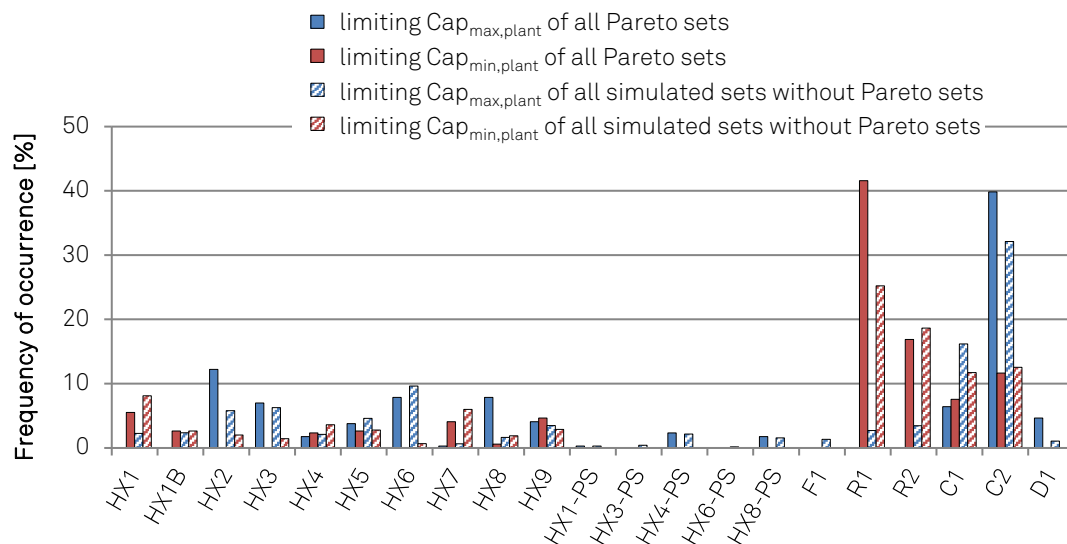


Figure 6-18: Frequency of occurrence of the limiting process units to $Cap_{max,plant}$ and $Cap_{min,plant}$ for all Pareto sets and all simulated and operable sets without Pareto sets

What becomes clear by Figure 6-18 is that $Cap_{min,plant}$ and $Cap_{max,plant}$ of the Pareto-optimal modular equipment sets is determined by different process units. Thus, a differentiation between the crucial process units regarding $Cap_{min,plant}$ and $Cap_{max,plant}$ is necessary. The fact

that for just 5 % of the Pareto sets $Cap_{min,plant}$ and $Cap_{max,plant}$ are limited by the same process unit underlines the necessity for this differentiation. The introduced Investment Cost Factor *ICF* by Seifert [23] does not consider whether a process unit is limiting or not. Thus, the *ICF* does not seem to be a suitable measure to identify the critical process units for equipment module selection leading to flexible modular production plants at low TCI.

In summary, the relationships between the large number of discrete parameters as the different equipment module sizes and numbers, as well as the nonlinear, discontinuous and non-monotonic behavior of $Cap_{min,plant}$, $Cap_{max,plant}$ and the TCI to select equipment modules for a flexible modular production plant are complex. Exchanging an equipment module for a single process unit can lead to changes in the operating windows of the other process units of the plant. Since for 95 % of all Pareto sets found for the case study the limiting process units that determine $Cap_{min,plant}$ and $Cap_{max,plant}$ are different process units, the influence of changes in the modular equipment set will have different effects on $Cap_{min,plant}$ and $Cap_{max,plant}$. Thus, a multi-objective evolutionary algorithm as *SPEA* that can handle the large number of discrete parameters as the different equipment module sizes and numbers seems to be essential to select equipment modules for a flexible modular production plant.

6.3.3 Market demand development

The acetone production process example (see chapter 5.2) is used to select equipment modules for a market demand development. The goal is to compare the equipment-wise capacity expansion strategies offered by applying module-based plant design to a line-wise capacity expansion where an entire production line is added if needed and a conventional large scale plant. First, the general framework for the comparison and evaluation is described. Subsequently, the different cases as the conventional design, the line-wise capacity expansion and the equipment-wise capacity expansion are explored. Finally, the reactors designed for a larger operating window are investigated in light of equipment-wise capacity expansions.

The market demand development used and the boundary conditions for the comparison are illustrated in Figure 6-19. The market development starts at an initial market demand of 28 kt acetone per year which corresponds to 40 % of the final market demand of 70 kt/a assuming that the production plant operates 8000 h/a. In case of the line-wise and the equipment-wise capacity expansions it is required to fulfill the initial market demand of 28 kt/a. The production plants are simulated at a yearly basis with discrete production rates along this demand as explained in chapter 4.3. Over ten years, the market demand is growing linearly. In year zero, the production starts with the initial modular equipment set. From this point, a capacity expansion can take place every year, which leaves ten decisions whether to

expand or not. After that period, the market demand stays at the maximum market demand for another ten years. This additional time of ten years is chosen to assure that the plant has been fully depreciated by the end of the regarded time span. As often in industry, the conventional plant is designed for the maximum capacity of that growing market demand development [10]. Due to its larger $Cap_{min,plant}$, the conventional plant can start its production approximately six years later compared to the stepwise expanded plants. The investment takes place three years before the start-up of the conventional plant. Sinnott assumes a distribution of 30 % of the $TCl_{initial}$ in the first year, 50 % in the second and 20 % in the third year [92].

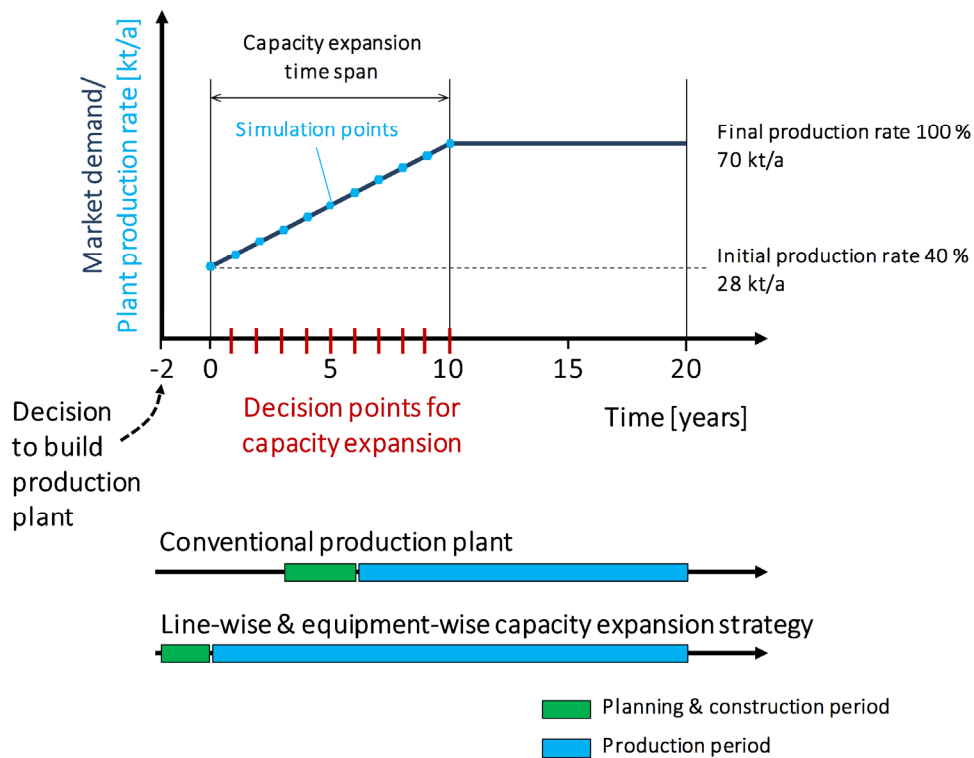


Figure 6-19: Illustration of the general evaluation framework to compare the different capacity expansion strategies

Due to the use of equipment modules, this time span is assumed to be reduced to two years for the line-wise as well as for the equipment-wise capacity expansion strategies [12,30]. 40 % of the $TCl_{initial}$ are invested during the first year and 60 % during the second. The investment for a capacity expansion takes place within half a year before the expanded equipment is ready to operate. The underlying parameters to calculate the FOB costs are summarized in appendix A.1.1, the prices of raw material and utilities can be found in appendix A.3.3 and the underlying staff costs in appendix A.1.4. The NPV considers a calculatory interest rate r of 12 %. All cash flows are assumed to take place in the middle of a year and are consequently discounted from this point in time.

The conventional design consists of the smallest possible single equipment modules for each process unit to fulfill the target production rate of 70 kt/a. Hence, the maximum capacity $Cap_{max,plant}$ of each process unit fits tightly on the edge at 70 kt/a avoiding an unnecessary and expensive overdesign. This leads to a reference plant representing the conventional design case that fulfills the required maximum production rate at minimum investment costs based on the available equipment module database. Figure 6-20 shows the operating windows of the different process units of the reference plant.

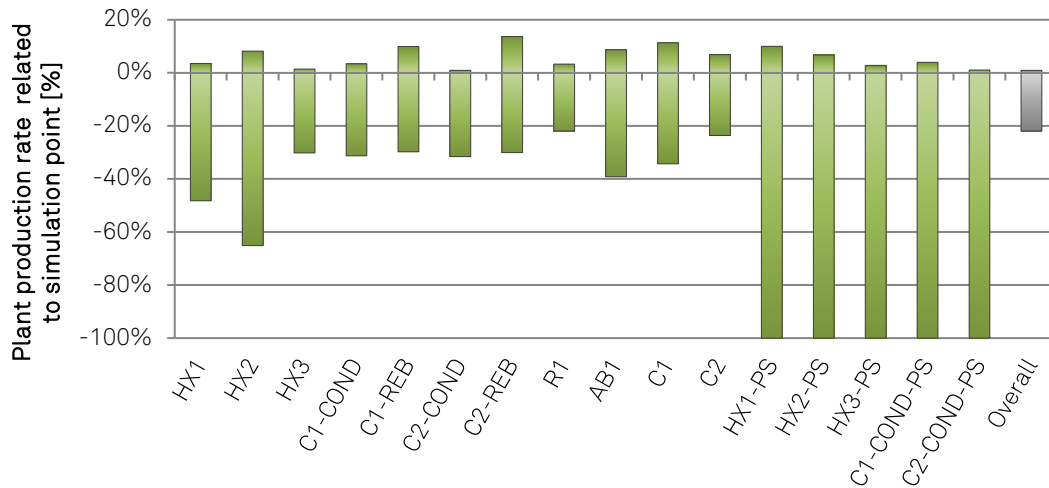


Figure 6-20: Operating windows of all process units from the reference plant representing the conventional case

It can be seen that the operating windows of all process units fit tightly on the edge regarding $Cap_{max,PU}$. The most restrictive process unit restricting $Cap_{max,plant}$ is with C2-COND the condenser of column C2 with +0.9 %. The reactor R1 limits the overall operating window of the plant regarding $Cap_{min,plant}$ with -21.9 %. A summary of the equipment modules used is shown in Table A.3-10. Figure 6-21 summarizes the distribution of the FOB costs for the reference plant, yielding in an overall TCI of \$ 5.54 million. The FOB costs are dominated by the column C1 and the reactor R1.

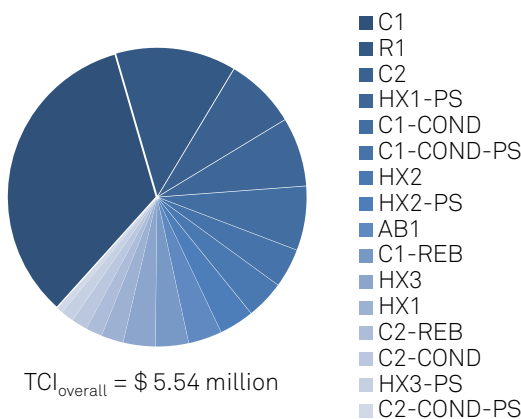


Figure 6-21: Distribution of total FOB costs for all process units of the reference plant

Hence, the trade-off between additional investment costs for an increased adaptability to the market demand is most relevant for C1 and R1. Less expensive process units can be numbered-up for an increased adaptability to the marked demand without significant changes to the TCI. Since Cap_{min} of the reference plant is determined to -21.9 % of the maximum production rate (70 kt/a), the reference plant can start its production a bit more than six years later compared to the line-wise and equipment-wise expanded plants at a market demand of 54.64 kt/a, which is equal to 78.1 % of the maximum production rate. The NPV of the conventional plant is \$ 12.87 million. To give a better understanding of the production potential utilized by the reference plant, the overall amount of product produced is compared to the maximum amount of product that the market demands, referred to as market volume. The reference plant satisfies 77.8 % of the possible market volume.

Investigating the line-wise capacity expansion strategies, two production lines satisfy the initial market demand of 28 kt/a, the 20 %- and the 40 %-production line. They consist of equipment modules that are designed conventionally for 20 % and 40 % of the maximum market demand, as 14 kt/a and 28 kt/a, respectively. The operating window of a single 30 %-production line is not large enough to cover the initial market demand and two 30 %-production lines result in a $Cap_{min,plant}$ that lies above the initial market demand. For the 50 %-production line, the initial market demand also lies below $Cap_{min,plant}$. Figure 6-22 illustrates the comparison of the 20 %- and 40 %-production lines to the conventional case in terms of production rate and overall TCI over the expansion timespan of 10 years. The 20 %-production line requires two capacity expansion steps in year 4 and 6, whereas the 40 %-production line requires only a single capacity expansion step in year 6. Additional capacity expansion steps are not possible due to the gap in the operating window that might occur by a numbering-up or are not profitable in terms of the NPV. The 20 %-production line satisfies with 92.6 % a larger share of the possible market volume compared to 89.6 % in case of the 40 %-production line due to the use of smaller expansion steps. By using four parallel 20 %-production lines in comparison to two parallel 40 %-production lines the overall TCI in case of the 20 %-production line increases by 35 % for approximately the same possible maximum production rate.

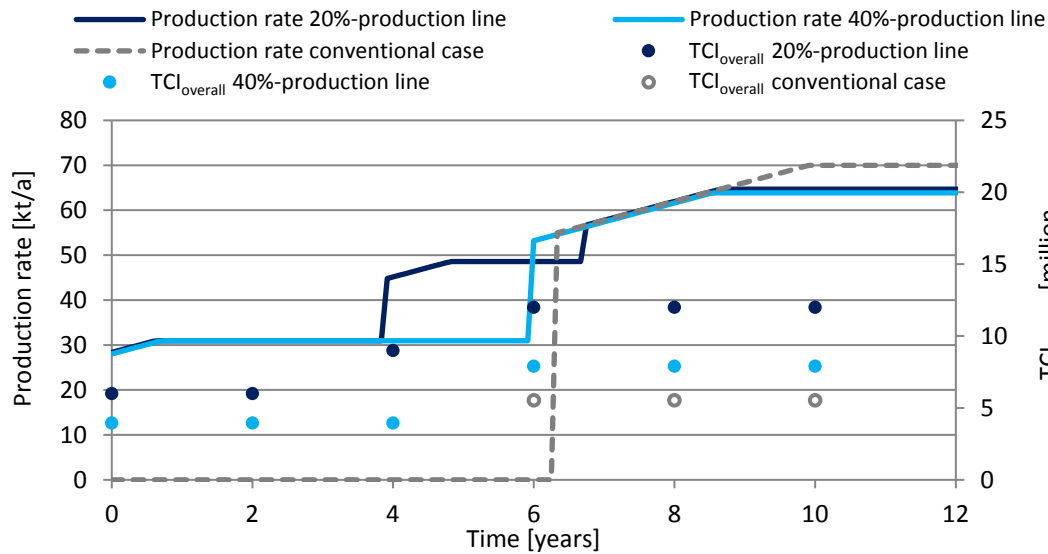


Figure 6-22: Comparison of conventional case to the 20 %- and 40 %-production lines regarding production rate (lines) and the overall TCI (dots)

Since a line-wise capacity expansion step needs to take place if a single process unit of a production line reached its maximum capacity, the operating windows of the other process units cannot be fully utilized. To illustrate this drawback in terms of additional investment costs and lost profit, the equipment modules of both production lines are used to investigate their equipment-wise capacity expansion scenarios. Figure 6-23 shows the production rate and the overall TCI for both production lines (blue) and its corresponding equipment-wise capacity expansion strategies (green). In case of the 20 % equipment-wise capacity expansion strategy it is clearly visible that an increased share of the possible market volume can be satisfied, namely 98.0 %, compared to the 92.6 % of the 20 %-production line. This results in an increased profitability, measured by the NPV of \$ 15.67 million compared to \$ 14.93 million in case of the 20 %-production line. The overall TCI of the equipment-wise case increased slightly by \$ 1.19 million mainly due to the addition of a fifth equipment module for the major cost drivers C1 and R1, as well as C1-COND and HX2, in year 10 to satisfy a larger share of the possible market volume. In contrast, just three equipment modules for C2-REB, AB1, HX2-PS, HX3-PS and two equipment modules for C2-COND-PS are used in year 10, instead of four in case of the 20 %-production line. A detailed comparison of the number of equipment modules used for each process unit over the expansion timespan of 10 years can be found in appendix A.3.7.

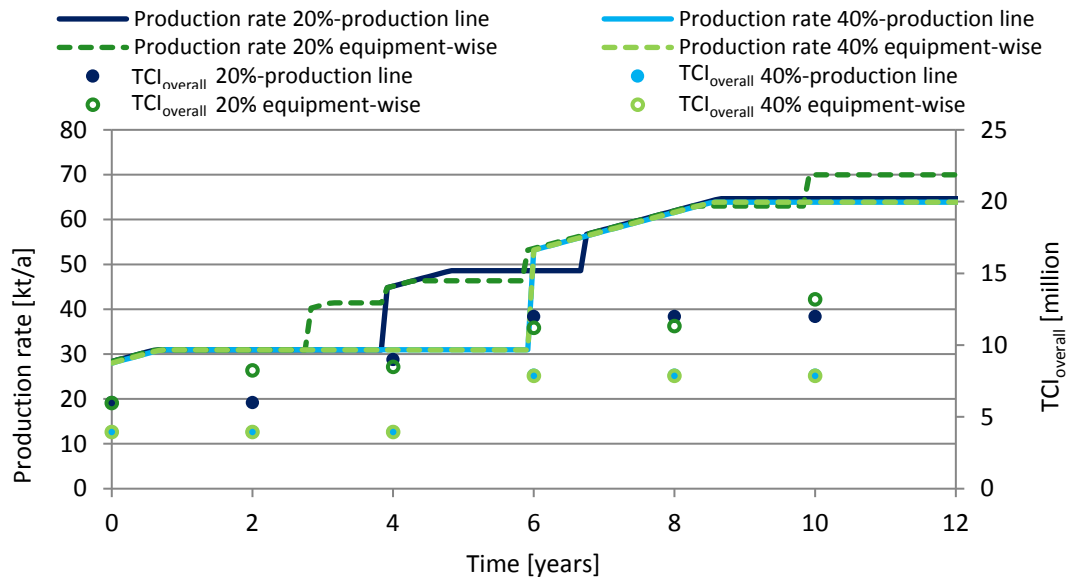


Figure 6-23: Production rate and overall TCI of production lines (blue) and its corresponding equipment-wise capacity expansion strategy (green)

Comparing both 40 %-cases with each other, the most profitable equipment-wise capacity expansion strategy in terms of NPV results nearly in the same production rate development for nearly the same overall TCI with \$ 7.87 million compared to \$ 7.91 million and an NPV \$ 16.67 million compared to \$ 16.68 million. The only difference is that in case of the equipment-wise capacity expansion strategy, a single equipment module for C2-COND-PS is used, instead of a forced expansion in the sixth year in case of the 40 %-production line. Thus, the 40 %-production line represents almost the best expansion strategy for the equipment modules used in terms of the objectives $TCl_{initial}$ and NPV. However, this cannot be taken as general statement, since the reason for the good performance of the 40 %-production line might be a coincidence of the required production rate in year zero and the market demand development considered.

The full potential of stepwise capacity expansion strategies is realized by an equipment-wise capacity expansion using all equipment modules available in the equipment module databases. Figure 6-24 shows the resulting five Pareto-optimal modular equipment sets with minimum $TCl_{initial}$ and a maximum NPV after 200 generations. From the 110th generation on, only minor improvements are observed in the Pareto front. The algorithm runs are continued to the 200th generation and stopped after an overall simulation time of 8 weeks. Figure 6-24 verifies that the equipment-wise capacity expansion does not have a single best solution but a collection of Pareto-optimal solutions. The modular equipment set ES1 shows the lowest $TCl_{initial}$, whereas modular equipment set ES2 achieves the highest NPV.

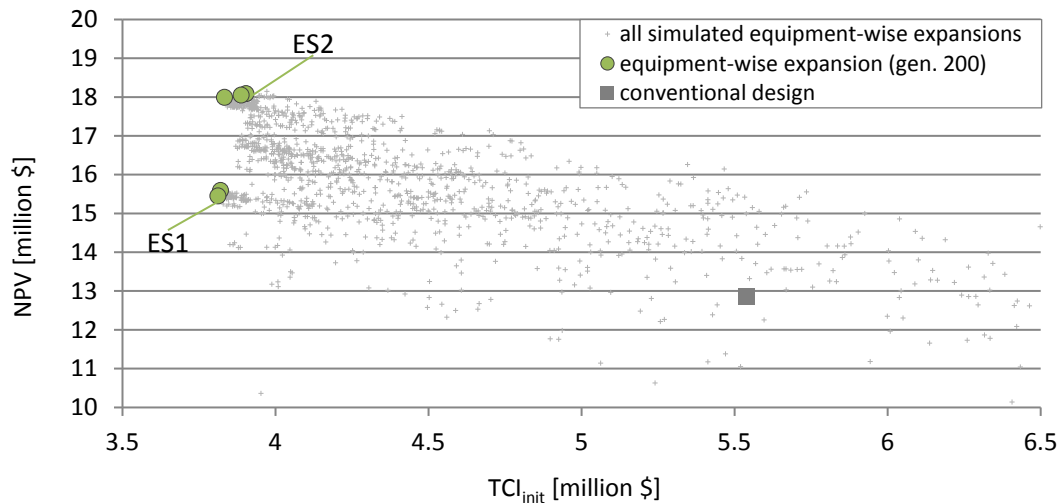


Figure 6-24: Pareto front of the equipment-wise capacity expansion strategies after the 200th generation, highlighting ES1 with the lowest $TCI_{initial}$ and ES2 with the highest NPV

A profit increase in terms of NPV for a little more initial investment can be achieved when comparing ES1 with ES2. More precisely, for 2.4 % more initial investment an NPV increase of 17.6 % can be achieved. To investigate and compare ES1 and ES2 in more detail, Figure 6-25 illustrates the production rates of the two modular equipment sets, as well as the development of the $TCI_{overall}$ to indicate the capacity expansions. Table 6-5 shows the size and numbers of the equipment modules selected for each process unit of ES1 and ES2.

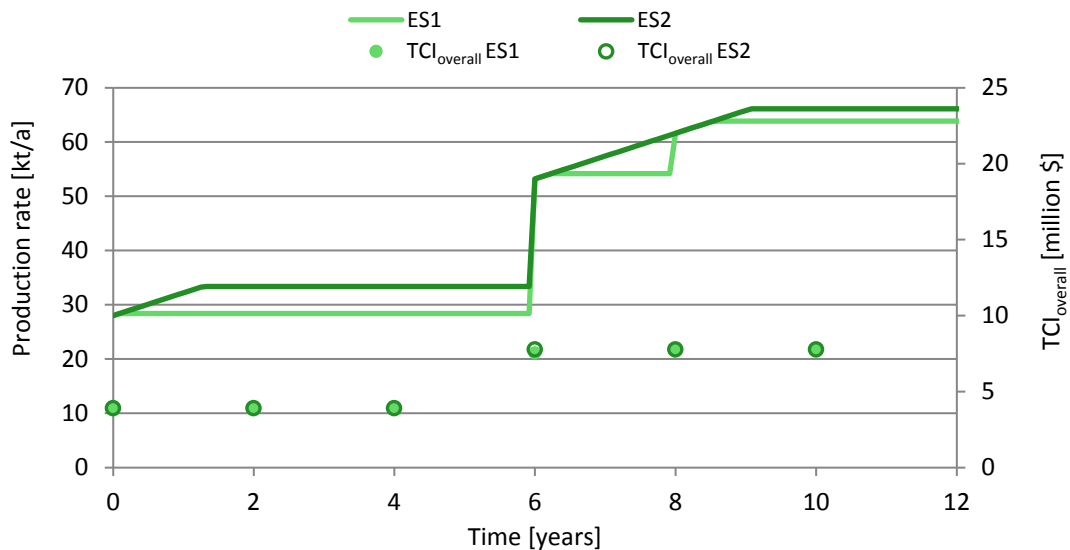


Figure 6-25: Production rate (lines) and overall TCI (dots) of modular equipment set ES1 (smallest $TCI_{initial}$) and modular equipment set ES2 (largest NPV)

The modular equipment set ES1 shows two capacity expansion steps, in year 6 adding second equipment modules except for C2-REB, and in year 8 adding a second equipment module for C2-REB and a third for HX3. The addition of a third equipment module for HX3 is necessary because ES1 uses a smaller HX3 compared to ES2. ES1 is the modular equipment set with the lowest $TCI_{initial}$, because it uses a smaller equipment module for HX3 and the

vapor-liquid separators HX1-PS, HX2-PS and C1-COND-PS. Furthermore, ES1 shifts the capacity expansion to a later point in time, although it uses three modules for HX3 compared to ES2. ES2 performs a single capacity expansion to two equipment modules in year 6 except for C2-COND-PS. Due to the larger final production rate of ES2, it shows with 92.7 % a higher satisfaction of the market volume compared to ES1 with 87.9 %.

Table 6-5: Number and size of equipment modules of two equipment-wise capacity expansion strategies

		ES1 (lowest $TCl_{initial}$)		ES2 (highest NPV)	
		Size ²	No. of modules after expansions	Size	No. of modules after expansions
HX1	[m ²]	14.1	2	14.1	2
HX2	[m ²]	12.0	2	12.0	2
HX3	[m ²]	11.2	3	13.8	2
C1-COND	[m ²]	51.2	2	51.2	2
C1-REB	[m ²]	18.3	2	18.3	2
C2-COND	[m ²]	3.2	2	3.2	2
C2-REB	[m ²]	2.1	2	2.1	2
R1	[-]	438	2	438	2
AB1	[m]	0.24	2	0.24	2
C1	[m]	1.30	2	1.30	2
C2	[m]	0.34	2	0.34	2
HX1-PS	[m ³]	7.95	2	11.58	2
HX2-PS	[m ³]	3.14	2	4.07	2
HX3-PS	[m ³]	0.81	2	0.81	2
C1-COND-PS	[m ³]	4.07	2	4.07	2
C2-COND-PS	[m ³]	0.15	2	0.29	1

Finally, all stepwise expansion strategies shall be compared to each other. Therefore, Figure 6-26 and Table 6-6 show the results of all expansion strategies.

² The 'size' of an equipment module refers to a characteristic size of the apparatus (i.e. area in case of a heat exchanger) that enables to relate the selected equipment module to the equipment module databases given in appendix A.3.4

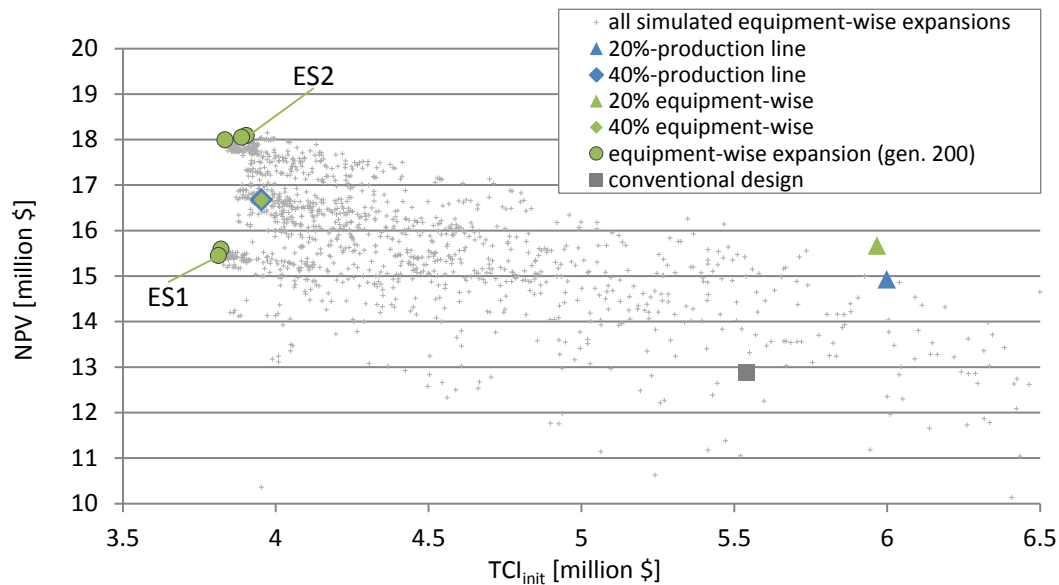


Figure 6-26: Results of all expansion strategies in terms of the objectives $TCI_{initial}$ and NPV

The equipment-wise expansion strategies and the 40 %-production line as well as the 40 % equipment-wise expansion offer a reduced initial investment risk, due to a lower $TCI_{initial}$, although the overall TCI is larger compared to the conventional plant. All stepwise expansion strategies show a larger absolute profit in terms of NPV and EAA due to the earlier market entry and the improved adaptability to the market demand development by the stepwise capacity expansions. Contrary results are obtained for the relative profit measured by the MIRR, where the conventional plant shows a superior performance compared to all stepwise capacity expansion strategies. The reason is based in the cost efficiency of the reference plant due to the economy of scale that favors a single investment in a large plant.

Table 6-6: Comparison of all expansion strategies by investment costs, NPV, EAA, MIRR and market satisfaction (PL = production line, EW = Equipment-wise)

		20 %-PL	40 %-PL	20 % EW	40 % EW	EW ES1	EW ES2	Conv. design
$TCI_{initial}$	[mio. \$]	6.00	3.95	5.97	3.95	3.81	3.90	5.54
$TCI_{overall}$	[mio. \$]	12.00	7.91	13.19	7.87	7.76	7.77	5.54
NPV	[mio. \$]	14.93	16.68	15.67	16.67	15.45	18.09	12.87
								22.68*
EAA	[mio. \$]	1.95	2.18	2.05	2.18	2.02	2.37	1.81
								3.19*
MIRR	[%]	18.0	20.3	18.0	20.3	20.1	20.7	24.0
Market satisfaction	[%]	92.6	89.6	98.0	89.6	87.9	92.7	77.8

*NPV and EAA discounted to the start of the planning period of the conventional plant

Finally, the reactor equipment modules of the equipment module database designed for a conversion of 90 % are replaced by the reactor modules with a larger operating window that are designed for a conversion of 85 %. Figure 6-27 shows the Pareto fronts of the equipment-

wise capacity expansion strategies using the conventional reactor modules in green and using the reactor modules with a larger operating window in orange of the 200th generation. It is clearly visible that by using the reactor modules with a larger operating window, the initial investment risk measured by the TCl_{initial} can be reduced while the absolute profit in terms of the NPV can be increased.

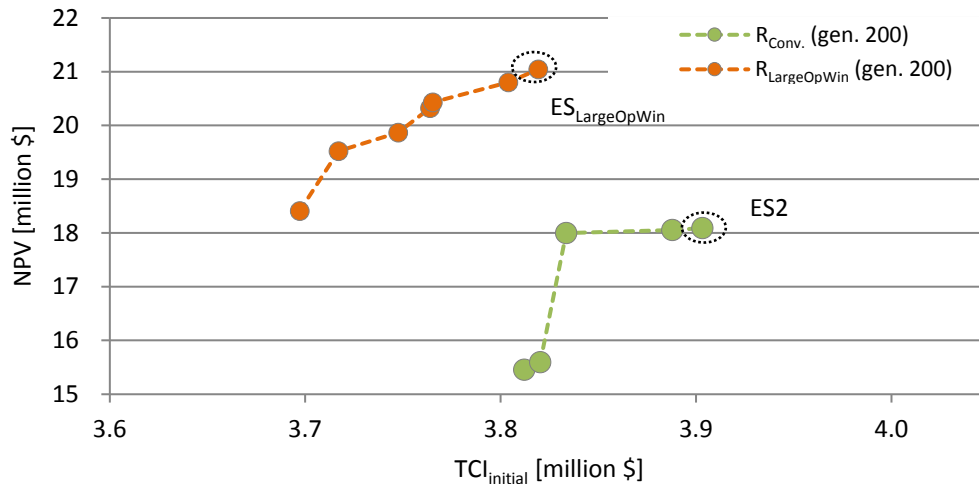


Figure 6-27: Pareto fronts of equipment-wise capacity expansion strategies with conventional reactor modules and reactor modules with a larger operating window

The two modular equipment sets with the largest NPV of both Pareto fronts ES2 and ES_{LargeOpWin} are used for a more detailed comparison. ES_{LargeOpWin} has with \$3.8 million a TCl_{initial} that is 2% lower compared to ES2 while the NPV is increased by 16% to \$21.04 million. Figure 6-28 shows the production rate and the overall TCI of both equipment-wise capacity expansion strategies and Table 6-7 gives an overview of the selected equipment modules. Both modular equipment sets use a single capacity expansion in year 6, whereby a second equipment module is added for each process unit except for C2-COND-PS in case of ES2. The reason is the larger C2-COND-PS equipment module selected for ES2. Besides the different reactor modules, ES_{LargeOpWin} uses a larger equipment module for HX1, AB1 and HX3-PS and a smaller equipment module for C1-REB and C2-COND-PS.

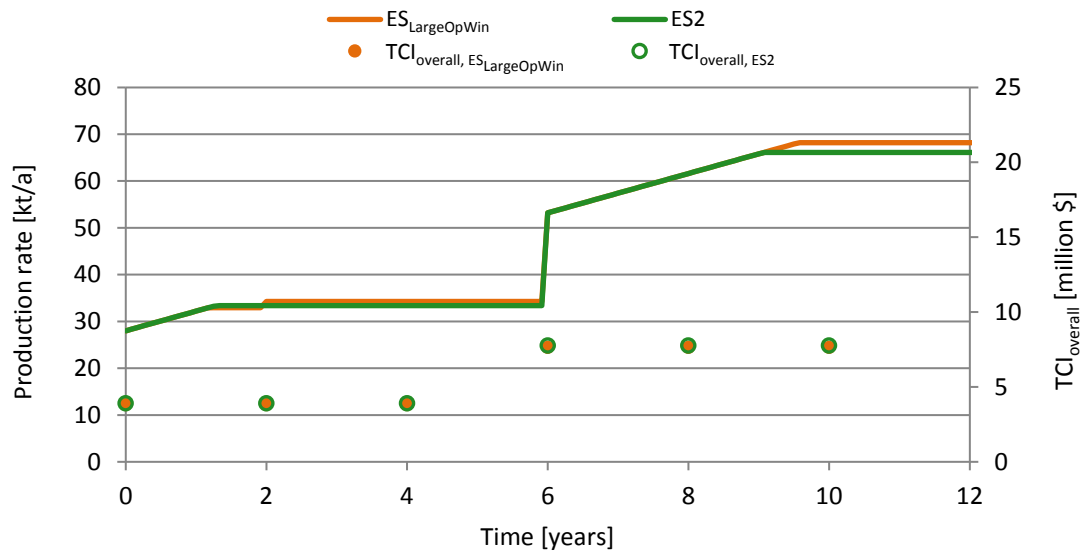


Figure 6-28: Production rate (lines) and overall TCI (dots) of modular equipment set ES_{LargeOpWin} (reactor modules with larger operating window) and modular equipment set ES2 (reactor modules designed for 90 % conversion)

By using the reactor modules with a larger operating window the reactor is limiting the overall operating window regarding $Cap_{min,plant}$ as well as $Cap_{max,plant}$ less often than in case of ES2. The small jump in the production rate of ES_{LargeOpWin} is due to the fact that the production rate is sampled yearly to estimate the operating window. Thus, two different production rates are simulated in year one and two, whereas the limiting process unit changes between both simulated production rates.

Table 6-7: Number and size of equipment modules of ES2 and ES_{LargeOpWin}

		ES _{LargeOpWin} (highest NPV)		ES2 (highest NPV)	
		Size	No. of modules after expansions	Size	No. of modules after expansions
HX1	[m ²]	14.9	2	14.1	2
HX2	[m ²]	12.0	2	12.0	2
HX3	[m ²]	13.8	2	13.8	2
C1-COND	[m ²]	51.2	2	51.2	2
C1-REB	[m ²]	17.6	2	18.3	2
C2-COND	[m ²]	3.2	2	3.2	2
C2-REB	[m ²]	2.1	2	2.1	2
R1	[-]	372	2	438	2
AB1	[m]	0.28	2	0.24	2
C1	[m]	1.30	2	1.30	2
C2	[m]	0.34	2	0.34	2
HX1-PS	[m ³]	11.58	2	11.58	2
HX2-PS	[m ³]	4.07	2	4.07	2
HX3-PS	[m ³]	1.15	2	0.81	2
C1-COND-PS	[m ³]	4.07	2	4.07	2
C2-COND-PS	[m ³]	0.15	2	0.29	1

As can be seen in Figure 6-28, the overall TCI of both modular equipment sets is nearly equal. To explain the increase in NPV of ES_{LargeOpWin} compared to ES2, the major cost differences are

investigated. On the one hand, the lower conversion of the reactor with the larger operating window increases the amount of unreacted IPA that is recycled. This leads to an increase in utility costs, especially for cooling water of condenser C2-COND. On the other hand, the lower conversion leads to an increased selectivity resulting in a lower raw material consumption and a slightly lower utility need for the reactor. In sum, the variable costs of $ES_{LargeOpWin}$ increased compared to ES2. However, this increasing variable costs are overcompensated by the increased earnings due to the larger $Cap_{max,plant}$ of $ES_{LargeOpWin}$ after the expansion timespan where it is able to produce 2.1 kt/a more compared to ES2, which is also visible comparing the different market volume satisfactions as 94.9 % compared to 92.7 % in case of ES2.

To show on the one hand the major obstacle in case of an equipment-wise capacity expansion and on the other hand the benefit of using equipment modules with a larger operating window Figure 6-29 and Figure 6-30 show the resulting operating windows of the of the equipment modules from ES2 and $ES_{LargeOpWin}$ after determining the required number of equipment modules to serve the market demand development at the final production rate of 70 kt/a. For a better orientation only the production rates at year 0, 2, 4, 6, 8, and 10 are shown. It is clearly visible that adding an equipment module for a process unit to enlarge the operating window often results in a gap of production rate. This happens when two times the minimum production rate of a single equipment module is larger than the maximum production rate of a single equipment module. Thus, adding an equipment module if a process unit reached its maximum production rate does not necessarily mean that the process unit is able to serve the next larger production rate. To enable a continuous operating window in case of using multiple equipment modules for a process unit, the precondition of $2 \times Cap_{min,singlePU} > Cap_{max,singlePU}$ must be fulfilled. Since in case of $ES_{LargeOpWin}$ the reactor has a larger operating window compared to ES2, no gap in the reactors' operating window occurs, although in both cases three reactor equipment modules are necessary to produce the final production rate of 70 kt/a. Due to a larger heat exchanger equipment module for HX1 in modular equipment set $ES_{LargeOpWin}$, the gap in the operating window disappeared due to a shift of the lower and upper capacity limit. Based on Figure 6-29 and Figure 6-30 it is also visible that some of the expansion steps required to serve the market demand development are not feasible due to the gaps in the operating windows and are thus not available as expansion steps. In case of the equipment modules from ES2 at 70 kt/a an expansion in year two, four, six and ten is not realizable due to gaps in the operating windows of process units. Compared to the equipment modules from ES2 at 70 kt/a, the expansion step in year six is realizable in case of the equipment modules from $ES_{LargeOpWin}$ at 70 kt/a, since the lower

operating boundaries of C2-COND and C2-REB moved, although identical equipment modules are used in both cases. This shows that changing an equipment module of a process unit can influence the operating windows of other process units.

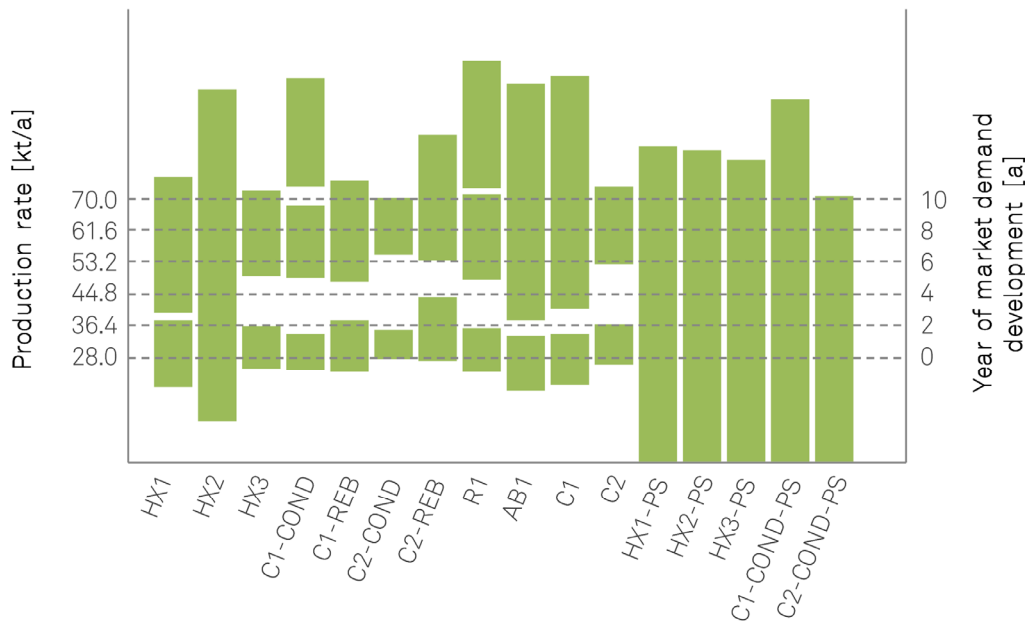


Figure 6-29: ES2 process units' operating windows after determining the required number of equipment modules to serve the market demand development at 70 kt/a

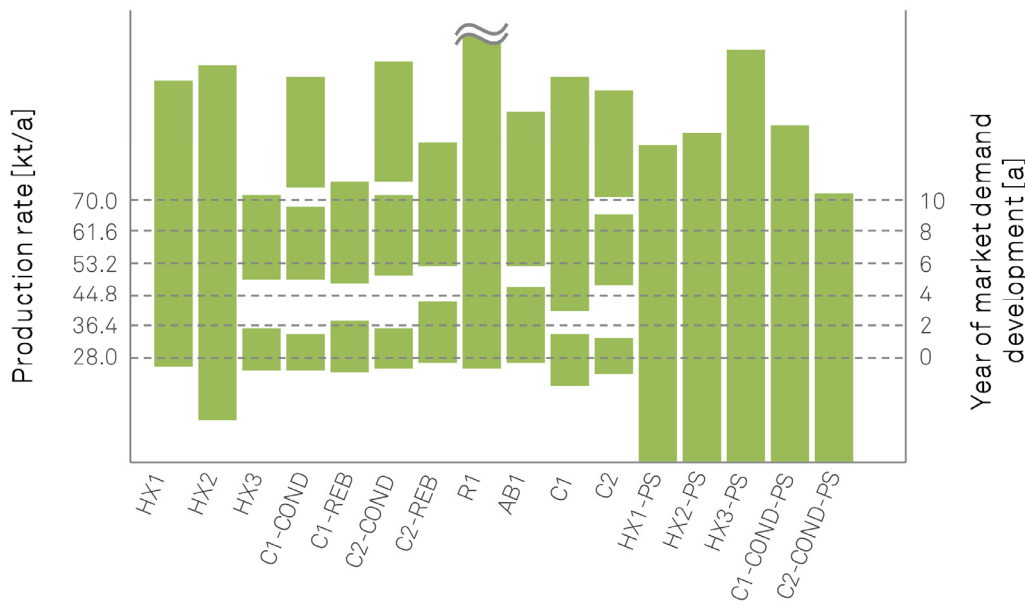


Figure 6-30: ES_{LargeOpWin} process units' operating windows after determining the required number of equipment modules to serve the market demand development at 70 kt/a

In summary, this study leads to two final key statements that are necessary to exploit the full potential of an equipment-wise capacity expansion: a) The determination of operating windows based on process-technological and mechanical operating constraints is important to enable the determination of gaps in case of numbering-up; and b) It is beneficial to design

equipment modules for a large operating window to offer a capacity expansion by numbering-up without a gap in the operating window.

6.4 Design for flexibility

The method to design equipment modules for flexibility, introduced in chapter 4.4, is applied to a liquid/liquid shell and tube heat exchanger without phase change based on the methanol cooler example of Sinnott et al. [122]. A sub-cooled condensate stream from a methanol condenser must be cooled from $T_{in,hot} = 95\text{ °C}$ to $T_{out,hot} = 40\text{ °C}$ using brackish water, as sketched in Figure 6-31.

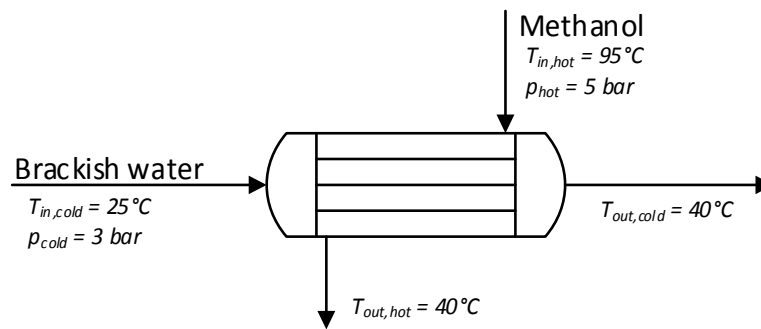


Figure 6-31: Sketch of the methanol cooler example

Since brackish water is the more corrosive of the two liquids handled, it is applied at the tube side [122]. The related heat capacities c_p , densities ρ , thermal conductivities k_f , fouling resistance factors R_f and viscosities μ are assumed to be constant [122]. Table A.7-1 provides an overview of the process conditions and the properties of the related liquids. A TEMA M-type rear head with fixed tube sheets is selected because the temperature difference does not exceed a value of 80 °C [122]. Carbon steel is used as material with a thermal conductivity of 54 W/m/K [123].

Since a liquid/liquid heat exchanger without phase change is investigated, the horizontal baffle orientation is considered only. The number of shell and tube passes are combined in the heat exchanger configuration which is represented in a double-digit number $N_{S,pass}N_{T,pass}$, whereby the shell passes are represented by the first digit and the number of tube passes by the second [124].

6.4.1 Development of the design approach and deduction of design rules of thumb

To individually sample all the design parameters, some adjustments to the design equations based on Kern's method [124] are necessary. A description of the basic approach to design a shell and tube heat exchanger with the corresponding equations is given in appendix A.7.2. Conventionally, the required heat transfer area is calculated from the heat balance (see Eq. A7-8 of Appendix A.7.2). Hence, the required heat transfer area and design parameters like the shell diameter d_s and the number of tubes directly depend on the design capacity. To overcome this dependency, the equations of Kern's method are customized as described in

the following. The inner shell diameter and the number of tubes at the design capacity are changed to an input design parameter. This is similar to other design procedures like the Bell-Delaware method [125] and the heat transfer area can be calculated as a function of d_s by Eq. 6-2, which is a reformulation of Eq. A7-10 from the appendix.

$$A = \frac{d_s^2 \cdot L_{eff} \cdot CTP}{0.637^2 \cdot PR^2 \cdot d_o \cdot CL} \quad \text{Eq. 6-2}$$

To verify whether the designed heat exchanger meets the required heat duty, the heat transfer area calculated by Eq. 6-2 is compared to the required heat transfer area from the heat balance in Eq. 6-3.

$$A = \frac{\dot{Q}}{U_{O,calc} \cdot \Delta T_m} \quad \text{Eq. 6-3}$$

Since the shell diameter represents an input design parameter now, the baffle spacing factor f_b needs to be adapted due to the percentage dependency of the baffle spacing factor on the shell diameter and the related range of variation. Therefore, the number of baffles N_b is used as input design parameter instead of the baffle spacing factor f_b of the conventional design procedure and Eq. 6-4 is used to calculate the baffle spacing.

$$l_b = \frac{N_b}{L_{eff}} \quad \text{Eq. 6-4}$$

This leads to an independent representation of l_b from d_s and avoids unrealistic baffle designs. To ensure a fixed orientation of the shell side nozzles, even numbers of baffles are used only. The discrete input design parameters resulting from the model adaptations and their range of variation are listed in Table 6-8. A constant tube thickness of 2 mm is used which is a recommended value for all tube OD sizes considered [126]. Additionally, a recommended value of the tube sheet thickness of 25 mm is applied [124].

Table 6-8: Adapted shell and tube heat exchanger design parameters and their possible values [122,126]

Design parameter	Unit	Values
Exchanger configuration $N_{S,pass}N_{T,pass}$	[-]	11, 12, 14, 16, 18, 22, 24, 26, 28, 33, 44
Tube OD d_o	[mm]	16, 20, 25, 30, 38
Tube length L	[m]	0.5, 1.0, 1.5, ..., 8
Tube pitch ratio PR	[-]	1.25, 1.33, 1.5
Layout angle a	[°]	30, 45, 60, 90
Inner shell diameter d_s	[m]	0.3, 0.35, 0.4, 0.5, ..., 2.5
Baffle cut b_c	[%]	15, 20, 25, 30, 35, 40, 45
Number of baffles N_b	[-]	2, 4, 6, 8, ..., 30

To ensure operability, the operating constraints summarized in Table 6-9 are utilized. As a large operating window is the key investigation goal in this work, pressure drop limitations have been neglected as they are typically applied for economic reasons only [125]. Equipment stability and secure operation are guaranteed by applying velocity boundaries v_s ,

and v_t on shell and tube side to avoid fouling in case of the lower boundary and stability problems like vibration and erosion in case of the upper boundary [124].

Table 6-9: Considered operating constraints for liquid/liquid shell and tube heat exchangers without phase change [122,126]

Operating constraint	Unit	Lower bound	Upper bound
v_t	[m/s]	1	2.5
v_s	[m/s]	0.3	1
Δp_t	[bar]	-	-
Δp_s	[bar]	-	-
Overdesign	[%]	-	5

To guarantee a sufficient heat transfer area and compensate the loss of heat transfer performance due to fouling, an overdesign of the heat exchanger is required [122] represented by the upper boundary of the overdesign constraint. The upper boundary is thereby the lower numerical value. The lower boundary of the overdesign is neglected in this work because it represents an economic limitation which restricts the increase of costs due to an oversized heat transfer area [127].

For the sampling generation, a base sample size of 1023 is used. To enable a statistical error estimation of the resulting sensitivity indices, the sampling is performed three times, generating 30 690 heat exchanger designs in total.

The capacity of the methanol cooler is described by the mass flow rate of methanol, because it is the process given duty that would change during market induced adaptations of a plant's production rate. Since the operating window of shell and tube heat exchangers is limited by different constraints, all operating constraints shown in Table 6-9 have to be fulfilled over the entire operating window. As described in chapter 4.4.3, the mass flow rate of the methanol stream is manipulated till the upper and lower operating constraints are reached. The resulting methanol mass flow rates represent the maximum and minimum capacity limitation regarding the related constraint.

In order to identify the design parameters with the strongest impact on the operating window, the described global sensitivity analysis (see chapter 4.4.4) is applied for ΔCap , Cap_{min} and Cap_{max} , respectively.

The sensitivity indices and interactions on ΔCap are shown in Figure 6-32. The exchanger configuration is the design parameter with the strongest impact on ΔCap . Its individual impact on ΔCap is represented by the first order index S_i and shows the highest value of 0.34. Furthermore, the shell diameter and the tube outside diameter (tube OD) show significant individual influences on the width of the operating window, whereas the influence of the shell diameter is dominated by interaction effects. The tube length, the tube pitch ratio and the number of baffles provide minor influences which are dominated by interactions. The

influences of the tube layout angle and the baffle cut are negligible because they do not show any significant sensitivity.

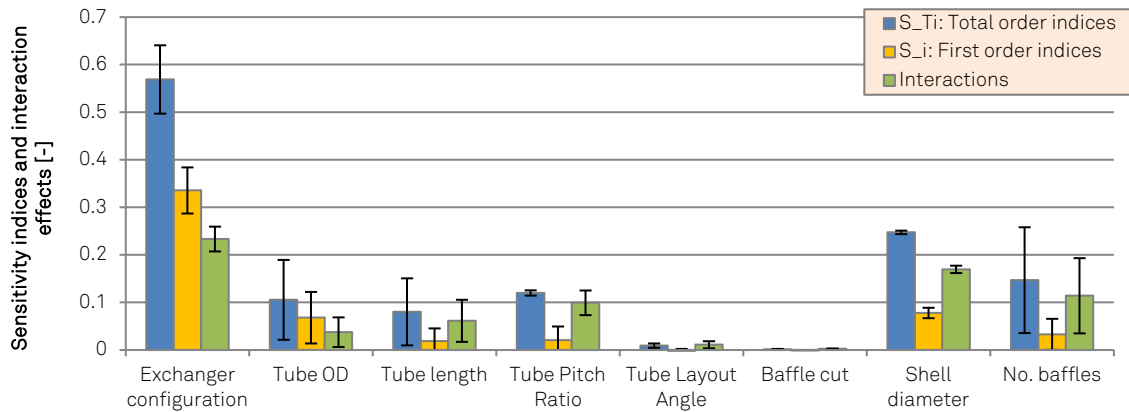


Figure 6-32: Sensitivity indices and interaction effects regarding ΔCap , bars represent the mean of three runs, $N_{base} = 1023$ per run

Figure 6-33 depicts the mean of the sensitivity indices and interaction effects for the triplet of runs according to Cap_{min} . The values of the sensitivity indices and interactions regarding Cap_{min} are dominated by the exchanger configuration and the shell diameter, with individual effects of 0.3 and 0.17, respectively. Like the measures of ΔCap , the tube layout angle and the baffle cut show a negligible impact on Cap_{min} . The other design parameters show a minor impact dominated by interactions.

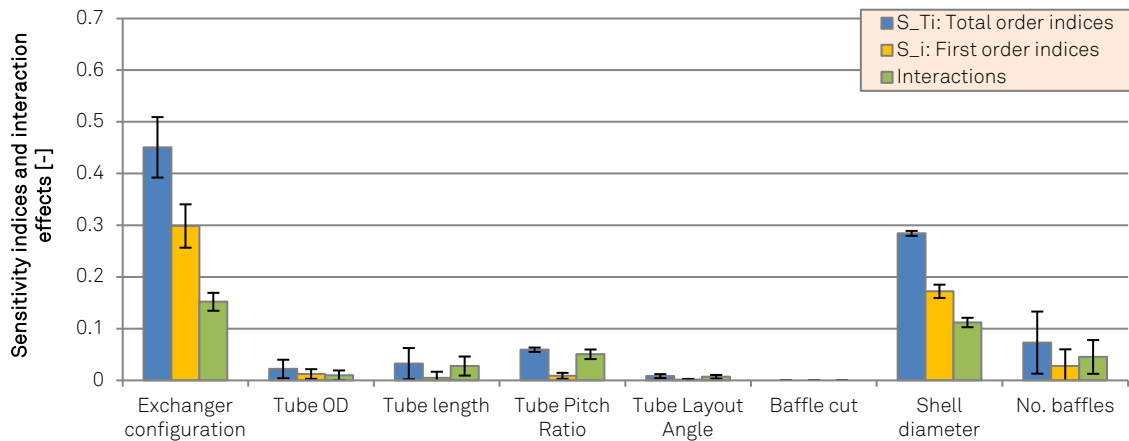


Figure 6-33: Sensitivity indices and interaction effects regarding Cap_{min} , bars represent the mean of three runs, $N_{base} = 1023$ per run

Analogously, Figure 6-34 illustrates the results regarding Cap_{max} . The tube length and the shell diameter show the largest impact with S_i values of 0.16, respectively. The tube OD follows as third most influential design parameter.

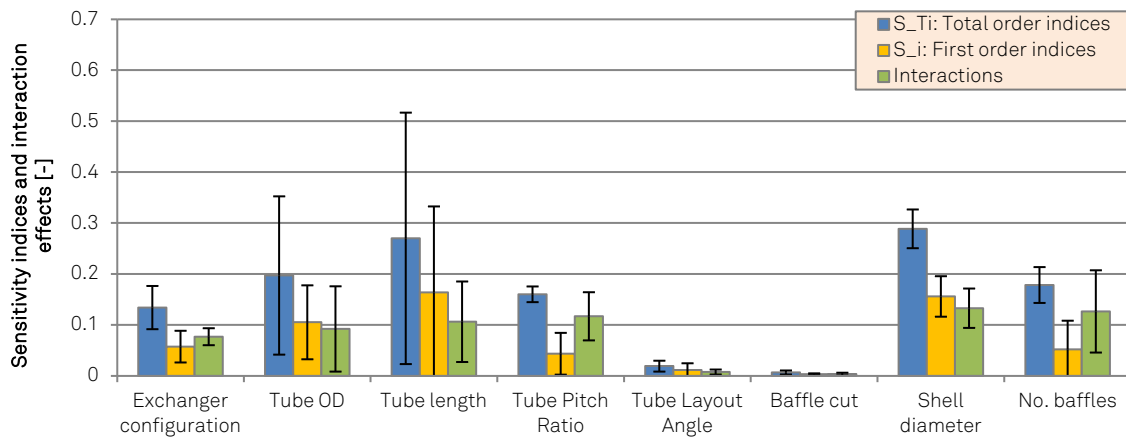


Figure 6-34: Sensitivity indices and interaction effects regarding Cap_{max} , bars represent the mean of three runs, $N_{base} = 1023$ per run

In contrast to the results for ΔCap and Cap_{min} , the exchanger configuration provides a small impact only, dominated by interactions. The number of baffles and the tube pitch ratio show a similar behavior with an influence dominated by interactions. Again, the tube layout angle and the baffle cut provide a negligible impact on Cap_{max} , as for ΔCap and Cap_{min} .

A summary of the design parameter influences on Cap_{min} , ΔCap and Cap_{max} is given in Table 6-10. Cap_{min} is mainly influenced by the same design parameters that are also responsible for the width of the operating window ΔCap . The most influential design parameters on Cap_{max} are different.

Table 6-10: Summary of influential design parameters on Cap_{min} , ΔCap and Cap_{max}

Rating measures	Cap_{min}	ΔCap	Cap_{max}	Negligible
Influential design parameters	- Exchanger config. - Shell diameter	- Exchanger config. - Tube OD - <i>Shell diameter</i>	- Tube length - Shell diameter - Tube OD - <i>Exchanger config.</i> - <i>Number of baffles</i> - <i>Tube pitch ratio</i>	- Tube layout angle - Baffle cut

* Italic parameters show an influence dominated by interactions

The first step of the design approach is to choose the corresponding design parameters with the major influence on Cap_{min} , namely the exchanger configuration and the shell diameter, to set Cap_{min} into a desired range. Since the influential design parameters on Cap_{min} are also influencing ΔCap , the first step of the design approach sets the values of design parameters according to the desired Cap_{min} with the potential of a large operating window ΔCap . Based on this potential, the most influential design parameters on Cap_{max} are set in the second step of the design approach aiming at a large value of Cap_{max} .

Regarding the first step of the design approach, the related design parameters according to Cap_{min} and ΔCap , namely the exchanger configuration, the shell diameter and the tube OD,

mainly influence the flow characteristics of the tube side. By setting these design parameters in the first design step, the degrees of freedom regarding the selection of the related design parameters according to Cap_{max} are reduced. Hence, Cap_{max} is increased by selecting the remaining influential design parameter values of tube length, number of baffles and tube pitch ratio in the second design step. The design parameters without any significant influence on Cap_{min} , ΔCap and Cap_{max} , namely the tube layout angle and the baffle cut, can be chosen independently. The resulting two-step design approach is depicted in Figure 6-35.

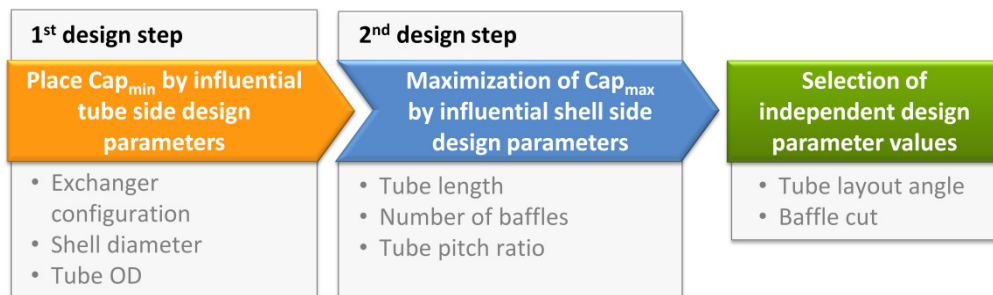


Figure 6-35: Two-step approach to design flexible liquid/liquid shell and tube heat exchangers without phase change

The dependencies that resulted in the two-step design approach are also reflected in the operating constraints limiting Cap_{min} and Cap_{max} . 68 % of all heat exchanger designs analyzed are restricted by the tube side velocity and 32 % by the shell side velocity according to Cap_{min} . On the other hand, Cap_{max} is restricted with 57 % by the overdesign, 33 % by the shell side velocity and only 10 % by the tube side velocity constraint. The small number of designs where Cap_{max} is restricted by the tube side constraint confirms the assumption that the tube side velocity mainly restricts Cap_{min} and that the related tube side design parameters should be selected in the first step of the design approach to set Cap_{min} into a desired interval.

To deduce design rules of thumb all technically feasible designs of the sampling are combined and the duplicates are deleted. Cap_{min} -intervals of 100 t/h are selected to cover a large capacity range with not too many intervals. In the following, 20 percent of the most flexible heat exchanger designs in terms of ΔCap_{rel} in each Cap_{min} -interval are investigated. Afterwards, the frequencies of occurrence of the design parameters in each Cap_{min} -interval are analyzed. It is important to note that the underlying number of designs differs within the intervals. By the sampling of designs heat exchangers with an operating window of up to 1000 t/h were found. Since fewer designs can be found in the larger capacity intervals and a realistic operation in such a high range is questionable, the consideration of the distributions is limited to the first five capacity intervals up to 500 t/h.

The design parameters of the first design step mainly related to the tube side are analyzed first. Figure 6-36 shows the distributions of the discrete values of the exchanger configuration $N_{S,pass}$ and $N_{T,pass}$ in the different Cap_{min} -intervals. The individual capacity intervals are dominated by different exchanger configurations, mainly differing by the number of tube passes.

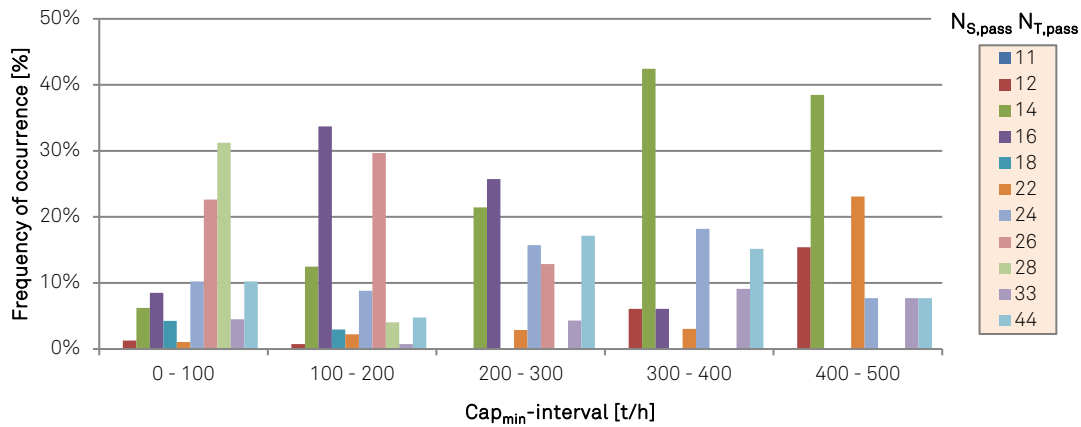


Figure 6-36: Distributions of the values for the exchanger configuration $N_{S,pass}N_{T,pass}$ in the considered intervals of Cap_{min}

The configurations with eight and six tube passes determine the distributions of the capacity intervals from 0 t/h to 100 t/h and 100 t/h to 200 t/h, respectively. The intervals from 300 t/h to 500 t/h are mainly dominated by the 14 configuration with a single shell and four tube passes.

The distributions of the shell diameter depicted in Figure 6-37 show a similar behavior. In the interval from 0 t/h to 100 t/h, the distribution is nearly uniform, slightly dominated by the smaller shell diameters from 0.6 m to 1.2 m. The distribution within the interval from 100 t/h to 200 t/h shows the highest bars for the middle range values of shell diameters from 1.9 m to 2.1 m. Larger capacities from 200 t/h to 500 t/h are dominated by the larger values of the shell diameter, as 1.7 m to 2.5 m. The shell diameter increases with an increasing Cap_{min} -interval due to the larger flow rates.

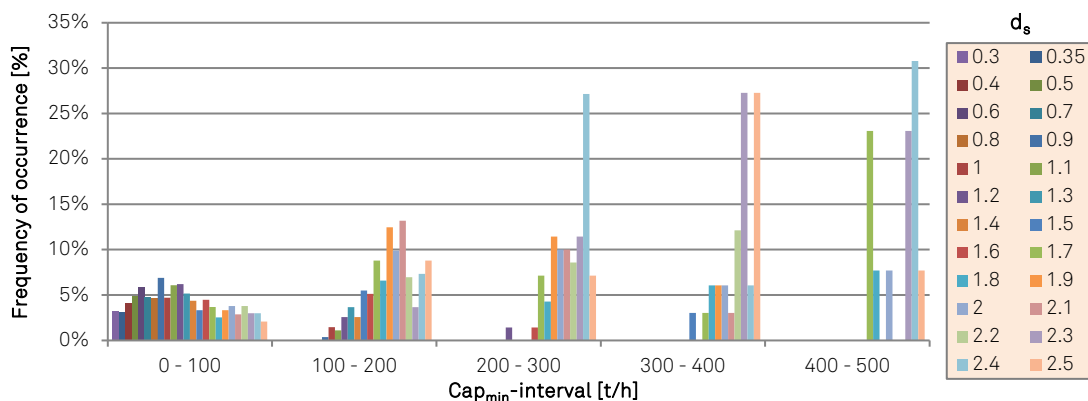


Figure 6-37: Distributions of the values for the shell diameter d_s in the considered intervals of Cap_{min}

The distributions of the tube OD are illustrated in Figure 6-38. In contrast to the distributions of the exchanger configuration and the shell diameter, there is no significant change of the distributions with an increasing Cap_{min} -interval visible.

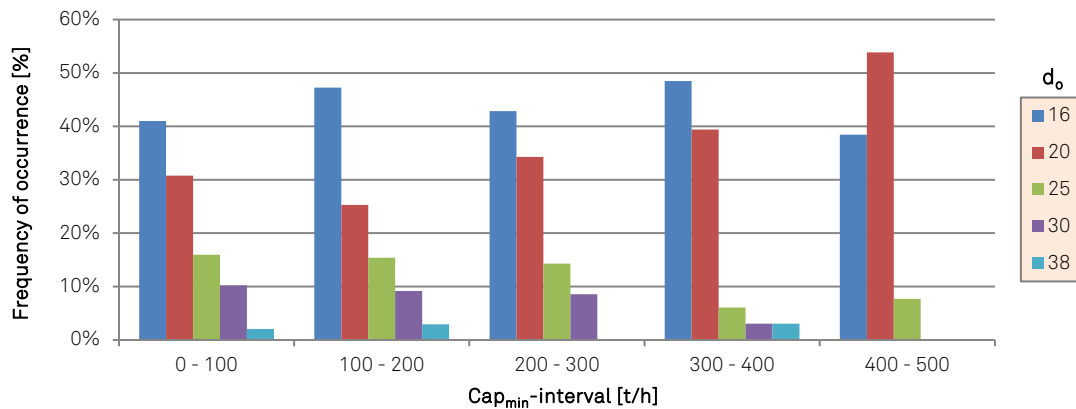


Figure 6-38: Distributions of the values for the tube OD d_o in the considered intervals of Cap_{min}

Small tube ODs, as 16 mm and 20 mm, are dominating the distributions over all capacity intervals. Since the exchanger configuration is the most influential design parameter on Cap_{min} and ΔCap it is selected first, according to the distributions within the different capacity intervals shown in Figure 6-36. The recommended values for the exchanger configurations based on these data are summarized in Table 6-11.

Table 6-11: Recommended values for the selection of the exchanger configuration

Interval of Cap_{min} [t/h]	Exchanger configuration [-]
0 – 100	26, 28
100 – 200	16, 26
200 – 300	14, 16, 24, 44
300 – 400	14
400 – 500	14, 22

Based on the fact that the exchanger configuration, the shell diameter and the tube OD influence the cross flow area of the tube side, rules of thumb are required considering combinations of these design parameters. Therefore, combinations of design parameters from 20 percent of the most flexible heat exchanger designs in terms of ΔCap_{rel} in each capacity interval with a small tube OD of 16 mm and 20 mm and an exchanger configuration according to the corresponding Cap_{min} -intervals as shown in Table 6-11 were analyzed. It was recognized that the designs can be classified regarding the ratio of the shell diameter to the number of tube passes for the different Cap_{min} -intervals. Many heat exchanger designs with large operating windows provide values of this ratio in defined ranges depending on the underlying Cap_{min} -intervals (see Table 6-12).

Table 6-12: Ratio of shell diameter to number of tube passes depending on Cap_{min} interval

Interval for Cap_{min} [t/h]	Range for $d_s/N_{T,pass}$ [1/m]	
	Lower Bound	Upper Bound
0 – 100	0.05	0.35
100 – 200	0.25	0.4
200 – 300	0.35	0.6
300 – 400	0.5	0.65
400 – 500	0.6	1.0

Summarizing the design rules of thumb for the first step of the design approach, the desired value of Cap_{min} can be realized by selecting the exchanger configuration according to Table 6-11. Next, the shell diameter d_s can be chosen based on the ratios of d_s to the number of tube passes of Table 6-12. For all capacity intervals, select a small tube OD of 16 mm or 20 mm to ensure that Cap_{min} lies in the desired interval.

The second step of the design approach aims at maximizing the value of Cap_{max} according to the defined interval of Cap_{min} . Therefore, the tube length, the number of baffles and the tube pitch ratio need to be selected. The frequency of occurrence distributions of these design parameters in the Cap_{min} -intervals are investigated for 20 percent of the heat exchanger designs with the largest Cap_{max} -value of each Cap_{min} -interval. Figure 6-39 shows the distributions according to the tube length.

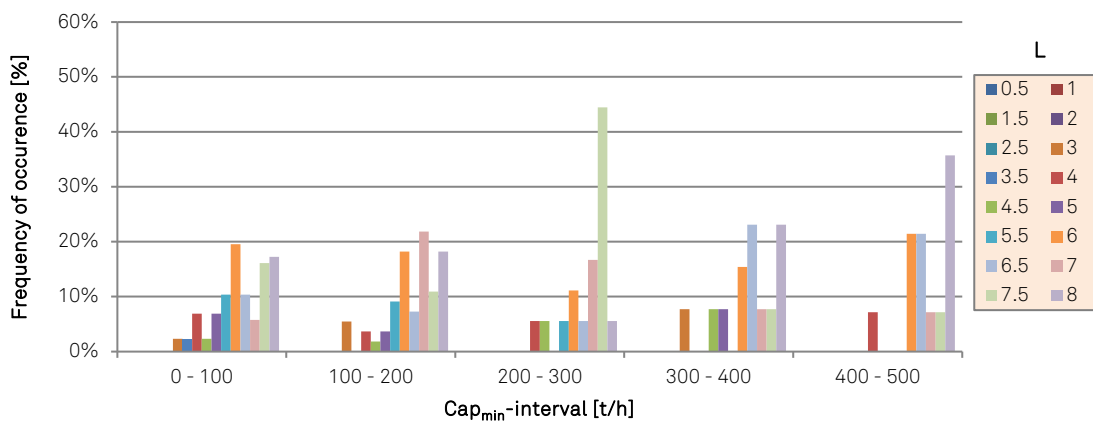


Figure 6-39: Distributions for the values of the tube length L in the considered intervals of Cap_{min}

Lower values of the tube length as 0.5 m to 2 m do not show up over the whole range of capacities. With an increasing capacity interval the distributions are more and more dominated by the larger tube lengths until the capacity interval from 400 t/h to 500 t/h with dominating tube lengths from 6 m to 8 m. This results from the required heat transfer area for the larger capacity intervals which can only be achieved using long tubes.

The distributions according to the number of baffles are illustrated in Figure 6-40. The lowest capacity interval from 0 t/h to 100 t/h shows mid-range to larger values of the baffle number,

which results from the related baffle spacing to ensure the required shell side velocities for the related low mass flow rates.

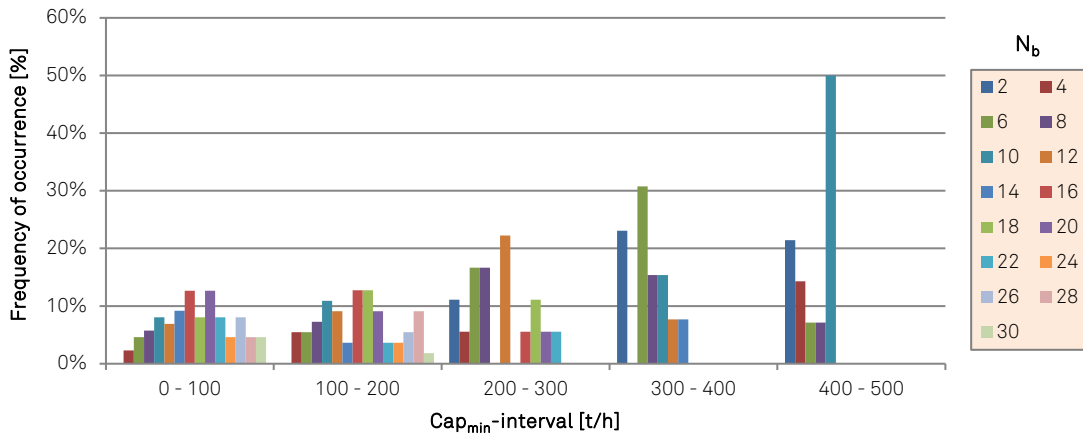


Figure 6-40: Distributions of the values for the number of baffles N_b in the considered intervals of Cap_{min}

With increasing Cap_{min} -intervals the distributions change from a middle-range dominated distribution between 100 t/h and 200 t/h to distributions that are dominated by the lower values of the baffle number between 200 t/h and 500 t/h.

As shown in Figure 6-41, no characteristic trend for the values of the tube pitch ratio can be observed over the Cap_{min} -intervals.

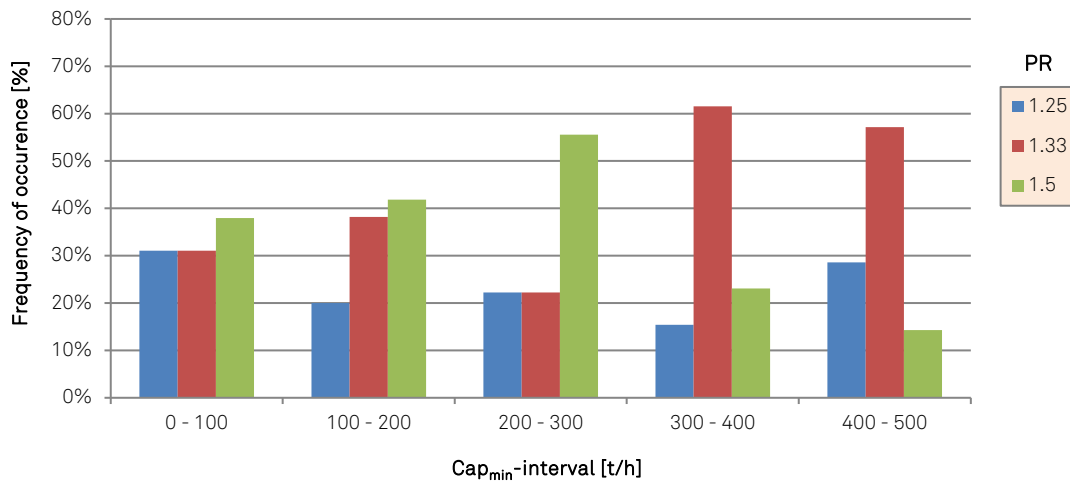


Figure 6-41: Distributions of the values for the tube pitch ratio PR in the considered intervals of Cap_{min}

To select the values of the design parameters according to the second step of the design approach to maximize Cap_{max} , it has to be noted that it was not possible to develop a specific rule of thumb for selecting the tube pitch ratio during the design analysis. All values for this design parameter were represented within the heat exchanger designs that provide a large Cap_{max} -value and there was no dependency to the capacity intervals detectable. As lower

tube pitch ratios provide an increased heat transfer [128], the lower values of the tube pitch ratio 1.25 and 1.33 are preferred in this work.

Since the tube length and the number of baffles determine the baffle spacing by the model adaption applied, rules of thumb are deduced which include both design parameters. To realize this goal, the heat exchangers with the largest Cap_{max} -value in each Cap_{min} -interval are analyzed according to the ratio of these design parameters. Additionally, the number of shell passes, which divides the shell side cross flow area, must be considered. Therefore, the ratio of the tube length to the number of baffles is divided by the number of shell passes. This ratio is defined as B according to Eq. 6-5.

$$B = \frac{L}{N_b N_{S,pass}} \quad \text{Eq. 6-5}$$

Since the value of Cap_{max} is mainly restricted by the oversize constraint, the tube length has to be chosen first, in order to ensure a sufficient heat transfer area. The analyzed heat exchanger designs are mainly dominated by the higher values of the tube length from 5 m to 8 m over the whole interval of capacities. Thus, a tube length within this range should be selected. To increase the possibility that the heat transfer area is sufficient the tube length should be increased with increasing capacity.

Depending on the selected length and the already determined exchanger configuration of the first step, 20 % of the heat exchanger designs with the largest Cap_{max} -value in each Cap_{min} -interval were analyzed according to the ratio B , shown in Table 6-13. Since the number of shell passes is already fixed by the selection of the exchanger configuration in the first step and the recommended value of the tube length, the number of baffles can be chosen from the ratio B .

Table 6-13: Recommended values for the ratio B to select the number of baffles

Interval of Cap_{min} [t/h]	Range of B [m]	
	Lower bound	Upper bound
0 – 100	0.1	0.4
100 – 200	0.2	0.45
200 – 300	0.3	0.9
300 – 400	0.5	1.1
400 – 500	0.6	1.5

As mentioned above, the tube layout angle and the baffle cut provide a negligible influence on the values for Cap_{min} , Cap_{max} and ΔCap . Therefore, they can be chosen independently from the design steps discussed. The tube layout angle should be chosen to 30 ° or 60 ° to provide a triangular arrangement which gives higher heat transfer rates than the square patterns but at the expense of an increasing pressure drop [124]. Furthermore, the recommended values

for the baffle cut from 20 % to 25 % are chosen in this work which provide the highest heat transfer coefficient [128].

The underlying number of designs for the deduction of the design rules of thumb are summarized in Figure A.7-1 of appendix A.7.3.

6.4.2 Evaluation of the design approach and the design rules of thumb for flexible shell and tube heat exchanger designs

The two-step design approach and the deduced design rules of thumb are applied to design a flexible methanol cooler. The flexible design will be compared to a design resulting from conventional design procedures.

The first step of the design approach requires the desired range of Cap_{min} . In this example Cap_{min} shall be in the range of 100 – 200 t/h.

First step:

- Select the exchanger configuration 16 from Table 6-11.
- Based on the exchanger configuration 16 choose a shell diameter of 2.0 m from Table 6-12 resulting in a ratio of 0.325, which lies in the middle of the recommended range.
- Set the tube OD to 20 mm which is a recommended low value.

Second step:

- Select a tube length of 6 m according to the low capacity interval.
- Choose a value of 18 for the number of baffles according to ratio B from Table 6-13. This provides a value of $B = 0.325$, which is in the middle of the desired range.
- Set the tube pitch ratio to 1.33.

Independent design parameter selection:

- Select a tube layout angle of 30 ° and a baffle cut of 25 %.

Using these design parameter values as input, the adapted model is applied to calculate the number of tubes and the heat transfer area. The final design of the shell and tube heat exchanger is summarized in Table 6-14.

Table 6-14: Design parameters of the exemplarily designed shell and tube heat exchanger with a large operating window for a desired Cap_{min} -interval of 100 to 200 t/h.

Design parameter	Unit	Value
Exchanger configuration	[-]	16
Shell diameter	[m]	2.0
Tube OD	[mm]	20
Tube length	[m]	6
Number of baffles	[-]	18
Tube pitch ratio	[-]	1.33
Tube layout angle	[°]	30
Baffle cut	[%]	25
Heat transfer area	[m ²]	1105
Number of tubes	[-]	2959

The operating window described by Cap_{min} , Cap_{max} and ΔCap of the designed flexible heat exchanger is shown in Figure 6-42.

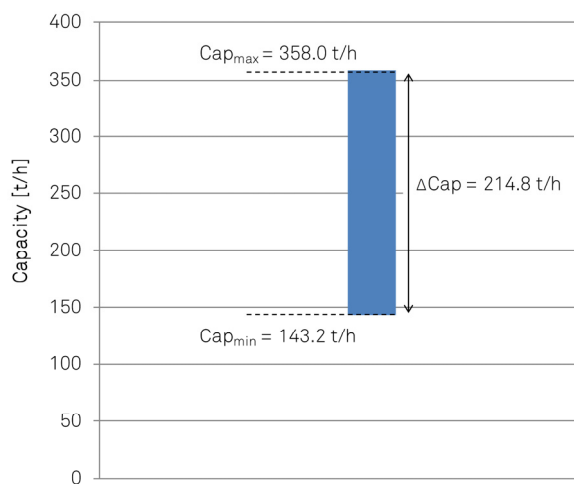


Figure 6-42: Operating window of the shell and tube heat exchanger designed for flexibility with design parameters listed in Table 6-14

Cap_{min} has been set to 143.2 t/h and was thus positioned in the desired capacity interval while Cap_{max} could be set to 358.0 t/h resulting in an ΔCap of 214.8 t/h.

A comparative analysis of a shell and tube heat exchanger designed for flexibility with a conventionally designed heat exchanger must consider the increase of the operating window and the related increase of investment and operating costs. Aspen EDR V8.4 is used as a reference for conventional shell and tube heat exchanger design at minimum investment costs. Most common cost models for shell and tube heat exchanger investment cost estimation are based on the heat transfer area, only. In order to analyze the differences between the flexible and the conventional heat exchangers in detail, a cost model suitable to consider small changes in the design parameter values is required. Therefore, a cost model calculating the costs based on the weight of the material used and the labor as in Aspen EDR is applied. Additionally, the operating costs are considered to determine the differences of the flexible and conventional design during the lifetime of the related heat exchanger. Hence, the total annual costs are used for a comparison, consisting of depreciated investment and

annual operating costs. A detailed description of the heat exchanger mass calculation can be found in appendix A.7.4. The values not calculated by the design procedure, as the shell thickness, the baffle thickness, the tie rod diameter and number, are estimated using recommended values according to the TEMA standards [129]. Working hours required for heat exchanger construction are estimated according to [124]. The total investment costs C_i of a shell and tube heat exchanger design are calculated by multiplying the total mass m_{tot} with $price_M$ as the price per kg of material used, adding the total number of working hours h_{tot} times the price per hour $price_h$. For a consistency check, investment costs calculated according to the method described above are compared with results obtained from Aspen EDR. The comparison led to a maximum deviation in equipment weight of 6 % and a mean of 3.25 %. To ensure comparability, the mean material price of 3.25 \$/kg was adapted for the calculations in this work from the Aspen EDR results. Analogously, the price for the working hours is assumed to 38.7 \$/h to realize a good comparability.

The operating costs of a shell and tube heat exchanger mainly consist of the pumping and utility costs [130]. The pumping power P depends on the mass flow rates and pressure drops of the shell and tube side and is calculated by Eq. 6-6, with a constant value of 0.8 for the pumping efficiency η [131].

$$P = \frac{1}{\eta} \cdot \left(\frac{\dot{m}_t}{\rho_t} \cdot \Delta p_t + \frac{\dot{m}_s}{\rho_s} \cdot \Delta p_s \right) \quad \text{Eq. 6-6}$$

Annual electricity costs C_{el} are calculated by multiplying the calculated pumping power P with 8232 annual operating hours n_{op} and the price for the electric power of 0.1 \$/kWh [132]. To determine the annual operating costs C_{op} , the price for the utility stream is set to 0.0382 \$/t [111]³ and the required mass flow rate is determined by a heat balance. The total annual costs C_{tot} are calculated by summing up the annual operating costs C_{op} and the investment costs C_i divided by a depreciation period of $n = 10$ years [132].

The design specifications and calculation methods used to generate the conventionally designed heat exchanger using Aspen EDR are summarized in Table A. 7-6 of appendix A.7.5. Since Aspen EDR selects the required tube length, the shell diameter, the baffle cut and the number of baffles according to the required heat duty, the ranges of variation for these design parameters are set according to Table 6-8 in chapter 6.4.1. The heat exchanger design with the lowest investment costs is selected. Heat exchanger designs with multiple shells in series or parallel are not considered. To ensure a good comparability, the operating windows of the conventionally designed heat exchangers are determined analogously to the

³ 1 € = 1.06 \$

procedure described for the heat exchangers designed for flexibility using the same operating constraints (cf. Table 6-9 in chapter 6.4.1). The conventionally designed heat exchanger is designed for a capacity of 150 t/h. The design parameters, related operating windows and costs of both shell and tube heat exchangers are compared in Table 6-15.

Table 6-15: Data of compared shell and tube heat exchangers for $Cap_{min} = 100 - 200$ t/h

Design parameters	Unit	Conventional Design	Flexible Design
Exchanger configuration	[-]	11	16
Shell diameter	[m]	0.675	2.0
Tube OD	[mm]	16	20
Tube length	[m]	8	6
Number of baffles	[-]	12	18
Tube pitch ratio	[-]	1.25	1.33
Tube layout angle	[°]	30	30
Baffle cut	[%]	45	25
Heat transfer area	[m ²]	354	1105
Number of tubes	[-]	888	2959
Δp_t @ 170.75 t/h	[bar]	0.174	0.611
Δp_s @ 170.75 t/h	[bar]	0.342	0.405
Cap_{min}	[t/h]	145.0	143.2
Cap_{max}	[t/h]	196.5	358.0
ΔCap	[t/h]	51.5	214.8
C_i	[\$]	59 000	201 000
C_{op} @ 170.75 t/h	[\$/a]	137 000	143 000
C_{tot}	[\$/a]	143 000	163 000

The shell diameter of the heat exchanger designed for flexibility is three times larger than the one of the conventionally designed heat exchanger. This results from the multi-pass arrangement of the flexible heat exchanger design which is also visible in the number of tubes that is increased by a factor of 3.3 in case of the design for flexibility. Since many design parameters are determined as a function of the shell diameter it is likely that the design procedure towards minimum investment costs aims at minimizing the values of these design parameters and thereby the amount of material used. Thus, the simplest exchanger configuration of 11 is used, which results in the smallest possible number of tubes and thereby minimizes the amount of material used to generate the required heat transfer area. The increased number of tube passes, the larger shell diameter of the flexible design and the related high number of tubes lead to investment costs increased by a factor of 3.4 compared to the conventional design towards minimum investment costs. The operating costs are calculated for the Cap_{mean} value of the conventionally designed heat exchanger as 170.75 t/h and show an increase of about 4 % for the flexible design. This results from the higher tube side pressure drop due to the multi-pass tube arrangement and the increased pressure drop on the shell side. It has to be noted that this value was calculated by the model in MS Excel. The pressure drop calculated by Aspen EDR is slightly different due to the differences in the

related calculation method. However, to ensure the comparability of the operating windows, the pressure drops calculated in MS Excel are used for comparison. Due to the high mass flow rates of the utility stream, the operating costs dominate the total annual costs. Therefore, the total annual costs show an increase of about 14 % for the flexible design, although the investment costs show a stronger increase. The costs determined are conservative estimations, since the main apparatus is considered only. For construction and installation, additional costs that are not size-dependent need to be considered, as the control system and electrical installations. This would bring the costs of the EDR design and the flexible design closer together. Figure 6-43 shows the different operating windows of the conventional and the flexible design.

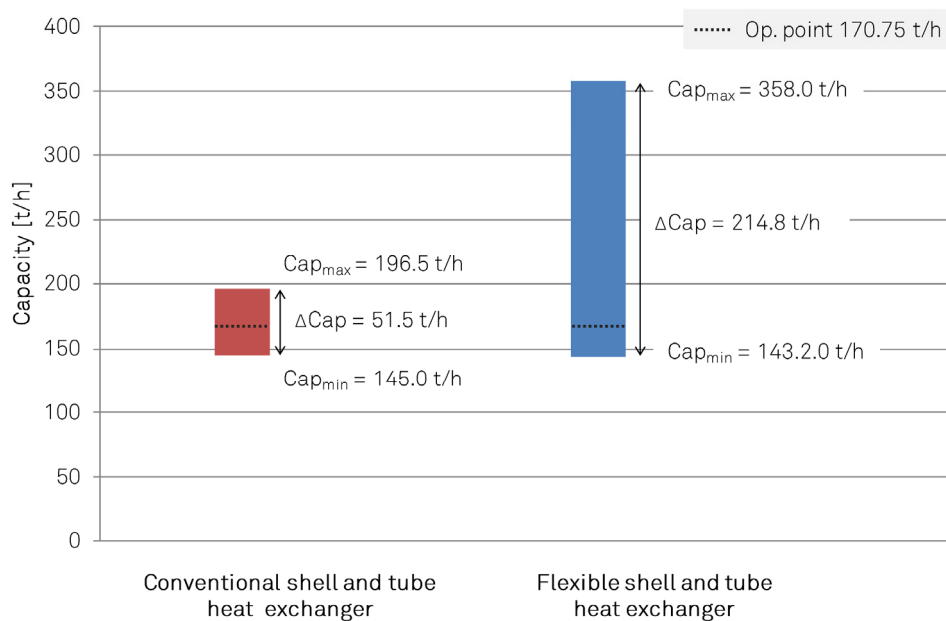


Figure 6-43: Comparative illustration of the operating windows of the designed shell and tube heat exchangers with $Cap_{min} = 100 - 200$ t/h

The heat exchanger designed for flexibility provides a strongly increased operating window. For 14 % higher annual cost a four-fold operating window can be obtained.

To compare the design for flexibility with a numbering-up of the conventionally designed heat exchanger, two of the conventionally designed heat exchangers in parallel are investigated. The resulting operating windows are compared to the design for flexibility in Figure 6-44.

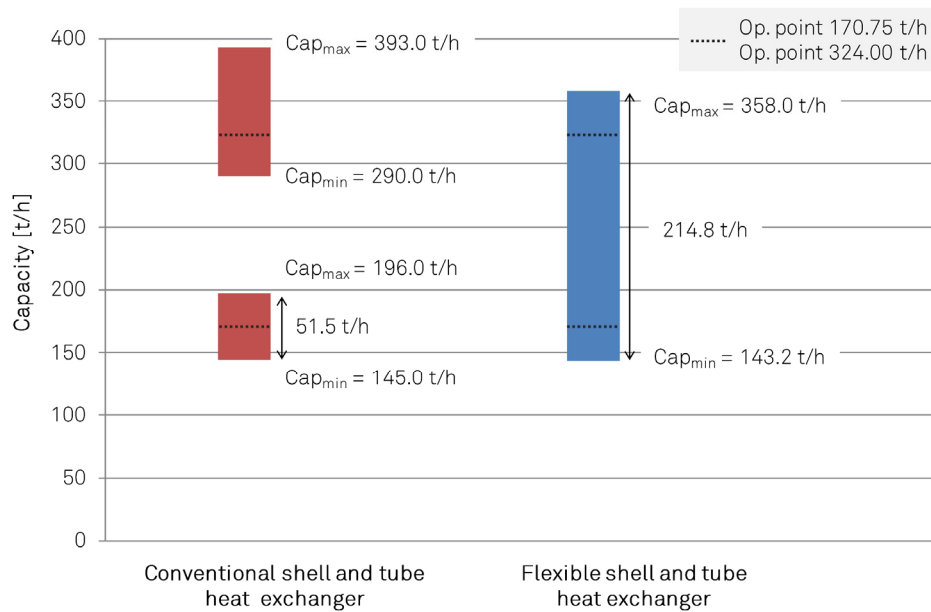


Figure 6-44: Comparative illustration of the operating windows of numbered-up conventional design and the shell and tube heat exchanger design for flexibility within $Cap_{min} = 100 - 200$ t/h

Increasing the operating window of the conventionally designed heat exchanger by numbering-up reveals a large gap in the operating window from 196 t/h to 290 t/h. This fact is often neglected when considering the increase of an operating window by numbering-up. In contrast, the operating window of the heat exchanger designed for flexibility enables a continuous operation over the entire operating window.

To compare the operating costs, a point of possible operation in the middle of the second overlapping section at 324 t/h is selected exemplarily, as indicated in Figure 6-44. The flexible design results in higher total annual costs of 334 000 \$/a compared to the conventionally designed and numbered-up heat exchanger with 272 000 \$/a. This results from the high investment costs of the heat exchanger designed for flexibility and the higher pressure drops at increasing loads. The detailed values are compared in Table 6-16.

Table 6-16: Data of compared shell and tube heat exchangers for $Cap_{min} = 100 - 200$ t/h

Design parameters	Unit	2x Conventional Design	Flexible Design
$Cap_{min,1}$	[t/h]	145.0	143.2
$Cap_{max,1}$	[t/h]	196.5	358.0
$Cap_{min,2}$	[t/h]	290.0	-
$Cap_{max,2}$	[t/h]	393.0	-
ΔCap	[t/h]	51.5 / 103.0	214.8
Δp_t (@ 324 t/h)	[bar]	0.318	1.942
Δp_s (@ 324 t/h)	[bar]	0.622	1.312
C_i	[\$]	117 000	201 000
C_{op} (@ 324 t/h)	[\$/a]	260 000	314 000
C_{tot}	[\$/a]	272 000	334 000

In the investigated case of the methanol cooler, the total annual costs at both operating points considered could not be reduced by the use of one heat exchanger designed for flexibility compared to the numbering-up of a conventionally designed apparatus. Thus, the preservation of the economy of scale by using a heat exchanger designed for flexibility instead of a numbering-up is not economically beneficial. The reason is the increase of the investment and operating costs for the flexible design compared to the conventional design. However, a major advantage of the heat exchanger designed for flexibility is the continuous coverage over the entire capacity interval. Again, the control system and electrical installations are size-independent and not considered. This would bring the costs of the conventional and the flexible design closer together. But more important, it has to be noted that additional costs as for the additional space requirement or process control devices which would increase the costs of numbering-up due to the use of two apparatuses, are not considered.

7 Major achievements

Within this work, an approach to determine the plants' overall operating window considering the design dependency and the often non-linear relationship between the operating constraints of a process unit and the production rate of a plant was developed and applied. A power-function-based approximation between the operating constraints of the process units to the production rate of the plant using the correlation exponents α considers the often non-linear relationships. This improves the determination of the operating window of a modular equipment set using the specific operating constraints of each process unit like flooding factors or velocities based on a single simulation point. Comparing the correlation-based approach to the assumption of a linear and constant relationship between operating constraints and production rate for the styrene production case study revealed a large difference in the resulting operating windows for certain process units. Although the limiting process unit does not change, it was shown that by assuming a linear and constant relationship the plants' operating window is overestimated. However, the correlation exponents determined are specific for each case study and depend on the modular equipment set that is used to determine them. Changing equipment modules of the modular equipment set will slightly change the correlation exponents. This is especially the case for process units that change the composition of a stream as reactors or distillation columns. Thus, strictly speaking the correlation exponents determined are only valid for the modular equipment set that is used to determine them. Nevertheless, the approach to determine the operating window of an entire plant consisting of the two steps: (1) Determination of the operating constraints based on a detailed simulation and the equipment modules' design parameters, and (2) Relating these operating constraints of the process units to the production rate of the plant, is a general approach that can be applied to other case studies. Furthermore, this work compared the impact of using equipment modules on operating costs versus investment costs. For the succinic acid production case study, it can be concluded that both investment and operating costs are equally important under the assumption of a 10-year depreciation period. Two new preselection approaches that consider both, investment and operating costs, have been developed, applied and evaluated. The most suitable preselection approach to decide on the use of equipment modules for process units of the case study investigated is the newly developed preselection approach *Inv&Op*, which allocates the operating costs directly by a distinction between avoidable and unavoidable raw material costs in combination with a position factor. Based on how much one is willing to pay for modularization with reference to investment and/or operating costs, the preselection criteria of the investigated preselection approaches can be adjusted. This may

relate to the critical CEX value of 0.6 or the average TCI in case of the preselection approach *Inv*. Further examples may include a different position factor or a different annualization of the investment costs. Additionally, the reference temperature and the handling of recycle streams in the case of the preselection approach *ExEco* may lead to different outcomes. All of these points require further investigation, especially in light of case studies that have a different characteristic cost structure compared to the case study of the fermentative succinic acid production investigated. Besides all uncertainties and limitations to a single case study, this work is a first step to think beyond investment costs when deciding on the use of equipment modules in module-based plant design and sets a basis for future investigations.

A multi-objective evolutionary algorithm was used to select equipment modules of discrete numbers and sizes for a flexible modular production plant. An analysis of the Pareto fronts of three independent runs revealed that the archive size N' should be increased for the case study used to reflect the characteristic shape of the Pareto front for the three objectives. Furthermore, an alternative clustering approach for the restriction of the archive size N' would help to maintain a uniform distribution of the Pareto sets stored in the archive. The trade-off solutions between flexibility in production rate and TCI of the case study show a characteristic shape with a plateau of Pareto-optimal modular equipment sets in a capacity range from -50 % to 40 %. On the edges of the lowest $Cap_{\min,plant}$ - and $Cap_{\max,plant}$ -values a large increase in TCI can be observed. The plateau is the most interesting region of the Pareto front as it offers a large increase in flexibility by a moderate increase in TCI. It is for example possible to achieve a 11-fold operating window compared to the conventional design for a 1.5-times increased TCI. The characteristic shape of the Pareto front can for example be used as fast shortcut cost estimation by engineering companies that offer modular production plants. The investigation of all Pareto-optimal modular equipment sets found within the three optimization runs of the case study revealed that no specific equipment module is preferably selected for a process unit of the Pareto sets. It was observed that both, a numbering-up of equipment modules and the use of oversized equipment modules were used to increase the operating window of process units while keeping the TCI low. This observation may strongly depend on the equipment module database used. Thus, when equipment modules designed for flexibility are present in the equipment module database, the need for a numbering-up of equipment modules for process units might be reduced. This might lead to a preferred use of such flexible equipment modules for the process units of the Pareto sets. Furthermore, it was observed that $Cap_{\min,plant}$ and $Cap_{\max,plant}$ of the Pareto-optimal modular equipment sets are determined by different process units. Thus, a

differentiation between the crucial process units regarding $Cap_{\min,plant}$ and $Cap_{\max,plant}$ is necessary to identify critical process units within equipment modules selection. In summary, the discrete, nonlinear, discontinuous and non-monotonic relations between the large number of different equipment module sizes and numbers, $Cap_{\min,plant}$, $Cap_{\max,plant}$ and the TCI lead to the final statement that a multi-objective evolutionary algorithm like SPEA seems to be currently essential to select equipment modules for a flexible modular production plant during module-based plant design.

By applying the extended equipment module selection framework to consider a market demand development with the objectives to minimize the initial TCI and maximize the NPV, the best trade-off solutions regarding a minimum investment risk and a better adaptability to improve the profit could be found. A comparison of the best equipment-wise capacity expansion strategies identified, to a line-wise capacity expansion strategy and the conventional approach in plant design revealed that the equipment-wise capacity expansion strategy seems to offer a promising approach. The initial investment risk can be reduced for the example considered by applying both stepwise capacity expansion strategies, although the overall investment increases compared to the conventional design approach. Furthermore, in terms of absolute profit measured by the NPV as well as the EAA the equipment-wise capacity expansion shows a superior performance followed by the line-wise capacity expansion strategy and the conventional design. This increased absolute profit results mainly from the earlier market entry enabling the satisfaction of a larger share of the possible market volume. However, in terms of relative profit measured by the MIRR, the cost-efficient conventional design that profits from economy of scale effects shows its strengths and outperforms both stepwise capacity expansion strategies. In summary, depending on the evaluation criteria used, different capacity expansion strategies are superior in case of the example considered. Whether the absolute profit, the relative profit or a minimum initial investment risk is the most important criterion depends on many boundary conditions and was not intended to be evaluated in this work. Notwithstanding this, a stepwise capacity expansion using equipment modules seems to provide a promising alternative to increase the profit of a plant in light of the changing and uncertain production requirements for the market scenario used. It needs to be mentioned that in case of storable products a conventional plant can start its production earlier to serve the market demand prior reaching $Cap_{\min,plant}$ and store product that is not being sold. This could improve the competitiveness of the conventional plant in terms of the absolute profit. Using the reactor modules with a larger operating window resulted in a larger NPV and a slightly decreased TCI_{initial} in case of the equipment-wise capacity expansion strategy. This increase in absolute profit resulted

from an increasing overall operating window leading to an increased satisfaction of the possible market volume. A detailed investigation revealed the huge impact of the process units' operating window size on the expansion steps. Although up to ten different and conventionally designed equipment modules were available in the equipment module database, gaps in the operating window often occurred hindering expansions to closely follow the market demand development. Therefore, the focus in equipment module design should not be limited to low investment and operating costs, it needs to include a large operating window. Only if a numbering-up without gaps in the operating windows is guaranteed by the equipment modules stored in the equipment module databases, the entire trade-off between initial investment risk and a better adaptability can be disclosed. Finally, a method to design equipment modules for flexibility based on a sampling and a global sensitivity analysis, leading to a two-step design approach and design rules of thumb was developed and applied. It was shown that the two-step design approach leads to shell and tube heat exchangers with a drastically increased operating window compared to the conventionally designed heat exchanger. Since the economic design boundaries of a conventional shell and tube heat exchanger design approach were neglected, a comparative analysis considering the investment and operating costs was performed. A detailed cost model was developed that takes small changes of design parameter values into account. It could be shown that the heat exchanger designed for flexibility provides a four times larger operating window for only 14 % higher total annual costs compared to a conventionally designed heat exchanger. A numbering-up of the conventionally designed shell and tube heat exchanger was compared to a flexible heat exchanger designed according to the derived design approach and the deduced design rules of thumb. This comparison showed that the heat exchanger designed for flexibility results in 23 % higher total annual costs compared to a numbering-up of the conventionally designed heat exchanger. However, a large gap in the resulting operating window was observed for the conventionally designed heat exchanger and size-independent costs were not considered. Including the size-independent costs would bring the costs of the conventional design and the flexible design closer together. The introduced design method is based on statistical analysis methods. Thus, it provides a statistical possibility to generate shell and tube heat exchanger designs with a large operating window for the used case study of a methanol cooler. Since the method introduced requires a mathematical model only enabling the determination of operating boundaries as basis, it can be applied to different types of equipment. So far, the design approach and the deduced design rules of thumb are limited to the underlying case study. In summary, the

introduced design method can set a promising basis to design equipment modules for the application in module-based plant design enabling an easy production rate adjustment.

8 Outlook & general conclusion

This work explored several important topics within module-based plant design at equipment level. Many of the developed and applied approaches are a first step to discover new and important aspects, where future research is required to deepen the understanding of essential points in module-based plant design at equipment level.

Future works should for example try to generalize the correlation-based approach to determine the plants' operating window since up to now the correlation exponents α are empirical and specific for each case study and equipment module used to determine them.

The approach for equipment module selection of this work should be extended to also allow the use of multiple equipment modules with different sizes for a process unit. Furthermore, it should be investigated which influence the equipment modules stored in the equipment module database have on the characteristic form of the Pareto front. It will be especially interesting to explore the influence of equipment modules designed for flexibility. This will give insights to the requirements for the development of equipment module databases. A combination of an evolutionary algorithm for equipment module selection and gradient-based mathematical programming for optimizing operational variables could be a promising extension of this work, since operating parameters can be used to enlarge or stay in an operating window of a process unit. Adjusting the operating parameters might also decrease the gaps that can occur by numbering-up equipment modules. Interesting to consider in future works would be uncertainties and market demand declines. Currently, the computational effort therefore is too high which is why such scenarios have not been included in this work. However, the proposed framework will also work for such cases. The consideration of additional space requirements for adding equipment modules during the plant layout and learning effects will bring the approach of stepwise capacity expansion strategies a step closer to reality.

The approach to design equipment modules for flexibility can be extended to consider also mechanical stability constraints of equipment modules. This will lead to a more realistic evaluation of the operating windows of shell and tube heat exchangers. Additionally, incorporating ranges of fluid property or application case data would enable the generation of a more generic design approach and design rules of thumb that are valid for a range of property or application case data. Finally, the approach to design equipment modules for flexibility should be applied to other equipment types to test and proof its general applicability.

The key goal in module-based plant design research must be a deeper understanding of the relation between operating constraints of process units and their respective investment and operating costs in light of an entire modular equipment set. As general conclusion it can be said that quick economic considerations to investigate and judge on module-based plant design are too superficial. It was shown that process technology as profound basis for an investigation and evaluation of module-based plant design is required and opens interesting and complex research challenges. This work investigated some areas in module-based plant design at equipment level beyond state of the art and should inspire future researchers to dig deeper and lay the path for a paradigm shift in plant design.

9 References

- [1] W.F. Furter, *A Century of chemical engineering: Based on the proceedings of an International symposium on the history of chemical engineering held at the 180th Meeting of the American chemical Society; Las Vegas, August 24-29, 1980*, Plenum Press, New York, London, 1982.
- [2] O. Krätz, *7000 Jahre Chemie: Alchemie, die schwarze Kunst, Schwarzpulver, Sprengstoffe, Teerchemie, Farben, Kunststoffe, Biochemie und mehr*, Lizenzausg, Nikol, Hamburg, 2000.
- [3] K. Sattler, *Verfahrenstechnische Anlagen: Planung, Bau und Betrieb*, John Wiley & Sons, 2000.
- [4] H. Silla, *Chemical process engineering: Design and economics*, M. Dekker, New York, 2003.
- [5] G.H. Vogel, *Process development: From the initial idea to the chemical production plant*, Wiley-VCH, Weinheim, Great Britain, 2010.
- [6] B.D. Fulks, *Planning and organizing for less-troublesome plant startups*, *Chem Eng (New York)* 89 (1982) 96–106.
- [7] R. Goedecke, *Fluidverfahrenstechnik. Grundlagen, Methodik, Technik, Praxis*, Wiley-VCH, Weinheim, 2006.
- [8] C. Tsay, R.C. Pattison, M.R. Piana, M. Baldea, *A survey of optimal process design capabilities and practices in the chemical and petrochemical industries*, *Comput. Chem. Eng.* 112 (2018) 180–189.
<https://doi.org/10.1016/j.compchemeng.2018.01.012>.
- [9] T.K. Buschulte, F. Heimann, *Verfahrensentwicklung durch Kombination von Prozeßsimulation und Miniplant-Technik*, *Chem Ing Tech* 67 (1995) 718–723.
<https://doi.org/10.1002/cite.330670604>.
- [10] H. Mothes, *No-Regret Solutions - Modular Production Concepts in Times of Complexity and Uncertainty [No-Regret-Lösungen - Modulare Produktionskonzepte Für komplexe, unsichere Zeiten]*, *Chem Ing Tech* 87 (2015) 1159–1172.
<https://doi.org/10.1002/cite.201400133>.
- [11] Kranenburg, K.J. van, Sofra, C., Verdoes, D., Graaff, M.P. de, *Small-scale flexible plant. Towards a more agile and competitive EU chemical industry*, 2015.
- [12] C. Bramsiepe, S. Sievers, T. Seifert, G.D. Stefanidis, D.G. Vlachos, H. Schnitzer, B. Muster, C. Brunner, J. Sanders, M.E. Bruins, G. Schembecker, *Low-cost small scale processing technologies for production applications in various environments-Mass produced factories*, *Chem. Eng. Process.: Process Intensif.* 51 (2012) 32–52.
<https://doi.org/10.1016/j.cep.2011.08.005>.
- [13] M. Eilermann, C. Post, H. Radatz, C. Bramsiepe, G. Schembecker, *A general approach to module-based plant design*, *Chem. Eng. Res. Des.* 137 (2018) 125–140.
<https://doi.org/10.1016/j.cherd.2018.06.039>.
- [14] L. Hohmann, K. Kössl, N. Kockmann, G. Schembecker, C. Bramsiepe, *Modules in process industry – A life cycle definition*, *Chem. Eng. Process.: Process Intensif.* 111 (2017) 115–126. <https://doi.org/10.1016/j.cep.2016.09.017>.
- [15] ISO 10628-1:2014, *Diagrams for the chemical and petrochemical industry - Part 1: Specification of diagrams*.
- [16] J.R. Coleman JR., R. York, *Optimum plant design for a growing market*, *Industrial and Engineering Chemistry* 56 (1964) 28–34. <https://doi.org/10.1021/ie50649a005>.
- [17] B. Bruns, M. Grünwald, J. Riese, *Analysis of Capacity Potentials in Continuously Operated Chemical Processes*, *Chem Ing Tech* (2020).
<https://doi.org/10.1002/cite.202000053>.
- [18] I.E. Grossmann, Sargent, R. W. H., *Optimum design of chemical plants with uncertain parameters*, *AIChE J* 24 (1978) 1021–1028.

- [19] I.E. Grossmann, K.P. Halemane, Decomposition strategy for designing flexible chemical plants, *AIChE J* 28 (1982) 686–694.
- [20] I.E. Grossmann, C. Floudas (Eds.), *New approach for evaluating flexibility in chemical process design*, Inst. of Chemical Engineers, distributed by Pergamon Press, Oxford, Cambridge, 1985.
- [21] Chien, D. C. H., P.L. Douglas, A. Penlidis, Method for flexibility analysis of continuous processing plants, *Can J Chem Eng* 69 (1991) 58–66.
- [22] P.M. Hoch, A.M. Eliceche, I.E. Grossmann, Evaluation of design flexibility in distillation columns using rigorous models, *Comput. Chem. Eng.* 19 (1995) 669–674. [https://doi.org/10.1016/0098-1354\(95\)87112-8](https://doi.org/10.1016/0098-1354(95)87112-8).
- [23] T. Seifert, *A contribution to the design of flexible modular chemical plants*, Dr. Hut, München, 2015.
- [24] N. Ishii, T. Fuchino, M. Muraki, Life cycle oriented process synthesis at conceptual planning phase, *Comput. Chem. Eng.* 21 (1997) 953–958.
- [25] V. Goyal, M.G. Ierapetritou, Integration of Data Analysis and Design Optimization for the Systematic Generation of Equipment Portfolio, *Ind. Eng. Chem. Res.* 42 (2003) 5204–5214. <https://doi.org/10.1021/ie020755+>.
- [26] V. Goyal, M.G. Ierapetritou, Multiobjective framework for modular design generation incorporating demand uncertainty, *Ind. Eng. Chem. Res.* 44 (2005) 3594–3606. <https://doi.org/10.1021/ie049336y>.
- [27] A.R. Sirdeshpande, M.G. Ierapetritou, M.J. Andrecovich, J.P. Naumovitz, Process synthesis optimization and flexibility evaluation of air separation cycles, *AIChE Journal* 51 (2005) 1190–1200. <https://doi.org/10.1002/aic.10377>.
- [28] J. Oldenburg, M. Schlegel, J. Ulrich, T.-L. Hong, B. Krepinsky, G. Grossmann, A. Polt, H. Terhorst, J.-W. Snoeck, A.P. Plesu V., A method for quick evaluation of stepwise plant expansion scenarios in the chemical industry, *Comput. Aided Chem. Eng.* 24 (2007) 563–568. [https://doi.org/10.1016/S1570-7946\(07\)80117-9](https://doi.org/10.1016/S1570-7946(07)80117-9).
- [29] A. Wiesner, M. Schlegel, J. Oldenburg, L. Würth, R. Hannemann, A. Polt, J.X. Braunschweig B., Model-based investment planning model for stepwise capacity expansions of chemical plants, *Comput. Aided Chem. Eng.* 25 (2008) 307–312. [https://doi.org/10.1016/S1570-7946\(08\)80056-9](https://doi.org/10.1016/S1570-7946(08)80056-9).
- [30] S. Lier, M. Grünwald, Net Present Value Analysis of Modular Chemical Production Plants, *Chem. Eng. Technol.* 34 (2011) 809–816. <https://doi.org/10.1002/ceat.201000380>.
- [31] S. Lier, D. Wörsdörfer, M. Grünwald, Real options for economic assessments of innovation projects in chemical production [Realoptionen zur Wirtschaftlichkeitsbewertung von Innovationsprojekten in der Chemieproduktion], *Chem Ing Tech* 84 (2012) 2164–2173. <https://doi.org/10.1002/cite.201200017>.
- [32] A. Harwardt, M. Skiborowski, W. Marquardt, Modular equipment design in optimization-based process synthesis, *Comput. Aided Chem. Eng.* 30 (2012) 517–521. <https://doi.org/10.1016/B978-0-444-59519-5.50104-0>.
- [33] M.-A. Cardin, M. Ranjbar-Bourani, R. de Neufville, Improving the lifecycle performance of engineering projects with flexible strategies: Example of on-shore LNG production design, *Systems Engineering* 18 (2015) 253–268. <https://doi.org/10.1002/sys.21301>.
- [34] A. Geraili, J.A. Romagnoli, A multiobjective optimization framework for design of integrated biorefineries under uncertainty, *AIChE Journal* 61 (2015) 3208–3222. <https://doi.org/10.1002/aic.14849>.
- [35] M. Heitmann, T. Huhn, S. Sievers, G. Schembecker, C. Bramsiepe, Framework to decide for an expansion strategy of a small scale continuously operated modular multi-product plant, *Chem. Eng. Process.: Process Intensif.* 113 (2017) 74–85. <https://doi.org/10.1016/j.cep.2016.09.004>.

- [36] T. Seifert, H. Schreider, S. Sievers, G. Schembecker, C. Bramsiepe, Real option framework for equipment wise expansion of modular plants applied to the design of a continuous multiproduct plant, *Chemical Engineering Research and Design* 93 (2015) 511–521. <https://doi.org/10.1016/j.cherd.2014.07.019>.
- [37] M. Baldea, B.A. Snowden, T.T. Do, Scaling Relations in Modular Process Design, in: *Proceedings of the 9th International Conference on Foundations of Computer-Aided Process Design*, Elsevier, 2019, pp. 481–485.
- [38] D.R. Woods, *Rules of thumb in engineering practice*, first ed., first repr, Wiley VCH, Weinheim, 2007.
- [39] T. Seifert, S. Sievers, C. Bramsiepe, G. Schembecker, Small scale, modular and continuous: A new approach in plant design, *Chem. Eng. Process.: Process Intensif.* 52 (2012) 140–150. <https://doi.org/10.1016/j.ccep.2011.10.007>.
- [40] T. Seifert, P. Fakner, S. Sievers, F. Stenger, B. Hamers, M. Priske, M. Becker, R. Franke, G. Schembecker, C. Bramsiepe, Intensified hydroformylation as an example for flexible intermediates production, *Chem. Eng. Process.: Process Intensif.* 85 (2014) 1–9. <https://doi.org/10.1016/j.ccep.2014.07.003>.
- [41] T. Seifert, J.M. Elischewski, S. Sievers, F. Stenger, B. Hamers, M. Priske, M. Becker, R. Franke, G. Schembecker, C. Bramsiepe, Multivariate risk analysis of an intensified modular hydroformylation process, *Chem. Eng. Process.: Process Intensif.* 95 (2015) 124–134. <https://doi.org/10.1016/j.ccep.2015.05.010>.
- [42] P.M. Hoch, A.M. Eliceche, Flexibility analysis leads to a sizing strategy in distillation columns, *Comput. Chem. Eng.* 20 (1996) S139–S144.
- [43] D. Sudhoff, M. Leimbrink, M. Schleinitz, A. Górak, P. Lutze, Modelling, design and flexibility analysis of rotating packed beds for distillation, *Chem. Eng. Res. Des.* 94 (2015) 72–89. <https://doi.org/10.1016/j.cherd.2014.11.015>.
- [44] M. Fesanghary, E. Damangir, I. Soleimani, Design optimization of shell and tube heat exchangers using global sensitivity analysis and harmony search algorithm, *Appl Therm Eng* 29 (2009) 1026–1031. <https://doi.org/10.1016/j.applthermaleng.2008.05.018>.
- [45] J. Szargut, D.R. Morris, F.R. Steward, *Exergy analysis of thermal, chemical, and metallurgical processes*, Hemisphere Publishing, New York, 1987.
- [46] A.P. Hinderink, F.P.J.M. Kerkhof, A.B.K. Lie, J.D.S. Arons, H.J. van der Kooi, Exergy analysis with a flowsheeting simulator--I. Theory; calculating exergies of material streams, *Chemical Engineering Science* (1996) 4693–4700.
- [47] G. Tsatsaronis, M.-H. Park, On avoidable and unavoidable exergy destructions and investment costs in thermal systems, *Energy Convers. Manag* (2002) 1259–1270.
- [48] K. Riedl, *Exergetische und Exergoökonomische Bewertung von Verfahren der Energie- und Stoffumwandlung*, Zentrum für Ingenieurwissenschaften, Halle-Wittenberg, 2007.
- [49] G. Wall, Exergy tools, *Proceedings of the Institution of Mechanical Engineers, Part A: Journal of Power and Energy* 217 (2003) 125–136. <https://doi.org/10.1243/09576500360611399>.
- [50] Nimkar, S.C. and Mewada, R.K., An overview of exergy analysis for chemical process industries, *International Journal of Exergy* (2014) 468–507.
- [51] E. Querol, B. Gonzalez-Reguer, J.L. Perez-Benedito, *Practical approach to exergy and thermoeconomic analyses of industrial processes*, Springer, London, Heidelberg, 2013.
- [52] B.V. Babu, S.A. Munawar, Differential evolution strategies for optimal design of shell-and-tube heat exchangers, *Chem. Eng. Sci.* 62 (2007) 3720–3739. <https://doi.org/10.1016/j.ces.2007.03.039>.
- [53] Coello Coello, Carlos A, G.B. Lamont, Van Veldhuizen, David A, *Evolutionary algorithms for solving multi-objective problems*, second ed., Springer, New York, 2007.

- [54] K. Deb, *Multi-objective optimization using evolutionary algorithms*, Wiley, Chichester, 2001.
- [55] E. Zitzler, L. Thiele, Multiobjective evolutionary algorithms: A comparative case study and the strength Pareto approach, *IEEE Transactions on Evolutionary Computation* 3 (1999) 257–271. <https://doi.org/10.1109/4235.797969>.
- [56] T. Bäck, H.-P. Schwefel, An Overview of Evolutionary Algorithms for Parameter Optimization, *Evol. Comput.* 1 (1993) 1–23. <https://doi.org/10.1162/evco.1993.1.1.1>.
- [57] P. Jäckel, *Monte Carlo methods in finance*, Wiley, Chichester u.a, 2002.
- [58] J.H. Halton, On the efficiency of certain quasi-random sequences of points in evaluating multi-dimensional integrals, *Numerische Mathematik* 2 (1960) 84–90. <https://doi.org/10.1007/BF01386213>.
- [59] J.H. Halton, Berichtigung, *Numerische Mathematik* 2 (1960) 196. <https://doi.org/10.1007/BF01386222>.
- [60] E. Braaten, G. Weller, An improved low-discrepancy sequence for multidimensional quasi-Monte Carlo integration, *Journal of Computational Physics* 33 (1979) 249–258. [https://doi.org/10.1016/0021-9991\(79\)90019-6](https://doi.org/10.1016/0021-9991(79)90019-6).
- [61] H. Faure, Discrépances de suites associées à un système de numération (en dimension un), *Bulletin de la Société Mathématique de France* 109 (1981) 143–182.
- [62] H. Faure, Good permutations for extreme discrepancy, *Journal of Number Theory* 42 (1992) 47–56. [https://doi.org/10.1016/0022-314X\(92\)90107-Z](https://doi.org/10.1016/0022-314X(92)90107-Z).
- [63] I.M. Sobol, Uniformly distributed sequences with an additional uniform property, *USSR Computational Mathematics and Mathematical Physics* 16 (1976) 236–242. [https://doi.org/10.1016/0041-5553\(76\)90154-3](https://doi.org/10.1016/0041-5553(76)90154-3).
- [64] I.A. Antonov, V.M. Saleev, An economic method of computing LP_{τ} -sequences, *USSR Computational Mathematics and Mathematical Physics* 19 (1979) 252–256. [https://doi.org/10.1016/0041-5553\(79\)90085-5](https://doi.org/10.1016/0041-5553(79)90085-5).
- [65] H. Niederreiter, *Random number generation and quasi-Monte Carlo methods*, Society for Industrial and Applied Mathematics, Philadelphia, 1992.
- [66] Sunderam V.S., Albada G.D., Sloot P.M.A., Dongarra J.J., H. Chi, P. Beerli, D.W. Evans, M. Mascagni (Eds.), *On the scrambled Sobol sequence*, Atlanta, 2005.
- [67] A. Saltelli, P. Annoni, I. Azzini, F. Campolongo, M. Ratto, S. Tarantola, Variance based sensitivity analysis of model output. Design and estimator for the total sensitivity index, *Comput Phys Commun* 181 (2010) 259–270. <https://doi.org/10.1016/j.cpc.2009.09.018>.
- [68] S. Joe, F.Y. Kuo, Remark on Algorithm 659: Implementing Sobol's quasirandom sequence generator, *ACM Trans Math Software* 29 (2003) 49–57. <https://doi.org/10.1145/641876.641879>.
- [69] A. B. Owen, Quasi-Monte Carlo Sampling, in: *Monte Carlo Ray Tracing: Siggraph 2003 Course 44*, SIGGRAPH, 2003, pp. 69–88.
- [70] E.I. Atanassov, A new efficient algorithm for generating the scrambled Sobol' sequence, In: Dimov I., Lirkov I., Margenov S., Zlatev Z. (eds) *Numerical Methods and Applications*, Springer, Berlin, Heidelberg, 2003.
- [71] P. Sabino, *Monte Carlo and Quasi-Monte Carlo Methods in Option Pricing and Hedging*, University of Bari, 2008.
- [72] H.S. Hong, F.J. Hickernell, Algorithm 823: Implementing scrambled digital sequences, *ACM Trans Math Software* 29 (2003) 95–109. <https://doi.org/10.1145/779359.779360>.
- [73] R. Statnikov, A. Bordetsky, J. Matusov, I. Sobol', A. Statnikov, Definition of the feasible solution set in multicriteria optimization problems with continuous, discrete, and mixed design variables, *Nonlinear Anal Theory Methods Appl* 71 (2009) 109–117. <https://doi.org/10.1016/j.na.2008.10.050>.

- [74] T. Seifert, A.-K. Lesniak, S. Sievers, G. Schembecker, C. Bramsiepe, Capacity Flexibility of Chemical Plants, *Chem. Eng. Technol.* 37 (2014) 332–342. <https://doi.org/10.1002/ceat.201300635>.
- [75] A. Saltelli (Ed.), *Sensitivity analysis*, Wiley, Chichester, 2000.
- [76] Haaker, M. P. R., Verheijen, P. J. T., Local and global sensitivity analysis for a reactor design with parameter uncertainty, *Chem. Eng. Res. Des.* 82 (2004) 591–598. <https://doi.org/10.1205/026387604323142630>.
- [77] A. Saltelli, *Global sensitivity analysis: The primer*, John Wiley, Chichester, England, Hoboken, NJ, 2008.
- [78] B.L. Fox, Algorithm 647: Implementation and relative efficiency of quasirandom sequence generators, *ACM Trans Math Software* 12 (1986) 362–376. <https://doi.org/10.1145/22721.356187>.
- [79] P. Bratley, B.L. Fox, Implementing Sobol's quasirandom sequence generator, *ACM Trans Math Software* 14 (1988) 88–100. <https://doi.org/10.1145/42288.214372>.
- [80] A.C. Dimian, C.S. Bildea, A.A. Kiss, *Integrated design and simulation of chemical processes*, secondnd edition, Elsevier Science, Amsterdam, 2014.
- [81] H.K. Baker, G.E. Powell, *Understanding Financial Management: A Practical Guide*, firstst ed., Wiley-Blackwell, Oxford, 2005.
- [82] D.H. James, W.M. Castor, Styrene, in: *Ullmann's Encyclopedia of Industrial Chemistry*, Wiley-VCH Verlag GmbH & Co. KGaA, 2000.
- [83] Elnashaie, Said S. E. H., S.S. Elshishini, *Modelling, simulation and optimization of industrial fixed bed catalytic reactors*, Gordon and Breach, Philadelphia, 1993.
- [84] R. Turton, *Analysis, synthesis, and design of chemical processes*, fourthth ed., international ed, Pearson, Upper Saddle River, NJ, 2013.
- [85] W.L. Luyben, Design and control of the styrene process, *Ind. Eng. Chem. Res.* 50 (2011) 1231–1246. <https://doi.org/10.1021/ie100023s>.
- [86] Sheel J.G.P., Crowe C.M., Simulation and optimization of an existing ethylbenzene dehydrogenation reactor, *Can. J. Chem. Eng.* 47 (1969) 183–187.
- [87] product focus, *Chemical Week* 170 (2008) 41.
- [88] S. Vasudevan, G.P. Rangaiah, N. Konda, W.H. Tay, Application and evaluation of three methodologies for plantwide control of the styrene monomer plant, *Ind. Eng. Chem. Res.* 48 (2009) 10941–10961. <https://doi.org/10.1021/ie900022h>.
- [89] B. Einfeld, *Pseudokontinuierliche Modellierung der Strömung in Schüttschichtreaktoren*. Diss., Cottbus, 1999.
- [90] H.F. Rase, *Chemical reactor design for process plants*, Wiley, New York, 1977.
- [91] Sheel, J. G. P., C.M. Crowe, Erratum: Simulation and optimization of an existing ethylbenzene dehydrogenation reactor (*Canadian Journal of Chemical Engineering* (1969) 47 (183-187)), *Can. J. Chem. Eng.* 78 (2000) 605.
- [92] R.K. Sinnott, *Chemical engineering design*, fourth ed., Elsevier/Butterworth-Heinemann, Amsterdam, 2005.
- [93] A.K. Coker, E.E. Ludwig, *Ludwig's applied process design for chemical and petrochemical plants*, fourth edition, Gulf Professional, Amsterdam, 2014.
- [94] DIN German Institute for Standardization, *Chemical equipment - Process equipment and vessels with two domed ends - Definitions, nominal capacity, nominal diameters, main dimensions: DIN 28105*, 2002.
- [95] C.R. Branan, A. Sherman, *Pocket Guide to Chemical Engineering*, Elsevier, Burlington, 1999.
- [96] S. Hall, *Rules of Thumb for Chemical Engineers*, fifth ed., Butterworth-Heinemann [Imprint]; Elsevier Science & Technology Books, San Diego, 2012.
- [97] J.R. Couper, W.R. Penney, J.R. Fair, S.M. Walas, *Chemical process equipment: Selection and design*, third ed., Elsevier/Butterworth-Heinemann, Amsterdam, Boston, 2012.

- [98] M. Weber, W. Pompetzki, R. Bonmann, Acetone: In Ullmann's Encyclopedia of Industrial Chemistry, (Ed.), 2014.
- [99] W.L. Luyben, Design and control of the acetone process via dehydrogenation of 2-propanol, *Ind. Eng. Chem. Res.* 50 (2011) 1206–1218. <https://doi.org/10.1021/ie901923a>.
- [100] R.M. Rioux, M.A. Vannice, Hydrogenation/dehydrogenation reactions: Isopropanol dehydrogenation over copper catalysts, *Journal of Catalysis* 216 (2003) 362–376. [https://doi.org/10.1016/S0021-9517\(02\)00035-0](https://doi.org/10.1016/S0021-9517(02)00035-0).
- [101] R.M. Rioux, M.A. Vannice, Dehydrogenation of isopropyl alcohol on carbon-supported Pt and Cu-Pt catalysts, *Journal of Catalysis* 233 (2005) 147–165. <https://doi.org/10.1016/j.jcat.2005.04.020>.
- [102] Knapsack AG GB804132.
- [103] L.H. Slaugh, G.W. Schoenthal, J.D. Richardson (Shell Oil Company) US4472593.
- [104] R.H. Perry, D.W. Green, J.O. Maloney, Perry's chemical engineers' handbook, seventh ed., McGraw-Hill, New York, 1997.
- [105] H.F. Rase, Fixed-bed reactor design and diagnostics: Gas-phase reactions, Butterworths, 1990.
- [106] A.K. Coker, E.E. Ludwig, Ludwig's applied process design for chemical and petrochemical plants, fourth ed., Elsevier Gulf Professional Pub., Amsterdam, Boston, 2007.
- [107] O. Levenspiel, The chemical reactor omnibook, fifth ed., Distributed by OSU Book Stores, Corvallis, Oregon, 1996.
- [108] H.F. Rase, Chemical reactor design for process plants: Volume Two: Case Studies and Design Data, Wiley, New York, 1977.
- [109] F.G. Helfferich, C.H. Bamford, R.G. Compton, N.J.B. Green, Kinetics of multistep reactions, second ed., Elsevier, Amsterdam, 2004.
- [110] J.M. Douglas, Conceptual design of chemical process, McGraw Hill, 1988.
- [111] M. Baerns, Technische Chemie, second ed., Wiley-VCH, 2013.
- [112] H. Kennedy, Biobased succinic acid report looks at technology, market, and applications, 2018. <http://biofuelsdigest.com/nuudigest/2018/02/28/biobased-succinic-acid-report-looks-at-technology-market-and-applications/> (accessed 3 July 2018).
- [113] P. Domínguez de María, Industrial biorenewables: A practical viewpoint, John Wiley & Sons, Inc, Hoboken, New Jersey, 2016.
- [114] A. Vlysidis, M. Binns, C. Webb, C. Theodoropoulos, Glycerol utilisation for the production of chemicals: Conversion to succinic acid, a combined experimental and computational study, *Biochem. Eng. J.* 58-59 (2011) 1–11. <https://doi.org/10.1016/j.bej.2011.07.004>.
- [115] A. Vlysidis, M. Binns, C. Webb, C. Theodoropoulos, A techno-economic analysis of biodiesel biorefineries: Assessment of integrated designs for the co-production of fuels and chemicals, *Energy* 36 (2011) 4671–4683. <https://doi.org/10.1016/j.energy.2011.04.046>.
- [116] P.F. Stanbury, A. Whitaker, S.J. Hall, Principles of fermentation technology, Third edition, Butterworth-Heinemann, Oxford, 2017.
- [117] M.J. van der Werf, M.V. Guettler, M.K. Jain, J.G. Zeikus, Environmental and physiological factors affecting the succinate product ratio during carbohydrate fermentation by *Actinobacillus* sp. 130Z, *Archives of Microbiology* 167 (1997) 332–342. <https://doi.org/10.1007/s002030050452>.
- [118] M. Carvalho, M. Matos, C. Roca, M.A. Reis, Succinic acid production from glycerol by *Actinobacillus succinogenes* using dimethylsulfoxide as electron acceptor, *New Biotechnology* 31 (2014) 133–139. <https://doi.org/10.1016/j.nbt.2013.06.006>.

- [119] Q. Li, D. Wang, Y. Wu, W. Li, Y. Zhang, J. Xing, Z. Su, One step recovery of succinic acid from fermentation broths by crystallization, *Separation and Purification Technology* 72 (2010) 294–300. <https://doi.org/10.1016/j.seppur.2010.02.021>.
- [120] E. Querol, B. Gonzalez-Reguer, A. Ramos, J.L. Perez-Benedito, Novel application for exergy and thermoeconomic analysis of processes simulated with Aspen Plus®, *Energy* 36 (2011) 964–974. <https://doi.org/10.1016/j.energy.2010.12.013>.
- [121] I. The MathWorks, Curve Fitting Toolbox™ User's Guide, 2001–2018. https://de.mathworks.com/help/pdf_doc/curvefit/index.html (accessed 30 March 2018).
- [122] R.K. Sinnott, J.M. Coulson, J.F. Richardson, *Chemical engineering design*, fourth ed., reprinted, Elsevier Butterworth-Heinemann, Amsterdam, 2006.
- [123] K. Gieck, R. Gieck, *Technische Formelsammlung*, thirty-first german ed., Gieck, Germering, 2005.
- [124] G. Towler, R.K. Sinnott, *Chemical engineering design: Principles, practice and economics of plant and process design*, Elsevier; Butterworth-Heinemann, Amsterdam, Boston, Heidelberg, 2012.
- [125] T. Kuppan, *Heat exchanger design handbook*, second. ed., [completely rev. and updated], CRC Press, Boca Raton, Fla., 2013.
- [126] *VDI heat atlas*, second. ed, Springer-Verlag Berlin Heidelberg, Berlin, 2010.
- [127] M.S. Peters, K.D. Timmerhaus, R.E. West, *Plant design and economics for chemical engineers*, fifth ed., internat. ed., McGraw-Hill, Boston, 2006.
- [128] J.P. Gupta, *Fundamentals of heat exchanger and pressure vessel technology*, Hemisphere Publ, Washington, 1986.
- [129] *Standards of the Tubular Exchanger Manufacturers Association*, ninth ed., TEMA, Tarrytown, NY, 2007.
- [130] R.K. Shah, D.P. Sekulić, *Fundamentals of heat exchanger design*, Wiley-Interscience, Hoboken, NJ, 2003.
- [131] M. Asadi, Y. Song, B. Sunden, G. Xie, Economic optimization design of shell-and-tube heat exchangers by a cuckoo-search-algorithm, *Appl Therm Eng* 73 (2014) 1030–1038. <https://doi.org/10.1016/j.applthermaleng.2014.08.061>.
- [132] S. Fettaka, J. Thibault, Y. Gupta, Design of shell-and-tube heat exchangers using multiobjective optimization, *Int. J. Heat Mass Transf.* 60 (2013) 343–354. <https://doi.org/10.1016/j.ijheatmasstransfer.2012.12.047>.
- [133] *Economic Indicators, Chemical Engineering* 124 (2017) 64.
- [134] R.G. Harrison, P. Todd, P.W. Todd, D.P. Petrides, S.R. Rudge, *Bioseparations science and engineering*, Oxford University Press, USA, 2015.
- [135] L.F. Albright (Ed.), *Albright's chemical engineering handbook*, Taylor & Francis Group, LLC, Estados Unidos, 2009.
- [136] SULZER Chemtech Ltd., 2013.
- [137] K.M. Sundaram, H. Sardina, J.M. Fernandez-Baujin, J.M. Hildreth, Styrene plant simulation and optimization, *Hydrocarbon Process* 70 (1991) 93–97.
- [138] Argus Media Inc., www.metalprices.com. <http://www.metalprices.com/metal/copper/copper-scrap-millberry-price-europe> (accessed 3 July 2015).
- [139] D.G. Austin, G.V. Jeffreys, *The manufacture of methyl ethyl ketone from 2-butanol*, London, 1979.
- [140] P. Prinzing, R. Roedel, D. Aichert, Capital Cost Estimation for Chemical Plant, *Chem Ing Tech* 57 (1985) 8–14.
- [141] J.R. Couper, *Process Engineering Economics*, Taylor & Francis Group, Philadelphia, 2003.
- [142] G.D. Ulrich, P.T. Vasudevan, *Chemical engineering process design and economics: A practical guide*, second ed., Process Publishing, Durham, 2004.

- [143] ICIS Pricing, Acetone, Isopropanol. <https://www.icis.com/chemicals/channel-info-chemicals-a-z/> (accessed 1 October 2015).
- [144] ICIS Pricing, Acetone Production and Manufacturing Process, 2007. <https://www.icis.com/resources/news/2007/11/01/9074860/acetone-production-and-manufacturing-process/> (accessed 7 October 2015).
- [145] R. Goedecke, *Fluidverfahrenstechnik: Grundlagen, Methodik, Technik, Praxis*, first ed., Wiley-VCH, Weinheim, 2011.
- [146] ICIS News, US crude glycerine prices could dip as spring nears, 2018. <https://www.icis.com/resources/news/2018/02/14/10193613/us-crude-glycerine-prices-could-dip-as-spring-nears/> (accessed 18 July 2018).
- [147] R. Davis, J. Markham, C. Kinchin, N. Grundl, E. Tan, D. Humbird, *Process Design and Economics for the Production of Algal Biomass: Algal Biomass Production in Open Pond Systems and Processing Through Dewatering for Downstream Conversion*, 2016. <https://www.nrel.gov/docs/fy16osti/64772.pdf>.
- [148] E. Heinzle, A.P. Biwer, C.L. Cooney, *Development of sustainable bioprocesses: Modeling and assessment*, Wiley, Chichester, 2006.
- [149] Carl Roth GmbH + Co. KG, *Silicon-Antischaumemulsion*, 2018. https://www.carlroth.com/de/de/Chemikalien/A-Z-Chemikalien/S/Silicon-Antischaumemulsion/Silicon-Antischaumemulsion/p/000000100002b69300080023_de?text=Silicone+antifoam (accessed 18 July 2018).
- [150] P.M. Doran, *Bioprocess engineering principles*, Reprint, Elsevier/Acad. Press, Amsterdam, 2004.
- [151] E. Molina Grima, E.-H. Belarbi, F.G. Acién Fernández, A. Robles Medina, Y. Chisti, Recovery of microalgal biomass and metabolites: Process options and economics, *Biotechnology Advances* 20 (2003) 491–515. [https://doi.org/10.1016/S0734-9750\(02\)00050-2](https://doi.org/10.1016/S0734-9750(02)00050-2).
- [152] R. Mukherjee, *Practical thermal design of shell-and-tube heat exchangers*, Begell House, Inc., Redding, Conn., 2004.
- [153] A. Górak, *Distillation: Fundamentals and principles*, Elsevier, Amsterdam, 2014.
- [154] J.D. Seader, E.J. Henley, D. Roper, *Separation process principles: Chemical and biochemical operations*, third ed., Wiley, Hoboken, N.J., 2011.
- [155] J.M. Coulson, J.F. Richardson, *Chemical engineering*, fifth ed., Butterworth Heinemann, Oxford, 1996.
- [156] W.L. Luyben, Design of cooled tubular reactor systems, *Ind. Eng. Chem. Res.* 40 (2001) 5775–5783.
- [157] E.B. Nauman, *Chemical reactor design, optimization, and scaleup*, second ed., Wiley, Hoboken, NJ, 2008.
- [158] L.M. Rose, *Chemical reactor design practice*, third impr., Elsevier, Amsterdam, 1985.
- [159] U. Mann, *Principles of chemical reactor analysis and design: New tools for industrial chemical reactor operations*, second ed., Wiley; John Wiley & Sons, Hoboken, N.J., 2009.
- [160] O. Bey, G. Eigenberger, Gas flow and heat transfer through catalyst filled tubes, *International Journal of Thermal Sciences* 40 (2001) 152–164. [https://doi.org/10.1016/S1290-0729\(00\)01204-7](https://doi.org/10.1016/S1290-0729(00)01204-7).
- [161] D. Wen, Y. Ding, Heat transfer of gas flow through a packed bed, *Chem. Eng. Sci.* 61 (2006) 3532–3542. <https://doi.org/10.1016/j.ces.2005.12.027>.
- [162] M.C. Flickinger, *Downstream industrial biotechnology: Recovery and purification*, John Wiley & Sons Inc, Hoboken, N.J., 2013.
- [163] M. Ambrosio, O.P. Taranto, The drying of solids in a modified fluidized bed, *Brazilian Journal of Chemical Engineering* 19 (2002) 355–358. <https://doi.org/10.1590/S0104-66322002000300010>.

- [164] A.S. Mujumdar, Handbook of Industrial Drying, Third Edition, third ed., CRC Press, Baton Rouge, 2006.
- [165] K. Sattler, Thermische Trennverfahren: Grundlagen, Auslegung, Apparate, third ed., VCH, Weinheim, Chichester, 2001.
- [166] S. Weiss, Verfahrenstechnische Berechnungsmethoden: Teil 2 Thermisches Trennen. Ausrüstungen und ihre Berechnung, VCH-Verl.-Ges, Weinheim, 1986.
- [167] A.E. Lewis, M. Seckler, H.J.M. Kramer, G. van Rosmalen, Industrial crystallization: Fundamentals and applications, Cambridge University Press, Cambridge, United Kingdom, 2015.
- [168] Y. Mori, G. Takahashi, H. Suda, S. Yoshida US 2013/0018206 A1, 2013.
- [169] G. Hofmann, Kristallisation in der industriellen Praxis, John Wiley & Sons, 2004.
- [170] I. Aspen Technology, Aspen Plus®: Help Manual, Aspen Technology, Inc., 2013.
- [171] E. Ehrfeld, Influence of Filter Cloth Behavior on the Layout of Cake Forming Filters, Chem. Eng. Technol. 33 (2010) 1349–1357. <https://doi.org/10.1002/ceat.201000135>.
- [172] J.B. McKinlay, Y. Shachar-Hill, J.G. Zeikus, C. Vieille, Determining Actinobacillus succinogenes metabolic pathways and fluxes by NMR and GC-MS analyses of ¹³C-labeled metabolic product isotopomers, Metabolic Engineering 9 (2007) 177–192. <https://doi.org/10.1016/j.ymben.2006.10.006>.
- [173] Y. Zhang, M.F. Doherty, Simultaneous prediction of crystal shape and size for solution crystallization, AIChE Journal 50 (2004) 2101–2112. <https://doi.org/10.1002/aic.10182>.
- [174] W. Jorisch, Vakuumtechnik in der chemischen Industrie, Wiley-VCH, Weinheim, 1999.
- [175] M. Kraume, Transportvorgänge in der Verfahrenstechnik: Grundlagen und apparative Umsetzungen, second ed., Springer Berlin, Berlin, 2012.
- [176] J. Stichlmair, Distillation, 1. Fundamentals, in: Ullmann's Encyclopedia of Industrial Chemistry, Wiley-VCH Verlag GmbH & Co. KGaA, 2000.
- [177] K. Ruff, T. Pilhofer, A. Mersmann, Vollständige Durchströmung von Lochböden bei der Fluid-Dispergierung, Chemie Ingenieur Technik 48 (1976) 759–764. <https://doi.org/10.1002/cite.330480906>.
- [178] J.M. Nesta, C.A. Bennett, Reduce fouling in shell-and-tube heat exchangers, Hydrocarbon Process 83 (2004) 77–82.
- [179] R.W. Johnson, The Handbook of fluid dynamics, CRC Press, Boca Raton, FL, 1998.
- [180] D.B. Spalding, J. Taborek, Heat exchanger design handbook (HEDH). - 1: Heat exchanger theory, VDI-Verlag, Düsseldorf, 1983.
- [181] V.C. Hass, R. Pörtner, Praxis der Bioprozesstechnik: Mit virtuellem Praktikum, second ed., Spektrum, Akad. Verl., Heidelberg, 2011.
- [182] W. Storhas, Bioverfahrensentwicklung, John Wiley & Sons, 2003.
- [183] H. Chmiel, Bioprozesstechnik, third ed., Spektrum Akademischer Verlag, Heidelberg, 2011.
- [184] J.R. Couper, Chemical process equipment: Selection and design, third ed., Elsevier, Amsterdam, 2012.
- [185] D.Q. Kern, Process heat transfer, McGraw-Hill, Tokyo, 1983.
- [186] S. Kakaç, H. Liu, Heat exchangers: Selection, rating, and thermal design, second ed., CRC Press, Boca Raton, 2002.
- [187] G.P. Towler, R.K. Sinnott, Chemical engineering design: Principles, practice, and economics of plant and process design, secondnd ed., Butterworth-Heinemann, Oxford, Waltham, Mass., 2013.
- [188] C. Dowidat, Ein Beitrag zur Reduktion des Energiebedarfs verfahrenstechnischer Batch-Prozesse, first ed., Verlag Dr. Hut, München, 2016.
- [189] I. Aspen Technology, Aspen Exchanger Design & Rating, Aspen Technology, Inc., 2014.
- [190] AD 2000-Regelwerk: Taschenbuch-Ausgabe 2015, ninth ed., Beuth, Berlin, 2015.

10 Appendix

A1 Cost calculations

A.1.1 Free on board (FOB) costs

FOB costs are calculated by the capacity method according to Eq. 4-30. The parameters used for each process unit are shown in Table A. 1-1 [38]. They consider a $CEPCI_{ref}$ of 1000 [38]. For 2015 a CEPCI of 556.8 is taken [133]. As an exception, the FOB costs for heat exchangers in the equipment module databases are calculated by Aspen EDR. In case of the crystallizers and the RDVFs, the characteristic sizes are not within the validity range for the CEX-values provided by Woods [38]. As no CEX-values for the MSMPR crystallizers and RDVFs with a larger range of validity could be found, the CEX-values of [38] are used. In the investment cost determination of the fermenters, the costs of the seed fermenters are not considered since not enough information was available for their OPEX calculation.

Table A. 1-1: FOB calculation parameters for each process unit [38,134,135]

Equipment	FOB_{ref} [\$]	$size_{ref}$	n [-]	$instr.$ [\$]
Adiabatic fixed-bed reactor ^{a)}	110 000	20 m ³	0.52	63 000
Multitubular reactor ^{b)}	350 000	1 200 m ²	0.68	63 000
Sieve tray column ^{b)}	545 000	100 m ^{2.5}	0.53	150 000
Sieve tray column ^{a), b)}				150 000
Column vertical excl. internals	100 000	20 m ^{2.5}	0.81	-
Trays	167 000	66 m ^{2.5}	0.39	-
Packed column				150 000
Column vertical excl. internals ^{a), b)}	100 000	20 m ^{2.5}	0.81	-
Structured packing ^{a), c)}	8 100	1 m ³	-	-
25 mm Raschig rings ^{b), d)}	3 300	1 m ³	-	-
Vapor-liquid separator	100 000	20 m ^{2.5}	0.81	17 400
Decanter	100 000	20 m ^{2.5}	0.81	17 400
Heat exchanger	Calculated by Aspen EDR [®]			27 000
Heat exchanger ^{d)}	70 000	100 [m ²]	0.71	27 000
RDVF	280 000	22 [m ²]	0.65	^{e)} 47 000
Dryer	350 000	2 [m ^{1.35} /s ^{0.35}]	0.73	^{e)} 47 000
Crystallizer	700 000	1 [kg/s]	0.63	^{e)} 47 000
Fermenter	^{g)} 436 000	350 [m ³]	0.51	^{f)} 75 500

^{a)} Styrene production process

^{b)} Acetone production process

^{c)} from [136]

^{d)} Succinic acid shortcut design

^{e)} average instr. costs of main plant item [135]

^{f)} average instr. costs of main plant item in highly automated batch process [135]

^{g)} $CEPCI_{ref}$ of 584.6 from 2012 [134]

The costs of the packings are taken times 1.5 to account for the costs of the distributors [104].

As price for the catalyst of the styrene production process 12.2 \$/kg are taken [137]. For the catalyst price of the acetone production process, the raw material costs for copper is

considered as 5.268 \$/kg [138]. According to Austin, this costs can be taken times four to estimate the catalyst costs, resulting in 21.07 \$/kg [139]. The resulting FOB costs for each equipment module can be found in appendices A.2.4, A.3.4 and A.4.5 for the styrene, acetone and succinic acid example processes, respectively.

To determine the costs of the control valves it is assumed that each process unit consists of three equipment modules. Based on [38] and a CEPCI of 556.8 for the styrene production process and of 579.8 for the acetone production process, the costs for the control valves per equipment module are calculated to 1 721 \$ and \$ 1 697, respectively. In case of the succinic acid production example, the costs for control valves per equipment module are calculated to \$ 1,752. All prices in Euro are converted to US Dollar with a conversion factor of 1.0961 \$/€.

A.1.2 Total capital investment (TCI)

Table A.1-2: Cost factors for TCI calculation

Cost positions	Source		
Free on Board (FOB)	100%		
+ Delivery to site (Freight, insurance, taxes)	20%	(of FOB)	[38]
+ Plant construction cost			
Plant construction work	61%	(of FOB)	[140]
Piping material	33%	(of FOB)	[140]
Material for electrical installations	25%	(of FOB)	[140]
Material for instrumentation & control system	(*)		[38]
Equipment insulation and painting	19%	(of FOB)	[140]
Ancillary work	6%	(of FOB)	[140]
Sum	144% + control	(of FOB)	
+ Assembly costs			
Assembly work (assembly of scaffolds, welding control, material control, equipment, piping, electrical installation)	90%	(of FOB)	[140]
= Direct plant costs (DPC)			
+ Overhead costs			
Contingency	20%	(of DPC)	[141]
Engineering and construction	35%	(of DPC)	[141]
= Total fixed capital investment (FCI)			
+ Working capital			
Start-up, raw materials for initial operation, spare parts	15%	(of TCI)	[127]
= Total capital investment (TCI)			

*fixed costs for instrumentation and valves

A.1.3 Free cash flow

Table A.1-3: Calculation of FCF and composition of fixed and variable operating costs

Cost positions		Sources	
+	Net sales	(from simulation)	
-	Variable costs		
	Production costs (Raw material, utilities)	(from simulation)	
	License fee	2 %	(of net sales) [111]
	Sales costs (Marketing, freight, sales organization)	15 %	(of net sales) [111]
	Generalia	3.5 %	(of net sales) [111]
	Research expenses	3.5 %	(of net sales) [111]
-	Fix costs		
	Staff costs		(cf. A.1.4) [111,142]
	Capital costs (Site related costs, maintenance, insurance)	7.5 %	(of TCI) [111]
	Depreciation (linear over 10 years)	10 %	(of TCI) [111]
	Sundry expenses (i.e. Analysis and quality control)	6 %	(of all fix costs) [111]
= Interim cash flow (ICF)			
-	Taxes (In case of loss: no taxes)	35%	(of ICF) [127]
= Cash flow incl. taxes			
+	Depreciation		
= Free Cash Flow (FCF)			

A.1.4 Staff costs

Table A. 1-4: Required workers per shift and process unit type for succinic acid production plant [142]

Process unit type	Workers per shift
Reactor (batch)	1
Heat exchanger	0.25
Crystallizer	0.16
Filter	0.1875
Dryer	1
Vapor-liquid separator	0

To calculate staff costs for the acetone production plant it is estimated that four skilled workers per shift are required for plant operation [142]. One shift leader per shift, one technician and an operation manager are needed as well. It is assumed that five shifts are necessary [111]. The salaries are estimated to 137,000 \$/a for a manager, 90,000 \$/a for a technician, 87,700 \$/a for a supervisor and 80,000 \$/a for a skilled worker. 13.1 % of the annual salaries are added to account for additional labor costs [111]. All prices in Euro are converted to US Dollar with a conversion factor of 1.0961 \$/€.

A2 Styrene production example

A.2.1 Boundary conditions of the styrene production process example

Table A.2-1: Specified boundary conditions for the process simulation of the styrene production process example

Plant capacity:	20 kt/year	target production rate
Operating time	8 000 h/year	
Product purity:	Styrene: 99.9 wt.-%	
Raw material:	Ethylbenzene-rich stream [84]	3 bar, 16 °C composition: 98.422 wt.-% EBZ 0.854 wt.-% TOL 0.724 wt.-% BZ
Utilities:	Low-pressure steam (LPS)	saturated steam, 4 bar
	High-pressure steam (HPS)	saturated steam, 42 bar
	Cooling water (CW)	1 bar inlet temperature: 20 °C outlet temperature: 30 °C
	Flue gas (FG)	1 bar inlet temperature: 700 °C outlet temperature: 500 °C composition: 77.5 wt.-% N ₂ 15.0 wt.-% CO ₂ 6.2 wt.-% H ₂ O 1.3 wt.-% O ₂

A.2.2 Specifications of implemented shortcut *HeatX* or *HXFlux* models of heat exchangers

Table A.2-2: Outlet conditions for process and utility streams of heat exchangers

Heat exchanger	Process stream	Utility stream
HX1*	$f_{vapor} = 0.15$	$f_{vapor} = 0$
HX1B	$T = 225\text{ °C}$	$T = 500\text{ °C}$
HX2	$T = 640\text{ °C}$	$T = 750\text{ °C}$
HX3	$T = 270\text{ °C}$	$f_{vapor} = 0.15$
HX4	$T = 180\text{ °C}$	$f_{vapor} = 0.15$
HX5	$T = 60\text{ °C}$	$T = 30\text{ °C}$
HX6	$\dot{Q}_{HeatX} = \dot{Q}_{RadFrac,Cond}$	$T = 30\text{ °C}$
HX7*	$f_{vapor} = 0.15$	$f_{vapor} = 0$
HX8	$\dot{Q}_{HeatX} = \dot{Q}_{RadFrac,Cond}$	$T = 30\text{ °C}$
HX9*	$f_{vapor} = 0.15$	$f_{vapor} = 0$

* forced circulation evaporators according to [7]

A.2.3 Design parameters and specifications of distillation columns C1 and C2

Table A.2-3: Input data for *RadFrac* distillation columns C1 and C2

	C1	C2
<i>NTP</i>	16	77
Feed stage (above stage)	9	35
Type of internal	Sieve trays	MellapakPlus 252.Y
d_h	0.005 m	/
Hole area/active area	12 %	/
Tray spacing / HETP	0.6 m	0.38
Pressure at condenser	0.4 bar	0.6 bar
K_1	0.1	/
Purities*	$x_{Ethylbenzene,T} = 1$ mole-% $x_{Toluene,B} = 1$ mole-%	$x_{Styrene,T} = 1$ mole-% $w_{Styrene,B} = 99.9$ wt.-%

* T = top, B = bottom

A.2.4 Equipment module database

Table A.2-4: Reactor modules for R1 and R2

	D [m]	L [m]	L/D [-]	m_{cat} [kg]	FOB [\$]
One reactor	1.90	1.52	0.8	9250	140 419
	2.00	1.60	0.8	10 788	161 487
	2.10	1.68	0.8	12 489	184 595
	2.10	1.26	0.6	9367	142 027
	2.20	1.32	0.6	10 769	161 230
	2.35	1.41	0.6	13126	193 212
	1.80	1.80	1.0	9831	148 397
	1.85	1.85	1.0	10 673	159 915
	1.95	1.95	1.0	12 499	184 734
Two reactors in parallel	1.65	0.99	0.6	4543	74 482
	1.75	1.05	0.6	5421	87 014
	1.85	1.11	0.6	6404	100 901
	1.90	0.76	0.4	4625	75 651
	2.00	0.80	0.4	5394	86 639
	2.10	0.84	0.4	6244	98 659
	1.50	1.20	0.8	4551	74 596
	1.60	1.28	0.8	5524	88 478
	1.70	1.36	0.8	6625	104 011
Three reactors in parallel	1.55	0.78	0.5	3159	54 310
	1.65	0.83	0.5	3809	63 854
	1.70	0.85	0.5	4141	68 673
	1.85	0.55	0.3	3173	54 520
	1.95	0.59	0.3	3782	63 456
	2.05	0.62	0.3	4392	72 303
	1.40	0.98	0.7	3238	55 477
	1.45	1.02	0.7	3615	61 021
	1.35	1.09	0.7	4414	72 624

Table A.2-5: Distillation column modules for C1 and C2

Column C1				Column C2			
NTP [-]	N _{Feed} [-]	D [m]	FOB [\$]	NTP [-]	N _{Feed} [-]	D [m]	FOB [\$]
11	8	0.9	55 574	72	31	1.4	493 388
11	8	1.0	60 564	72	31	1.6	630 386
11	8	1.1	65 521	72	31	1.8	783 632
16	9	0.7	55 506	77	32	1.2	397 365
16	9	0.8	61 906	77	32	1.4	526 187
16	9	0.9	68 255	77	32	1.6	672 441
21	10	0.6	56 743	82	34	1.2	421 971
21	10	0.7	64 396	82	34	1.4	558 911
21	10	0.8	71 984	82	34	1.6	714 408
11	8	0.6	40 291	72	31	1.0	268 388
11	8	0.7	45 454	72	31	1.1	318 489
11	8	0.8	35 025	72	31	1.2	372 698
16	9	0.4	35 744	77	32	0.9	236 996
16	9	0.5	42 464	77	32	1.0	286 053
16	9	0.6	49 036	77	32	1.1	339 515
21	10	0.4	41 100	82	34	0.9	251 542
21	10	0.5	48 994	82	34	1.0	303 670
21	10	0.6	56 743	82	34	1.1	360 484
11	8	0.5	35 025	72	31	0.8	180 562
11	8	0.6	40 291	72	31	0.9	222 407
11	8	0.7	45 454	72	31	1.0	268 388
16	9	0.4	35 744	77	32	0.7	152 165
16	9	0.5	42 464	77	32	0.8	192 360
16	9	0.6	49 036	77	32	0.9	236 996
21	10	0.35	37 073	82	34	0.7	161 423
21	10	0.4	41 100	82	34	0.8	204 119
21	10	0.5	48 994	82	34	0.9	251 542

Table A.2-6: Heat exchanger modules for HX1

Capacity factor	Tube OD [mm]	Shell ID [mm]	Tube length [mm]	Baffle pitch [mm]	No. baffles [-]	No. Tubes [-]	Tube passes [-]	FOB [\$]
0.4*	-	-	-	-	-	-	-	-
0.5*	-	-	-	-	-	-	-	-
0.67 ^a	20	500	1000	30	16	279	1	32 828
1	25	600	1000	30	14	261	1	37 743
1.5	20	700	1400	40	18	588	1	52 866
2	25	800	1000	50	5	495	1	55 882
2.5	38	1000	2000	60	17	349	1	80 410

BES-type

Vertical with 15 % vaporization in tubes

SS: $v_{\min, \text{in}} > 4.1$ m/s, $v_{\min, \text{out}}$ not consideredTS: $v_{\min, \text{in}}$ not considered, v_{out} : 1.0-2.0 m/s

* no suitable design could be found with only one shell in series or one shell in parallel

^a v_{SS} was too small, but design was kept

Table A.2-7: Heat exchanger modules for HX1B

Capacity factor	Tube OD [mm]	Shell ID [mm]	Tube length [mm]	Baffle pitch [mm]	No. baffles [-]	No. Tubes [-]	Tube passes [-]	FOB [\$]
0.4	16	152.3	1000	80	7	22	1	7 614
0.5	20	204.9	1000	90	6	31	1	9 353
0.67	38	204.9	1500	135	7	8	1	9 312
1	20	204.9	1500	135	7	31	1	9 713
1.5	20	257	1000	175	3	57	1	11 536
2	25	257	5000	250	18	36	1	14 381
2.5	25	306.3	4000	230	15	55	1	15 743

BES-type

Vertical exchanger with hot heating gas stream on shell side

SS: $v_{\min,in} > 22.6$ m/s, $v_{\min,out} > 20.1$ m/sTS: $v_{\min,in}$ 10-30 m/s, $v_{\min,out}$: 10-30 m/s

Table A.2-8: Heat exchanger modules for HX2

Capacity factor	Tube OD [mm]	Shell ID [mm]	Tube length [mm]	Baffle pitch [mm]	No. baffles [-]	No. Tubes [-]	Tube passes [-]	FOB [\$]
0.4	38	900	2000	70.05	2	267	1	175 486
0.5	30	900	2000	100	2	438	1	179 401
0.67	16	900	2500	70	11	1600	1	221 153
1	25	1300	2600	90	3	1395	1	450 259
1.5	30	1400	2800	151.75	2	1122	1	538 065
2	30	1800	3000	130	4	1907	1	975 794
2.5	30	1900	3000	160	3	2138	1	1 108 359

BES-type

Vertical exchanger with hot superheated steam on shell side

SS: $v_{\min,in} > 6.49$ m/s, $v_{\min,out} > 6.33$ m/sTS: $v_{\min,in}$ 10-30 m/s, $v_{\min,out}$: 10-30 m/s

Table A.2-9: Heat exchanger modules for HX3

Capacity factor	Tube OD [mm]	Shell ID [mm]	Tube length [mm]	Baffle pitch [mm]	No. baffles [-]	No. Tubes [-]	Tube passes [-]	FOB [\$]
0.4	16	800	4000	85	30	1243	1	164 473
0.5	16	900	4000	95	25	1597	1	207 799
0.67	16	1000	4000	115	19	2002	1	258 516
1	20	1200	5000	135	21	1864	1	386 570
1.5	20	1400	5000	180	14	2555	1	537 507
2	20	1600	5000	200	12	3375	1	723 559
2.5	20	1800	5000	250	10	4316	1	932 872

BES-type

Horizontal exchanger with condensation in tubes

SS: $v_{\min,in} > 0.6$ m/s, $v_{\min,out} > 0.6$ m/sTS: v_{in} 10-30 m/s, v_{out} : 10-30 m/s

Table A.2-10: Heat exchanger modules for HX4

Capacity factor	Tube OD [mm]	Shell ID [mm]	Tube length [mm]	Baffle pitch [mm]	No. baffles [-]	No. Tubes [-]	Tube passes [-]	FOB [\$]
0.4*	-	-	-	-	-	-	-	-
0.5	20	600	2500	30	65	421	1	35 604
0.67	20	800	2000	35	39	782	1	50 402
1	25	900	3000	45	51	649	1	60 147
1.5	25	1100	3000	60	37	988	1	82 279
2	25	1300	3000	65	34	1399	1	108 969
2.5	25	1400	2800	75	25	1633	1	117 601

BES-type

Horizontal exchanger with hot gas stream in tubes

10 % evaporation on shell side

SS: $v_{\min, \text{in}} > 0.6 \text{ m/s}$, $v_{\min, \text{out}} > 0.6 \text{ m/s}$ TS: $v_{\text{in}} 10\text{-}30 \text{ m/s}$, $v_{\text{out}}: 10\text{-}30 \text{ m/s}$

* no suitable design could be found with only one shell in series or one shell in parallel

Table A.2-11: Heat exchanger modules for HX5

Capacity factor	Tube OD [mm]	Shell ID [mm]	Tube length [mm]	Baffle pitch [mm]	No. baffles [-]	No. Tubes [-]	Tube passes [-]	FOB [\$]
0.4	25	600	3000	140	16	258	1	28 493
0.5	25	700	3000	180	12	354	1	34 998
0.67	16	700	2000	170	7	909	1	41 420
1	20	800	2500	400	4	729	1	45 041
1.5	38	900	6000	400	13	253	1	54 394
2	20	1300	2600	300	5	2095	1	105 695
2.5*	-	-	-	-	-	-	-	-

BES-type

Vertical tube side condenser

SS: $v_{\min, \text{in}} > 0.6 \text{ m/s}$, $v_{\min, \text{out}} > 0.6 \text{ m/s}$ TS: $v_{\text{in}} 10\text{-}30 \text{ m/s}$, $v_{\text{out}}: 1.0\text{-}2.0 \text{ m/s}$

* no suitable design could be found with only one shell in series or one shell in parallel

Table A.2-12: Heat exchanger modules for HX6

Capacity factor	Tube OD [mm]	Shell ID [mm]	Tube length [mm]	Baffle pitch [mm]	No. baffles [-]	No. Tubes [-]	Tube passes [-]	FOB [\$]
0.4 ^a	30	257	3000	35	80	30	1	13 201
0.5	38	257	3000	50.8	53	19	1	12 197
0.67	16	335.6	750	65	7	215	1	14 977
1	38	335.6	3000	85	31	34	1	14 676
1.5	38	437	3000	90	29	58	1	19 265
2	30	437	3000	60	44	99	1	20 742
2.5	25	500	3000	65	41	202	1	25 359

BEM-type

Vertical tube side condenser

SS: $v_{\min, \text{in}} > 0.6 \text{ m/s}$, $v_{\min, \text{out}} > 0.6 \text{ m/s}$ TS: $v_{\text{in}} 10\text{-}30 \text{ m/s}$, v_{out} not considered^a v_{SS} was too small, but design was kept

Table A.2-13: Heat exchanger modules for HX7

Capacity factor	Tube OD [mm]	Shell ID [mm]	Tube length [mm]	Baffle pitch [mm]	No. baffles [-]	No. Tubes [-]	Tube passes [-]	FOB [\$]
0.4*	-	-	-	-	-	-	-	-
0.5*	-	-	-	-	-	-	-	-
0.67	30	1000	1000	30	25	592	1	50 367
1	25	1100	1000	40	18	1050	1	62 258
1.5	30	1300	1000	45	15	1017	1	73 791
2	38	1600	1000	50	12	960	1	93 263
2.5	38	1800	1000	60	10	1229	1	111 477

BEM-type

Vertical exchanger with 15 % vaporization in tubes

SS: $v_{\min, \text{in}} > 13.0$ m/s, $v_{\min, \text{out}}$ not consideredTS: v_{in} not considered, v_{out} 1-2 m/s

* no suitable design could be found with only one shell in series or one shell in parallel

Table A.2-14: Heat exchanger modules for HX8

Capacity factor	Tube OD [mm]	Shell ID [mm]	Tube length [mm]	Baffle pitch [mm]	No. baffles [-]	No. Tubes [-]	Tube passes [-]	FOB [\$]
0.4	38	500	1000	100	4	73	1	19 002
0.5	38	550	1000	110	4	88	1	20 754
0.67	38	600	1000	120	2	106	1	21 916
1	38	700	1000	140	2	152	1	26 297
1.5	38	900	1800	80	15	268	1	40 951
2	38	900	1800	60	18	265	1	41 037
2.5	38	1300	3000	140	15	582	1	81 155

BES-type

Vertical tube side condenser

SS: $v_{\min, \text{in}} > 0.6$ m/s, $v_{\min, \text{out}} > 0.6$ m/sTS: v_{in} 10-30 m/s, v_{out} not considered

Table A.2-15: Heat exchanger modules for HX9

Capacity factor	Tube OD [mm]	Shell ID [mm]	Tube length [mm]	Baffle pitch [mm]	No. baffles [-]	No. Tubes [-]	Tube passes [-]	FOB [\$]
0.4	38	1500	1000	45	14	839	1	82 012
0.5	38	1700	1000	55	11	1090	1	101 933
0.67	38	1800	1000	65	10	1229	1	110 829
1	38	2200	1000	80	7	1845	1	151 631
1.5	38	2600	1000	90	4	2593	1	200 992
2*	-	-	-	-	-	-	-	-
2.5*	-	-	-	-	-	-	-	-

BEM-type

Vertical exchanger with 15 % vaporization in tubes

SS: $v_{\min, \text{in}} > 13.0$ m/s, $v_{\min, \text{out}}$ not consideredTS: v_{in} not considered, v_{out} 1-2 m/s

* no suitable design could be found with only one shell in series or one shell in parallel

Table A.2-16: Decanter modules for D1

Capacity factor	D [m]	L _{tot} [m]	V [m ³]	FOB [\$]
1/3	0.25	3.35	0.16	*2 430
	0.3	2.9	0.20	*2 698
	0.35	2.55	0.25	2 932
	0.4	2.35	0.30	3 228
	0.5	2	0.39	3 715
	0.6	1.75	0.49	4 161
	0.7	1.6	0.62	4 667
0.5	0.35	3.55	0.34	3 833
	0.4	3.2	0.40	4 145
	0.5	2.65	0.52	4 666
	0.6	2.35	0.66	5 283
	0.7	2.1	0.81	5 816
	0.8	1.9	0.96	6 308
	0.9	1.75	1.11	6 810
1	0.9	2.9	1.84	10 252
	1.0	2.65	2.08	10 832
	1.1	2.5	2.38	11 601
	1.2	2.35	2.66	12 264
	1.4	2.1	3.23	13 502
	1.6	1.9	3.82	14 644
	1.8	1.75	4.45	15 808

* slightly out of the validity range of the cost function

Table A.2-17: Vapor-liquid separator modules

	D [m]	L [m]	V [m ³]	FOB [\$]		D [m]	L [m]	V [m ³]	FOB [\$]
HX1-PS 3 bar	0.9	2.7	1.7	9 676	F1 1.2 bar	0.8	2.4	1.2	7 622
	0.8	3.7	1.9	10 823		0.9	2.7	1.7	9 676
	0.9	3.7	2.4	12 489		0.9	2.7	1.7	9 676
	1.0	3.7	2.9	14 194		1.0	3.0	2.4	11 977
	1.5	4.5	8.0	27 222		1.0	4.2	3.3	15 729
	2.2	6.6	25.1	59 121		1.2	4.2	4.8	19 629
	3.0	9.0	63.6	110 791		1.4	4.2	6.5	23 672
	3.7	11.1	119.3	169 411		1.6	4.8	9.7	31 022
	4.3	12.9	187.3	229 671		1.7	5.1	11.6	35 075
HX3-PS 42 bar	0.8	2.4	1.2	12 196	HX6-PS 0.4 bar	0.3	0.9	0.1	*1 046
	0.9	2.7	1.7	15 481		0.3	0.9	0.1	*1 046
	0.9	4.1	2.6	21 714		0.4	1.2	0.2	*1 873
	1.2	4.1	4.6	30 800		0.4	1.7	0.2	*2 483
	1.8	5.4	13.7	63 006		0.6	1.9	0.5	4 447
	2.7	8.1	46.4	143 207		0.8	2.4	1.2	7 622
	3.7	11.1	119.3	271 058		1.1	3.3	3.1	14 526
	4.5	13.5	214.7	402 910		1.4	4.2	6.5	23 672
5.4	16.2	371.0	582 842	1.6	4.8	9.7	31 022		
HX4-PS 4 bar	0.5	1.5	0.3	2 943	HX8-PS 0.6 bar	0.6	1.8	0.5	4 257
	0.6	1.8	0.5	4 257		0.7	2.1	0.8	5 816
	0.7	2.1	0.8	5 816		0.8	2.4	1.2	7 622
	0.7	3.2	1.2	8 181		1.0	3.0	2.4	11 977
	1.1	3.3	3.1	14 526		1.3	3.9	5.2	20 374
	1.6	4.8	9.7	31 022		1.6	4.8	9.7	31 022
	2.1	6.3	21.8	53 806		2.0	6.0	18.8	48 744
	2.6	7.8	41.4	82 919		2.0	9.0	28.3	67 694
3.2	9.6	77.2	126 259	2.6	7.8	41.4	82 919		

* outside of cost function

A.2.5 Details of the exemplary modular equipment sets shown in Figure 6-16

Table A.2-18: Number and FOB costs of selected equipment modules for each process unit of exemplary modular equipment sets in Figure 6-16

	conv. design		set1		set2		set3		set4		set5		set6	
	No. of modules	FOB per module [\$]	No. of modules	FOB per module [\$]	No. of modules	FOB per module [\$]	No. of modules	FOB per module [\$]	No. of modules	FOB per module [\$]	No. of modules	FOB per module [\$]	No. of modules	FOB per module [\$]
HX1	1	37 743	2	55 882	2	37 743	2	37 743	3	55 882	3	37 743	5	32 828
HX1B	1	9 713	3	15 743	5	9 353	6	9 353	6	9 312	4	9 713	4	14 381
HX2	1	450 259	2	179 401	3	175 486	3	175 486	3	175 486	2	221 153	4	221 153
HX3	1	386 570	2	207 799	3	164 473	3	164 473	3	207 799	4	258 516	4	207 799
HX4	1	60 147	2	50 402	3	35 604	2	50 402	2	50 402	5	108 969	6	60 147
HX5	1	45 041	3	41 420	2	34 998	2	34 998	4	41 420	6	41 420	2	54 394
HX6	1	14 676	5	13 201	3	14 676	4	14 977	3	19 265	4	14 676	6	19 265
HX7	1	62 258	4	50 367	2	73 791	3	62 258	2	50 367	3	93 263	2	93 263
HX8	1	26 297	3	20 754	2	20 754	2	20 754	6	41 037	5	26 297	4	40 951
HX9	1	151 631	3	82 012	2	151 631	2	151 631	3	110 829	3	82 012	6	82 012
HX1-PS	1	27 222	1	59 121	2	27 222	3	10 823	2	12 489	2	12 489	6	27 222
HX3-PS	1	63 006	5	12 196	2	15 481	5	30 800	4	21 714	5	15 481	4	15 481
HX4-PS	1	14 526	6	14 526	3	2 943	3	2 943	1	8 181	4	126 259	1	126 259
HX6-PS	1	4 447	4	14 526	6	1 046	6	1 046	5	4 447	1	7 622	2	23 672
HX8-PS	1	20 374	1	7 622	5	4 257	5	4 257	5	4 257	4	31 022	4	82 919
F1	1	15 729	3	23 672	2	15 729	2	15 729	3	35 075	5	9 676	3	31 022
R1	1	161 487	3	72 624	2	88 478	2	88 478	3	72 624	3	55 477	3	68 673
R2	1	161 487	3	55 477	3	55 477	3	55 477	3	61 021	3	55 477	3	72 624
C1	1	61 906	2	48 994	3	49 036	3	49 036	3	42 464	3	45 454	3	48 994
C2	1	526 187	2	268 388	2	372 698	2	372 698	2	360 484	3	251 542	3	268 388
D1	1	12 264	1	10 832	2	4 145	2	4 145	3	2 932	1	13 502	1	14 644

A3 Acetone production example

A.3.1 Specifications of implemented shortcut HeatX models of heat exchangers

Table A.3-1: Outlet conditions of process and utility streams of heat exchangers

Heat exchanger	Process stream	Utility stream
HX1*	$f_{vapor} = 0.15$	$f_{vapor} = 0$
HX2*	$T = 162\text{ °C}$	$f_{vapor} = 0.15$
HX3	$T = 47\text{ °C}$	$T = 25\text{ °C}$
C1-COND	$\dot{Q}_{HeatX} = \dot{Q}_{RadFrac,Cond}$	$T = 25\text{ °C}$
C1-REB*	$f_{vapor} = 0.15$	$f_{vapor} = 0$
C2-COND	$\dot{Q}_{HeatX} = \dot{Q}_{RadFrac,Cond}$	$T = 25\text{ °C}$
C2-REB*	$f_{vapor} = 0.15$	$f_{vapor} = 0$

* forced circulation evaporators according to [7]

A.3.2 Design parameters and specifications of distillation columns C1 and C2

Table A.3-2: Input data for *RadFrac* distillation columns C1 and C2

	C1	C2
<i>NTP</i>	54	19
Feed stage (above stage)	44	16
d_h	0.005 m	0.005 m
Hole area/active area	12 %	12 %
Tray spacing	0.6 m	0.6 m
pressure at condenser	1 atm	1 atm
K_1	0.1	0.1
Purities*	$x_{Acetone,T} = 99.8\text{ mole-}\%$ $x_{Acetone,B} = 0.01\text{ mole-}\%$	$x_{IPA,T} = 65\text{ mole-}\%$ $x_{IPA,B} = 0.1\text{ mole-}\%$

* T = top, B = bottom

A.3.3 Raw material and utility costs

Acetone prices found in literature are cheaper than the price for IPA [143]. That is, because the majority of acetone is produced by the cheaper cumene route [98,144]. However, the acetone produced by the dehydrogenation of IPA is free from aromatic impurities and is therefore used in the pharmaceutical industry where tighter restrictions apply. Typical gross margins in the pharmaceutical industry are more than 40 %, often higher than 80 % [124]. A gross margin of 60 % has been considered for acetone to determine an appropriate product price. Prices in Euro are converted to US Dollar with a conversion factor from Euro to US Dollar of 1.0961 \$/€.

Table A. 3-3: Costs of used raw material and utilities

Utility	Specification	Costs	Source
Low-pressure steam	5 bar	19.73 \$/t	[111]
High-pressure steam	25 bar	24.11 \$/t	[111]
Molten salt	Costs energy consumption for fired heater	9.83 \$/GJ	[99]
Cooling water	Inlet 20°C, outlet 25°C	0.066 \$/m ³	[111]
Process water	-	0.493 \$/m ³	[111]
Wastewater	-	0.145 \$/m ³	[142]
Hydrogen/Propylene	Calculated as heating gas using combustion heat	9.83 \$/GJ	[99]
Isopropanol	-	1 400 \$/t	[143]
Acetone	-	2 240 \$/t	[92,124,143]

A.3.4 Equipment module database

Table A.3-4: Conventional reactor R1 modules ($d_T = 0.025$ m, $L_{T,\text{total}} = 4.7$ m) and reactor R1 modules with a larger operating window ($d_T = 0.025$ m, $L_{T,\text{total}} = 3.5$ m)

Conventional R1				R1 with larger operating window			
N_T [-]	V [m ³]	A [m ²]	FOB [\$]	N_T [-]	V [m ³]	A [m ²]	FOB [\$]
1095	2.30	367.3	117 036	931	1.45	232.6	82 268
985	2.07	330.6	108 021	838	1.31	209.3	76 012
876	1.84	293.8	98 788	744	1.16	186.0	69 565
766	1.61	257.1	89 299	651	1.02	162.8	62 992
657	1.38	220.4	79 505	558	0.87	139.5	56 164
532	1.12	178.7	67 922	465	0.73	116.3	49 062
438	0.92	146.9	58 689	372	0.58	93.0	41 609
328	0.69	110.2	47 396	279	0.44	69.8	33 684
219	0.46	73.5	35 146	186	0.29	46.5	25 056
109	0.23	36.7	23 575	93	0.15	23.3	15 182

Table A.3-5: Absorption column AB1 modules

d [m]	FOB [\$]
0.44	10 076
0.42	9 461
0.40	8 858
0.36	7 689
0.34	7 123
0.32	6 571
0.28	5 505
0.24	4 496
0.20	3 545
0.14	*2 239

* out of valid range for cost function, but considered

Table A.3-6: Distillation column modules of C1 and C2

Column C1			Column C2		
d [m]	H [m]	FOB [\$]	d [m]	H [m]	FOB [\$]
2.06	31.8	293 702	0.54	11.4	49 395
1.96	31.8	282 310	0.50	11.4	44 801
1.84	31.8	268 480	0.48	11.4	43 295
1.72	31.8	254 465	0.44	11.4	40 273
1.58	31.8	237 856	0.42	11.4	38 756
1.44	31.8	220 943	0.38	11.4	35 709
1.30	31.8	203 689	0.34	11.4	32 638
1.12	31.8	180 930	0.30	11.4	29 535
0.92	31.8	154 737	0.24	11.4	*24 797
0.64	31.8	115 957	0.18	11.4	*19 906

* out of valid range for cost function of trays, but considered

Table A.3-7: Vapor-liquid separator modules

	V [m ³]	L [m]	d [m]	FOB [\$]		V [m ³]	L [m]	d [m]	FOB [\$]
HX1-PS	46.38	8.1	2.7	89 505	HX2-PS	16.16	5.7	1.9	43 935
	41.41	7.8	2.6	82 920		13.74	5.4	1.8	39 379
	32.57	7.2	2.4	70 512		11.58	5.1	1.7	35 075
	28.67	6.9	2.3	64 690		9.65	4.8	1.6	31 023
	21.82	6.3	2.1	53 806		7.95	4.5	1.5	27 222
	16.16	5.7	1.9	43 935		6.47	4.2	1.4	23 673
	11.58	5.1	1.7	35 075		4.07	3.6	1.2	17 326
	7.95	4.5	1.5	27 222		3.14	3.3	1.1	14 527
	4.07	3.6	1.2	17 326		1.72	2.7	0.9	9 676
	1.84	2.9	0.9	10 253		0.54	1.9	0.6	4 448
HX3-PS	2.36	3.0 ^{b)}	1.0	11 977	C1-COND-PS	25.09	6.6	2.2	59 121
	1.91	3.0 ^{b)}	0.9	10 538		21.82	6.3	2.1	53 806
	1.51	3.0	0.8	9 133		18.85	6.0	2.0	48 744
	1.15	3.0 ^{b)}	0.7	7 765		13.74	5.4	1.8	39 379
	0.81	2.1	0.7	5 817		11.58	5.1	1.7	35 075
	0.51	1.8	0.6	4 257		9.65	4.8	1.6	31 023
C2-COND-PS	0.29	1.5	0.5	2 943		6.47	4.2	1.4	23 673
	0.47	2.4	0.5	4 307		4.07	3.6	1.2	17 326
	0.51	1.8 ^{a)}	0.6	4 257		2.36	3.0	1.0	11 977
	0.29	1.5 ^{a)}	0.5	2 943		0.81	2.1	0.7	5 817
	0.15	1.2 ^{b),*}	0.4	1 873					
	0.06	0.9 [*]	0.3	1 046					

^{a)} 3 times, ^{b)} 2 times

* outside of cost function but considered

Table A.3-8: Heat exchanger modules

	A	Tube OD	Shell ID	Tube length	Baffle Pitch	No Baffles	No Tubes	Tube Passes	HX in series	HX in parallel	FOB
	[m ²]	[mm]	[mm]	[mm]	[mm]	[mm]	[mm]	[mm]	[mm]	[mm]	[\$]
HX1	24.8	16	300	3000	150	18	168	1	1	1	17 557
BEM	20.6*	16	300	2500	155	14	168	1	1	1	16 980
Vertical	14.9	25	350	2500	80	27	78	2	1	1	16 702
	14.1	25	300	3000	130	21	61	2	1	1	15 190
	12.2	20	300	2000	100	17	100	2	1	1	15 456
	9.2	25	250	3000	80	34	40	2	1	1	13 488
	6.1	25	300	1500	190	6	54	4	1	1	13 394
	3.0	25	200	2000	50.8	35	20	2	1	1	11 005
HX2	27.0*	25	500	3000	125	17	129	2	1	1	32 903
BES	22.4**	25	450	3000	115	19	106	2	1	1	29 311
Vertical	16.3	25	400	3000	105	21	77	2	1	1	25 536
	12.0	25	350	3000	90	26	56	2	1	1	21 892
	8.1	25	300	2500	60	31	46	2	1	1	17 795
	6.1	25	250	3000	65	37	28	2	1	1	15 866
	3.6	20	250	1500	50.8	20	46	2	1	1	12 269
HX3	29.9**	30	500	3000	100	23	112	1	1	1	27 063
BES	29.3	30	500	3000	135	17	112	1	1	1	26 582
Horizontal	28.4	25	500	2500	135	13	159	1	1	1	26 199
	22.5	30	450	3000	130	18	86	1	1	1	23 856
	16.8	30	400	3000	85	28	64	1	1	1	22 010
	13.8	30	400	2500	75	26	64	1	1	1	20 501
	11.2	25	350	2500	90	22	62	1	1	1	17 254
	8.2	20	300	2000	50.8	29	72	1	1	1	14 910
	4.5	20	250	1500	50.8	21	55	1	1	1	12 150
C1-COND	136.5	38	800	3000	295	8	196	2	1	2	68 574
BEM	105.0	30	700	2500	300	6	230	2	1	2	58 396
Horizontal	102.4	38	700	3000	335	7	147	2	1	2	57 234
	89.0	38	900	3000	365	6	256	2	1	1	40 090
	71.4	30	800	2500	415	4	313	2	1	1	35 330
	68.3	38	800	3000	320	7	196	2	1	1	34 341
	51.2	38	700	3000	335	7	147	2	1	1	28 617
	39.0	30	600	2500	280	7	171	2	1	1	24 279
	23.3	20	400	2500	320	6	152	1	1	1	17 076
	12.6	20	300	2000	270	6	104	1	1	1	13 041
C1-REB	37.4*	38	700	2000	225	7	163	1	1	1	27 618
BEM	26.8**	38	600	2000	180	9	117	1	1	1	23 026
Vertical	18.3	38	500	2000	155	10	80	1	1	1	19 398
	17.6	38	500	2000	155	11	77	1	1	1	19 274
	10.5	38	400	2000	155	11	46	1	1	1	14 920
	7.8	38	350	2000	120	14	34	1	1	1	13 195
	3.9	30	250	1500	60	20	29	1	1	1	10 500
C2-COND	5.2	25	250	2000	200	7	34	1	1	1	10 565
BEM	5.1	30	250	2000	150	11	28	1	1	1	10 617
Horizontal	5.1	25	250	1500	145	8	45	1	1	1	10 407
	4.9	20	250	1500	200	6	54	1	1	1	10 499
	3.7	20	200	1500	200	6	41	1	1	1	9 076
	3.2	25	200	1500	135	9	28	1	1	1	8 875
	2.7	20	200	1500	180	7	30	1	1	1	8 865
	2.4	30	250	1500	80	15	18	2	1	1	10 032
	1.5	16	150	1000	120	6	31	1	1	1	7 352
	0.8	20	150	750	50.8	11	18	2	1	1	7 118

* three times, ** two times

Table A.3-8 (continued): Heat exchanger modules

	A	Tube OD	Shell ID	Tube length	Baffle Pitch	No Baffles	No Tubes	Tube Passes	HX in series	HX in parallel	FOB
	[m ²]	[mm]	[mm]	[mm]	[mm]	[mm]	[mm]	[mm]	[mm]	[mm]	[\$]
C2-REB	3.2**	38	250	1500	60	20	19	1	1	1	10 372
BEM	2.9**	30	300	750	50.8	10	46	2	1	1	11 213
Vertical	2.1**	25	200	1000	50.8	15	29	1	1	1	8 745
	1.2**	38	150	1500	50.8	25	7	1	1	1	7 678
	0.8	38	150	1500	50.8	5	7	1	1	1	7 601
	0.4	38	150	500	50.8	6	7	1	1	1	6 811

* three times, ** two times

A.3.5 Correlation exponents of each process units' operating constraint

Table A.3-9: Correlation exponents for the operating constraints of each process unit

Process units	Correlation exponents				
Heat exchangers		$\alpha_{v_{tube}}$	$\alpha_{v_{shell}}$	$\alpha_{\Delta p_{tube}}$	$\alpha_{\Delta p_{shell}}$
	HX1	1.00	1.17	1.73	2.80
	HX2	0.97	1.01	1.69	2.08
	HX3	2.72	1.14	5.25	2.08
	C1-COND	2.36	1.01	4.56	1.86
	C1-REB	2.45	1.05	2.72	2.40
	C2-COND	2.62	1.18	4.98	2.47
	C2-REB	2.26	1.48	2.52	6.82
Reactors		$\alpha_{\Delta p}$	$\alpha_{Conv.}$	$\alpha_{Sel.}$	
	R1	1.92	-0.0159	0.0163	
Distillation columns			$\alpha_{F-factor}$		
	C1		1.00		
	C2		1.15		
Absorption column		α_{FFmin}		α_{FFmax}	
	AB1	1.04		1.06	
Vapor-liquid separators		α_{τ}		α_v	
	HX1PS	-1.02		1.02	
	HX2PS	-1.00		1.05	
	HX3PS	-1.02		1.08	
	C1CONDPS	-1.00		1.26	
	C2CONDPS	-1.13		3.96	

A.3.6 Used equipment modules for the conventional design case

Table A.3-10: Size of used equipment modules of reference plant representing conventional design case

Process unit	Size	Process unit	Size		
HX1	[m ²]	20.6	AB1	[m]	0.36
HX2	[m ²]	27.0	C1	[m]	1.96
HX3	[m ²]	29.3	C2	[m]	0.50
C1-COND	[m ²]	105.0	HX1-PS	[m ³]	28.67
C1-REB	[m ²]	37.4	HX2-PS	[m ³]	9.65
C2-COND	[m ²]	5.1	HX3-PS	[m ³]	1.51
C2-REB	[m ²]	3.2	C1-COND-PS	[m ³]	11.58
R1	[-]	985	C2-COND-PS	[m ³]	0.29

A.3.7 Number of equipment modules per process unit for 20 %-production line and 20 % equipment-wise expansion strategy

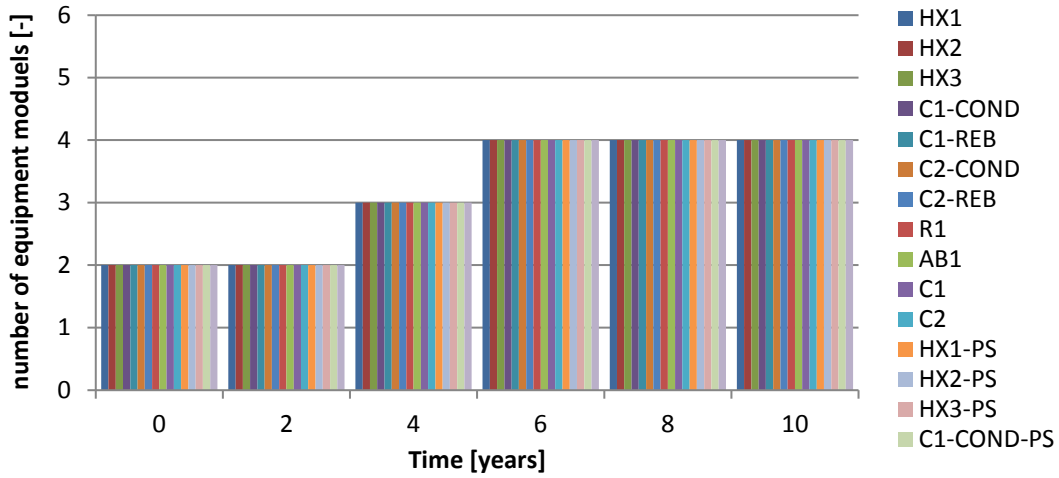


Figure A.3-1: Number of equipment modules for each process unit in case of the 20 %-production line over the expansion timespan of 10 years

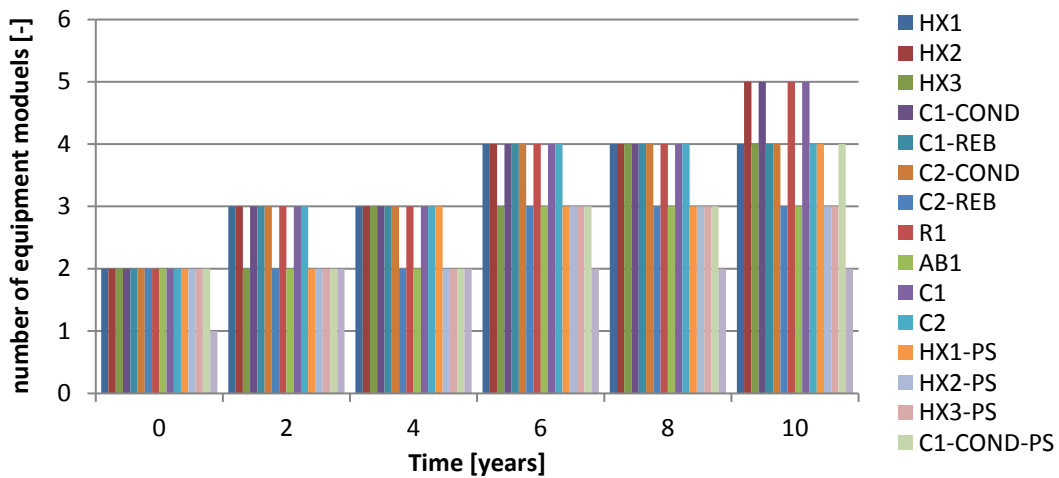


Figure A.3-2: Number of equipment modules for each process unit in case of the 20 % equipment-wise expansion strategy over the expansion timespan of 10 years

A4 Fermentative succinic acid production example

A.4.1 Basis for shortcut design of heat exchangers

Table A.4-1: Overall heat transfer coefficients used for shortcut heat exchanger design in Aspen Plus® for the heat exchangers of the succinic acid production process [92,126]

Heat exchanger	U [W/m ² /K]
HX1	750
HX2	675
HX3	1950
HX4	1950
HX5	1950

A.4.2 Correlation exponents of each process units' operating constraint

Table A.4-2: Correlation exponents for the operating constraints of each process unit of the succinic acid production process

Process units		Correlation exponents α			
Heat exchangers		$\alpha_{v_{tube}}$	$\alpha_{v_{shell}}$	$\alpha_{\Delta p_{tube}}$	$\alpha_{\Delta p_{shell}}$
	HX1	1.00	1.07	1.39	2.59
	HX2	1.99	1.00	1.05	1.92
	HX3	0.88	1.18	0.85	14.87
	HX4	0.73	1.11	1.07	6.44
	HX5	0.85	1.08	0.77	2.42
Fermenter		$\alpha_{Filling\ level}$			
	Ferm	1.00			
Rotary drum vacuum filters		$\alpha_{\Delta p}$			
	RDVF1	2.00			
	RDVF2	2.00			
Dryer		α_{ϵ}	$\alpha_{solids\ hold-up}$	$\alpha_{w_{g,min}}$	
	DRY	0.00	0.00	0.00	
Crystallizer		$\alpha_{Filling\ level}$			$\alpha_{A_{req}}$
	CrystCas1	1.00			0.97
	CrystCas2	1.00			1.00
	CrystCas3	1.00			1.00
	CrystCas4	1.00			1.00
Vapor-liquid separators		α_{τ}	α_v		
	2PS1	-1.00	1.01		
	2PS2	-1.00	1.03		
	2PS3	-1.00	1.04		

A.4.3 Specifications of implemented shortcut *HeatX* or *HXFlux* models of heat exchangers

Table A.4-3: Outlet conditions for process and utility streams of heat exchangers

Heat exchanger	Process stream	Utility stream
HX1	$T = 140\text{ }^{\circ}\text{C}$	$f_{vapor} = 0$
HX2	$T = 37\text{ }^{\circ}\text{C}$	$T = 25\text{ }^{\circ}\text{C}$
HX3	$f_{vapor} = 0.15$	$f_{vapor} = 0$
HX4	$f_{vapor} = 0.15$	$f_{vapor} = 0$
HX5	$f_{vapor} = 0.15$	$f_{vapor} = 0$

* forced circulation evaporators according to [145]

A.4.4 Raw material and utility costs

The prices for raw materials and utilities used to calculate the OPEX are summarized in Table A.4-4. As the bacteria are bred, they are considered part of the initial costs for a succinic acid production plant and not part of the OPEX.

Table A.4-4: Costs for raw material and utilities

	Costs		Source
Glycerol feed	200	\$/t	[146]
Carbon dioxide	45	\$/t	[147]
Yeast extract	4 384	\$/t	[148]
Hydrochloric acid (37 % w/w)	750	\$/t	[134]
Sodium hydroxide	350	\$/t	[134]
Silicon antifoam	65 656	\$/t	[149]
Process water	0.493	\$/m ³	[111]
Low-pressure steam (5 bar)	19.73	\$/t	[111]
High-pressure steam (25 bar)	24.11	\$/t	[111]
Cooling water	0.066	\$/m ³	[111]
Electric power	0.1	\$/kWh	[134]

For the fermenters, the average power consumption by stirring per volume can be estimated to 1 to 2 kW/m³ for industrial bioreactors with a vessel volume of 100 m³ [150]. As the fermenter vessels used are larger and the power consumption per unit volume decreases for an increasing vessel volume, 1 kW/m³ is used in this work. The electrical power consumption of the continuous rotary drum vacuum filters RDVF1 and RDVF2 is estimated to 5.9 kWh/m³ according to [151]. It is assumed that the heat stream supplied by hot air is generated by electricity using its specific enthalpy to estimate the utility costs of the fluidized bed dryer. To calculate the amount and costs of cooling water required for the batch fermenters, the heat of reaction is estimated according to [150] by using the heats of combustion Δh_c of substrate S , nitrogen source N – *source*, biomass BM and products P according to Eq. A4-1:

$$\Delta H_{rxn} = (n \cdot \Delta h_c)_S + (n \cdot \Delta h_c)_{N-source} - (n \cdot \Delta h_c)_{BM} - (n \cdot \Delta h_c)_P \quad \text{Eq. A4-1}$$

The heat of combustion of the nitrogen source is estimated by using the heat of combustion of L-Glutamic acid as its main component. Carbon dioxide and water are not considered as their values are zero. By using an estimated value for the heat of combustion of biomass (bacteria) of -23.2 kJ/kg [150], the heat of reaction of the fermentative production of succinic acid is determined to be -1.001 kJ/mol.

A.4.5 Equipment module database of succinic acid production process

Table A. 4-5: Fermenter equipment modules in equipment module database

V [m ³]	FOB [\$]
360	421 276
365	424 250
420	455 732
435	463 961
455	474 721
465	480 013
485	490 434

* less than ten equipment modules, since equal sizes are used with different numbers in conventional design

Table A.4-6: Dryer equipment modules in equipment module database

A [m ²]	H [m]	FOB [\$]
2.3	1.060	164 891
6.2	1.045	236 144
7.9	1.052	258 347
11.0	1.050	291 059
13.3	1.052	312 465
17.3	1.048	343 817
15.8	1.061	332 237
18.7	1.059	353 179
19.5	1.064	358 607
27.5	1.050	407 018

Table A. 4-7: Vapor-liquid separator modules in equipment module database

2PS1				2PS3			
V [m ³]	L [m]	D [m]	FOB [\$]	V [m ³]	L [m]	D [m]	FOB [\$]
2.4	3.0	1.0	11 977	1.7	2.7	0.9	9 676
6.5	4.2	1.4	23 672	5.2	3.9	1.3	20 374
11.6	5.1	1.7	35 075	9.7	4.8	1.6	31 022
18.8	6.0	2.0	48 744	13.7	5.4	1.8	39 379
25.1	6.6	2.2	59 121	18.8	6.0	2.0	48 744
32.6	7.2	2.4	70 512	25.1	6.6	2.2	59 121
41.4	7.8	2.6	82 919	28.7	6.9	2.3	64 689
51.7	8.4	2.8	96 345	36.8	7.5	2.5	76 588
57.5	8.7	2.9	103 440	46.4	8.1	2.7	89 504
70.2	9.3	3.1	118 397	51.7	8.4	2.8	96 345
2PS2							
2.4	3.0	1.0	11 977				
6.5	4.2	1.4	23 672				
11.6	5.1	1.7	35 075				
18.8	6.0	2.0	48 744				
25.1	6.6	2.2	59 121				
32.6	7.2	2.4	70 512				
41.4	7.8	2.6	82 919				
46.4	8.1	2.7	89 504				
57.5	8.7	2.9	103 440				
70.2	9.3	3.1	118 397				

Table A.4-8: Crystallizer equipment modules of crystallization cascade CrystCas in equipment module database

V [m ³]	^a FOB [\$]
0.4	50 278
0.8	77 806
1.1	100 427
1.5	120 420
1.8	138 569
2.2	155 471
2.5	171 310
2.9	186 322
3.2	200 695
3.6	214 472

^a out of range of validity of cost function, but used anyway

^b L/D-ratio of fourth crystallizer is set to two

Table A.4-9: Rotary drum vacuum filter equipment modules in equipment module database

RDVF1			RDVF2		
L [m]	D [m]	FOB [\$]	L [m]	D [m]	FOB [\$]
0.26	0.13	27 471	0.21	0.11	21 450
0.36	0.18	41 938	0.29	0.15	32 367
0.44	0.22	54 438	0.36	0.18	41 938
0.51	0.26	66 794	0.41	0.21	50 447
0.57	0.29	77 084	0.46	0.23	57 677
0.62	0.31	85 021	0.50	0.25	64 280
0.67	0.34	94 950	0.54	0.27	71 044
0.72	0.36	103 264	0.58	0.29	77 960
0.76	0.38	110 783	0.62	0.31	85 021
0.80	0.40	118 422	0.65	0.33	91 309

Table A.4-10: Heat exchanger modules in equipment module database of succinic acid production plant

	A	Tube OD	Shell ID	Tube length	Baffle Pitch	No Baffles	No Tubes	Tube Passes	HX in series	HX in parallel	FOB
	[m ²]	[mm]	[mm]	[mm]	[mm]	[mm]	[mm]	[mm]	[mm]	[mm]	[\$]
HX1	3.3	16	150	4000	100	36	17	2	1	1	9 195
BES	4.7	16	200	3000	150	17	33	3	1	1	10 393
Horizontal	7.7	16	200	4000	200	18	40	2	1	1	11 110
hot @SS	8.9	16	250	3000	240	11	63	3	1	1	12 595
	13.6	20	250	5000	240	19	45	2	1	1	14 875
	15.1	20	300	4000	265	13	63	3	1	1	15 215
	17.0	25	350	4000	265	13	57	4	1	1	17 220
	21.9	25	350	5000	295	15	58	3	1	1	19 553
	21.9	25	350	5000	295	15	58	3	1	1	19 553
	23.3	20	400	3000	235	11	132	4	1	1	19 846
HX2	4.5	20	250	1500	25	44	55	1	1	1	12 610
BES	7.8	25	300	2000	40	40	55	1	1	1	14 782
Horizontal	14.5	30	350	3000	60	42	55	1	1	1	17 805
hot @SS	19.8	25	400	2500	70	28	109	1	1	1	20 149
	24.5	25	450	2500	80	24	135	1	1	1	22 143
	31.5	25	500	2500	80	24	174	1	1	1	24 557
	33.0	38	500	4000	90	38	73	1	1	1	25 876
	39.1	30	600	3000	100	24	181	1	1	1	27 624
	47.6	30	600	3000	100	24	181	1	1	1	28 478
	47.6	30	600	3000	100	24	181	1	1	1	28 478
HX3	7.3	30	300	2000	130	12	40	1	1	1	12 017
BEM	14.5	30	400	2000	210	8	80	1	1	1	16 155
Vertical	22.8	38	500	2500	260	8	79	1	1	1	20 454
hot @SS	27.9	38	500	3000	285	9	80	1	1	1	21 176
	34.4	38	600	2500	165	12	119	1	1	1	24 011
	47.1	38	700	2500	330	6	163	1	1	1	28 359
	56.8	38	700	3000	400	6	163	1	1	1	29 123
	61.8	38	800	2500	345	6	214	1	1	1	34 184
	74.6	38	800	3000	600	3	214	1	1	1	34 536
	74.6	38	800	3000	345	7	214	1	1	1	35 348
HX4	5.7	38	300	2000	95	18	25	1	1	1	11 945
BEM	11.7	38	400	2000	210	8	51	1	1	1	15 676
Vertical	18.5	30	450	2000	255	6	102	1	1	1	18 198
hot @SS	22.8	38	500	2500	345	6	79	1	1	1	20 484
	26.8	38	600	2000	145	11	117	1	1	1	23 072
	34.4	38	600	2500	340	6	119	1	1	1	23 558
	37.4	38	700	2000	140	11	163	1	1	1	27 881
	47.1	38	700	2500	330	6	163	1	1	1	28 491
	50.2	38	800	2000	260	6	219	1	1	1	33 033
	63.3	38	800	2500	345	6	219	1	1	1	34 272
HX5	5.3	30	250	2000	120	15	29	1	1	1	10 566
BEM	10.1	25	350	1500	95	13	89	1	1	1	14 104
Vertical	18.7	25	400	2000	255	6	123	1	1	1	16 674
hot @SS	21.6	38	450	3000	235	11	62	1	1	1	18 818
	27.5	38	500	3000	345	7	79	1	1	1	21 132
	33.8	38	600	2500	215	10	117	1	1	1	23 740
	41.5	38	600	3000	410	6	119	1	1	1	24 161
	48.2	38	700	2500	330	6	167	1	1	1	28 573
	56.8	38	700	3000	355	7	163	1	1	1	29 372
	56.8	38	700	3000	400	6	163	1	1	1	29 238

A.4.6 Details of Pareto sets from preselection case study

Table A.4-11: Number and size of equipment modules of the Pareto sets
(modular equipment sets are sorted in ascending order based on TCI for each preselection case)

	HX1	HX2	Ferm	RDVF1	HX3	2PS1	HX4	2PS2	HX5	2PS3	CrystCas	RDVF2	DRY	TCI ^a	OPEX													
	No. [m ²]	No. [m ²]	No. [m ³]	No. [m]*	No. [m ²]	No. [m ³]	No. [m ²]	No. [m ³]	No. [m ²]	No. [m ³]	No. [m ³]	No. [m]*	No. [m ²]	[mio. \$/a]	[mio. \$/a]													
Conv	1	21.9	1	0.72	1	61.8	1	47.1	1	46.4	1	48.2	1	36.8	1	2.9	1	0.58	1	18.7	3.38	9.9363						
Set 1	1	21.9	2	19.8	7	485	1	0.72	1	74.6**	2	11.6	1	63.3	5	2.4	2	33.8	1	25.1	1	2.9	1	0.46	1	10.99	2.99	9.6737
Set 2	1	21.9	2	19.8	7	485	1	0.72	1	74.6**	6	2.4	3	26.8	5	2.4	2	33.8	6	1.7	1	2.9	1	0.46	1	10.99	3.04	9.6575
Set 3	1	21.9	2	19.8	7	485	2	0.44	4	34.4	6	2.4	1	63.3	3	6.5	2	33.8	1	36.8	1	2.9	1	0.46	1	10.99	3.07	9.5824
Set 4	3	7.7	2	19.8	7	485	2	0.44	4	34.4	6	2.4	3	26.8	3	6.5	2	33.8	6	1.7	1	2.9	1	0.46	1	10.99	3.12	9.5559
Set 5	7	3.3	2	19.8	7	485	1	0.72	4	34.4	2	11.6	3	26.8	5	2.4	7	10.1	1	25.1	1	2.9	1	0.46	1	10.99	3.17	9.5414
Set 6	7	3.3	2	19.8	7	485	2	0.44	4	34.4	2	11.6	3	26.8	5	2.4	7	10.1	1	36.8	1	2.9	1	0.46	1	10.99	3.19	9.5413
Set 7	7	3.3	2	19.8	7	485	5	0.26	4	34.4	2	11.6	3	26.8	3	6.5	7	10.1	6	1.7	1	2.9	1	0.46	1	10.99	3.22	9.5410
Set 1	1	21.9	1	33	8	485	1	0.67	1	56.8	1	32.6	1	63.3	5	2.4	1	56.8***	1	25.1	1	2.9	1	0.46	1	6.2	3.24	9.8282
Set 2	1	21.9	2	19.8	8	485	1	0.67	3	34.4	1	32.6	1	63.3	5	2.4	1	56.8***	1	25.1	1	2.9	1	0.46	1	6.2	3.29	9.6216
Set 3	3	7.7	2	19.8	8	485	1	0.67	4	34.4	1	32.6	1	63.3	5	2.4	1	56.8***	1	25.1	1	2.9	1	0.46	1	6.2	3.32	9.5858
Set 4	3	7.7	2	19.8	8	485	1	0.67	4	34.4	1	32.6	3	37.4	5	2.4	1	56.8***	1	25.1	1	2.9	1	0.46	1	6.2	3.36	9.5573
Set 5	3	7.7	2	19.8	8	485	1	0.67	4	34.4	1	32.6	3	37.4	5	2.4	8	10.1	1	25.1	1	2.9	1	0.46	1	6.2	3.44	9.5306
Set 6	3	7.7	2	19.8	8	485	5	0.26	4	34.4	3	32.6	3	37.4	5	2.4	8	10.1	1	25.1	1	2.9	1	0.46	1	6.2	3.49	9.5305
Set 7	3	7.7	2	19.8	8	485	5	0.26	4	34.4	8	6.5	3	37.4	10	11.6	8	10.1	8	9.4	1	2.9	1	0.46	1	6.2	3.91	9.5305
Set 1	1	21.9	2	19.8	8	485	1	0.57	1	61.8	1	32.6	1	47.1	3	6.5	1	48.2	1	25.1	1	2.9	1	0.46	1	2.3	3.20	9.8548
Set 2	1	21.9	2	19.8	8	485	1	0.57	1	61.8	1	32.6	1	47.1	6	2.4	1	48.2	1	25.1	1	2.9	1	0.46	1	2.3	3.21	9.8548
Set 3	1	21.9	2	19.8	8	485	1	0.57	1	61.8	1	32.6	1	47.1	6	2.4	1	48.2	6	1.7	1	2.9	1	0.46	1	2.3	3.22	9.8545
Set 4	1	21.9	2	19.8	8	485	5	0.26	1	61.8	6	2.4	1	47.1	3	6.5	1	48.2	1	25.1	1	2.9	1	0.46	1	2.3	3.27	9.8543
Set 5	1	21.9	2	19.8	8	485	5	0.26	1	61.8	6	2.4	1	47.1	3	6.5	1	48.2	1	25.1	2	1.5	1	0.46	1	2.3	3.33	9.8543
Set 6	1	21.9	2	19.8	8	485	5	0.26	1	61.8	10	6.5	1	47.1	3	6.5	1	48.2	1	25.1	1	2.9	1	0.46	1	2.3	3.39	9.8540
Set 7	1	21.9	2	19.8	8	485	5	0.26	1	61.8	10	6.5	1	47.1	3	6.5	1	48.2	1	25.1	2	1.5	1	0.46	1	2.3	3.44	9.8540
Set 1	1	23.3	2	19.8	8	485	1	0.72	1	61.8	5	2.4	2	26.8	2	11.6	2	33.8	2	9.7	1	2.9	1	0.58	1	18.7	3.39	9.7853
Set 2	1	23.3	2	19.8	8	485	1	0.72	1	61.8	1	51.7	3	37.4	2	11.6	9	10.1	2	9.7	1	2.9	1	0.58	1	18.7	3.50	9.7186
Set 3	7	3.3	2	19.8	8	485	1	0.72	1	61.8	1	51.7	3	37.4	2	11.6	9	10.1	2	9.7	1	2.9	1	0.58	1	18.7	3.55	9.7082
Set 4	7	3.3	2	19.8	8	485	1	0.72	1	61.8	5	2.4	4	26.8	2	11.6	9	10.1	8	13.7	1	2.9	1	0.58	1	18.7	3.72	9.7078
Set 5	7	3.3	2	19.8	8	485	1	0.72	1	61.8	3	70.2	4	26.8	1	32.6	9	10.1	2	18.8	1	2.9	1	0.58	1	18.7	3.75	9.7077
Set 6	7	3.3	2	19.8	8	485	1	0.72	1	61.8	4	18.8	4	26.8	3	6.5	9	10.1	2	18.8	4	0.8	1	0.58	1	18.7	3.77	9.7077
Set 7	7	3.3	2	19.8	8	485	1	0.72	1	61.8	5	2.4	4	26.8	3	6.5	9	10.1	5	9.7	1	2.9	1	0.58	1	18.7	3.80	9.7075

* [m] according length
 ** with 7 baffles
 *** with 7 baffles
 a depreciation period of 10 years

A.4.7 Overall operating windows of case *Conv* and Pareto-optimal modular equipment sets of the cases *Inv*, *Inv&Op* and *ExEco*

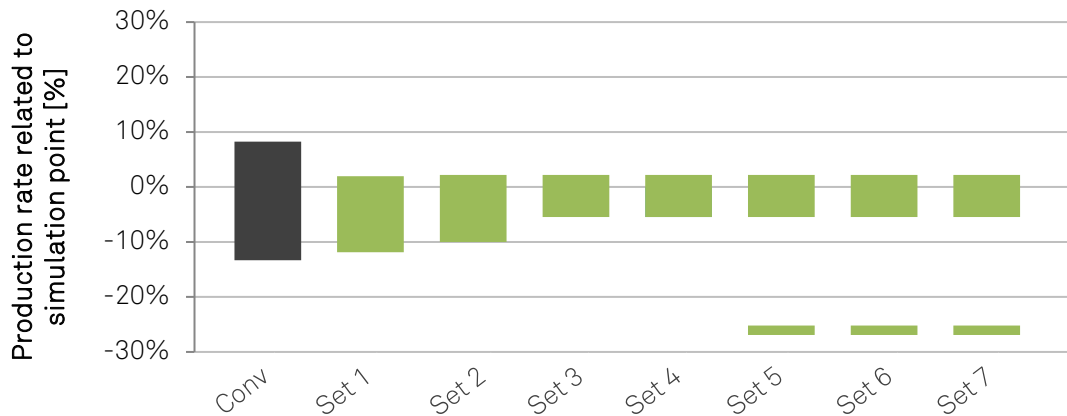


Figure A.4-1: Overall operating windows of case *Conv* (black) and Pareto-optimal modular equipment sets of case *Inv* (green, numbered consecutively as shown in Table A.4-11 from left to right)

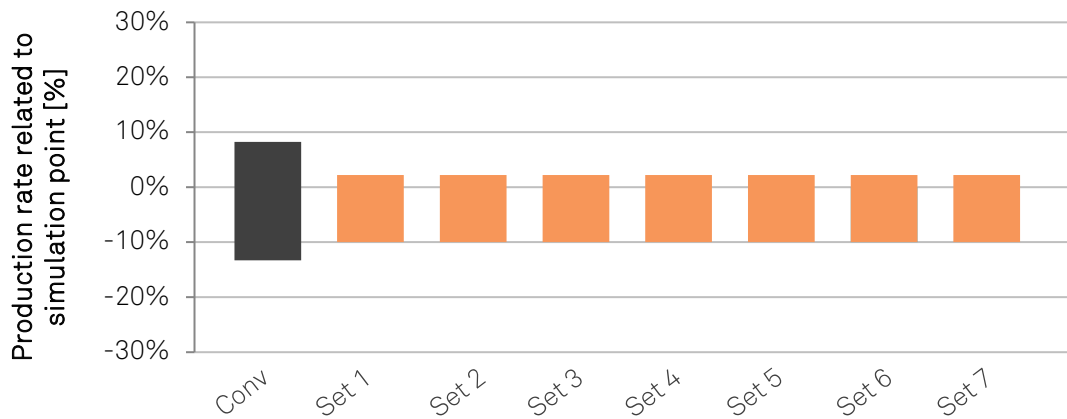


Figure A.4-2: Overall operating windows of case *Conv* (black) and Pareto-optimal modular equipment sets of case *Inv&Op* (orange, numbered consecutively as shown in Table A.4-11 from left to right)

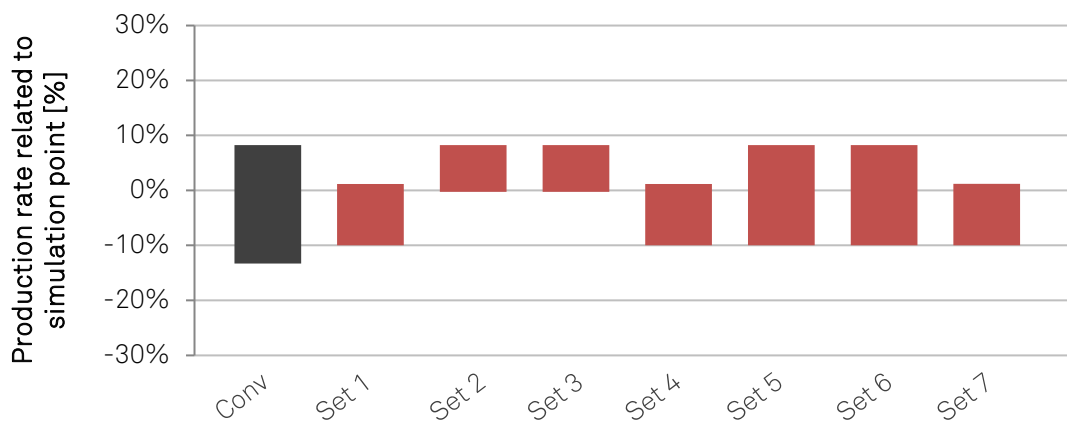


Figure A.4-3: Overall operating windows of case *Conv* (black) and Pareto-optimal modular equipment sets of case *ExEco* (red, numbered consecutively as shown in Table A.4-11 from left to right)

A5 General conventional design approach for process units

A.5.1 Heat exchangers

To design and simulate the shell and tube heat exchangers Aspen Exchanger Design & Rating (EDR) V8.4 is used. Aspen EDR selects the design with the lowest investment costs out of the feasible designs. To design a heat exchanger with the help of Aspen EDR the process requirements from a *HeatX* model block in shortcut simulation mode of the flowsheet simulation are transferred to Aspen EDR. Thus, the inlet and outlet conditions are specified for the hot and cold stream, as well as all physical property parameters. In order to design a shell and tube heat exchanger in Aspen EDR, some basic design parameters as TEMA designation, tube pitch ratio, tube diameter, baffle layout and baffle cut orientation need to be fixed first. With these boundary conditions Aspen EDR searches for feasible designs by varying tube length, shell length and diameter, baffle cut, baffle pitch and number of tube passes. Aspen EDR performs these calculations based on the *Construction Specifications* listed in Table A.5-1 using the *Standard* simulation method.

Table A.5-1: Construction specifications in Aspen EDR

Design code	EN13445
Service class	Normal
TEMA class	B – chemical service
Material standard	EN
Dimensional standard	ISO - international

The main design parameters are fixed for every heat exchanger in the process. This work is limited to one pass shells (TEMA Type E) and bonnet front end heads (type B), because they are most commonly used in chemical process industry [92]. For the rear end two types can be chosen. A fixed tubesheet (type M) is the simplest and cheapest alternative. However, they are not recommended for large temperature differences between shell and tube due to thermal expansion. For temperature differences above 80 °C a floating head with backing device, which is most commonly used is chosen [92,152]. Evaporators are built as forced circulation evaporators, which typically evaporate 6 to 15 %, whereas 15 % are chosen within this work [7,126]. The remaining liquid flow is separated in a vapor-liquid separator and recycled back to the evaporator. In case of column reboilers, the bottom of the columns serves as vapor-liquid separator. The orientation and allocation of streams is given for each heat exchanger in the respective equipment module database. Table A.5-2 summarizes the main design parameters for shell and tube heat exchangers used in this work.

Table A.5-2: Fixed design parameter values for shell and tube heat exchangers

Design parameter		Source
Basic type	Shell and tube heat exchanger	[125]
Shell type	One pass shell (type E)	[92]
Front end heat type	Bonnet (B type)	[92]
Rear end head type	Fixed tubesheet (M type) or Floating head with backing device (S type)	[92] [152]
Tube arrangement pattern	Triangular (30°)	[125]
Tube pitch ratio	1.25	[92]
Baffle layout	Single segmental baffles	[92]
Baffle cut orientation	Vertical	[125]

The other design parameters that are varied by Aspen EDR to design the heat exchanger according to the process requirements are shown in Table A.5-3.

Table A.5-3: Ranges and values of variable shell and tube heat exchangers design parameters [126]

Design parameter	Unit	Values / value ranges
Tube outer diameter	[mm]	16, 20, 25, 30, 38
Tube length	[mm]	500-8000
Shell inner diameter	[mm]	150-2500
Baffle cut	[%]	14-45
Baffle pitch	[mm]	> 30
Number of tube passes	[-]	1-4

These variables are varied by Aspen EDR using a *Scenario Table* to find a feasible and inexpensive heat exchanger design. All operating constraints of the resulting feasible designs are checked. If for example the shell side velocity is lower than the required minimum, the baffle pitch is adjusted. 30 mm is the smallest baffle pitch that is used. The resulting heat exchanger designs are stored in an EDR-File which the Aspen Plus® flowsheet simulation can use. Additionally to the individual design of each heat exchanger, all designed heat exchanger equipment modules of a design case are tested together in the flowsheet simulation. If heat exchanger modules do not fit any longer it is redesigned until it fits.

A.5.2 Distillation columns

The number of theoretical plates is determined with the *DSTWU* model in Aspen Plus®, which uses the Winn-Underwood-Gilliland shortcut calculation. To determine the minimum reflux ratio RR_{min} a large number of theoretical stages is used for the *DSTWU* model in a first step. The resulting RR_{min} is multiplied by 1.3 to get the actual reflux ratio RR [153]. Afterwards the actual reflux ratio RR is applied to calculate the *NTP*, the distillate to feed ratio $D:F$ and the initial feed stage. These design values are transferred to the *RadFrac* model, which allows a rigorous simulation and is therefore used for further design and simulation. The feed stage is determined by minimizing the costs for condenser and reboiler duty with a sensitivity

analysis. Finally, the *TraySizing* or the *PackSizing* feature is used to determine the diameter of every column equipment module, respectively. All column equipment modules are designed at 80 % of their flooding velocity.

A.5.3 Randomly packed absorption column

The required absorbent flow rate is calculated based on a balance around the column as shown by Eq. A5-1 [154]. X and Y are loadings of the liquid and the vapor stream, respectively. To calculate the minimum required absorbent flow rate, thermodynamic equilibrium of the liquid flow entering and the gas flow leaving the column is assumed. The equilibrium constant K is calculated according to Eq. A5-2 for non-ideal solutions [154].

$$\dot{n}_{L,min} = \dot{n}_v \cdot \frac{Y_{in} - Y_{out}}{\frac{Y_{in}}{K} - X_{in}} \quad \text{Eq. A5-1}$$

$$K_i = \frac{\gamma_{i,L}^{\infty} \cdot p_i^{LV}}{p} \quad \text{Eq. A5-2}$$

The practical absorbent flow rate ranges between 1.1 and 2 times the calculated minimal flow rate, whereas a value of 1.5 is taken within this work [154]. Next, the number of theoretical plates NTP is calculated using the Colburn equation shown by Eq. A5-3 [104].

$$NTP = \frac{\ln\left(\left(1 - \frac{1}{A_{ab}}\right) \cdot \left(\frac{y_{in} - K \cdot x_{in}}{y_{out} - K \cdot x_{in}}\right) + \frac{1}{A}\right)}{\ln(A_{ab})} \quad \text{Eq. A5-3}$$

Eq. A5-3 is valid for straight operating and equilibrium lines, a non-reacting system and dilute concentrations. The absorption factor A_{ab} is defined by Eq. A5-4 [154].

$$A_{ab} = \frac{\dot{n}_L}{K \cdot \dot{n}_v} \quad \text{Eq. A5-4}$$

Subsequently, the column diameter can be determined by Aspen Plus[®] using the *PackSizing* feature of the *RadFrac* column model. To calculate the overall height of the column, the height equivalent to a theoretical plate (HETP) needs to be determined according to Eq. A5-5 [38].

$$HETP = \frac{\ln\left(\frac{1}{A_{ab}}\right)}{\frac{1}{A} - 1} \cdot HTU_{OG} \quad \text{Eq. A5-5}$$

HTU_{OG} represents the overall gas transfer unit and can be determined by Eq. A5-6 [155].

$$HTU_{OG} = HTU_G + \frac{HTU_L}{A_{ab}} \quad \text{Eq. A5-6}$$

The height of a liquid-film transfer unit HTU_L and the height of the gas-film transfer unit HTU_G depend on the used packing internals [155].

A.5.4 Multi-tubular reactor

The tube diameter is determined first. Generally, the tube diameter is determined based on heat transfer characteristics. The smaller the tube diameter, the larger is the specific heat transfer area of the multi-tubular reactor. Smaller tube diameters increase the heat transfer, whereas larger tube diameters reduce the material costs [156,157]. Simulations in Aspen Plus® showed that the reaction progress is limited by heat transfer and the smallest practical tube diameter of 25 mm according to [158] is chosen. The consideration to determine the tube diameter mainly depends on the reaction and does not change with varying throughput [159]. Consequently, the tube diameter is equal for all ten reactor modules. Next, the tube length L_T is determined with the help of a *Design Spec* in Aspen Plus® such that the pressure drop is about 5 % of the reactor inlet pressure [105]. To avoid condensation of the saturated vapor on the catalyst pellets, the tube length is increased to offer an overheating section at the first part of the reactor tubes. This preheating section does not contain catalyst and therefore acts as a shell and tube heat exchanger. To overheat the saturated process steam by 50 °C an additional tube length of 0.35 m is added resulting in an overall tube length $L_{T,total}$ of 4.7 m. The catalyst particle diameter should not be larger than a tenth of the tube diameter [38,90]. Due to no mass transfer restriction, the maximum diameter of the catalyst particle d_p of 2.5 mm is selected. This also assures sufficient mixing based on the recommended ratio of tube length to catalyst particle diameter [38]. Finally, the number of tubes N_T is determined to fulfill the process requirements in terms of production rate for each design production rate at a minimum conversion of 90 %. To keep the pressure drop in the reactor low and assure a decent operation of the following absorption column, the number of tubes of each of the designed reactor equipment modules is raised by 10 %.

To model the heat transfer from the molten salt to the process fluid a correlation for the *Nusselt* number Nu is used for the tube section without catalyst pellets and with catalyst pellets, respectively. Typically, the heat transfer in packed tubes is increased compared to empty tubes due to the higher heat conduction of the packing [92]. The correlation of Bey and Eigenberger specifically addresses this influence of the packing and is used in this work as shown in Eq. A5-7 [160] and Eq. A5-8 [161]:

$$Nu = 2.4 \cdot \left(\frac{\lambda_{cat}}{\lambda_{fluid}} \right)^n + 0.054 \cdot \left(1 - \frac{d_p}{d_T} \right) \cdot Re_p \cdot Pr^{1/3} \quad \text{Eq. A5-7}$$

with:

$$n = 0.28 - 0.757 \cdot \log(\varepsilon) - 0.057 \cdot \log\left(\frac{\lambda_{cat}}{\lambda_{fluid}}\right) \quad \text{Eq. A5-8}$$

with λ as thermal conductivity of the catalyst and the fluid, respectively, and ε representing the void fraction of the catalyst packing. The thermal conductivity of the catalyst is assumed to be $\lambda_{cat} = 2 \text{ W}/(\text{m}\cdot\text{K})$ and ε is taken as 0.4. Re_p is the particle *Reynolds* number calculated by Eq. A5-9 and Pr is the *Prandtl* number that can be calculated according to Eq. A5-10, with ρ as mass density, v as fluid velocity, η as dynamic viscosity, c_p as specific heat and λ as thermal conductivity.

$$Re_p = \frac{\rho \cdot v \cdot d_p}{\eta} \quad \text{Eq. A5-9}$$

$$Pr = \frac{\eta \cdot c_p}{\lambda} \quad \text{Eq. A5-10}$$

In the preheating section of the reactor tubes, catalyst pellets do not need to be taken into account and Eq. A5-11 is used to calculate the heat transfer for empty tubes, whereby C is set to 0.021 for gases [92].

$$Nu = C \cdot Re^{0.8} \cdot Pr^{1/3} \quad \text{Eq. A5-11}$$

These *Nusselt* numbers are used to calculate the respective heat transmission coefficients α of both reactor tube sections, respectively. This allows to calculate the overall heat transfer coefficient, which is transferred to the *RPlug* model block in Aspen Plus®. All physical properties of the process fluid are averaged using the value at the reactor in- and outlet. The tube wall thickness of the reactor tubes is assumed to 2 mm, the thermal conductivity of the tubes λ_T is taken as $16 \text{ W}/(\text{m}\cdot\text{K})$ and for the heat transmission coefficient of the molten salt α_{MS} a value of $1000 \text{ W}/(\text{m}^2\cdot\text{K})$ is used [38].

A.5.5 Vapor-liquid separators

Vapor-liquid separators can be designed as either horizontal or vertical pressure vessels depending on the volume of liquid compared to the volume of vapor. Vertical separators are used to separate liquid from vapor when the volume of liquid is small compared to the vapor volume like for compressor knockout drums. Horizontal separators are preferred for larger liquid volumes. [93]

The design of both is based on the maximum vapor velocity, as well as the liquid surge volume. For separation, the entrained liquid droplets need to disengage from the vapor flow. To avoid a carryover of these droplets the vapor velocity should not exceed the maximum vapor velocity $v_{V,max}$ determined by Eq. A5-12, with k as the design vapor velocity factor and ρ_L and ρ_V as the liquid and vapor density, respectively [93].

$$v_{V,max} = k \cdot \sqrt{\frac{\rho_L - \rho_V}{\rho_V}} \quad \text{Eq. A5-12}$$

The design vapor velocity factor for a vertical vapor liquid separator $k_{vert.}$ is calculated according to [95], using an empirical correlation based on the vapor-liquid separation factor $S.Fac$ calculated according to Eq. A5-13 [95,96]:

$$S.Fac = \frac{\dot{m}_L}{\dot{m}_V} \cdot \sqrt{\frac{\rho_V}{\rho_L}} \quad \text{Eq. A5-13}$$

Subsequently, $k_{vert.}$ is calculated by Eq. A5-14 and Eq. A5-15 [95].

$$k_{vert.} = \exp(A + BX + CX^2 + DX^3 + EX^4 + FX^5) \quad \text{Eq. A5-14}$$

where: $A = -1.942936$
 $B = -0.814894$
 $C = -0.179390$
 $D = -0.0123790$
 $E = 0.000386235$
 $F = 0.000259550$

$$X = \ln(S.Fac) \quad \text{Eq. A5-15}$$

It needs to be noted that the empirical correlation results in $k_{vert.}$ with the unit [ft/s] which needs to be converted to [m/s].

$k_{horiz.}$ is generally set to $1.25 \cdot k_{vert.}$ [38,96]. The separator is usually operated between 0.5 to 0.85 of the maximum velocity [38], whereas $v_V = 0.675 \cdot v_{V,max}$ is used. The required vapor flow is used to determine the cross-sectional area of the vapor flow. For horizontal separators the vapor flow \dot{V}_V makes up 20 % of the cross-sectional area and the liquid surge volume is 80 % [38]. The resulting vessel diameter can be calculated using Eq. A5-16.

$$D_{horiz.} = \sqrt{\frac{4 \cdot \dot{V}_V}{0.2 \cdot \pi \cdot v_V}} \quad \text{Eq. A5-16}$$

If the L/D-ratio of the first calculation is not in the range of $3 \leq \frac{L}{D} \leq 5$, the length is increased and the diameter is kept constant to ensure $v_V = 0.675 \cdot v_{V,max}$. The resulting diameters and lengths are rounded up to the first digit

A.5.6 Decanter

The decanter design is performed as described in Couper et al. by using a horizontal, cylindrical vessel that is operated full [97]. To identify the dispersed phase the dispersion factor c is used as shown in Eq. A5-17.

$$c = \frac{\dot{V}_l}{\dot{V}_h} \cdot \left(\frac{\rho_l \cdot \mu_h}{\rho_h \cdot \mu_l} \right)^{0.3} \quad \text{Eq. A5-17}$$

The indices l and h refer to the light and the heavy phase, respectively. The holdup of the two liquid phases in the vessel is in the proportions as in the feed. Figure A.5-1 shows the geometry of the cross section. The ratio of the cross sectional areas A_1 to A_2 is equal to the ratio of the volumetric flow rates of the two liquid phases.

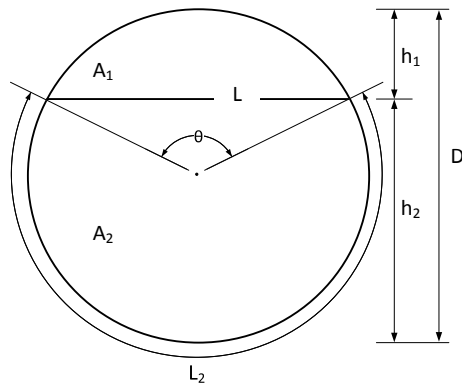


Figure A.5-1: Schematic geometry of the cross section (adjusted from [97])

To assure a proper separation of the two liquid phases the Reynolds number Re based on the hydraulic diameter D_{hyd} is used as indicator. The hydraulic diameter of the heavy liquid phase can be calculated based on the cross sectional geometry shown in Figure A.5-1 by Eq. A5-18 to Eq. A5-20.

$$D_{hyd} = \frac{4 \cdot A_2}{L + L_2} \quad \text{Eq. A5-18}$$

with:

$$L = D \cdot \sin\left(\frac{\theta}{2}\right) \quad \text{Eq. A5-19}$$

$$L_2 = D \cdot \left(\pi - \frac{\theta}{2}\right) \quad \text{Eq. A5-20}$$

Subsequently, the Reynolds number of the heavy and continuous phase is calculated by Eq. A5-21:

$$Re = D_{hyd} \cdot \left(\frac{\dot{V}_h \cdot 4}{\pi \cdot D^2}\right) \cdot \frac{\rho_h}{\mu_h} \quad \text{Eq. A5-21}$$

where ρ_h and μ_h are the specific density and the dynamic viscosity of the heavy phase.

Hooper and Jacobs indicate that an Re number of 5 000 or less would lead to little separation problems only, while $5\,000 < Re < 20\,000$ would cause some hindrance [97]. Within this work, a maximum Reynolds number of 10 000 is used.

As shown by Eq. A5-22, the settling or rising velocity of the dispersed droplets is determined by Stokes' law,

$$v = \frac{g \cdot (\rho_h - \rho_l) \cdot d^2}{18 \cdot \mu} \quad \text{Eq. A5-22}$$

where ρ_l are the specific gravities, μ is the dynamic viscosity of the continuous phase and d is the droplet diameter. A conservative droplet diameter of $150\ \mu\text{m}$ is assumed. The necessary flow distance of the decanter L_f is calculated using the settling or rising time of the dispersed droplets t and the forward velocity of the continuous phase v_f as shown in Eq. A5-23:

$$L_f = v_f \cdot t \quad \text{Eq. A5-23}$$

In addition to the calculated flow length L_f , 24 in (60.96 cm) are added for inlet and outlet nozzles and baffles to get the total length of the decanter L_{tot} .

A.5.7 Fermenter

To determine the required number of batch fermenters to reach the target production rate of succinic acid, the overall batch sequence needs to be considered. First, the filling time t_{fill} is determined by the volume of the fermenter V_{ferm} , its liquid content q_{fill} and the volume flow rate entering the fermenter \dot{V}_{ferm} from the Aspen Plus® flowsheet simulation as shown by Eq. A5-24:

$$t_{fill} = \frac{V_{ferm} \cdot q_{fill}}{\dot{V}_{ferm}} \quad \text{Eq. A5-24}$$

The draining time t_{drain} is assumed to be equal to the filling time t_{fill} . All times calculated are rounded up to 15 min. The time for succinic acid production t_{prod} is computed by the kinetic model. At the end of a batch sequence a Cleaning-in-Place (CIP) is carried out with an overall duration t_{CIP} of 105 min [162]. Summing up t_{fill} , t_{prod} , t_{drain} and t_{CIP} yields the time of a batch-cycle $t_{batchcycle}$. The number of batch-cycles $n_{batchcycle}$ and the number of fermenters n_{ferm} can be calculated according to Eq. A5-25 and Eq. A5-26:

$$n_{batchcycle} = \frac{t_{operating}}{t_{batchcycle}} \quad \text{Eq. A5-25}$$

$$n_{ferm} = \frac{\dot{m}_{DCW,initial} \cdot 3600 \cdot t_{operating}}{c_{DCW,initial} \cdot V_{ferm} \cdot q_{fill} \cdot n_{batchcycle}} \quad \text{Eq. A5-26}$$

The annual time of operation $t_{operating}$ is set to 8000 h. In order to determine the required number of fermenters, it is assumed that the initial dry cell weight concentration $c_{DCW,initial}$ is equal in each vessel. Since the number of fermenters needs to be an integer, it is rounded up and the liquid content in each fermenter is adjusted. In case of using equipment modules for the fermenter, the volume and number of the fermenter modules is given and the liquid level q_{fill} is determined iteratively.

A.5.8 Fluidized bed dryer

To design and model the fluidized bed dryer in Aspen Plus® the drying behavior needs to be estimated. The three phases of convective drying are characterized by a warming up period, followed by a constant rate drying period until the critical moisture content X_c and the falling drying rate period with a declining drying rate till the equilibrium moisture content X_e is reached [134]. As critical solid moisture content X_c a value of 0.00074 kg/kg is taken from experimental studies using salicylic acid [163]. Since succinic acid and salicylic acid are both carboxylic acids, it is assumed that both components have similar drying properties.

Furthermore, a drying curve shape factor of 0.75 is assumed because succinic acid is a non-hygroscopic component [134]. Further input parameters are summarized in Table A.5-4.

Table A.5-4: Input parameters for Dryer model in Aspen Plus®

Parameter	Unit	Value	Source
Solids residence time	[s]	1100	[38]
Heat transfer coefficient	[kW/m ² /K]	0.06	[38]
Critical solids moisture content X_c	[kg/kg]	0.00074	[163]
Equilibrium solid moisture content X_e	[kg/kg]	0	[164]
Drying curve shape factor	[-]	0.75	

The main design parameters of a fluidized bed dryer are dryer area and height, whereby the area can be calculated according to Eq. A5-27 [165]:

$$A_{FBD} = \frac{\dot{m}_g}{\rho_g \cdot v_g} \quad \text{Eq. A5-27}$$

with \dot{m}_g as mass flow rate, ρ_g as density and v_g as optimum velocity of the drying gas. The optimum gas velocity depends on the mean particle diameter d_p and the gravitational acceleration g as shown by Eq. A5-28 [165].

$$v_g \approx 7.5 \cdot \sqrt{d_p \cdot g} \quad \text{Eq. A5-28}$$

Using a minimum fluidization void fraction ε_{min} of 0.55 [166] the bed height at minimum fluidization $Z_{FBD,min}$ can be determined using Eq. A5-29 [165]:

$$\varepsilon_{min} = 1 - \frac{m_s}{\rho_s \cdot A_{FBD} \cdot Z_{FBD,min}} \quad \text{Eq. A5-29}$$

m_s represents the mass and ρ_s the density of the solids. Subsequently, the actual bed height Z_{FBD} is determined according to Eq. A5-30 [165]:

$$Z_{FBD} = Z_{FBD,min} \cdot \frac{1 - \varepsilon_{min}}{1 - \varepsilon} \quad \text{Eq. A5-30}$$

The real void fraction ε can be estimated based on Eq. A5-31 to Eq. A5-33 [165] with Re_g as Reynolds number of the gas stream, Ar as Archimedes number, and ν_g as kinematic viscosity of the gas.

$$\varepsilon \approx \left(\frac{18 \cdot Re_g + 0.36 \cdot Re_g^2}{Ar} \right)^{0.21} \quad \text{Eq. A5-31}$$

$$Re_g = \frac{w_g \cdot d_p}{\nu_g} \quad \text{Eq. A5-32}$$

$$Ar = \frac{g \cdot d_p^3}{\nu_g^2} \cdot \frac{\rho_s - \rho_g}{\rho_g} \quad \text{Eq. A5-33}$$

To finally obtain the height of the dryer Z_{Dryer} 1 m for disengagement is added to the actual bed height Z_{FBD} [38].

A.5.9 Crystallizer

To design and model the crystallization cascade, the number of crystallizers n_{cryst} , their volume V_{cryst} and the temperature steps need to be determined. The number of vessels is usually between three and five [167], whereas four vessels are used in this work. To determine the volume of a crystallizer, the residence time needs to be estimated. Assuming the initial size of crystals equal to a seed crystal size of 200 μm [168], a final crystal size of around 400 μm and a crystal growth rate G of 10^{-8} m/s [169], the residence time τ can be estimated to 5.56 h. Rounding this residence time up to 6 h and assuming an equal residence time in each vessel, the residence time in each crystallizer τ_{cryst} is 1.5 h. A multiplication with the volume flow rate to the crystallizer results in the vessel volume V_{cryst} . Next, the temperature profile of the crystallizer cascade is determined based on the entering succinic acid concentration of 485 g/L after the last evaporator HX5. Using the solubility curve of succinic acid of Li et al. [119], the temperature steps in the four-staged MSMPR crystallizer cascade are set to 64.4 °C, 56.5 °C, 44.4 °C and 20.0 °C to achieve an equal yield of 105.7 g/L in each crystallization vessel. This results in an overall yield of 423 g/L. It must be noted that the metastable zone width is not known and experiments are necessary to clarify whether primary nucleation occurs or can be neglected. Since space for the stirrer and installations in the crystallization vessels needs to be considered, the actual size of a crystallization vessel is enlarged, such that a filling level of 85 % provides the required volume of V_{cryst} . The heat that needs to be removed in a crystallization vessel is obtained from the Aspen Plus® model. The corresponding required heat exchanger area $A_{cryst,req}$ is calculated according to Eq. A5-34, with U as heat transfer coefficient and ΔT_{ln} as logarithmic temperature difference between the cooling medium and the process stream.

$$A_{cryst,req} = \frac{\dot{Q}}{U \cdot \Delta T_{ln}} \quad \text{Eq. A5-34}$$

It is assumed that each MSMPR crystallizer is ideally mixed and the temperature inside the crystallizer T_{cryst} is constant. An overall heat transfer coefficient of 625 W/m²/K is used [126] and an L/D-ratio of one is assumed, except for the fourth crystallizer where an L/D-ratio of two is necessary to offer the required heat transfer area. A maximum filling level of 90 % determines the height of the cooling jacket to remove the heat at the maximum filling level.

A.5.10 Rotary drum vacuum filter

The design mode of the *Drum Filter* model in Aspen Plus® is used to determine the filter diameter and length, as well as the cake thickness, using the input parameters summarized in Table A.5-5.

Table A.5-5: Input parameters for RDVF models in Aspen Plus®

Parameter	Unit	Value	Source
max. allowable Δp_{RDVF1}	[bar]	0.3	[115]
max. allowable Δp_{RDVF2}	[bar]	0.31	[115]
Drum speed	[rpm]	0.4	[170]
Width to diameter ratio	[-]	2	[170]
Filter medium resistance	[1/m]	0	(assumed)
Specific cake resistance	[m/kg]	8e+08	[38]
Compressibility	[-]	0	
Porosity ϵ	[-]	0.55	[171]
Mass fraction of solids in filter cake of RDVF1	[kg/kg]	0.8	[115]
Mass fraction of solids in filter cake of RDVF2	[kg/kg]	0.85	[115]
Average solids sphericity	[-]	0.75	
Average solids diameter RDVF1	[mm]	0.00063	[172]
Average solids diameter RDVF2 (worst case estimation)	[mm]	0.15	[168,173]

In simulation mode, when equipment modules are used, the same input parameters except the pressure drop are required. Additionally, the filter diameter and length as well as a filtration angle of 120 ° are used [174]. Since non-operable filter equipment modules in simulation mode would lead to errors of the overall flowsheet, the filter equipment modules are modeled in design mode within the flowsheet and transfer blocks are used to activate the model blocks in simulation mode.

A6 Calculating upper and lower operating constraints of process units

A.6.1 Fixed-bed catalytic reactors

The operating constraints of the fixed-bed catalytic reactors are set by a minimum and maximum pressure drop of 3 and 15 % of the reactor inlet pressure [90], respectively. Eq. A6-1 to Eq. A6-3 show the pressure drop calculation equations used which consider wall effects according to [89]:

$$\frac{\Delta p}{\rho_o v_o^2} \frac{d_p}{L} = \frac{K_1}{Re_p} \cdot A_w^2 \cdot \frac{(1-\varepsilon)^2}{\varepsilon^3} + \frac{A_w}{B_w} \cdot \frac{1-\varepsilon}{\varepsilon^3} \quad \text{Eq. A6-1}$$

$$A_w = 1 + \frac{2}{3 \cdot \left(\frac{D}{d_p}\right) \cdot (1-\varepsilon)} \quad \text{Eq. A6-2}$$

$$B_w = \left[k_1 \cdot \left(\frac{d}{d_p}\right)^2 + k_2 \right] \quad \text{Eq. A6-3}$$

In Eq. A6-1 Δp is the pressure drop over the catalyst bed, d_p the diameter of the catalyst pellet which is 4.7 mm for the styrene production [83,86,91], ε the voidage of the catalyst bed and L and d the length and diameter of the packed bed. The mean fluid mass density is represented by ρ_o and the mean fluid velocity by v_o . Re_p is the particle related Reynolds number, with the particle diameter d_p as characteristic length. A_w and B_w are wall correlation terms addressing the wall effects, whereby K_1 , k_1 and k_2 are empirical factors. For spherical pellets [89] determined K_1 to 154, k_1 to 1.15 and k_2 to 0.87. For the acetone production process, conversion and selectivity are considered as operating constraints, too.

A.6.2 Sieve tray columns

The upper operating constraint of a sieve tray column is determined by flooding which occurs at high vapor rates. If flooding occurs, liquid droplets are entrained to the next stage and the separation efficiency decreases. To avoid flooding, sieve tray columns should be operated below the flooding factor calculated according to Eq. A6-4 [175]:

$$F_{max} = K_1 \cdot \sqrt{\rho_L - \rho_V} \quad \text{Eq. A6-4}$$

Constant K_1 depends on the tray spacing and the ratio of vapor and liquid flow rate. The lower capacity constraint of a sieve tray column is determined by a non-uniform distribution of the vapor flow through the tray or weeping of the liquid, which also decrease the separation efficiency. A non-uniform distribution in sieve tray columns occurs for a flooding factor below $F_{min,distribution}$ calculated according to Eq. A6-5 [176]:

$$F_{min,distribution} = \Phi \cdot \sqrt{2 \cdot \frac{\sigma}{d_h}} \quad \text{Eq. A6-5}$$

with σ as liquid surface tension and Φ as ratio of sieve hole area to tray active area. Weeping occurs at low gas flow rates when liquid can leak through the sieve holes. This happens for F-factors lower than $F_{min,weeping}$ according to Eq. A6-6 [176,177]:

$$F_{min,weeping} = \Phi \cdot \sqrt{0.37 \cdot d_h \cdot g \cdot \frac{(\rho_L - \rho_V)^{1.25}}{\rho_V^{0.25}}} \quad \text{Eq. A6-6}$$

All operating constraints need to be checked for each tray. Aspen Plus® provides the reduced F-factors F_{red} for each tray which have to be multiplied with the cross-sectional area to get the F-factor. Finally, the most restrictive trays regarding the upper and lower operating constraint determine the operating window of a sieve tray distillation column.

A.6.3 Packed columns

As for a sieve tray column, the upper operating constraint of a packed column is flooding. The lower operating constraint is determined by dewetting, which occurs at low liquid loads. To avoid both effects Coker recommends an operation between 50 and 95 % of the flooding factor [93]. However, the lower constraint is not a strict boundary and is set to 40 % for this work. Aspen Plus® provides the fractional capacity for each stage of a packed column which can be used to determine the lower and upper operating constraints. Both operating constraints are checked for each stage and the most restrictive stages determine the operating window of the packed distillation column.

A.6.4 Heat Exchangers

This work is limited to shell and tube heat exchangers as they are the most commonly used heat exchangers due to their versatility [125]. The operating constraints have to be calculated for the shell and tube side, respectively. They are determined by the maximum allowable pressure drop and vibrations as an upper operating constraint for the fluid velocity, and fouling as the lower operating constraint for the fluid velocity. The maximum pressure drops given in Table A.6-1 are economic design recommendations given by [92]. For gases between 2 and 10 bar the allowed pressure drop is linearly interpolated using at least two rows of Table A.6-1.

Table A.6-1: Allowable pressure drops in shell and tube heat exchangers [92]

Fluid	Allowable pressure drop	Condition
Liquid	30 kPa	Viscosity \leq 1 mPas
	50 to 70 kPa	Viscosity 1 to 10 mPas
Gas/Vapor	0.4 to 0.8 kPa	High vacuum operating pressure
	0.1 x absolute pressure	Medium vacuum operating pressure
	0.5 x system gauge pressure	Operating pressure of 1 to 2 bar
	0.1 x system gauge pressure	Operating pressure > 10 bar

The upper velocity constraint related to vibrations is calculated by Aspen EDR. Therefore, Aspen EDR performs a TEMA vibration analysis to determine vibrations on the shell side. This analysis is based on the calculation of natural frequencies which result in critical velocities as an upper operating constraint. These critical velocities are calculated at four points inside the shell: shell inlet, baffle window, between the baffles and shell outlet.

To prevent shell side fouling, Nesta recommends a minimum shell side velocity $v_{shell,min,water}$ of 0.6 m/s for water and other liquids [178]. For vapor, such value was not found in literature. However, fouling is prevented by shear forces τ_{shear} acting on the wall [178]. A dimensionless number to describe the characteristic of shear stress is the *Fanning friction factor* $f = 2 \cdot \tau_{shear} / (\rho v^2)$. It relates the shear force to the dynamic pressure [179]. Assuming shear stress conditions similar to water, the minimum shell side velocity of vapor can be calculated according to Eq. A6-7.

$$v_{shell,min,v} = v_{shell,min,water} \cdot \sqrt{\frac{\rho_{water}}{\rho_v}} \quad \text{Eq. A6-7}$$

To prevent tube side vibrations and fouling, the tube side fluid velocity has to stay within the velocity ranges for given fluid conditions as shown in Table A.6-2 [92].

Table A.6-2: Tube side velocity operating constraints [92,180]

Fluid	Condition	Velocity range [m/s]
Liquid	Organic	1 – 2
	Water	0.9 – 2.5
Gas/Vapor	Vacuum	50 – 70
	Atmospheric pressure	10 – 30
	High pressure	5 – 10

In this work it is assumed that high pressure refers to pressures higher than 5 bar.

A.6.5 Vapor-liquid separators

For vapor-liquid separators no lower operating constraints are considered. Upper operating constraints are a minimum residence time τ_{min} of 300 s and a maximum vapor velocity $v_{V,max}$ [96], determined by Eq. A6-8:

$$v_{V,max} = k \cdot \sqrt{\frac{\rho_L - \rho_V}{\rho_V}} \quad \text{Eq. A6-8}$$

with k as the design vapor velocity factor and ρ_L and ρ_V as the liquid and vapor density, respectively.

A.6.6 Decanter

A lower operating constraint for a decanter is not considered. As upper operating constraint a maximum Reynolds number Re_{max} of the heavy and continuous phase of 10 000 is used [97]. The Reynolds number is thereby calculated according to Eq. A6-9:

$$Re = D_{hyd} \cdot \left(\frac{\dot{V}_h \cdot 4}{\pi \cdot D^2} \right) \cdot \frac{\rho_h}{\mu_h} \quad \text{Eq. A6-9}$$

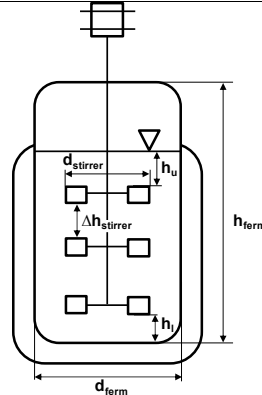
where ρ_h and μ_h are the specific density and viscosity of the heavy phase.

A.6.7 Fermenter

An upper and lower filling level are used as operating constraints of the fermenters. To guarantee a sufficient head space required for liquid drop settling and foam deposition a maximum filling level of 80 % should not be exceeded [181]. Regarding the lower operating constraint, it is assumed that an adequate liquid level above the stirrer is necessary. Therefore, the height of a stirrer is estimated based on a 3-stage turbine stirrer with the design ratios as shown in Table A.6-3 since this is the most commonly used stirrer for fermentation processes [182].

Table A.6-3: Values of design ratios to estimate the lower liquid level in a fermenter

Parameter	Value	Source
h_{ferm}/d_{ferm}	2.5	[183]
$d_{stirrer}/d_{ferm}$	0.3	[182]
$\Delta h_{stirrer}/d_{stirrer}$	1.5	[182]
$h_l/d_{stirrer}$	0.33	[184]
$h_u/d_{stirrer}$	1	



h_{ferm} and d_{ferm} are the height and diameter of the fermenter, $d_{stirrer}$ is the diameter of the stirrer, $\Delta h_{stirrer}$ is the distance between the stirrer blades and h_l and h_u are the distance below and above the stirrer. On this basis, the minimum filling level is determined to 52 %.

A.6.8 Rotary drum vacuum filters

The pressure drop serves as lower and upper operating constraints in case of the rotary drum vacuum filters, which should be above 0.2 bar [170] and below 0.8 bar [38].

A.6.9 Crystallizer

On the one hand, as lower and upper operating constraints of a crystallizer the filling level is oriented at a chemical reaction vessel, which should be between 60 % and 90 % [124]. On the other hand, the actual heat exchange area must be at least as large as the required heat exchange area and thus serves as additional upper operating constraint.

A.6.10 Fluidized bed dryer

To enable a fluidized bed, the voids fraction needs to be between ε_{min} and 1, whereby the lower boundary ensures fluidization and the upper boundary avoids elutriation and pneumatic transport of solids [165]. The minimum fluidization velocity is confirmed by comparing $v_{g,min}$ calculated according to Eq. A6-10 [165] with the optimum fluidization velocity v_g .

$$v_{g,min} = 7.19 \cdot (1 - \varepsilon) \cdot v_g \cdot a_p \cdot \left[\sqrt{1 + 0.067 \cdot \frac{\varepsilon_{min}^3 \cdot (\rho_s - \rho_g) \cdot g}{(1 - \varepsilon_{min})^2 \cdot \rho_g \cdot v_g^2 \cdot a_p^3}} - 1 \right] \quad \text{Eq. A6-10}$$

The volume specific surface of the particles is calculated assuming cylindrical crystals with a diameter of 150 μm and a length of 400 μm [173]. Furthermore, a maximum solids hold-up of 500 kg per m^3 dryer volume is considered as upper operating constraint [38].

A7 Design of equipment modules for flexibility

A.7.1 Characterization of the liquid/liquid methanol cooler example

Table A.7-1: Process parameters and physical property data of the liquid/liquid methanol cooler without phase change [122]

Parameter	Unit	Process stream Shell side (Methanol)	Utility stream Tube Side (Brackish water)
T_{in}	[°C]	95	25
T_{out}	[°C]	40	40
p	[bar]	5	3
c_p	[kJ/kg/K]	2.84	4.2
ρ	[kg/m ³]	750	995
μ	[mNs/m ²]	0.34	0.8
k_f	[W/m/K]	0.19	0.59
R_f	[m ² °C/W]	0.0002	0.0002

A.7.2 Heat exchanger design equations

If the utility stream (e.g. \dot{m}_{cold}) is not defined, it is calculated by a heat balance as shown by Eq. A7-1.

$$\dot{m}_{cold} = \frac{\dot{Q}}{(T_{cold,out} - T_{cold,in}) \cdot c_{p,cold}} \quad \text{Eq. A7-1}$$

To estimate the required heat transfer area, the true mean temperature difference ΔT_m calculated by Eq. A7-2 is required. ΔT_m consists of the mean logarithmic temperature difference ΔT_{lm} computed by Eq. A7-3 and the temperature correction factor F_t which considers the influence of a multi-pass arrangement on the temperature driving-force. F_t is calculated using the dimensionless temperature ratios R and S , according to Eq. A7-4 and Eq. A7-5. For one shell and two or a multiple of two tube passes, F_t is computed using Eq. A7-6. For two shell passes and four or more tube passes, Eq. A7-7 is applied [122,185].

$$\Delta T_m = F_t \cdot \Delta T_{lm} \quad \text{Eq. A7-2}$$

$$\Delta T_{lm} = \frac{(T_{hot,in} - T_{cold,out}) - (T_{hot,out} - T_{cold,in})}{\ln \frac{T_{hot,in} - T_{cold,out}}{T_{hot,out} - T_{cold,in}}} \quad \text{Eq. A7-3}$$

$$R = \frac{T_{hot,in} - T_{hot,out}}{T_{cold,out} - T_{cold,in1}} \quad \text{Eq. A7-4}$$

$$S = \frac{T_{cold,out} - T_{cold,in1}}{T_{hot,in} - T_{hot,out}} \quad \text{Eq. A7-5}$$

$$F_t = \frac{\sqrt{R^2 + 1} \cdot \ln \frac{(1-S)}{(1-RS)}}{(R-1) \cdot \ln \frac{2 - S(R+1 - \sqrt{R^2 + 1})}{2 - S(R+1 + \sqrt{R^2 + 1})}} \quad \text{Eq. A7-6}$$

$$F_t = \frac{\frac{\sqrt{R^2 + 1}}{2(R-1)} \cdot \ln \frac{(1-S)}{(1-RS)}}{\ln \frac{\left(\frac{2}{S}\right) - 1 - R + \left(\frac{2}{S}\right) \cdot \sqrt{(1-S)(1-RS)} + \sqrt{R^2 + 1}}{\left(\frac{2}{S}\right) - 1 - R + \left(\frac{2}{S}\right) \cdot \sqrt{(1-S)(1-RS)} - \sqrt{R^2 + 1}}} \quad \text{Eq. A7-7}$$

Next, the required heat transfer area A_{req} can be estimated by Eq. A7-8, using an assumed heat transfer coefficient $U_{O,ass}$, i.e. estimated from [122].

$$A_{req} = \frac{\dot{Q}}{U_{O,ass} \cdot \Delta T_m} \quad \text{Eq. A7-8}$$

Afterwards, the basic dimensioning is performed by calculating the number of tubes N_T and the inner shell diameter d_s which depends on the tube OD d_o and the tube pitch ratio PR as well as the tube layout constant CL and the tube count calculation constant CTP [186]. These constants account for the incomplete coverage of the shell by the tubes due to clearances induced by the multi-pass arrangements. CL assumes a value of 1 for quadratic tube patterns and 0.87 for triangular arrangements according to the compactness of a triangular pattern [125].

CTP depends on the number of tube passes and can be estimated by Eq. A7-11 which is extrapolated to eight tube passes by the CTPs for one, two and three tube passes [186].

To calculate the inner tube diameter d_i with Eq. A7-12, a tube thickness δ_t has to be chosen [126]. The effective length of the tubes L_{eff} is calculated subtracting the tubesheet thickness δ_{ts} two times from the tube length L as shown in Eq. A7-13.

$$N_T = 0.785 \cdot \frac{CTP}{CL} \cdot \frac{d_s^2}{PR^2 \cdot d_o^2} \quad \text{Eq. A7-9}$$

$$d_s = 0.637 \cdot \sqrt{\frac{CL}{CTP}} \cdot \sqrt{\frac{A \cdot PR^2 \cdot d_o}{L_{eff}}} \quad \text{Eq. A7-10}$$

$$CTP = (-0.01 \cdot x^2) + 0.94 \quad \text{Eq. A7-11}$$

$$d_i = d_o - 2\delta_t \quad \text{Eq. A7-12}$$

$$L_{eff} = L - 2\delta_{ts} \quad \text{Eq. A7-13}$$

In order to calculate the heat transfer coefficient on the tube side, the corresponding flow characteristics have to be determined. Hence, the linear velocity v_t is calculated using Eq. A7-17 which depends on the cross flow area of one tube $A_{cross,t}$ and the flow area per tube pass $A_{flow,pass}$ as well as on the mass velocity G_t (see Eq. A7-14 to Eq. A7-16).

$$A_{cross,t} = \frac{\pi \cdot d_i^2}{4} \quad \text{Eq. A7-14}$$

$$A_{flow,pass} = A_{cross,t} \cdot N_{T,pass} \quad \text{Eq. A7-15}$$

$$G_t = \frac{\dot{m}_{cold}}{A_{flow,pass}} \quad \text{Eq. A7-16}$$

$$v_t = \frac{G_t}{\rho_t} \quad \text{Eq. A7-17}$$

With this, the flow characteristics can be described by the Reynolds number Re , the Prandtl number Pr and the mean Nusselt number Nu_m . These dimensionless indicators depend on the liquid properties density ρ , heat capacity c_p , viscosity μ , thermal conductivity k_f and the tube side friction coefficient ξ_t [126]. Next, the heat transfer coefficient for the tube side h_t can be calculated. It should be noted that the calculation of Nu_m is only valid for turbulent flow regimes [126]. The related calculations are represented by Eq. A7-18 to Eq. A7-22 [122].

$$Re_t = \frac{\rho_t \cdot v_t \cdot d_i}{\mu_t} \quad \text{Eq. A7-18}$$

$$Pr_t = \frac{c_{p,t} \cdot \mu_t}{k_{f,t}} \quad \text{Eq. A7-19}$$

$$\xi_t = (1.8 \log_{10} Re_t - 1.5)^{-2} \quad \text{Eq. A7-20}$$

$$Nu_{m,t} = \frac{\frac{\xi_{tube}}{8} \cdot Re_t \cdot Pr_t}{1 + 12.7 \sqrt{\frac{\xi_t}{8}} \cdot (Pr_t^{2/3} - 1)} \cdot \left[1 + \left(\frac{d_i}{L_{eff}} \right)^{2/3} \right] \quad \text{Eq. A7-21}$$

$$h_t = \frac{Nu_{m,t} \cdot k_{f,t}}{d_i} \quad \text{Eq. A7-22}$$

Similarly, the heat transfer coefficient for the shell side h_s is calculated using the shell cross flow area A_s depending on the baffle spacing l_b , the tube pitch p_t and the number of shell passes $N_{s,pass}$. For the shell side, the calculation of Re depends on the hydraulic diameter d_e . The representation of the mean Nusselt number depends on the shell side heat transfer factor $j_{h,s}$ which describes a correction factor according to the flow characteristics of the shell side. The calculations of $j_{h,s}$ are shown in Table A.7-2 and are functions of Reynolds number and baffle cut. The related equations were derived from a diagram in [122].

Table A.7-2: Calculations of the shell side heat transfer factor

Baffle cut [%]	Calculation of $j_{h,s}$
15	$j_{h,s} = 0.6018 \cdot Re^{-0.486}$
20	$j_{h,s} = 0.5530 \cdot Re^{-0.484}$
25	$j_{h,s} = 0.5193 \cdot Re^{-0.482}$
30	$j_{h,s} = 0.4959 \cdot Re^{-0.483}$
35	$j_{h,s} = 0.4725 \cdot Re^{-0.484}$
40	$j_{h,s} = 0.4589 \cdot Re^{-0.487}$
45	$j_{h,s} = 0.4440 \cdot Re^{-0.490}$

The calculations regarding to the shell side are listed in Eq. A7-23 to Eq. A7-32 [122].

$$l_b = f_b \cdot d_s \quad \text{Eq. A7-23}$$

$$p_t = PR \cdot d_o \quad \text{Eq. A7-24}$$

$$A_s = \frac{1}{N_{s,pass}} \cdot \left(\frac{(p_t - d_o) \cdot d_s \cdot l_b}{p_t} \right) \quad \text{Eq. A7-25}$$

$$G_s = \frac{\dot{m}_{hot}}{A_s} \quad \text{Eq. A7-26}$$

$$v_s = \frac{G_s}{\rho_s} \quad \text{Eq. A7-27}$$

$$d_e = \frac{1.10}{d_o} \cdot (p_t^2 - 0.917 \cdot d_o^2) \quad (\text{for triangular arrangements}) \quad \text{Eq. A7-28}$$

$$d_e = \frac{1.27}{d_o} \cdot (p_t^2 - 0.785 \cdot d_o^2) \quad (\text{for quadratic arrangements}) \quad \text{Eq. A7-29}$$

$$Re_s = \frac{\rho_s \cdot v_s \cdot d_e}{\mu_s} \quad \text{Eq. A7-30}$$

$$Nu_{m,s} = j_{h,s} \cdot Re_s \cdot Pr_s^{1/3} \quad \text{Eq. A7-31}$$

$$h_s = \frac{Nu_{m,s} \cdot k_s}{d_e} \quad \text{Eq. A7-32}$$

Afterwards, the computation of the overall heat transfer coefficient $U_{o,calc}$ is performed using Eq. A7-33. The overall heat transfer coefficient depends on the fouling factors of the liquids R_f and the thermal conductivity k_w of the heat exchanger material. The fouling factors are estimated from [187]. [122]

$$U_{o,calc} = \left(\frac{1}{h_s} + R_{f,o} + \frac{d_o \cdot \ln\left(\frac{d_o}{d_i}\right)}{2 \cdot k_w} + \frac{R_{f,i} \cdot d_o}{d_i} + \frac{d_o}{h_t \cdot d_i} \right)^{-1} \quad \text{Eq. A7-33}$$

Finally, the pressure drops for both sides Δp_t and Δp_s are calculated using Eq. A7-34 and Eq. A7-35.

$$\Delta p_t = N_{T,pass} \cdot \left[8 \cdot j_{f,t} \cdot \frac{L_{eff}}{d_i} + 2.5 \right] \cdot \frac{\rho_t \cdot v_t^2}{2} \quad \text{Eq. A7-34}$$

$$\Delta p_s = \left[8 \cdot j_{f,s} \cdot \frac{D_s}{d_e} \cdot \frac{L_{eff}}{l_b} \right] \cdot \frac{\rho_s \cdot v_s^2}{2} \quad \text{Eq. A7-35}$$

Similar to the shell side heat transfer factor, friction factors j_f are used to consider the prevailing flow conditions. Therefore, the tube side friction factor depends on Re and the shell side factor is a function of the baffle cut and Re . These factors are calculated as described in Table A.7-3 and Table A.7-4.

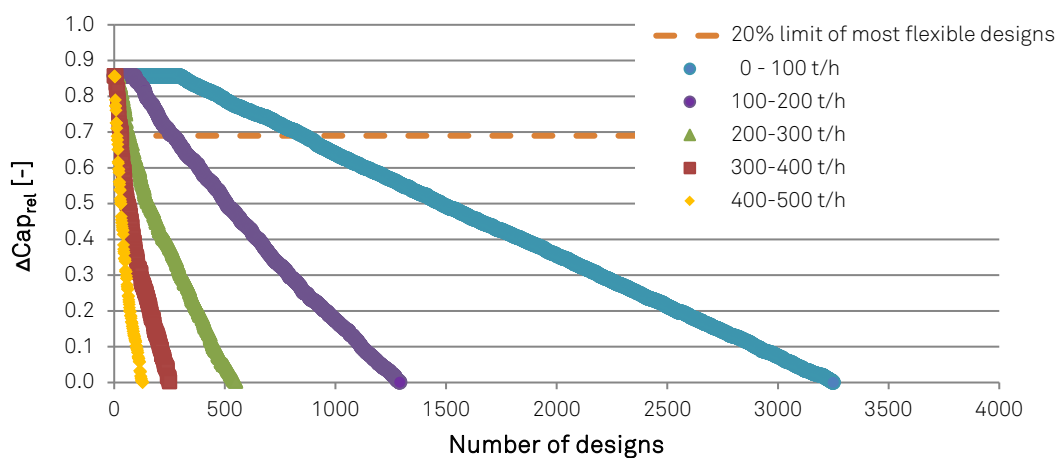
Table A.7-3: Calculations of the tube side friction factor derived from [122]

Reynolds number	Calculation of $j_{f,t}$
< 1000	$j_{f,t} = 8.0800 \cdot Re^{-1.003}$
> 1000	$j_{f,t} = 0.0449 \cdot Re^{-0.240}$

Table A.7-4: Calculations of the shell side friction factor derived from [122]

Baffle cut [%]	Calculation of $j_{f,s}$ for $Re \leq 300$	Calculation of $j_{f,s}$ for $Re > 300$
15	$j_{f,s} = 31.069 \cdot Re^{-0.948}$	$j_{f,s} = 0.3781 \cdot Re^{-0.181}$
20	$j_{f,s} = 24.070 \cdot Re^{-0.932}$	$j_{f,s} = 0.3047 \cdot Re^{-0.175}$
25	$j_{f,s} = 19.129 \cdot Re^{-0.926}$	$j_{f,s} = 0.2310 \cdot Re^{-0.164}$
30	$j_{f,s} = 17.131 \cdot Re^{-0.918}$	$j_{f,s} = 0.2258 \cdot Re^{-0.170}$
35	$j_{f,s} = 15.245 \cdot Re^{-0.907}$	$j_{f,s} = 0.2304 \cdot Re^{-0.181}$
40	$j_{f,s} = 15.371 \cdot Re^{-0.930}$	$j_{f,s} = 0.2032 \cdot Re^{-0.178}$
45	$j_{f,s} = 15.176 \cdot Re^{-0.950}$	$j_{f,s} = 0.1706 \cdot Re^{-0.171}$

A.7.3 Basis for the design analysis and the deduction of design rules of thumb

Figure A.7-1: Representation of most flexible designs in Cap_{min} -intervals in terms of ΔCap_{rel} Table A.7-5: Summary of number of designs in each Cap_{min} -interval considered for the deduction of design rules of thumb

Cap_{min} -range	No. designs in each Cap_{min} -range	1 st step of design approach		2 nd step of design approach	
		No. designs considered for frequency distributions	No. designs considered for $d_s/N_{T,pass}$	No. designs considered for frequency distributions	No. designs considered for B
0 – 100	3250	871	277	87	40
100 – 200	1291	273	120	55	27
200 – 300	549	70	45	18	14
300 – 400	251	33	13	13	5
400 – 500	129	13	8	14	8

A.7.4 Mass determination of a heat exchanger design

The tube bundle consists mainly of the tubes, the baffles and the tie rods which are stabilizing this arrangement. The mass of the tubes m_t is calculated using Eq. A7-36 which depends on the number of tubes, the tube OD, the effective length and the density of the material used [188]. Related to this calculation, the mass of the baffles m_b is calculated

based on the number of baffles, the shell inside diameter and the baffle thickness δ_b according to Eq. A7-37. The mass losses due to the holes for the tubes and the cut part according to the baffle cut are subtracted afterwards. For multi-pass heat exchangers, the mass of the longitudinal baffles m_{lb} is estimated with respect to Eq. A7-38 under the assumption that the thickness is similar to the baffles [189]. The mass of the tie rods m_{trod} is calculated using Eq. A7-39, under the assumption that the volume of the tie rods is represented by n_{tr} cylinders of diameter d_{tr} and length L . The individual masses related to the tube bundle are summed up to m_{tb} by Eq. A7-40.

$$m_t = N_T \cdot \rho \cdot \frac{\pi}{4} \cdot (d_o^2 - (d_o - 2\delta_t)^2) \cdot L_{eff} \quad \text{Eq. A7-36}$$

$$m_b = (N_b \cdot \rho \cdot \frac{\pi}{4} \cdot d_s^2 \cdot \delta_b - N_T \cdot \rho \cdot \frac{\pi}{4} \cdot d_o^2 \cdot \delta_b) \cdot (1 - b_c) \quad \text{Eq. A7-37}$$

$$m_{lb} = (N_{s,pass} - 1) \cdot L_{eff} \cdot d_s \cdot \delta_b \cdot \rho \quad \text{Eq. A7-38}$$

$$m_{trod} = n_{tr} \cdot \frac{\pi}{4} \cdot d_{tr}^2 \cdot L \cdot \rho \quad \text{Eq. A7-39}$$

$$m_{tb} = m_t + m_b + m_{trod} \quad \text{Eq. A7-40}$$

Afterwards, the mass of the shell m_s is calculated by Eq. A7-41, depending on the shell diameter, the thickness δ_s and the effective length.

$$m_s = \rho \cdot \frac{\pi}{4} \cdot ((d_s + 2\delta_s)^2 - d_s^2) \cdot L_{eff} \quad \text{Eq. A7-41}$$

The mass of the heads m_{heads} is calculated using Eq. A7-42, under the assumption that their shell is represented by a semi-sphere. To cover the required space for the tube side nozzles, a shell part is added to the equation with the length of the outer nozzle diameter $d_{o,nozz}$. Additionally, the mass of the tube sheets m_{ts} is calculated by Eq. A7-43 depending on the shell diameter and the tube sheet thickness δ_{ts} , whereby the holes of the tubes are subtracted.

$$m_{heads} = 2 \cdot \rho \cdot \frac{\pi}{6} \cdot ((d_s + 2\delta_s)^3 - d_s^3) + \rho \cdot \frac{\pi}{4} \cdot ((d_s + 2\delta_s)^2 - d_s^2) \cdot d_{o,nozz} \quad \text{Eq. A7-42}$$

$$m_{ts} = 2 \cdot \rho \cdot \frac{\pi}{4} \cdot d_s^2 \cdot \delta_{ts} - N_T \cdot \rho \cdot \frac{\pi}{4} \cdot d_o^2 \cdot \delta_{ts} \quad \text{Eq. A7-43}$$

Finally, the mass of the nozzles m_{nozz} is calculated by Eq. A7-44 depending on the number of nozzles n_{nozz} , their inner diameter $d_{i,nozz}$ and their length l_{nozz} . The nozzle length is estimated by Eq. A7-45 according to [190]. To avoid velocity changes inside the nozzles, the inner diameter is calculated based on the equation of continuity by Eq. A7-46, using the mass flow rates and velocities according to the mean capacity of the heat exchanger.

$$m_{Nozz} = n_{nozz} \cdot \rho \cdot \frac{\pi}{4} \cdot (d_{o,nozz}^2 - d_{i,nozz}^2) \cdot l_{nozz} \quad \text{Eq. A7-44}$$

$$l_{nozz} = 1.25 \cdot \sqrt{d_{o,nozz} \cdot (d_{o,nozz} - d_{i,nozz})} \quad \text{Eq. A7-45}$$

$$d_{i,nozz} = \sqrt{4 \cdot \frac{\left(\frac{\dot{m}_{t/s}}{\rho_{t/s}}\right)}{v_{t/s} \cdot \pi}} \quad \text{Eq. A7-46}$$

A.7.5 Design specifications in Aspen EDR

Table A. 7-6: Design specifications in Aspen EDR

Specifications	Value
Design code	EN13445
Service class	Normal
TEMA Class	B – chemical service
Material standard	DIN
Dimensional standard	DIN-German
Calculation method	Standard

Curriculum vitae

Personal Details

Name: Heiko Radatz (born Grabs)
Date of birth: April 10th, 1988
Place of birth: Forst (L.)
Nationality: German

Professional Experience

since 10/2018 Technology Expert Process Modeling
Covestro Deutschland AG, Leverkusen, Germany

10/2013 – 12/2017 Scientific assistant and PhD student
Laboratory of Plant and Process Design
Department of Biochemical and Chemical Engineering
TU Dortmund University, Dortmund, Germany

04/2012 – 08/2012 Internship, Conceptual Process Engineering
BASF SE, Ludwigshafen am Rhein, Germany

10/2011 – 04/2012 Student Trainee, Electrolysis Plants
ThyssenKrupp Uhde GmbH, Dortmund, Germany

03/2011 – 10/2011 Student assistant, Laboratory for technical chemistry B -
Reaction engineering
Department of Biochemical and Chemical Engineering
TU Dortmund University, Dortmund, Germany

01/2010 – 02/2010 Stay at construction site, PR China

10/2007 – 10/2010 Dual studies, Linde AG, Division Linde Engineering

07/2007 – 10/2007 Pre-internship for dual studies, Linde AG, Division Linde
Engineering

Education

10/2010 – 08/2013 Master of Science studies (M.Sc.), Chemical Engineering
TU Dortmund University, Dortmund, Germany

08/2012 – 01/2013 Semester abroad, KTH Royal Institute of Technology,
Stockholm, Sweden

10/2007 – 10/2010 Dual Bachelor of Engineering studies (B.Eng.)
Duale Hochschule Baden-Württemberg (DHBW), Mannheim,
Germany

08/2000 – 06/2007 Secondary School
Europaschule Friedrich-Ludwig-Jahn-Gymnasium, Forst (L.),
Germany